Supplementary Materials A

Figure S1. Dose concentration distribution over time for meteorological conditions in Urumqi, Xinjiang.

Figure S2. Exposure-response association between dry eye disease outpatient visits and $PM_{2.5}$ exposure.

Figure S3. The relative risks (RRs) of per 10 μg/m^3 increase in $PM_{2.5}$ on dry eye disease outpatient visits at various lag days.

Figure S4. 3D graph and contour map of $PM_{2.5}$ exposure on dry eye disease outpatient visits.

Figure S5. Exposure-response association between dry eye disease outpatient visits and $PM_{2.5}$ exposure after adjusted for other air pollution.

Figure S6. The relative risks (RRs) of per 10 μg/m^3 increase in $PM_{2.5}$ on dry eye disease outpatient visits at various lag days after adjusted for NO_2 exposure.

Figure S7. 3D graph and contour map of $PM_{2.5}$ exposure on dry eye disease outpatient visits after adjusted for NO_2 exposure.

Figure S8. The relative risks (RRs) of per 10 μg/m^3 increase in $PM_{2.5}$ on dry eye disease outpatient visits at various lag days after adjusted for PM_{10} exposure.

Figure S9. 3D graph and contour map of $PM_{2.5}$ exposure on dry eye disease outpatient visits after adjusted for PM_{10} exposure.

Figure S10. The relative risks (RRs) of per 10 μg/m^3 increase in $PM_{2.5}$ on dry eye disease outpatient visits at various lag days after adjusted for CO exposure.

Figure S11. 3D graph and contour map of $PM_{2.5}$ exposure on dry eye disease outpatient visits after adjusted for CO exposure.

Figure S12. The relative risks (RRs) of per 10 μg/m^3 increase in $PM_{2.5}$ on dry eye disease outpatient visits at various lag days after adjusted for SO_2 exposure.

Figure S13. 3D graph and contour map of $PM_{2.5}$ exposure on dry eye disease outpatient visits after adjusted for SO_2 exposure.

Figure S14. The relative risks (RRs) of per 10 μg/m^3 increase in $PM_{2.5}$ on dry eye

disease outpatient visits at various lag days after adjusted for O_3 exposure.

Figure S15. 3D graph and contour map of $PM_{2.5}$ exposure on dry eye disease outpatient visits after adjusted for O_3 exposure.

Figure S16. The relative risks (RRs) of per 10 μg/m^3 increase in $PM_{2.5}$ on dry eye disease outpatient visits at various lag days after adjusted for others exposure.

Figure S17. 3D graph and contour map of $PM_{2.5}$ exposure on dry eye disease outpatient visits after adjusted for others exposure.

Figure S18. Exposure-response association between dry eye disease outpatient visits and PM2.5 exposure in male patients.

Figure S19. The relative risks (RRs) of per 10 μg/m^3 increase in $PM_{2.5}$ on dry eye disease outpatient visits at various lag days in male patients.

Figure S20. Exposure-response association between dry eye disease outpatient visits and PM2.5 exposure in female patients.

Figure S21. The relative risks (RRs) of per 10 μg/m^3 increase in $PM_{2.5}$ on dry eye disease outpatient visits at various lag days in female patients.

Figure S22. Exposure-response association between dry eye disease outpatient visits and PM2.5 exposure in age 0-5 patients.

Figure S23. The relative risks (RRs) of per 10 μg/m^3 increase in $PM_{2.5}$ on dry eye disease outpatient visits at various lag days in age 0-5 patients.

Figure S24. Exposure-response association between dry eye disease outpatient visits and $PM_{2.5}$ exposure in age 6-18 patients.

Figure S25. The relative risks (RRs) of per 10 μg/m^3 increase in $PM_{2.5}$ on dry eye disease outpatient visits at various lag days in age 6-18 patients.

Figure S26. Exposure-response association between dry eye disease outpatient visits and $PM_{2.5}$ exposure in age 19-64 patients.

Figure S27. The relative risks (RRs) of per 10 μg/m^3 increase in $PM_{2.5}$ on dry eye disease outpatient visits at various lag days in age 19-64 patients.

Figure S28. Exposure-response association between dry eye disease outpatient visits

and $PM_{2.5}$ exposure in age ≥65 patients.

Figure S29. The relative risks (RRs) of per 10 μg/m^3 increase in $PM_{2.5}$ on dry eye disease outpatient visits at various lag days in age ≥65 patients.

Figure S30. Exposure-response association between dry eye disease outpatient visits and $PM_{2.5}$ exposure in the warm season.

Figure S31. The relative risks (RRs) of per 10 μg/m^3 increase in $PM_{2.5}$ on dry eye disease outpatient visits at various lag days in the warm season.

Figure S32. Exposure-response association between dry eye disease outpatient visits and $PM_{2.5}$ exposure in the cold season.

Figure S33. The relative risks (RRs) of per 10 μg/m^3 increase in $PM_{2.5}$ on dry eye disease outpatient visits at various lag days in the cold season.

Figure S34. Exposure-response association between dry eye disease outpatient visits and PM_{10} exposure.

Figure S35. The relative risks (RRs) of per 10 μg/m^3 increase in PM_{10} on dry eye disease outpatient visits at various lag days.

Figure S36. 3D graph and contour map of PM_{10} exposure on dry eye disease outpatient visits.

Figure S37. Exposure-response association between dry eye disease outpatient visits and PM_{10} exposure after adjusting for other air pollution.

Figure S38. The relative risks (RRs) per 10 μg/m^3 increase in PM_{10} on dry eye disease outpatient visits at various lag days after adjusted for NO_2 exposure.

Figure S39. 3D graph and contour map of PM_{10} exposure on dry eye disease outpatient visits after adjusting for NO_2 exposure.

Figure S40. The relative risks (RRs) per 10 μg/m^3 increase in PM_{10} on dry eye disease outpatient visits at various lag days after adjusted for $PM_{2.5}$ exposure.

Figure S41. 3D graph and contour map of PM_{10} exposure on dry eye disease outpatient visits after adjusted for $PM_{2.5}$ exposure.

Figure S42. The relative risks (RRs) of per 10 μg/m^3 increase in PM_{10} on dry eye disease

outpatient visits at various lag days after adjusted for SO_2 exposure.

Figure S43. 3D graph and contour map of PM_{10} exposure on dry eye disease outpatient visits after adjusted for SO_2 exposure.

Figure S44. The relative risks (RRs) of per 10 $\mu g/m^3$ increase in PM_{10} on dry eye disease outpatient visits at various lag days after adjusted for CO exposure.

Figure S45. 3D graph and contour map of PM_{10} exposure on dry eye disease outpatient visits after adjusted for CO exposure.

Figure S46. The relative risks (RRs) of per 10 $\mu g/m^3$ increase in PM_{10} on dry eye disease outpatient visits at various lag days after adjusted for O_3 exposure.

Figure S47. 3D graph and contour map of PM_{10} exposure on dry eye disease outpatient visits after adjusted for O_3 exposure.

Figure S48. The relative risks (RRs) of per 10 $\mu g/m^3$ increase in PM_{10} on dry eye disease outpatient visits at various lag days after adjusted for others exposure.

Figure S49. 3D graph and contour map of PM_{10} exposure on dry eye disease outpatient visits after adjusted for others exposure.

Figure S50. Exposure-response association between dry eye disease outpatient visits and PM_{10} exposure in male patients.

Figure S51. The relative risks (RRs) of per 10 $\mu g/m^3$ increase in PM_{10} on dry eye disease outpatient visits at various lag days in male patients.

Figure S52. Exposure-response association between dry eye disease outpatient visits and PM_{10} exposure in female patients.

Figure S53. The relative risks (RRs) of per 10 $\mu g/m^3$ increase in PM_{10} on dry eye disease outpatient visits at various lag days in female patients.

Figure S54. Exposure-response association between dry eye disease outpatient visits and PM_{10} exposure in age 0-5 patients.

Figure S55. The relative risks (RRs) of per 10 $\mu g/m^3$ increase in PM_{10} on dry eye disease outpatient visits at various lag days in age 0-5 patients.

Figure S56. Exposure-response association between dry eye disease outpatient visits

and PM_{10} exposure in age 19-64 patients.

Figure S57. The relative risks (RRs) of per 10 μg/m^3 increase in PM_{10} on dry eye disease outpatient visits at various lag days in age 19-64 patients.

Figure S58. Exposure-response association between dry eye disease outpatient visits and PM_{10} exposure in age ≥65 patients.

Figure S59. The relative risks (RRs) of per 10 μg/m^3 increase in PM_{10} on dry eye disease outpatient visits at various lag days in age ≥65 patients.

Figure S60. Exposure-response association between dry eye disease outpatient visits and PM_{10} exposure in the warm season.

Figure S61. The relative risks (RRs) of per 10 μg/m^3 increase in PM_{10} on dry eye disease outpatient visits at various lag days in the warm season.

Figure S62. Exposure-response association between dry eye disease outpatient visits and PM_{10} exposure in the cold season.

Figure S63. The relative risks (RRs) of per 10 μg/m^3 increase in PM_{10} on dry eye disease outpatient visits at various lag days in the cold season.

Figure S64. Exposure-response association between dry eye disease outpatient visits and CO exposure.

Figure S65. The relative risks (RRs) of per 10 mg/m^3 increase in CO on dry eye disease outpatient visits at various lag days.

Figure S66. 3D graph and contour map of CO exposure on dry eye disease outpatient visits.

Figure S67. Exposure-response association between dry eye disease outpatient visits and CO exposure after adjusted for other air pollution.

Figure S68. The relative risks (RRs) of per 10 mg/m^3 increase in CO on dry eye disease outpatient visits at various lag days after adjusted for NO_2 exposure.

Figure S69. 3D graph and contour map of CO exposure on dry eye disease outpatient visits after adjusted for NO_2 exposure.

Figure S70. The relative risks (RRs) of per 10 mg/m^3 increase in CO on dry eye disease

outpatient visits at various lag days after adjusted for PM_{10} exposure.

Figure S71. 3D graph and contour map of CO exposure on dry eye disease outpatient visits after adjusted for PM_{10} exposure.

Figure S72. The relative risks (RRs) of per 10 mg/m^3 increase in CO on dry eye disease outpatient visits at various lag days after adjusted for $PM_{2.5}$ exposure.

Figure S73. 3D graph and contour map of CO exposure on dry eye disease outpatient visits after adjusted for $PM_{2.5}$ exposure.

Figure S74 The relative risks (RRs) of per 10 mg/m^3 increase in CO on dry eye disease outpatient visits at various lag days after adjusted for SO_2 exposure.

Figure S75 3D graph and contour map of CO exposure on dry eye disease outpatient visits after adjusted for SO_2 exposure.

Figure S76 The relative risks (RRs) of per 10 mg/m^3 increase in CO on dry eye disease outpatient visits at various lag days after adjusted for O_3 exposure.

Figure S77 3D graph and contour map of CO exposure on dry eye disease outpatient visits after adjusted for O_3 exposure.

Figure S78The relative risks (RRs) of per 10 mg/m^3 increase in CO on dry eye disease outpatient visits at various lag days after adjusted for others exposure.

Figure S79. 3D graph and contour map of CO exposure on dry eye disease outpatient visits after adjusted for others exposure.

Figure S80. Exposure-response association between dry eye disease outpatient visits and CO exposure in male patients.

Figure S81. The relative risks (RRs) of per 10 mg/m^3 increase in CO on dry eye disease outpatient visits at various lag days in male patients.

Figure S82. Exposure-response association between dry eye disease outpatient visits and CO exposure in female patients.

Figure S83. The relative risks (RRs) of per 10 mg/m^3 increase in CO on dry eye disease outpatient visits at various lag days in female patients.

Figure S84. Exposure-response association between dry eye disease outpatient visits

and CO exposure in age 0-5 patients.

Figure S85. The relative risks (RRs) of per 10 mg/m^3 increase in CO on dry eye disease outpatient visits at various lag days in age 0-5 patients.

Figure S86. Exposure-response association between dry eye disease outpatient visits and CO exposure in age 6-18 patients.

Figure S87. The relative risks (RRs) of per 10 mg/m^3 increase in CO on dry eye disease outpatient visits at various lag days in age 6-18 patients.

Figure S88. Exposure-response association between dry eye disease outpatient visits and CO exposure in age 19-64 patients.

Figure S89. The relative risks (RRs) of per 10 mg/m^3 increase in CO on dry eye disease outpatient visits at various lag days in age 19-64 patients.

Figure S90. Exposure-response association between dry eye disease outpatient visits and CO exposure in age ≥65 patients.

Figure S91. The relative risks (RRs) of per 10 mg/m^3 increase in CO on dry eye disease outpatient visits at various lag days in age ≥65 patients.

Figure S92. Exposure-response association between dry eye disease outpatient visits and CO exposure in the warm season.

Figure S93. The relative risks (RRs) of per 10 mg/m^3 increase in CO on dry eye disease outpatient visits at various lag days in the warm season.

Figure S94. Exposure-response association between dry eye disease outpatient visits and CO exposure in the cold season.

Figure S95. The relative risks (RRs) of per 10 mg/m^3 increase in CO on dry eye disease outpatient visits at various lag days in the cold season.

Figure S96. Exposure-response association between dry eye disease outpatient visits and NO_2 exposure.

Figure S97. The relative risks (RRs) of per 10 $\mu g/m^3$ increase in NO_2 on dry eye disease outpatient visits at various lag days.

Figure S98. 3D graph and contour map of NO_2 exposure on dry eye disease outpatient

visits.

Figure S99. Exposure-response association between dry eye disease outpatient visits and NO2 exposure after adjusted for other air pollution.

Figure S100. The relative risks (RRs) of per 10 μg/m^3 increase in NO_2 on dry eye disease outpatient visits at various lag days after adjusted for $PM_{2.5}$ exposure.

Figure S101. 3D graph and contour map of NO_2 exposure on dry eye disease outpatient visits after adjusted for $PM_{2.5}$ exposure.

Figure S102. The relative risks (RRs) of per 10 μg/m^3 increase in NO_2 on dry eye disease outpatient visits at various lag days after adjusted for PM_{10} exposure.

Figure S103. 3D graph and contour map of NO_2 exposure on dry eye disease outpatient visits after adjusted for PM_{10} exposure.

Figure S104. The relative risks (RRs) of per 10 μg/m^3 increase in NO_2 on dry eye disease outpatient visits at various lag days after adjusted for CO exposure.

Figure S105. 3D graph and contour map of NO_2 exposure on dry eye disease outpatient visits after adjusted for CO exposure.

Figure S106. The relative risks (RRs) of per 10 μg/m^3 increase in NO_2 on dry eye disease outpatient visits at various lag days after adjusted for SO_2 exposure.

Figure S107. 3D graph and contour map of NO_2 exposure on dry eye disease outpatient visits after adjusted for SO_2 exposure.

Figure S108. The relative risks (RRs) of per 10 μg/m^3 increase in NO_2 on dry eye disease outpatient visits at various lag days after adjusted for O_3 exposure.

Figure S109. 3D graph and contour map of NO_2 exposure on dry eye disease outpatient visits after adjusted for O_3 exposure.

Figure S110. The relative risks (RRs) of per 10 μg/m^3 increase in NO_2 on dry eye disease outpatient visits at various lag days after adjusted for others exposure.

Figure S111. 3D graph and contour map of NO_2 exposure on dry eye disease outpatient visits after adjusted for others exposure.

Figure S112. Exposure-response association between dry eye disease outpatient visits

and NO_2 exposure in male patients.

Figure S113. The relative risks (RRs) of per 10 μg/m^3 increase in NO_2 on dry eye disease outpatient visits at various lag days in male patients.

Figure S114. Exposure-response association between dry eye disease outpatient visits and NO_2 exposure in female patients.

Figure S115. The relative risks (RRs) of per 10 μg/m^3 increase in NO_2 on dry eye disease outpatient visits at various lag days in female patients.

Figure S116. Exposure-response association between dry eye disease outpatient visits and NO_2 exposure in age 0-5 patients.

Figure S117. The relative risks (RRs) of per 10 μg/m^3 increase in NO_2 on dry eye disease outpatient visits at various lag days in age 0-5 patients.

Figure S118. Exposure-response association between dry eye disease outpatient visits and NO_2 exposure in age 6-18 patients.

Figure S119. The relative risks (RRs) of per 10 μg/m^3 increase in NO_2 on dry eye disease outpatient visits at various lag days in age 6-18 patients.

Figure S120. Exposure-response association between dry eye disease outpatient visits and NO_2 exposure in age 19-64 patients.

Figure S121. The relative risks (RRs) of per 10 μg/m^3 increase in NO_2 on dry eye disease outpatient visits at various lag days in age 19-64 patients.

Figure S122. Exposure-response association between dry eye disease outpatient visits and NO_2 exposure in age ≥65 patients.

Figure S123. The relative risks (RRs) of per 10 μg/m^3 increase in NO_2 on dry eye disease outpatient visits at various lag days in age ≥65 patients.

Figure S124. Exposure-response association between dry eye disease outpatient visits and NO_2 exposure in the warm season.

Figure S125. The relative risks (RRs) of per 10 μg/m^3 increase in NO_2 on dry eye disease outpatient visits at various lag days in the warm season.

Figure S126. Exposure-response association between dry eye disease outpatient visits

and NO_2 exposure in the cold season.

Figure S127. The relative risks (RRs) of per 10 μg/m^3 increase in NO_2 on dry eye disease outpatient visits at various lag days in the cold season.

Figure S128. Exposure-response association between dry eye disease outpatient visits and SO_2 exposure.

Figure S129. The relative risks (RRs) of per 10 μg/m^3 increase in SO_2 on dry eye disease outpatient visits at various lag days.

Figure S130. 3D graph and contour map of SO_2 exposure on dry eye disease outpatient visits.

Figure S131. Exposure-response association between dry eye disease outpatient visits and SO_2 exposure after adjusted for other air pollution.

Figure S132. The relative risks (RRs) of per 10 μg/m^3 increase in SO_2 on dry eye disease outpatient visits at various lag days after adjusted for NO_2 exposure.

Figure S133. 3D graph and contour map of SO_2 exposure on dry eye disease outpatient visits after adjusted for NO_2 exposure.

Figure S134. The relative risks (RRs) of per 10 μg/m^3 increase in SO_2 on dry eye disease outpatient visits at various lag days after adjusted for PM_{10} exposure.

Figure S135. 3D graph and contour map of SO_2 exposure on dry eye disease outpatient visits after adjusted for PM_{10} exposure.

Figure S136. The relative risks (RRs) of per 10 μg/m^3 increase in SO_2 on dry eye disease outpatient visits at various lag days after adjusted for CO exposure.

Figure S137. 3D graph and contour map of SO_2 exposure on dry eye disease outpatient visits after adjusted for CO exposure.

Figure S138. The relative risks (RRs) of per 10 μg/m^3 increase in SO_2 on dry eye disease outpatient visits at various lag days after adjusted for $PM_{2.5}$ exposure.

Figure S139. 3D graph and contour map of SO_2 exposure on dry eye disease outpatient visits after adjusted for $PM_{2.5}$ exposure.

Figure S140. The relative risks (RRs) of per 10 μg/m^3 increase in SO_2 on dry eye disease

outpatient visits at various lag days after adjusted for O_3 exposure.

Figure S144. 3D graph and contour map of SO_2 exposure on dry eye disease outpatient visits after adjusted for O_3 exposure.

Figure S142. The relative risks (RRs) of per 10 μg/m^3 increase in SO_2 on dry eye disease outpatient visits at various lag days after adjusted for others exposure.

Figure S143. 3D graph and contour map of SO_2 exposure on dry eye disease outpatient visits after adjusted for others exposure.

Figure S144. Exposure-response association between dry eye disease outpatient visits and SO_2 exposure in male patients.

Figure S145. The relative risks (RRs) of per 10 μg/m^3 increase in SO_2 on dry eye disease outpatient visits at various lag days in male patients.

Figure S146. Exposure-response association between dry eye disease outpatient visits and SO_2 exposure in female patients.

Figure S147. The relative risks (RRs) of per 10 μg/m^3 increase in SO_2 on dry eye disease outpatient visits at various lag days in female patients.

Figure S148. Exposure-response association between dry eye disease outpatient visits and SO_2 exposure in age 0-5 patients.

Figure S149. The relative risks (RRs) of per 10 μg/m^3 increase in SO_2 on dry eye disease outpatient visits at various lag days in age 0-5 patients.

Figure S150. Exposure-response association between dry eye disease outpatient visits and SO_2 exposure in age 6-18 patients.

Figure S151. The relative risks (RRs) of per 10 μg/m^3 increase in SO_2 on dry eye disease outpatient visits at various lag days in age 6-18 patients.

Figure S152. Exposure-response association between dry eye disease outpatient visits and SO_2 exposure in age 19-64 patients.

Figure S153. The relative risks (RRs) of per 10 μg/m^3 increase in SO_2 on dry eye disease outpatient visits at various lag days in age 19-64 patients.

Figure S154. Exposure-response association between dry eye disease outpatient visits

and SO_2 exposure in age ≥65 patients.

Figure S155. The relative risks (RRs) of per 10 μg/m^3 increase in SO_2 on dry eye disease outpatient visits at various lag days in age ≥65 patients.

Figure S156. Exposure-response association between dry eye disease outpatient visits and SO_2 exposure in the warm season.

Figure S157. The relative risks (RRs) of per 10 μg/m^3 increase in SO_2 on dry eye disease outpatient visits at various lag days in the warm season.

Figure S158. Exposure-response association between dry eye disease outpatient visits and SO_2 exposure in the cold season.

Figure S159. The relative risks (RRs) of per 10 μg/m^3 increase in SO_2 on dry eye disease outpatient visits at various lag days in the cold season.

Figure S160. Exposure-response association between dry eye disease outpatient visits and O_3 exposure.

Figure S161. The relative risks (RRs) of per 10 μg/m^3 increase in O_3 on dry eye disease outpatient visits at various lag days.

Figure S162. 3D graph and contour map of O_3 exposure on dry eye disease outpatient visits.

Figure S163. Exposure-response association between dry eye disease outpatient visits and O_3 exposure after adjusted for other air pollution.

Figure S164. The relative risks (RRs) of per 10 μg/m^3 increase in O_3 on dry eye disease outpatient visits at various lag days after adjusted for NO_2 exposure.

Figure S165. 3D graph and contour map of O_3 exposure on dry eye disease outpatient visits after adjusted for NO_2 exposure.

Figure S166. The relative risks (RRs) of per 10 μg/m^3 increase in O_3 on dry eye disease outpatient visits at various lag days after adjusted for PM_{10} exposure.

Figure S167. 3D graph and contour map of O_3 exposure on dry eye disease outpatient visits after adjusted for PM_{10} exposure.

Figure S168. The relative risks (RRs) of per 10 μg/m^3 increase in O_3 on dry eye disease

outpatient visits at various lag days after adjusted for CO exposure.

Figure S169. 3D graph and contour map of O_3 exposure on dry eye disease outpatient visits after adjusted for CO exposure.

Figure S170. The relative risks (RRs) of per 10 μg/m^3 increase in O_3 on dry eye disease outpatient visits at various lag days after adjusted for $PM_{2.5}$ exposure.

Figure S171. 3D graph and contour map of O_3 exposure on dry eye disease outpatient visits after adjusted for $PM_{2.5}$ exposure.

Figure S172. The relative risks (RRs) of per 10 μg/m^3 increase in O_3 on dry eye disease outpatient visits at various lag days after adjusted for SO_2 exposure.

Figure S173. 3D graph and contour map of O_3 exposure on dry eye disease outpatient visits after adjusted for SO_2 exposure.

Figure S174. The relative risks (RRs) of per 10 μg/m^3 increase in O_3 on dry eye disease outpatient visits at various lag days after adjusted for others exposure.

Figure S175. 3D graph and contour map of O_3 exposure on dry eye disease outpatient visits after adjusted for others exposure.

Figure S176. Exposure-response association between dry eye disease outpatient visits and O_3 exposure in male patients.

Figure S177. The relative risks (RRs) of per 10 μg/m^3 increase in O_3 on dry eye disease outpatient visits at various lag days in male patients.

Figure S178. Exposure-response association between dry eye disease outpatient visits and O_3 exposure in female patients.

Figure S189. The relative risks (RRs) of per 10 μg/m^3 increase in O_3 on dry eye disease outpatient visits at various lag days in female patients.

Figure S180. Exposure-response association between dry eye disease outpatient visits and O_3 exposure in age 0-5 patients.

Figure S181. The relative risks (RRs) of per 10 μg/m^3 increase in O_3 on dry eye disease outpatient visits at various lag days in age 0-5 patients.

Figure S182. Exposure-response association between dry eye disease outpatient visits

and O_3 exposure in age 6-18 patients.

Figure S183. The relative risks (RRs) of per 10 μg/m^3 increase in O_3 on dry eye disease outpatient visits at various lag days in age 6-18 patients.

Figure S184. Exposure-response association between dry eye disease outpatient visits and O_3 exposure in age 19-64 patients.

Figure S185. The relative risks (RRs) of per 10 μg/m^3 increase in O_3 on dry eye disease outpatient visits at various lag days in age 19-64 patients.

Figure S186. Exposure-response association between dry eye disease outpatient visits and O_3 exposure in age ≥65 patients.

Figure S187. The relative risks (RRs) of per 10 μg/m^3 increase in O_3 on dry eye disease outpatient visits at various lag days in age ≥65 patients.

Figure S188. Exposure-response association between dry eye disease outpatient visits and O_3 exposure in the warm season.

Figure S189. The relative risks (RRs) of per 10 μg/m^3 increase in O_3 on dry eye disease outpatient visits at various lag days in the warm season.

Figure S190. Exposure-response association between dry eye disease outpatient visits and O_3 exposure in the cold season.

Figure S191. The relative risks (RRs) of per 10 μg/m^3 increase in O_3 on dry eye disease outpatient visits at various lag days in the cold season.

Figure S192. Overall exposure-response association and meteorological conditions: Multi-pollutant model.

Figure S1. Dose concentration distribution over time for air pollution in Urumqi, Xinjiang.

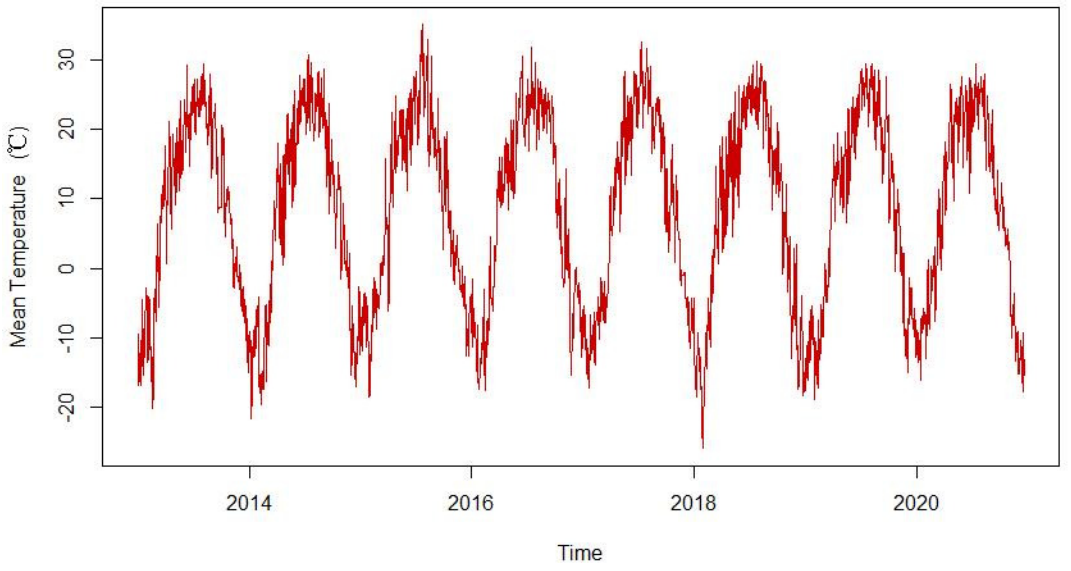

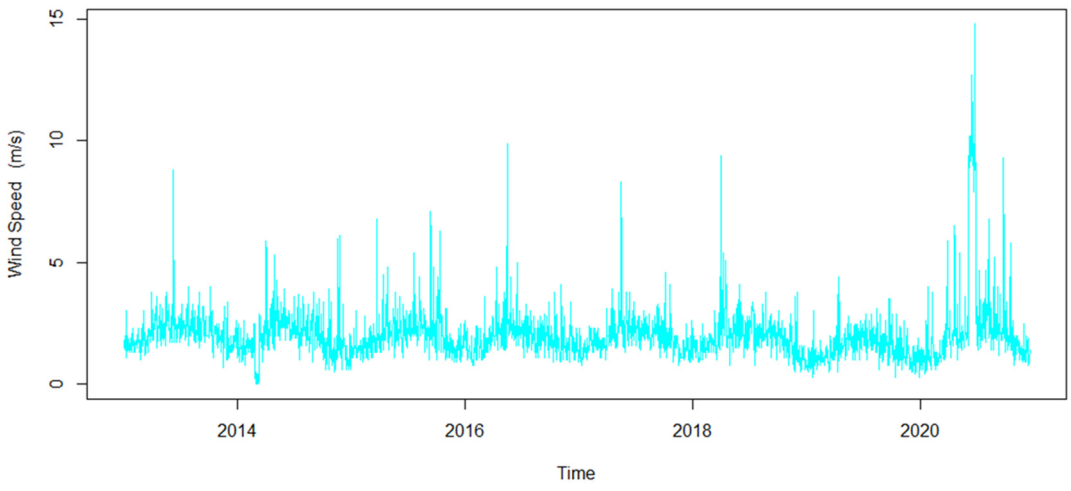

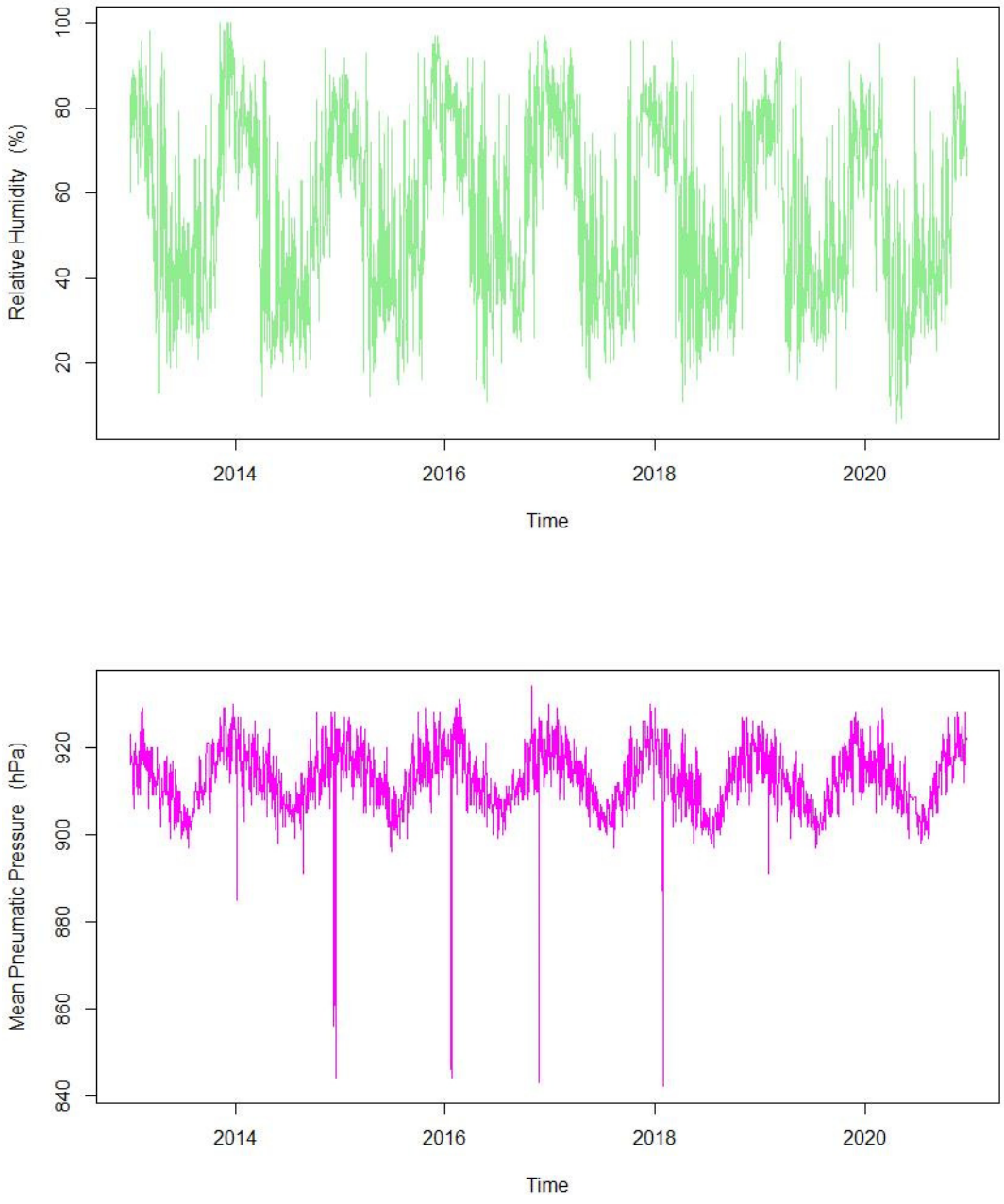

Figure S2. Exposure-response association between dry eye disease outpatient visits and $PM_{2.5}$ exposure.

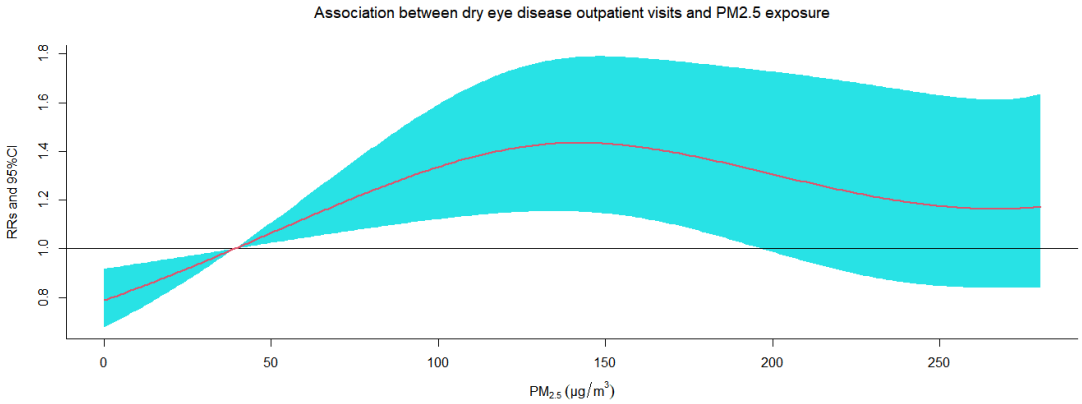

Figure S3. The relative risks (RRs) of per 10 μg/m^3 increase in $PM_{2.5}$ on dry eye disease outpatient visits at various lag days.

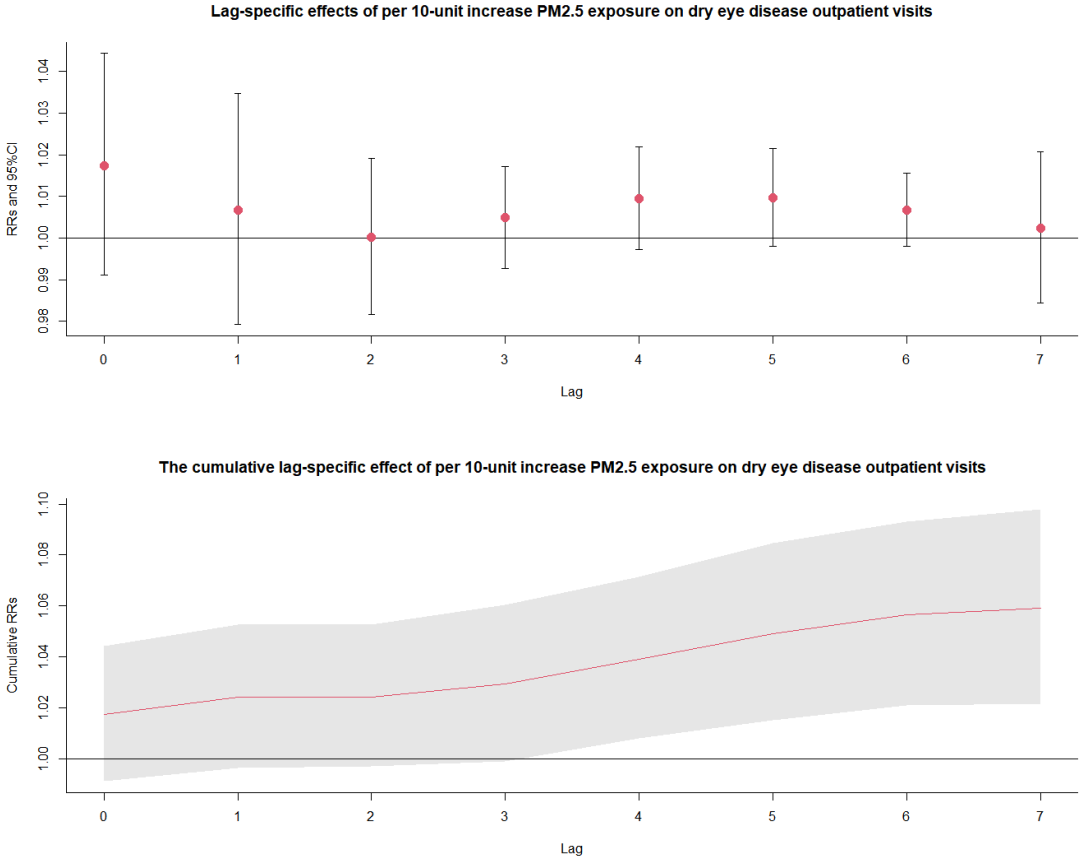

Figure S4. 3D graph and contour map of $PM_{2.5}$ exposure on dry eye disease outpatient visits.

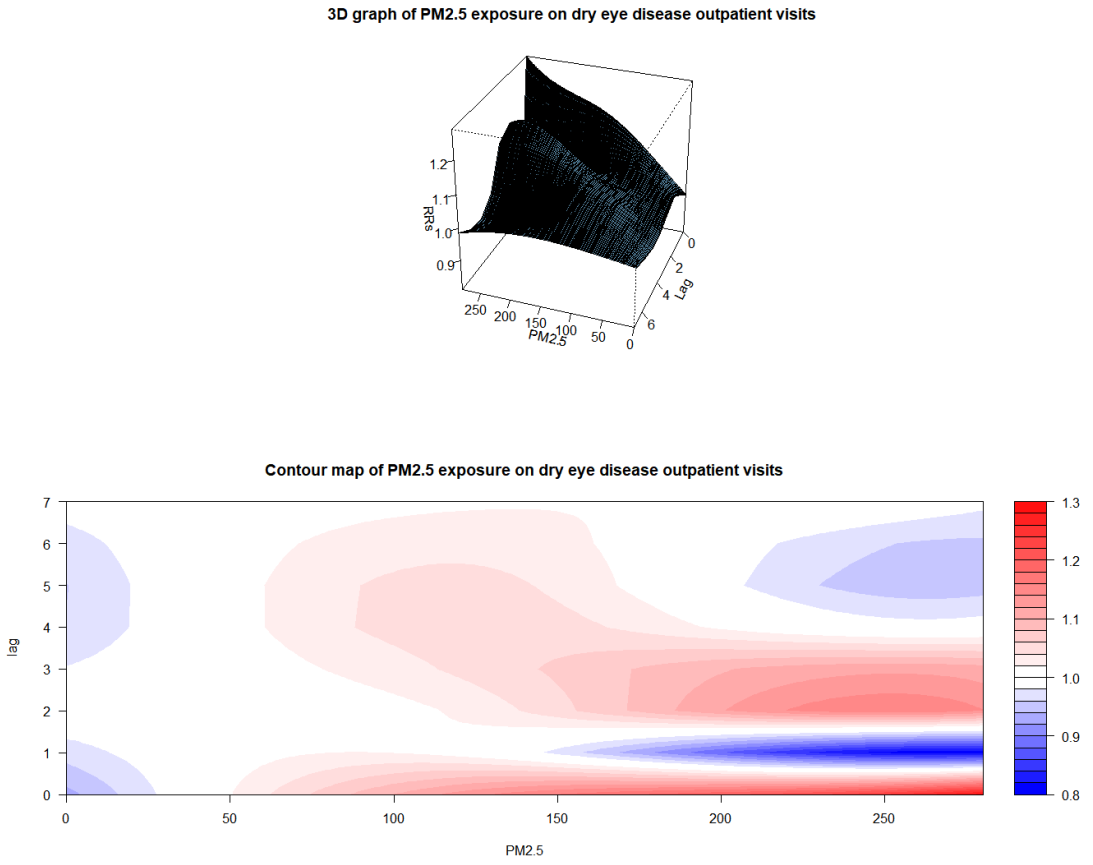

Figure S5. Exposure-response association between dry eye disease outpatient visits and $PM_{2.5}$ exposure after adjusted for other air pollution.

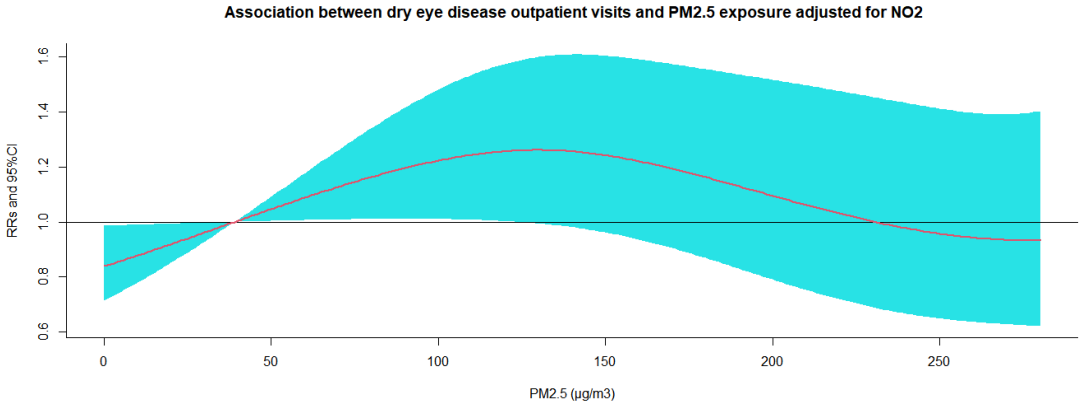

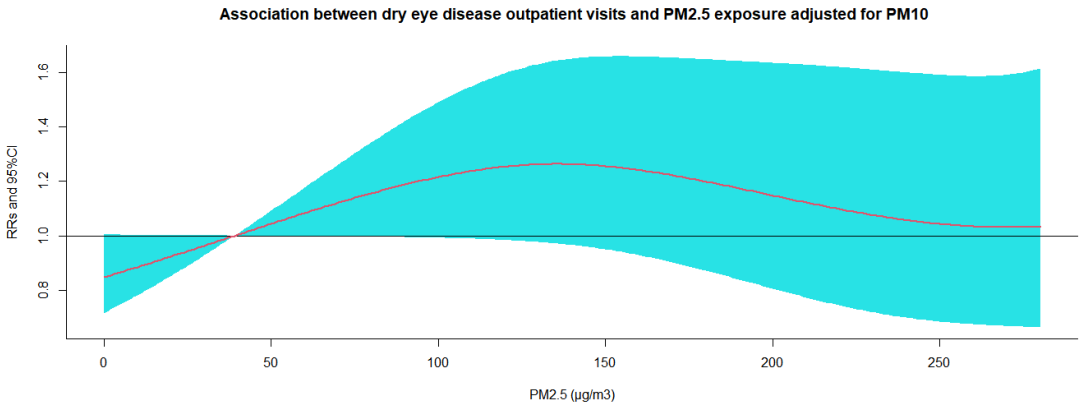
Association between dry eye disease outpatient visits and PM2.5 exposure adjusted for PM10
RRs and 95%CI
0.8
1.0
1.2
1.4
1.6
0
50
100
150
200
250
PM2.5 (μg/m3)

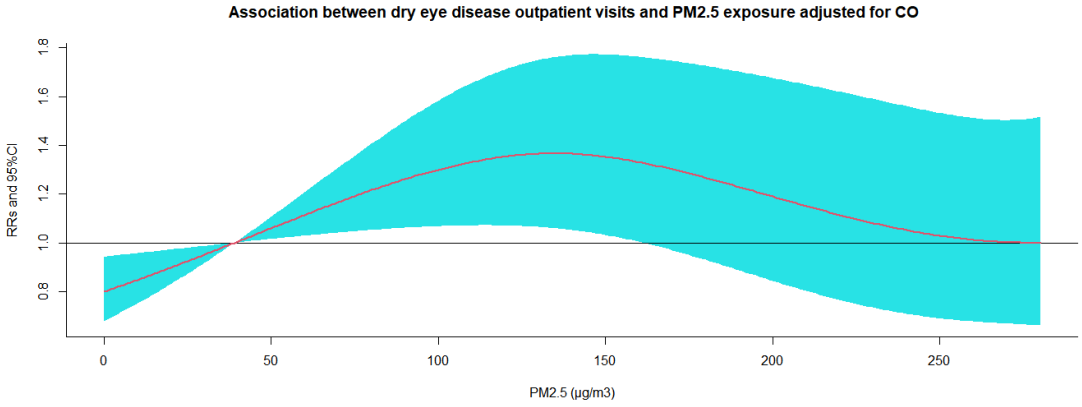
Association between dry eye disease outpatient visits and PM2.5 exposure adjusted for CO
RRs and 95%CI
0.8
1.0
1.2
1.4
1.6
1.8
0
50
100
150
200
250
PM2.5 (μg/m3)

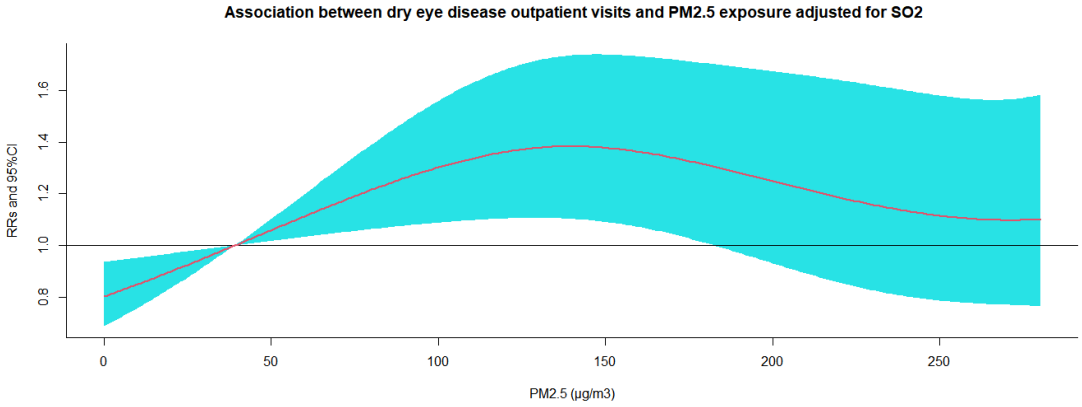
Association between dry eye disease outpatient visits and PM2.5 exposure adjusted for SO2
RRs and 95%CI
0.8
1.0
1.2
1.4
1.6
0
50
100
150
200
250
PM2.5 (μg/m3)

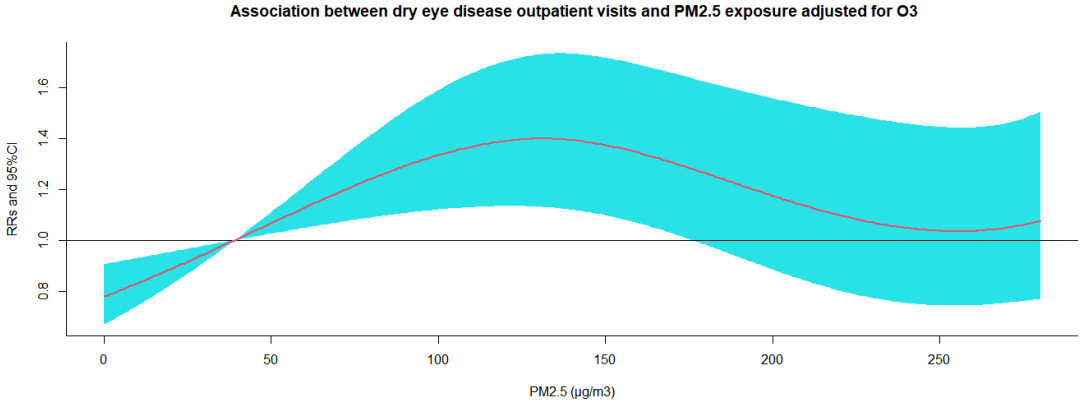
Association between dry eye disease outpatient visits and PM2.5 exposure adjusted for O3
RRs and 95%CI
0.8
1.0
1.2
1.4
1.6
0
50
100
150
200
250
PM2.5 (μg/m3)

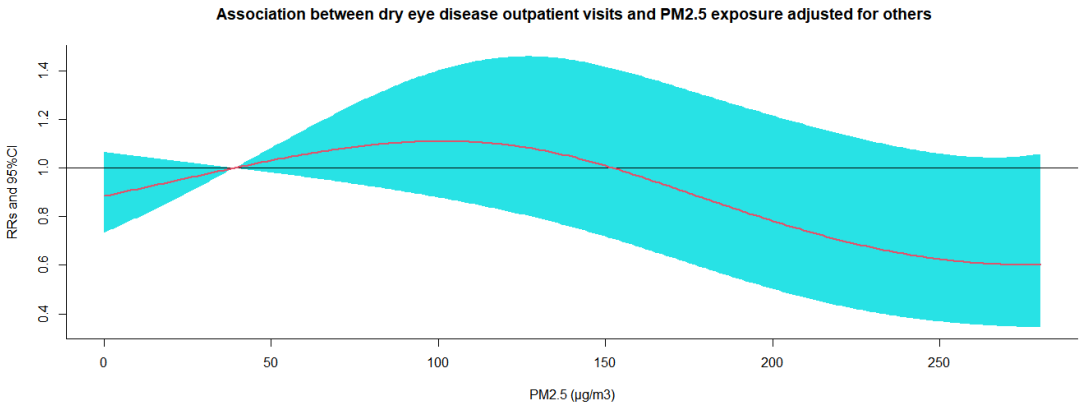

Figure S6. The relative risks (RRs) of per 10 μg/m^3 increase in $PM_{2.5}$ on dry eye disease outpatient visits at various lag days after adjusted for NO_2 exposure.

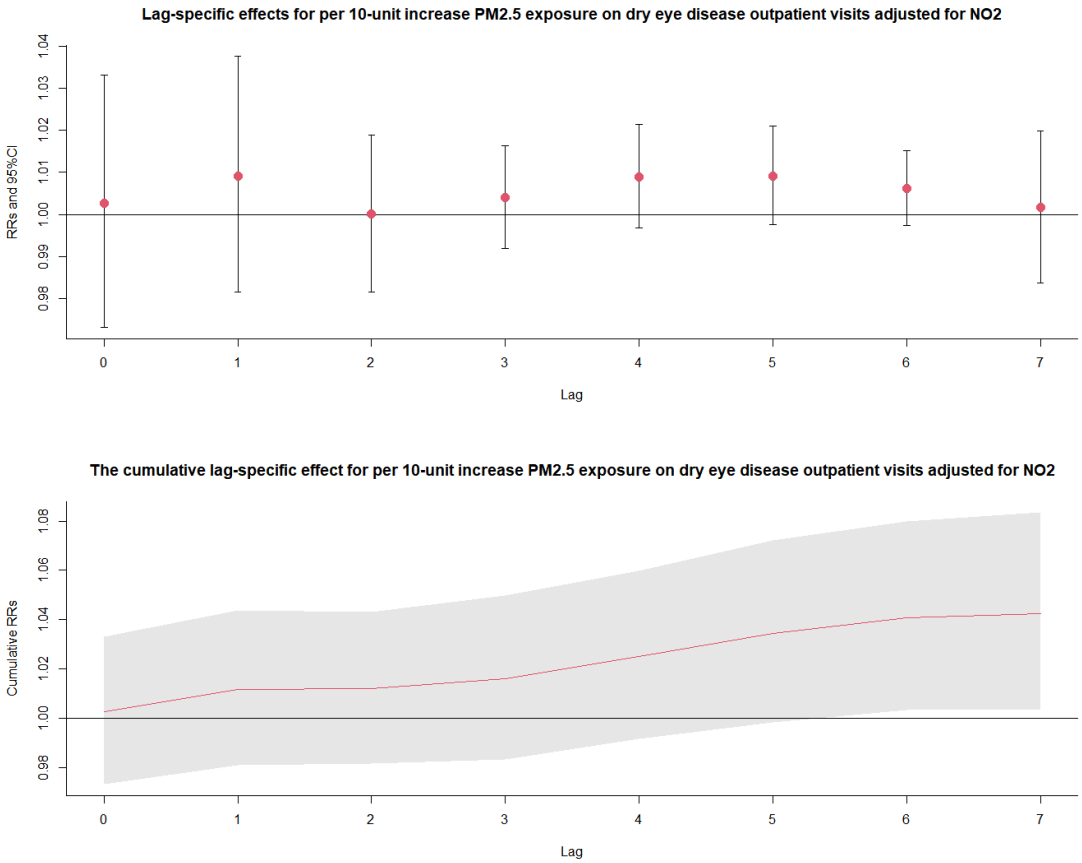

Figure S7. 3D graph and contour map of $PM_{2.5}$ exposure on dry eye disease outpatient visits after adjusted for NO_2 exposure.

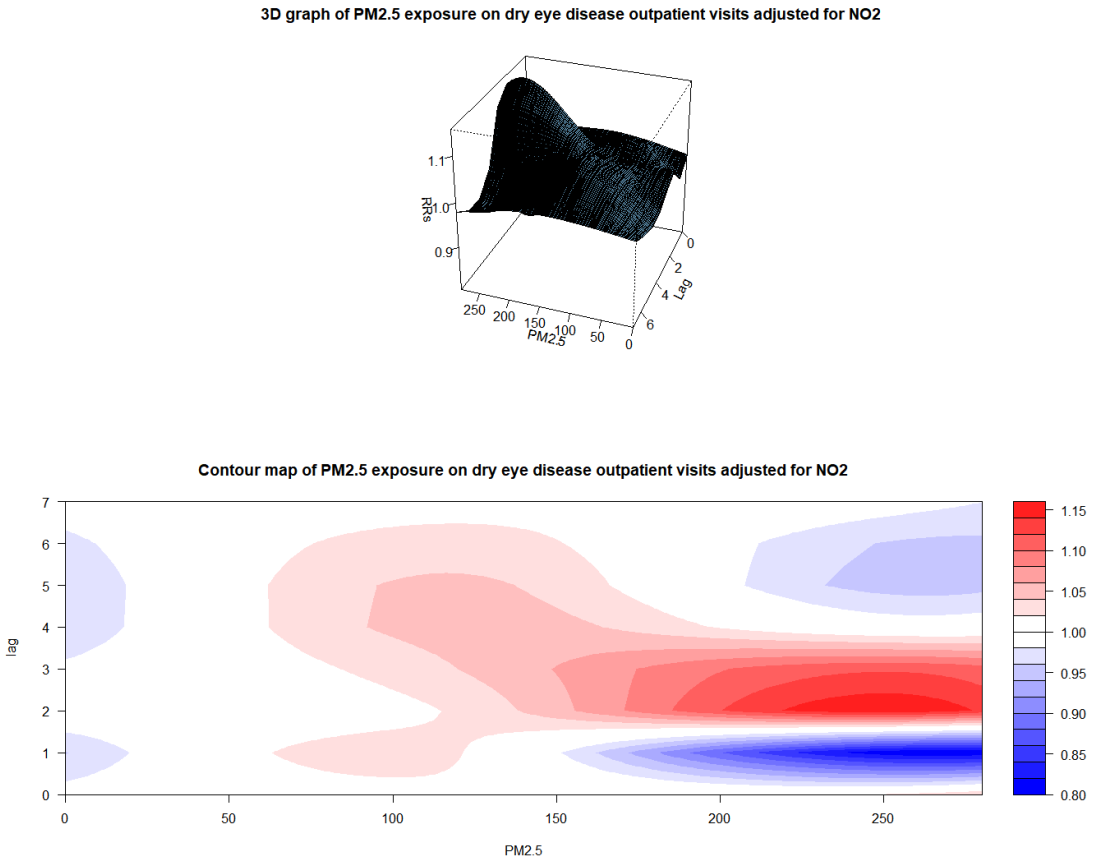

Figure S8. The relative risks (RRs) of per 10 μg/m^3 increase in $PM_{2.5}$ on dry eye disease outpatient visits at various lag days after adjusted for PM_{10} exposure.

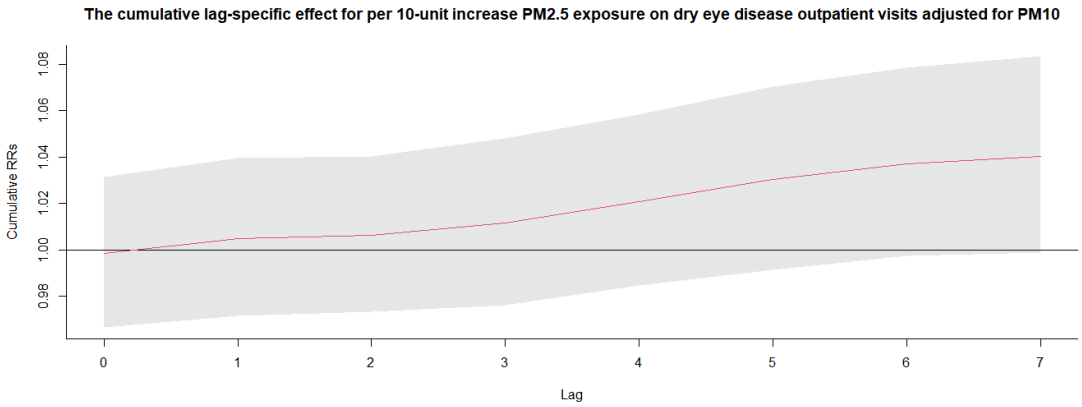

Figure S9. 3D graph and contour map of $PM_{2.5}$ exposure on dry eye disease outpatient visits after adjusted for PM_{10} exposure.

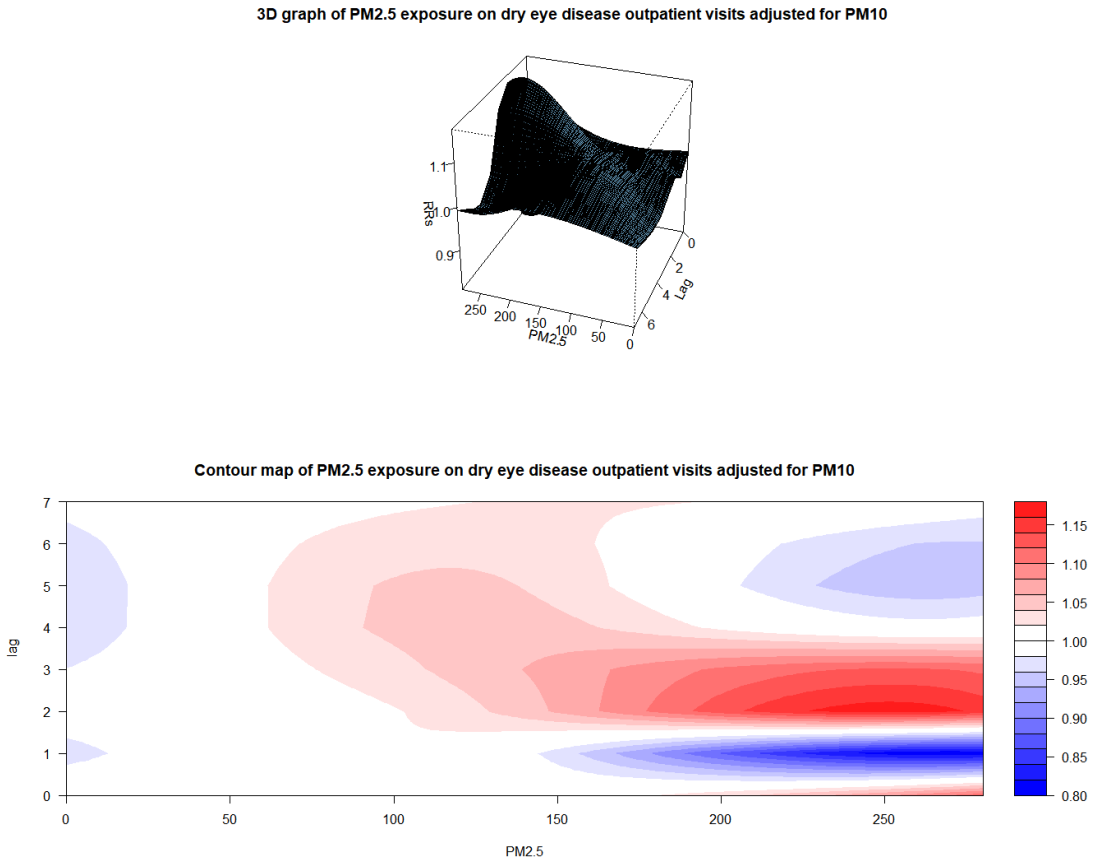

Figure S10. The relative risks (RRs) of per 10 $\mu g/m^3$ increase in $PM_{2.5}$ on dry eye disease outpatient visits at various lag days after adjusted for CO exposure.

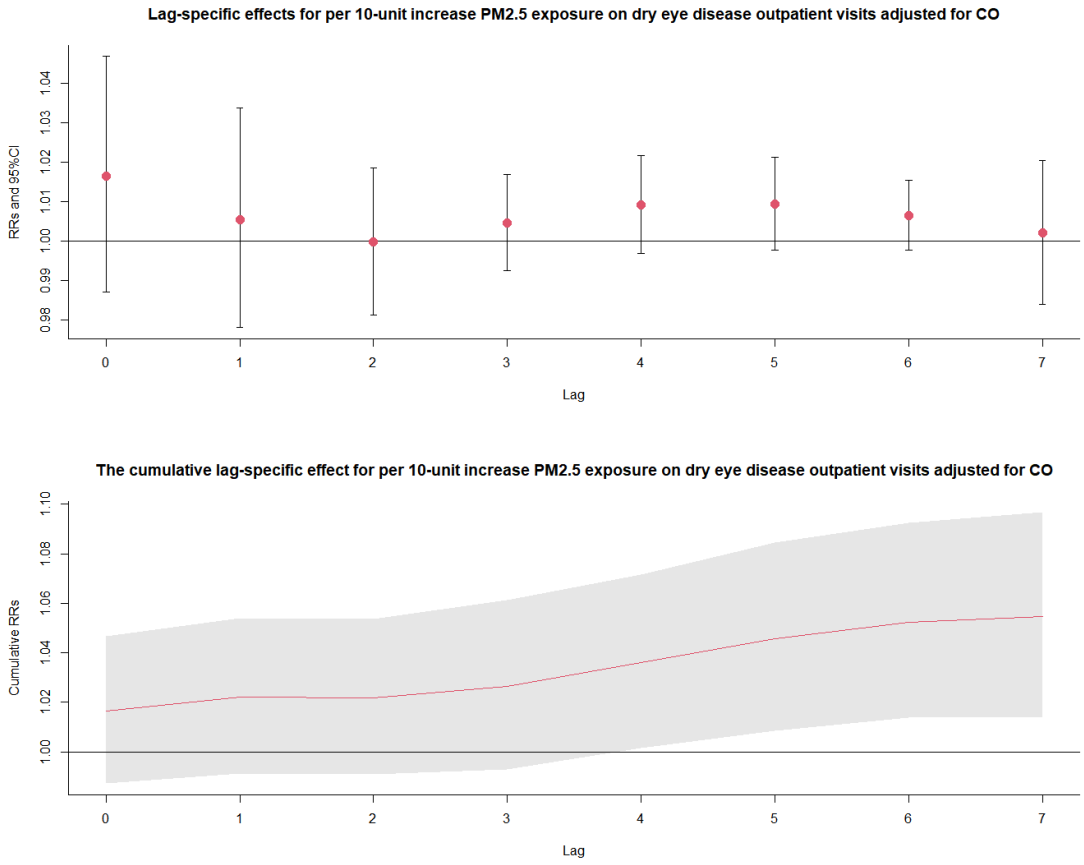

Figure S11. 3D graph and contour map of $PM_{2.5}$ exposure on dry eye disease outpatient visits after adjusted for CO exposure.

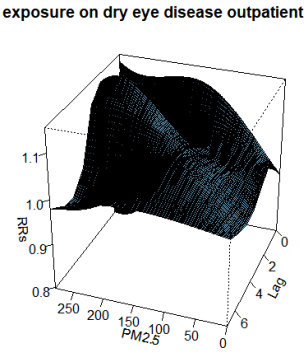

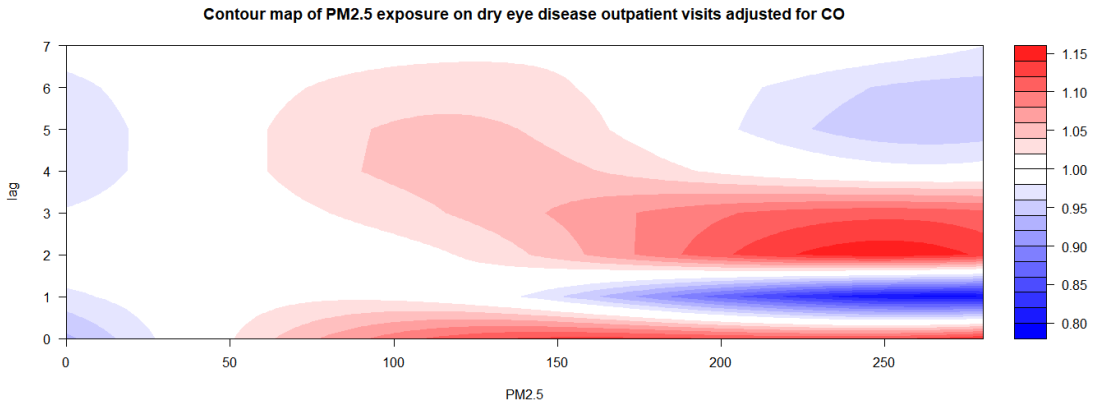

Figure S12. The relative risks (RRs) of per 10 μg/m^3 increase in $PM_{2.5}$ on dry eye disease outpatient visits at various lag days after adjusted for SO_2 exposure.

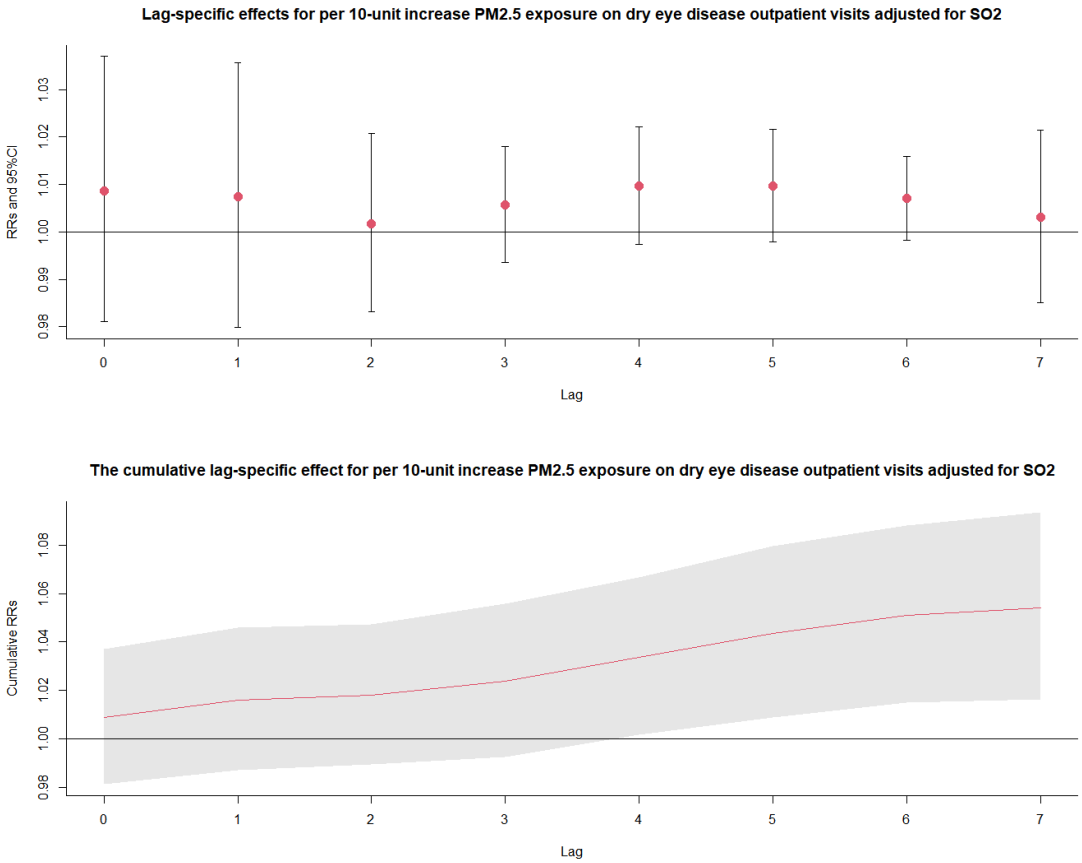

Figure S13. 3D graph and contour map of $PM_{2.5}$ exposure on dry eye disease outpatient visits after adjusted for SO_2 exposure.

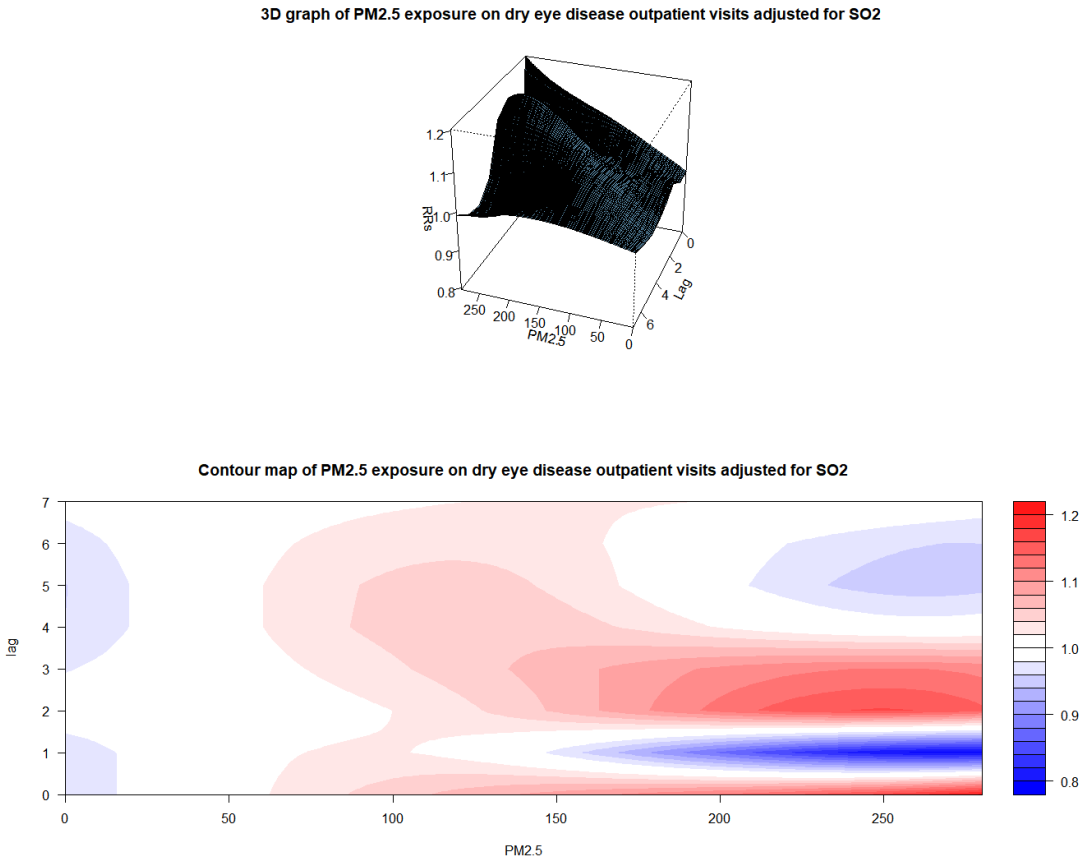

Figure S14. The relative risks (RRs) of per 10 μg/m^3 increase in $PM_{2.5}$ on dry eye disease outpatient visits at various lag days after adjusted for O_3 exposure.

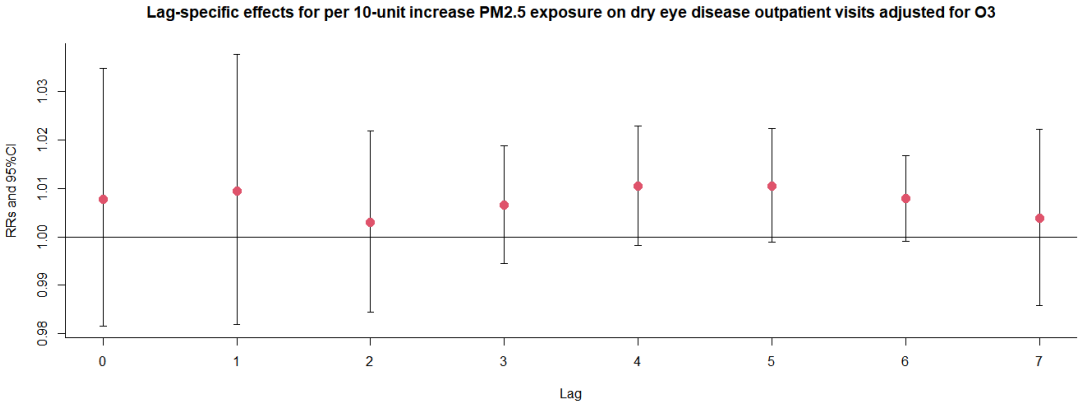

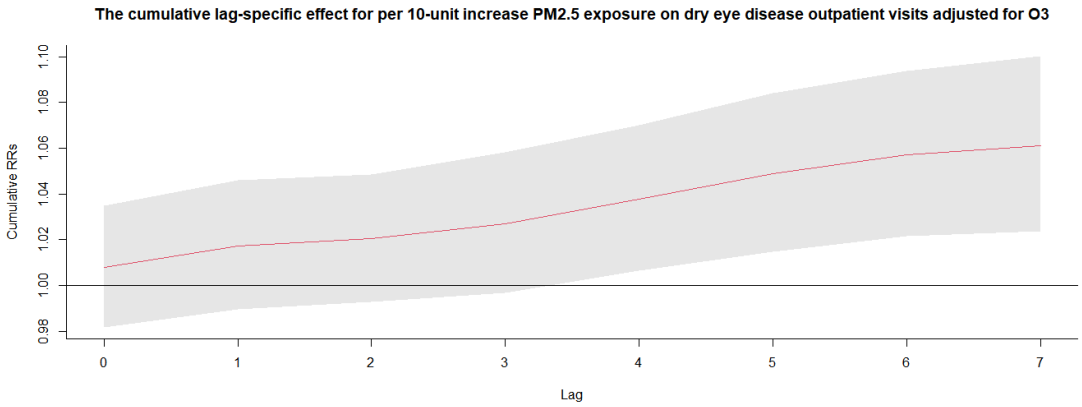

Figure S15. 3D graph and contour map of $PM_{2.5}$ exposure on dry eye disease outpatient visits after adjusted for O_3 exposure.

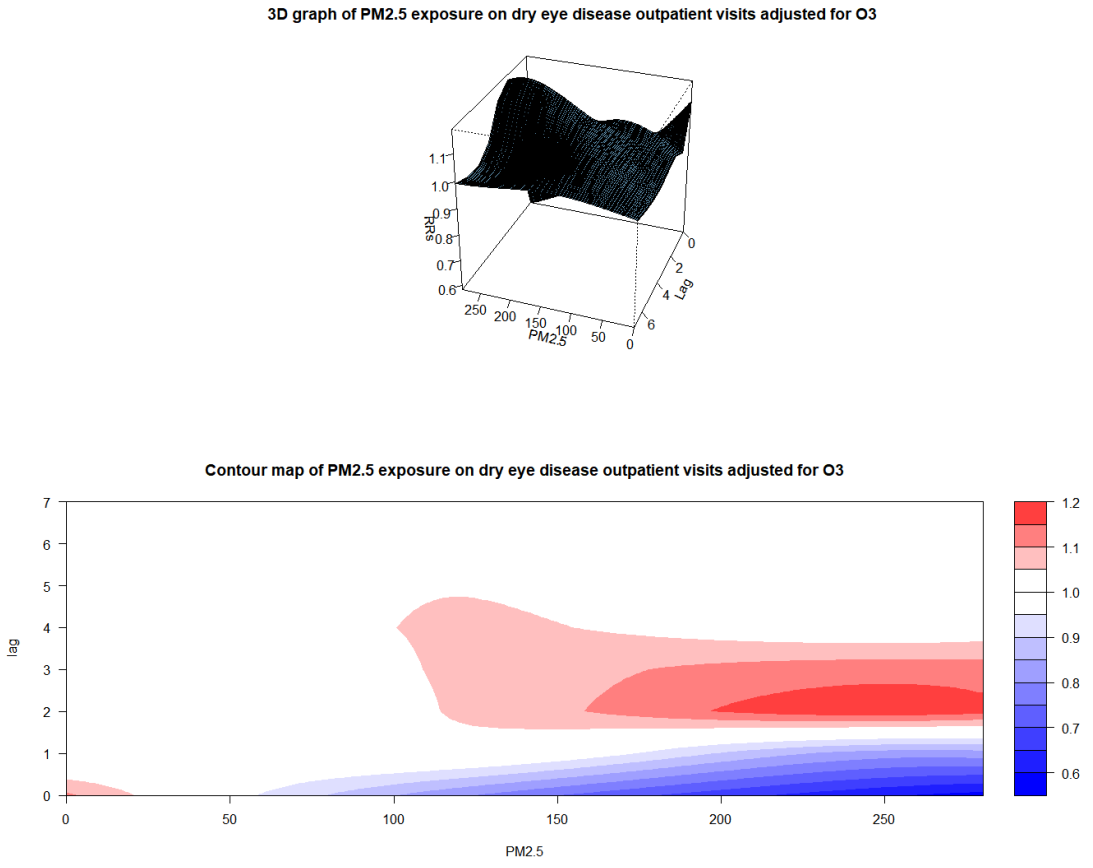

Figure S16. The relative risks (RRs) of per 10 $\mu g/m^3$ increase in $PM_{2.5}$ on dry eye disease outpatient visits at various lag days after adjusted for others exposure.

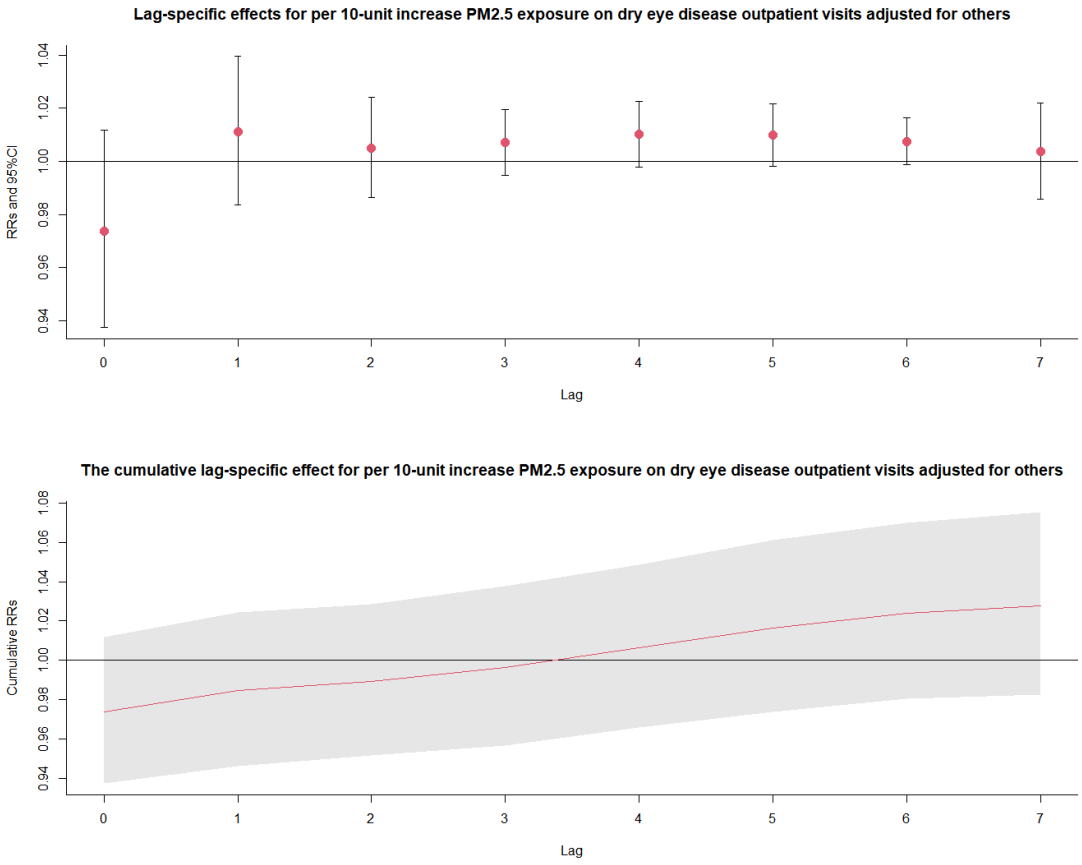

Figure S17. 3D graph and contour map of $PM_{2.5}$ exposure on dry eye disease outpatient visits after adjusted for others exposure.

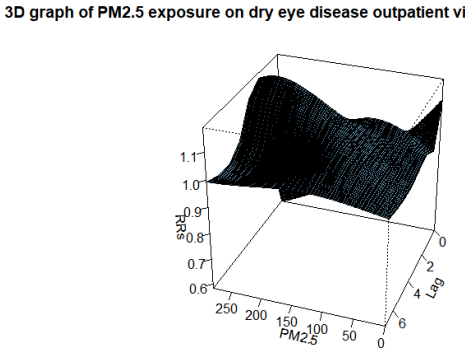

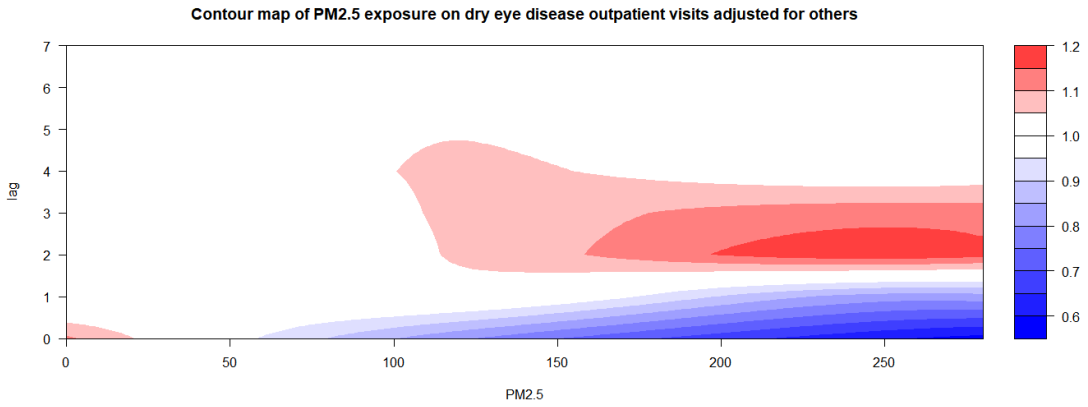

Figure S18. Exposure-response association between dry eye disease outpatient visits and $PM_{2.5}$ exposure in male patients.

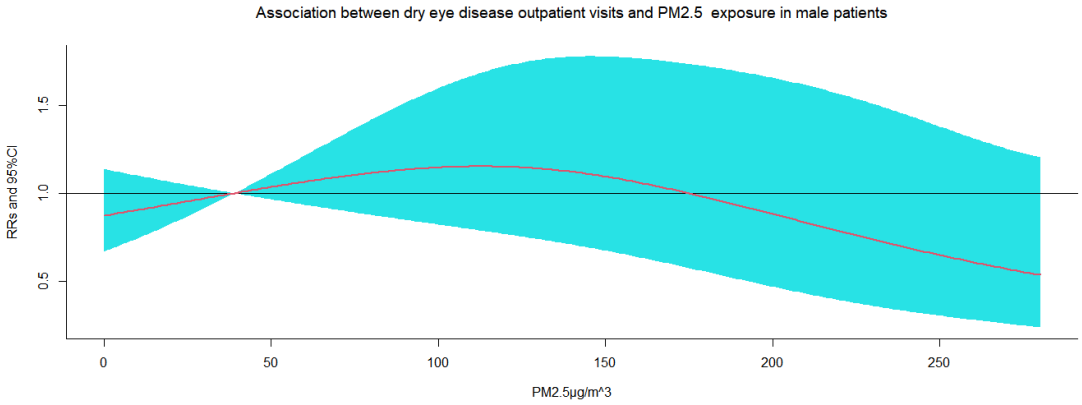

Figure S19. The relative risks (RRs) of per 10 $\mu g/m^3$ increase in $PM_{2.5}$ on dry eye disease outpatient visits at various lag days in male patients.

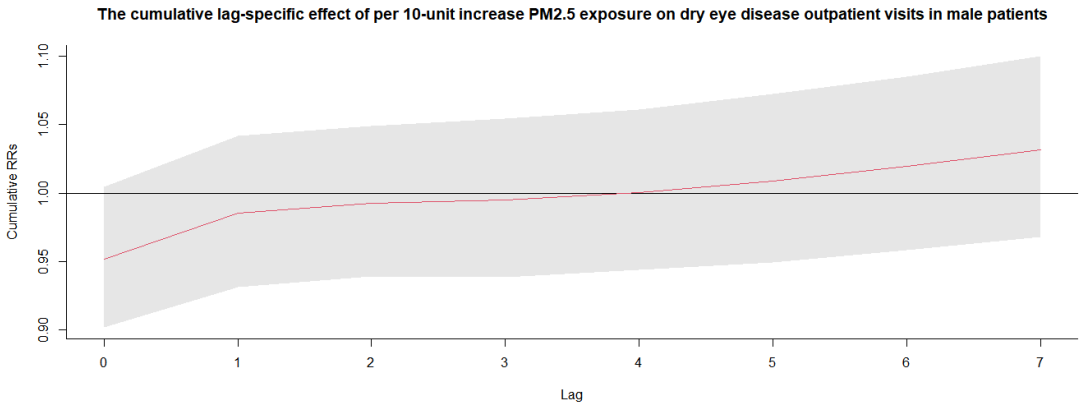

Figure S20. Exposure-response association between dry eye disease outpatient visits and $PM_{2.5}$ exposure in female patients.

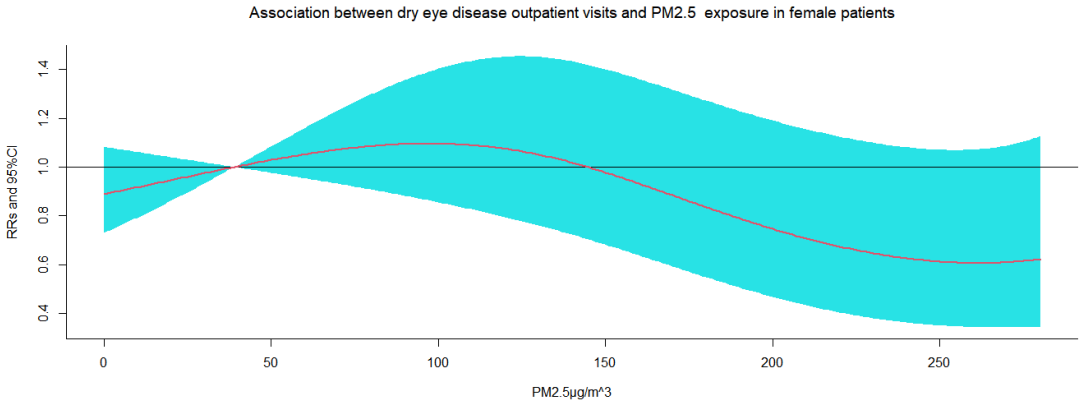

Figure S21. The relative risks (RRs) of per 10 $\mu g/m^3$ increase in $PM_{2.5}$ on dry eye disease outpatient visits at various lag days in female patients.

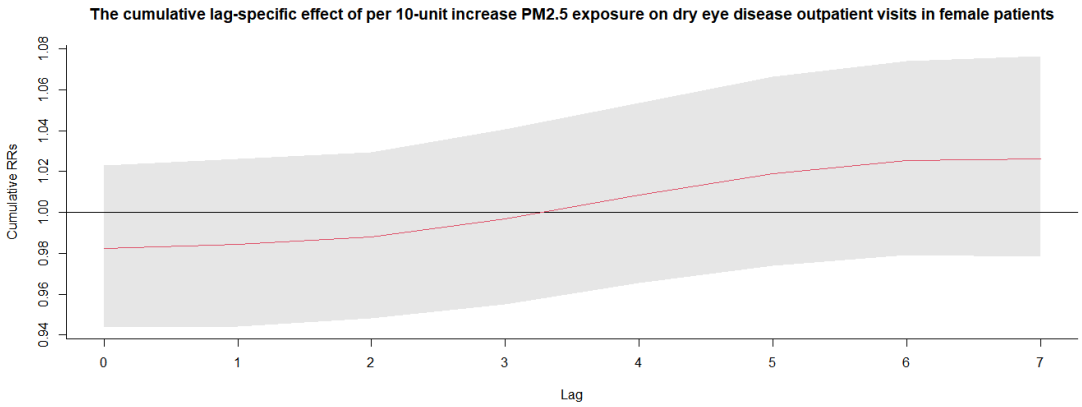

Figure S22. Exposure-response association between dry eye disease outpatient visits and $PM_{2.5}$ exposure in age 0-5 patients.

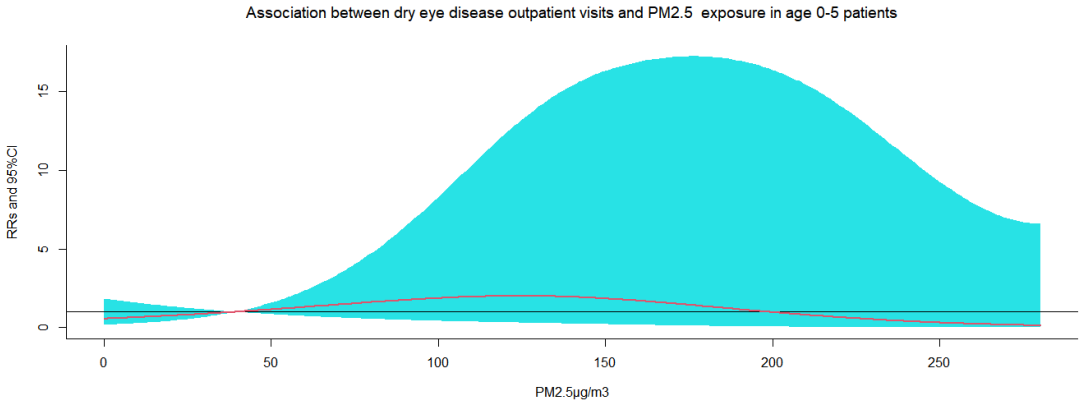

Figure S23. The relative risks (RRs) of per 10 μg/m^3 increase in $PM_{2.5}$ on dry eye disease outpatient visits at various lag days in age 0-5 patients.

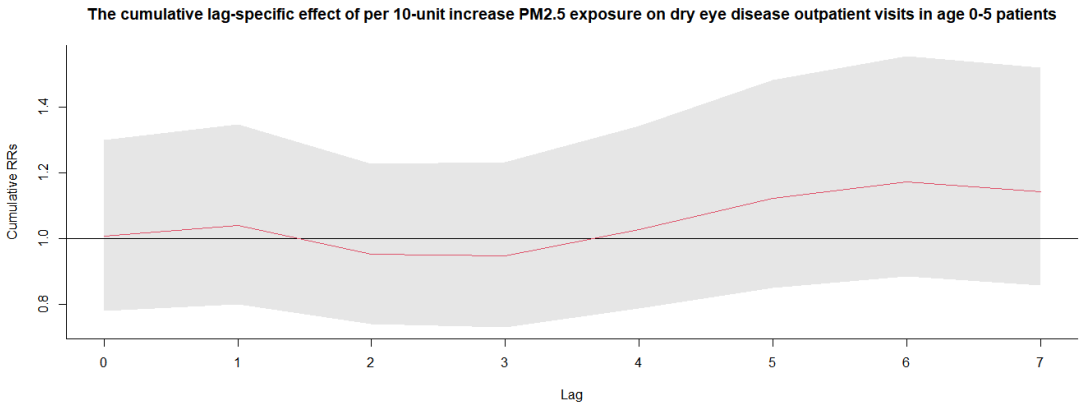

Figure S24. Exposure-response association between dry eye disease outpatient visits and $PM_{2.5}$ exposure in age 6-18 patients.

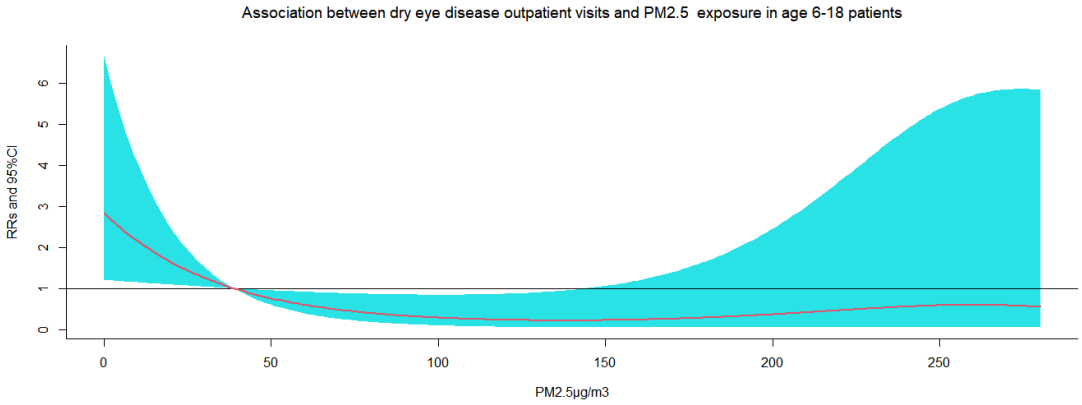

Figure S25. The relative risks (RRs) of per 10 μg/m^3 increase in $PM_{2.5}$ on dry eye disease outpatient visits at various lag days in age 6-18 patients.

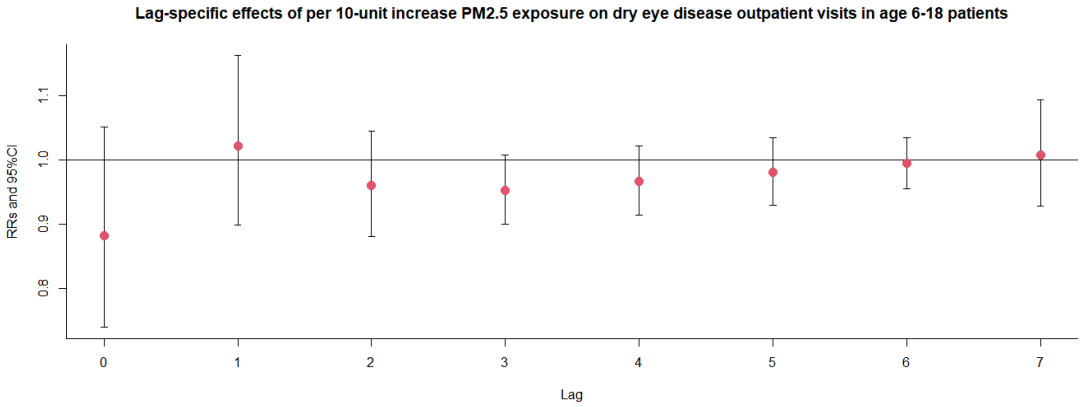

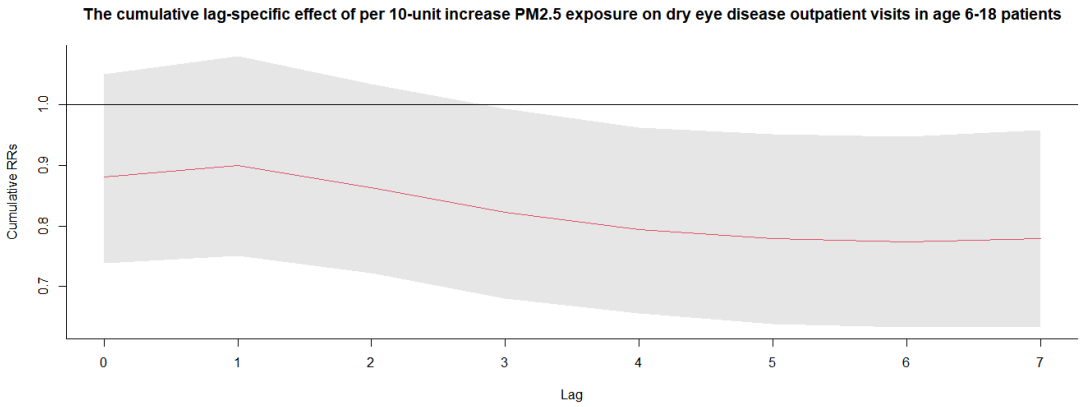

Figure S26. Exposure-response association between dry eye disease outpatient visits and $PM_{2.5}$ exposure in age 19-64 patients.

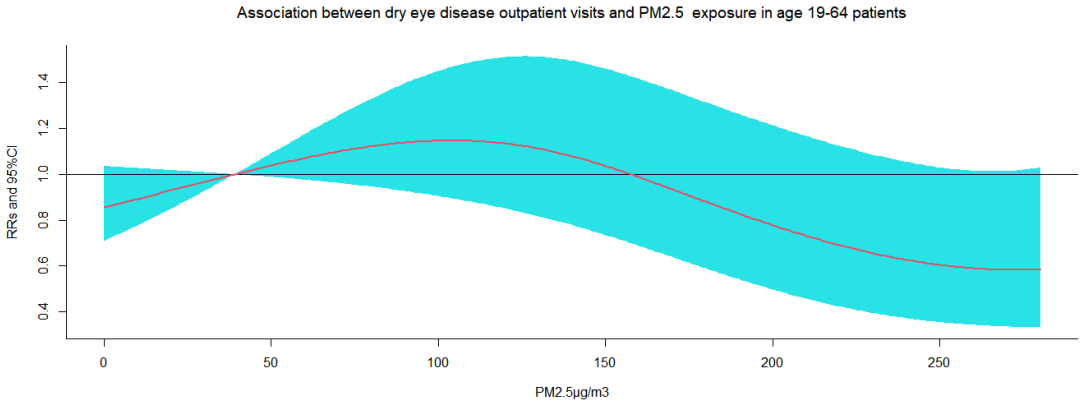

Figure S27. The relative risks (RRs) of per 10 $\mu g/m^3$ increase in $PM_{2.5}$ on dry eye disease outpatient visits at various lag days in age 19-64 patients.

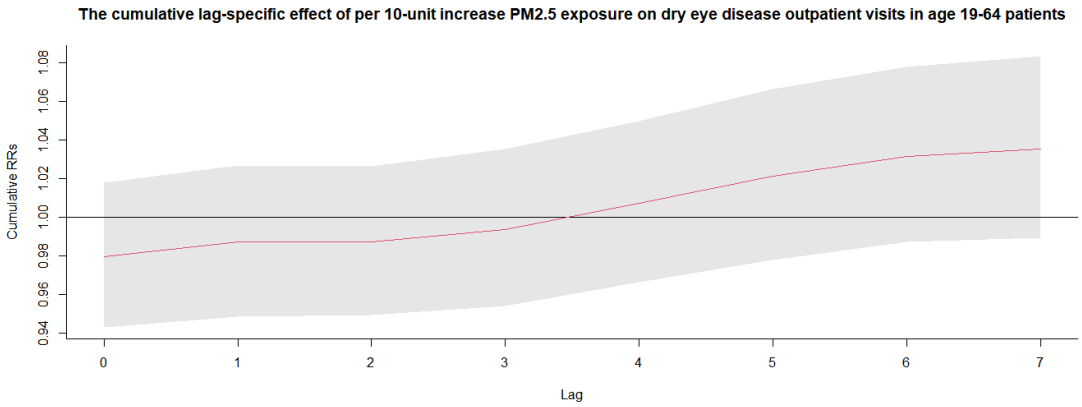

Figure S28. Exposure-response association between dry eye disease outpatient visits and $PM_{2.5}$ exposure in age ≥65 patients.

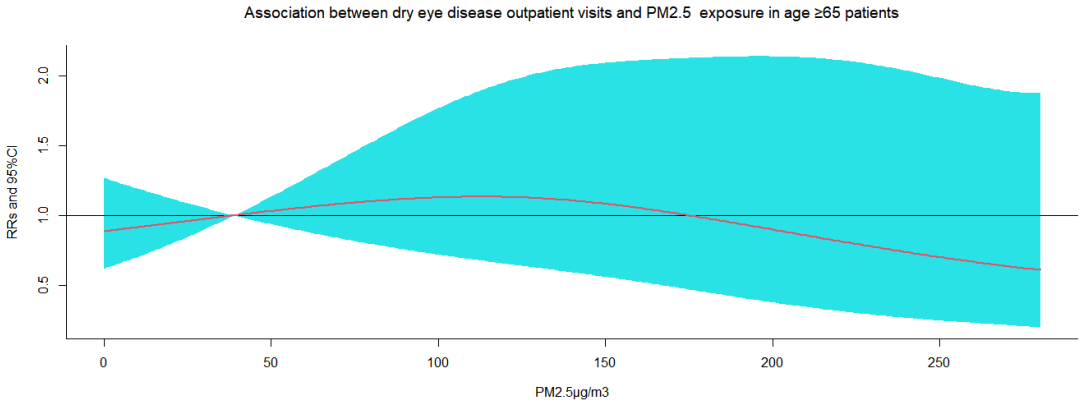

Figure S29. The relative risks (RRs) of per 10 μg/m^3 increase in $PM_{2.5}$ on dry eye disease outpatient visits at various lag days in age ≥65 patients.

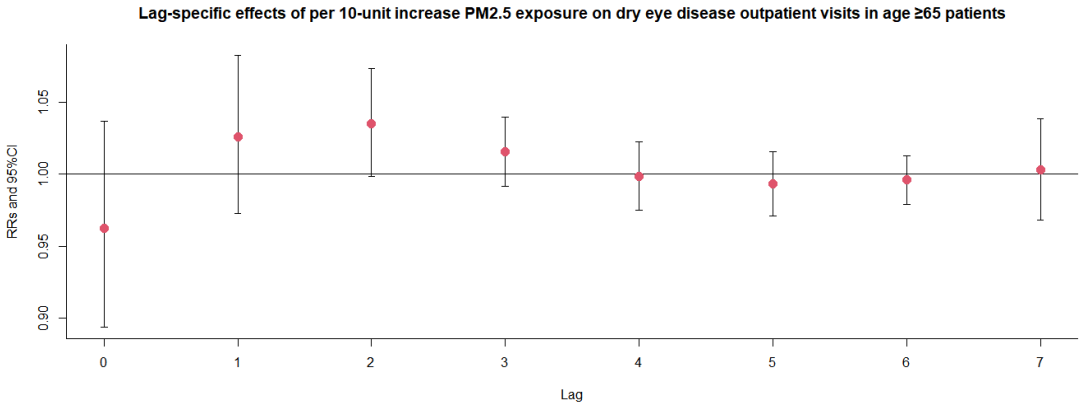

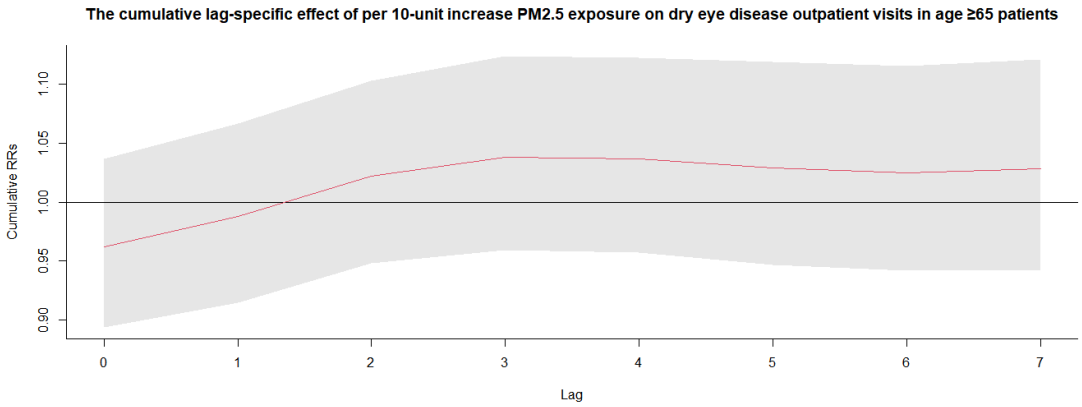

Figure S30. Exposure-response association between dry eye disease outpatient visits and $PM_{2.5}$ exposure in the warm season.

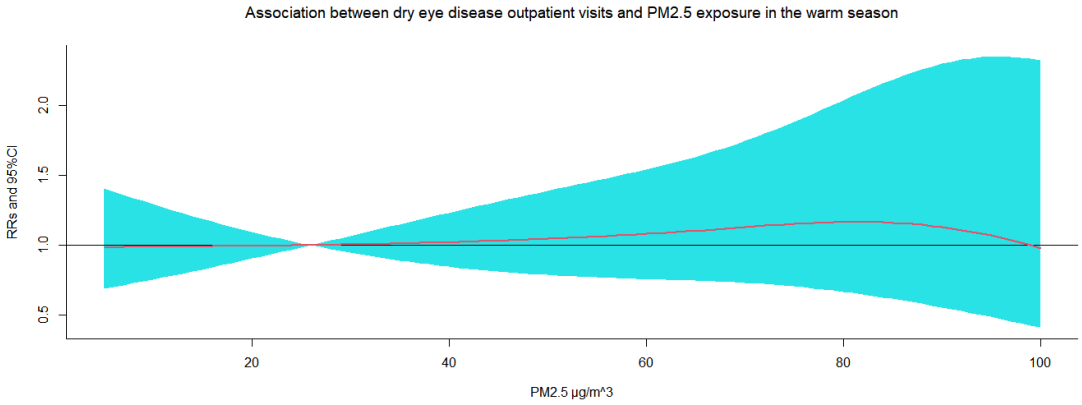

Figure S31. The relative risks (RRs) of per 10 $\mu g/m^3$ increase in $PM_{2.5}$ on dry eye disease outpatient visits at various lag days in the warm season.

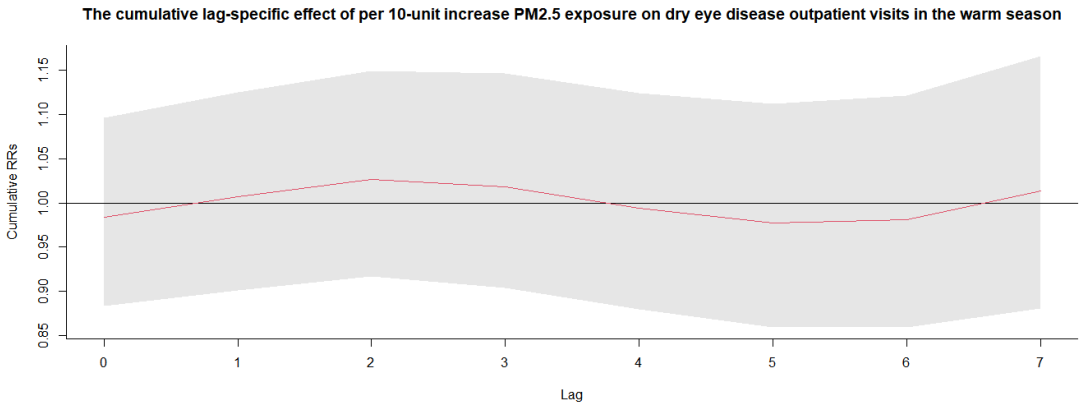

Figure S32. Exposure-response association between dry eye disease outpatient visits and $PM_{2.5}$ exposure in the cold season.

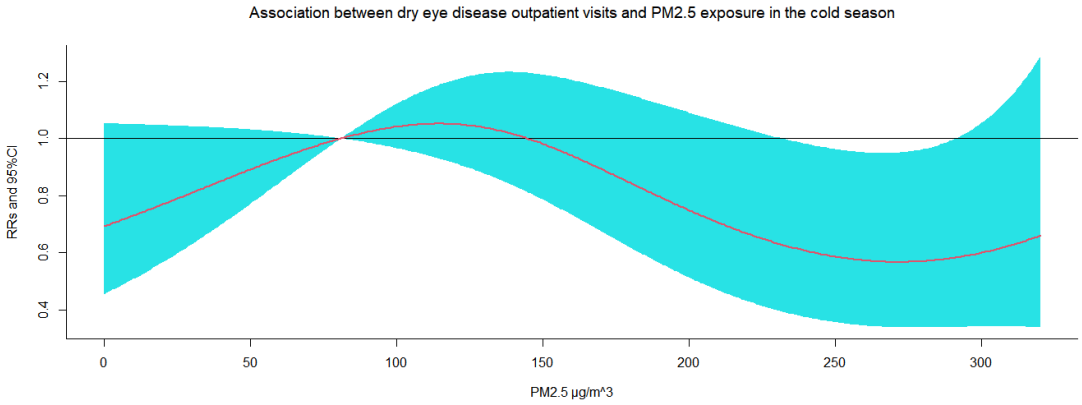

Figure S33. The relative risks (RRs) of per 10 $\mu g/m^3$ increase in $PM_{2.5}$ on dry eye disease outpatient visits at various lag days in the cold season.

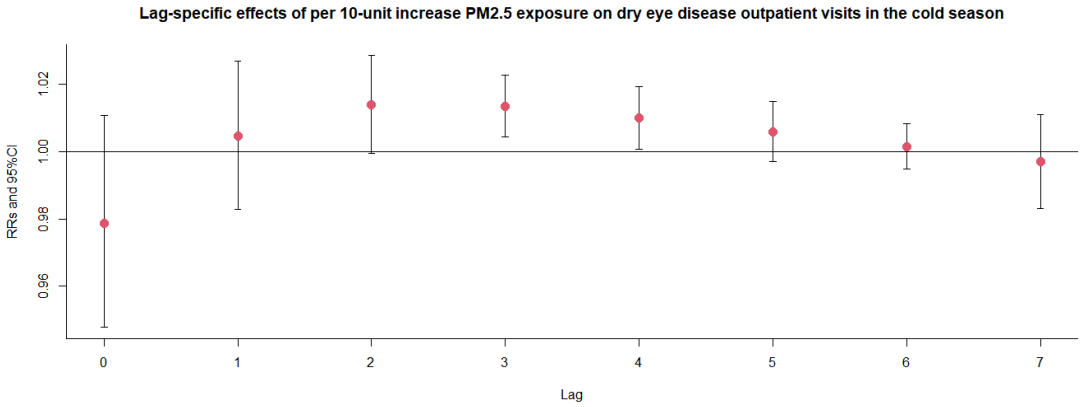

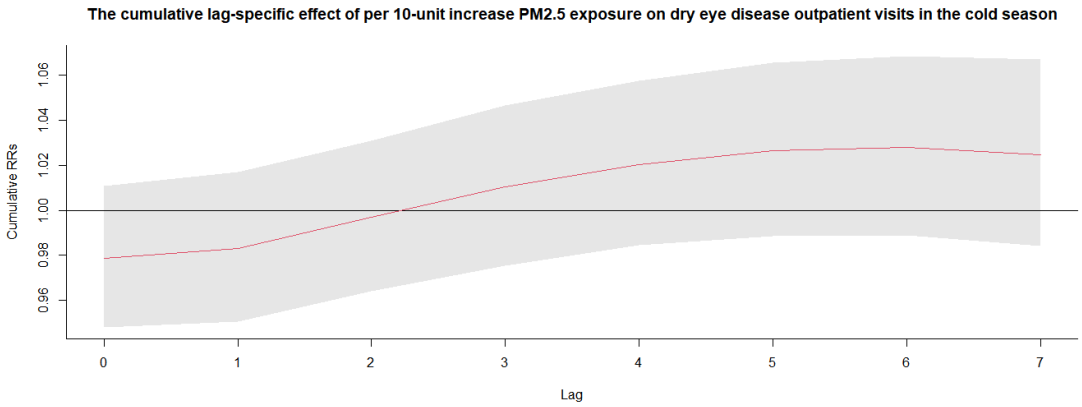

Figure S34. Exposure-response association between dry eye disease outpatient visits and PM_{10} exposure.

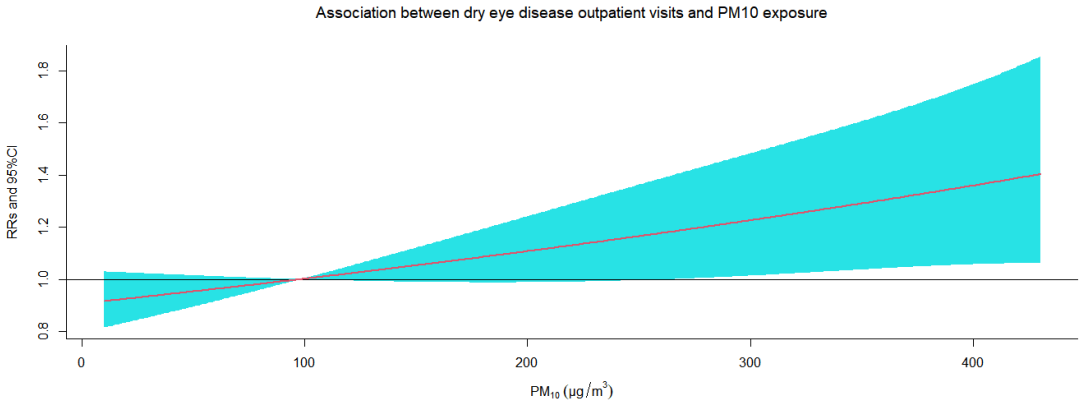

Figure S35. The relative risks (RRs) of per 10 μg/m^3 increase in PM_{10} on dry eye disease outpatient visits at various lag days.

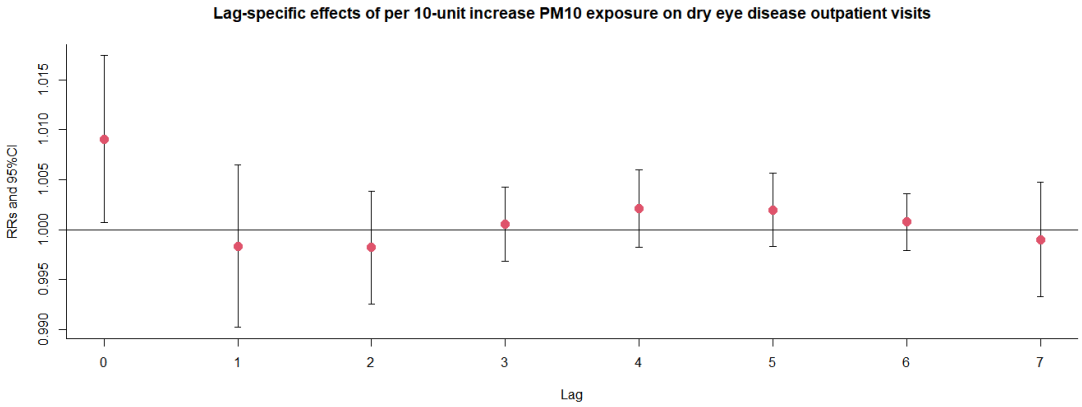

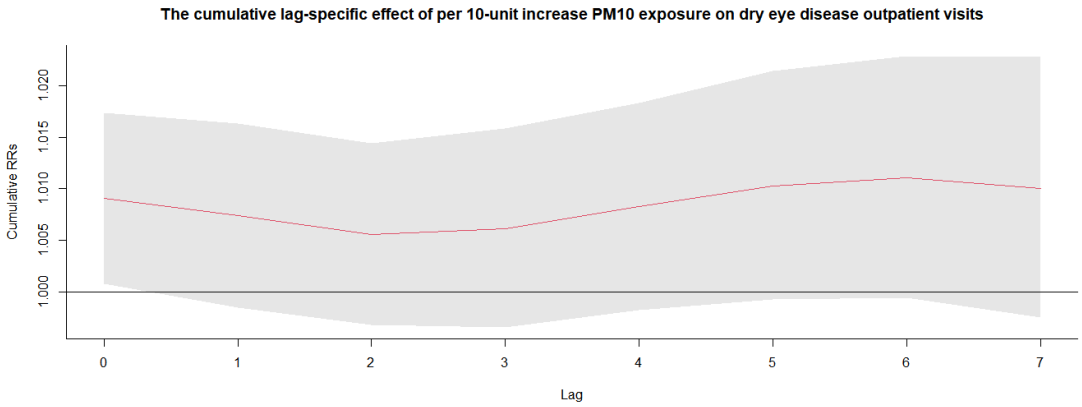

Figure S36. 3D graph and contour map of PM_{10} exposure on dry eye disease outpatient visits.

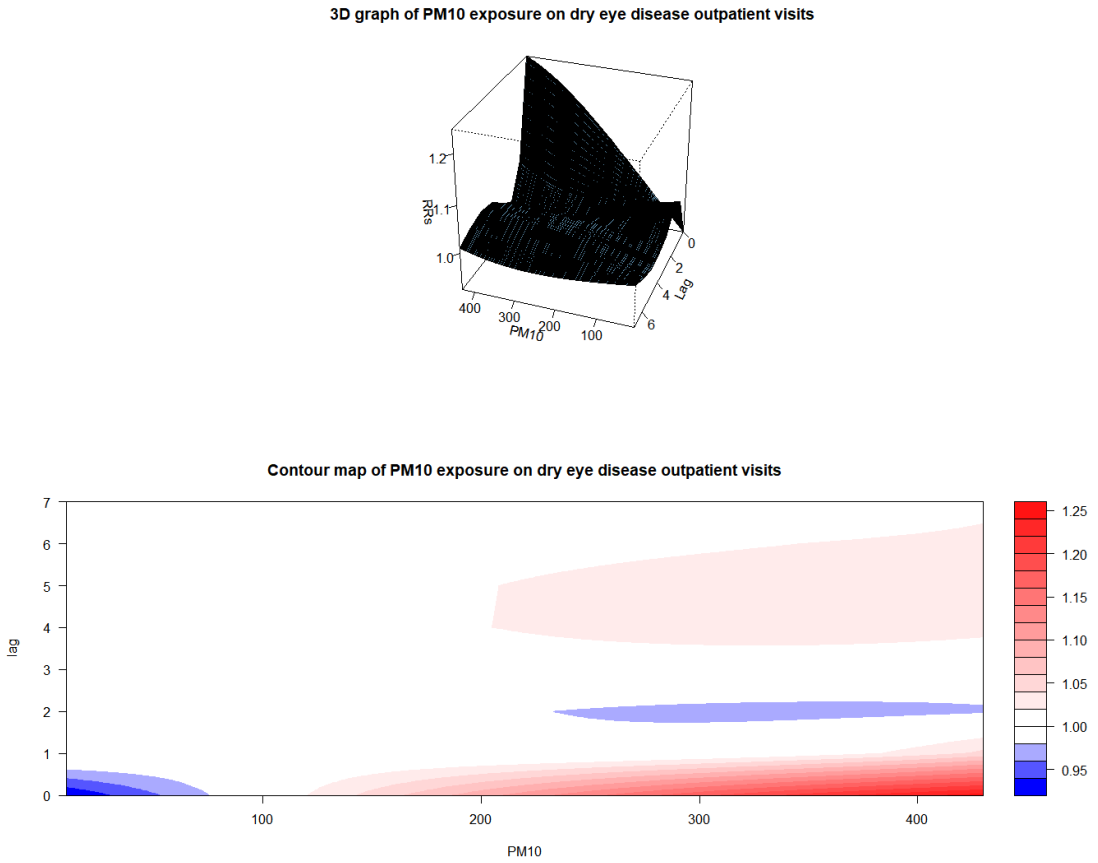

Figure S37. Exposure-response association between dry eye disease outpatient visits and PM_{10} exposure after adjusted for other air pollution.

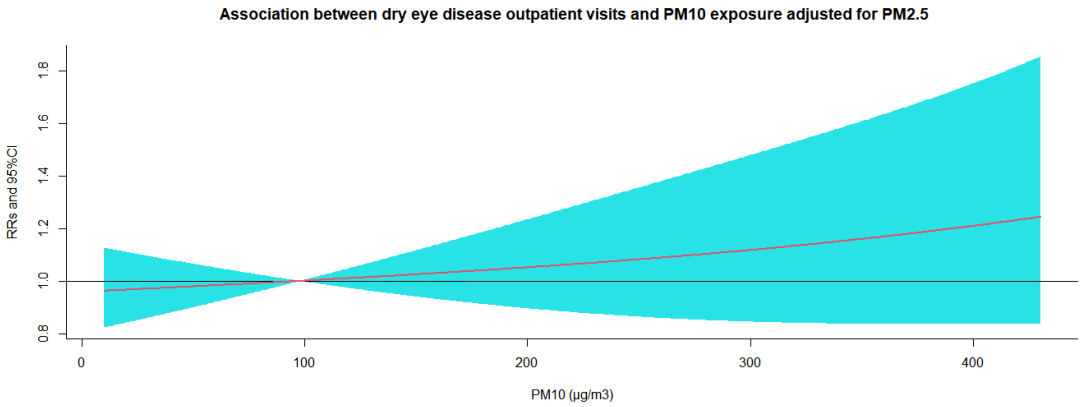
Association between dry eye disease outpatient visits and PM10 exposure adjusted for PM2.5
RRs and 95%CI
0.8
1.0
1.2
1.4
1.6
1.8
0
100
200
300
400
PM10 (μg/m3)

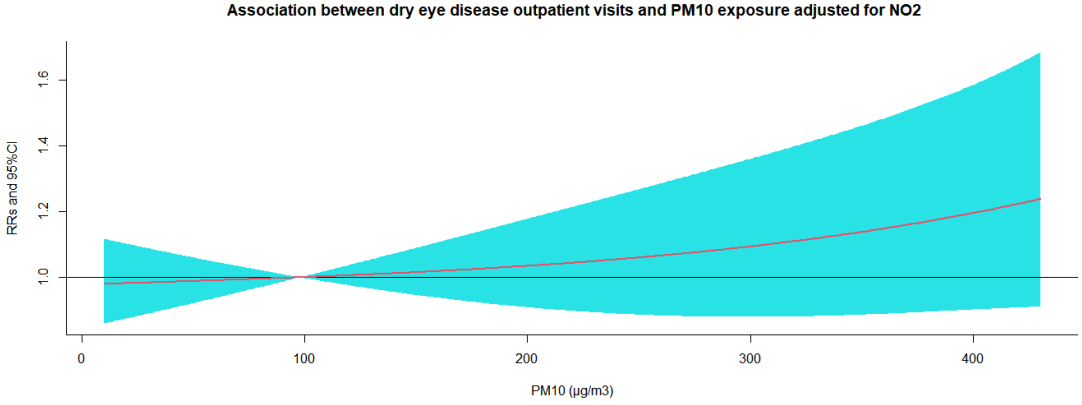
Association between dry eye disease outpatient visits and PM10 exposure adjusted for NO2
RRs and 95%CI
1.0
1.2
1.4
1.6
0
100
200
300
400
PM10 (μg/m3)

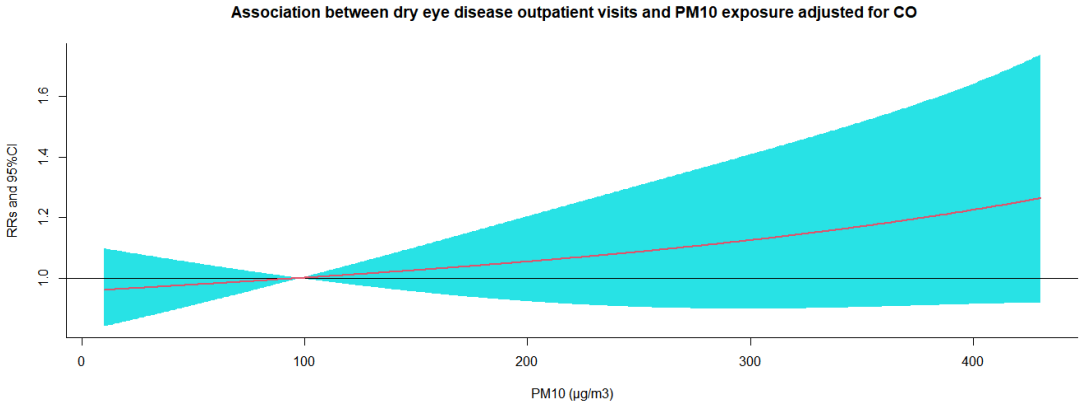
Association between dry eye disease outpatient visits and PM10 exposure adjusted for CO
RRs and 95%CI
1.0
1.2
1.4
1.6
0
100
200
300
400
PM10 (μg/m3)

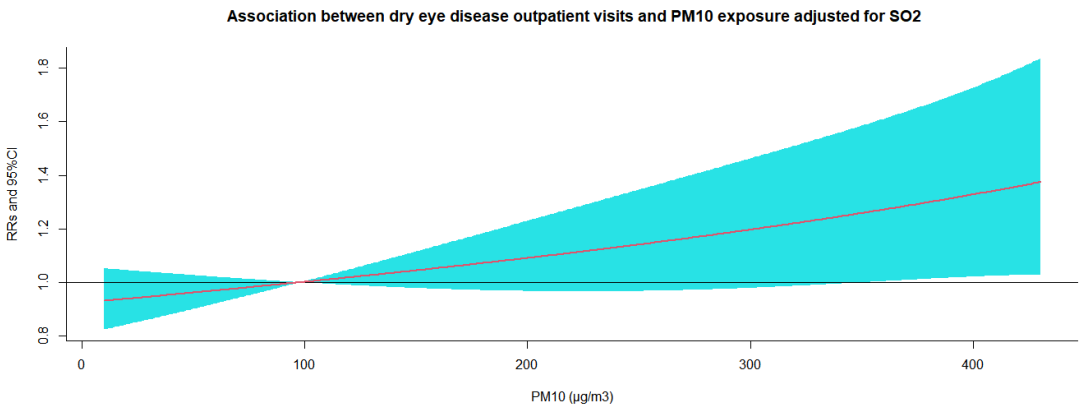
Association between dry eye disease outpatient visits and PM10 exposure adjusted for SO2
RRs and 95%CI
0.8
1.0
1.2
1.4
1.6
1.8
0
100
200
300
400
PM10 (μg/m3)

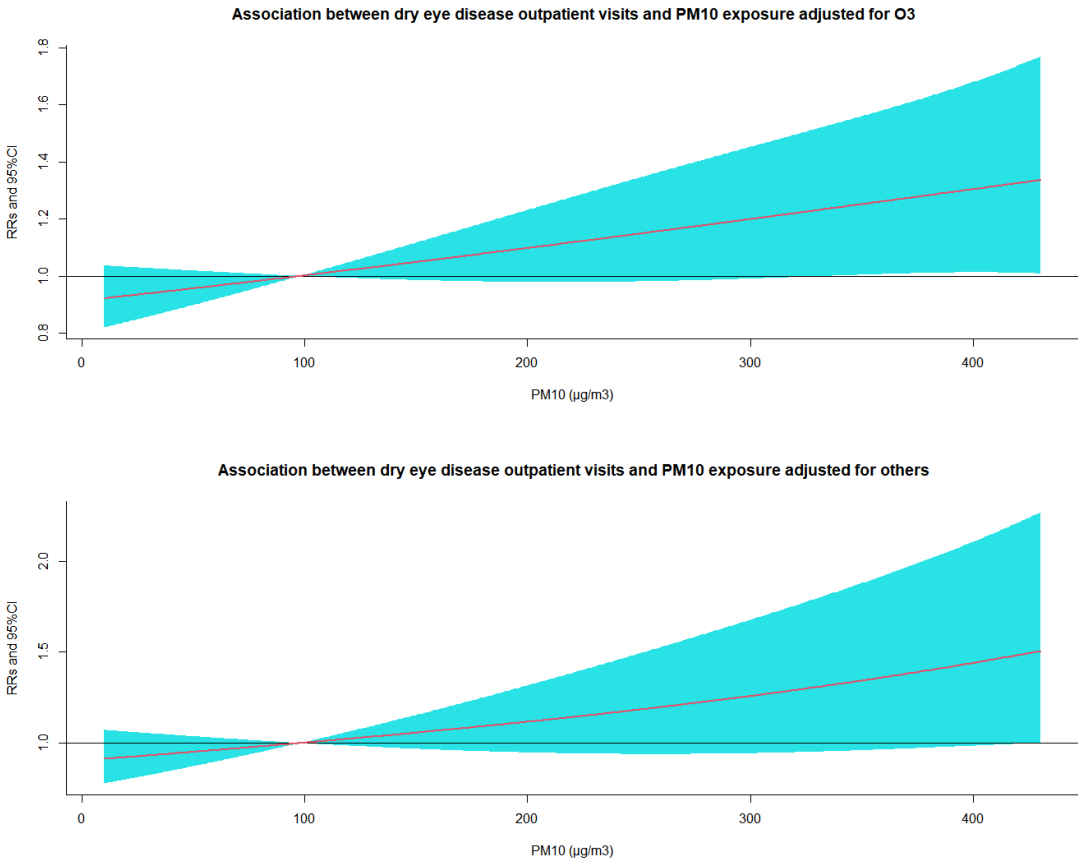

Figure S38. The relative risks (RRs) of per 10 μg/m^3 increase in PM_{10} on dry eye disease outpatient visits at various lag days after adjusted for NO_2 exposure.

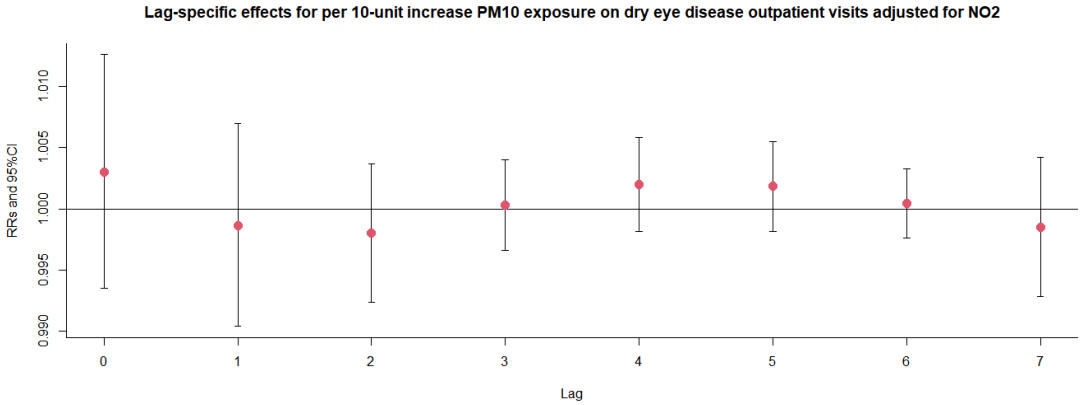

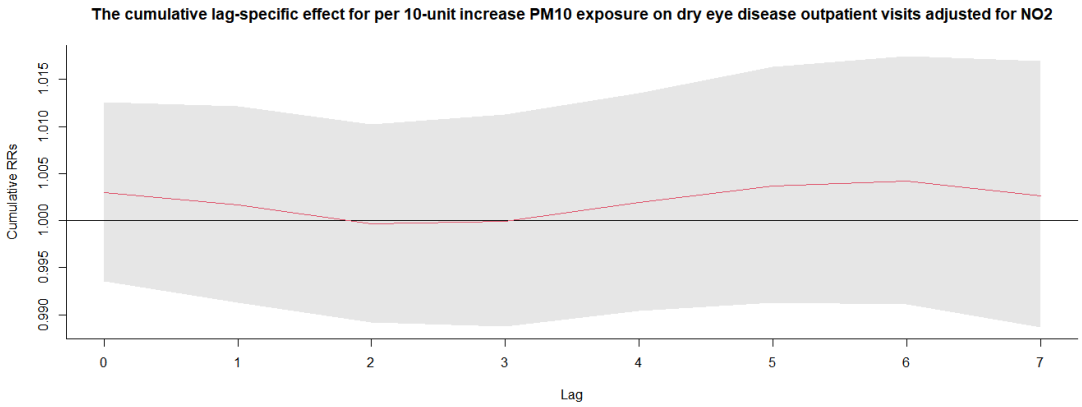

Figure S39. 3D graph and contour map of PM_{10} exposure on dry eye disease outpatient visits after adjusted for NO_2 exposure.

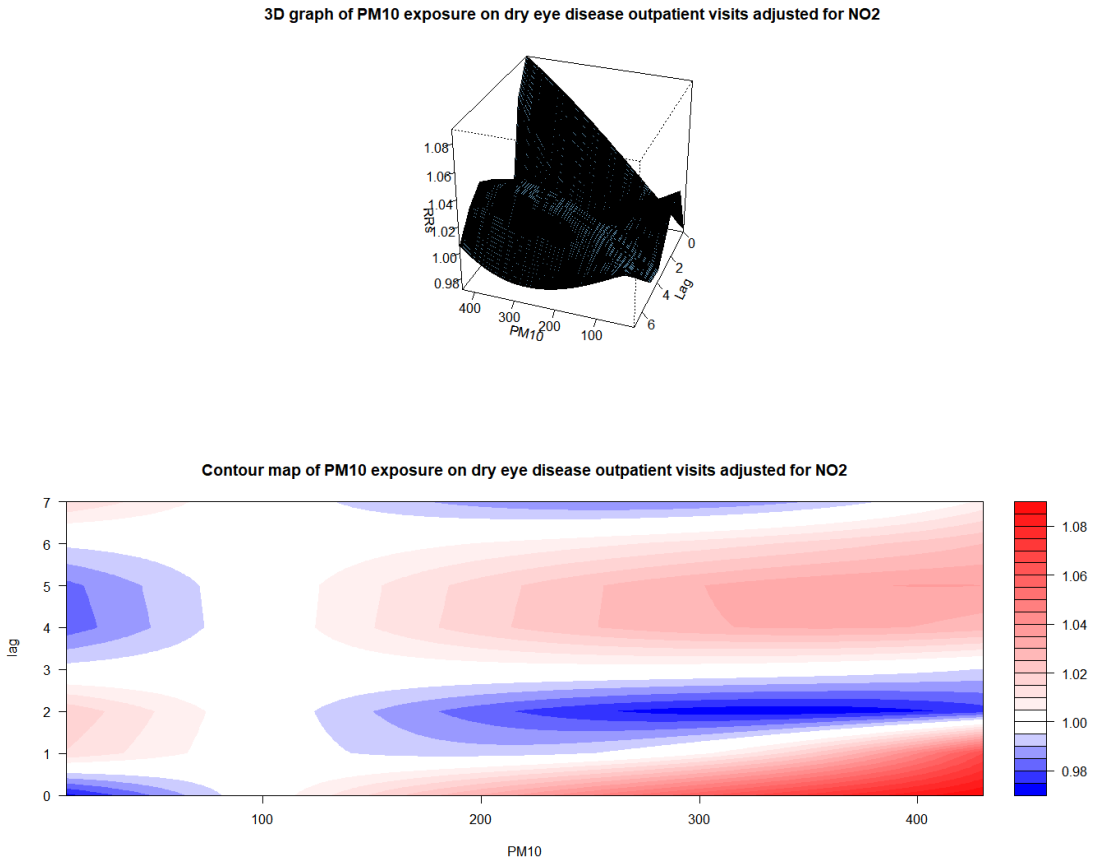

Figure S40. The relative risks (RRs) of per 10 $\mu g/m^3$ increase in PM_{10} on dry eye disease outpatient visits at various lag days after adjusted for $PM_{2.5}$ exposure.

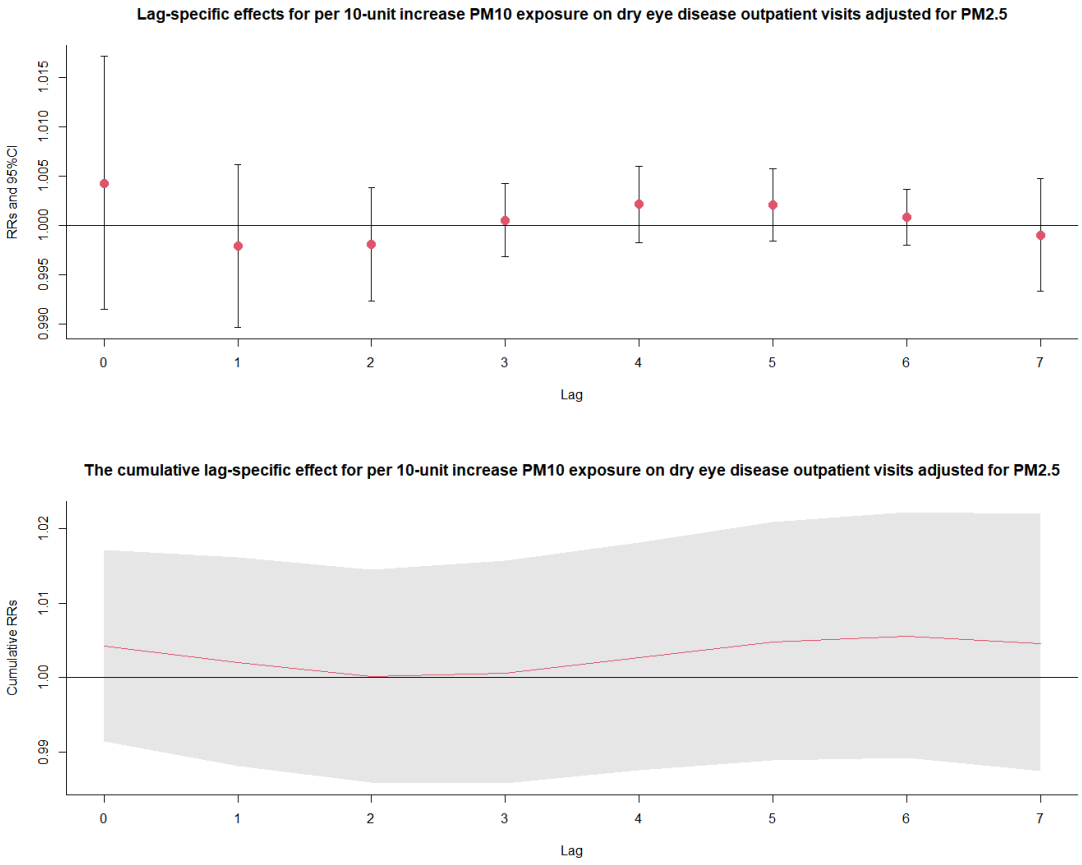

Figure S41. 3D graph and contour map of PM_{10} exposure on dry eye disease outpatient visits after adjusted for $PM_{2.5}$ exposure.

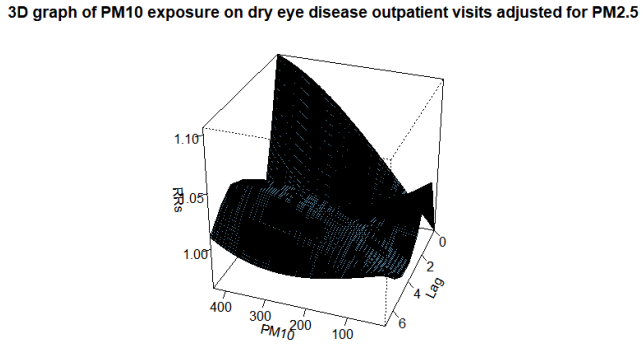

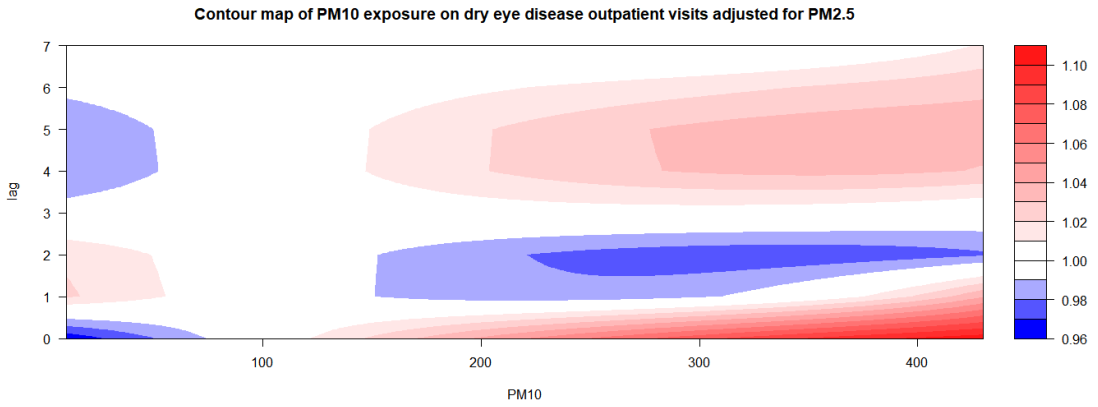

Figure S42. The relative risks (RRs) of per 10 μg/m^3 increase in PM_{10} on dry eye disease outpatient visits at various lag days after adjusted for SO_2 exposure.

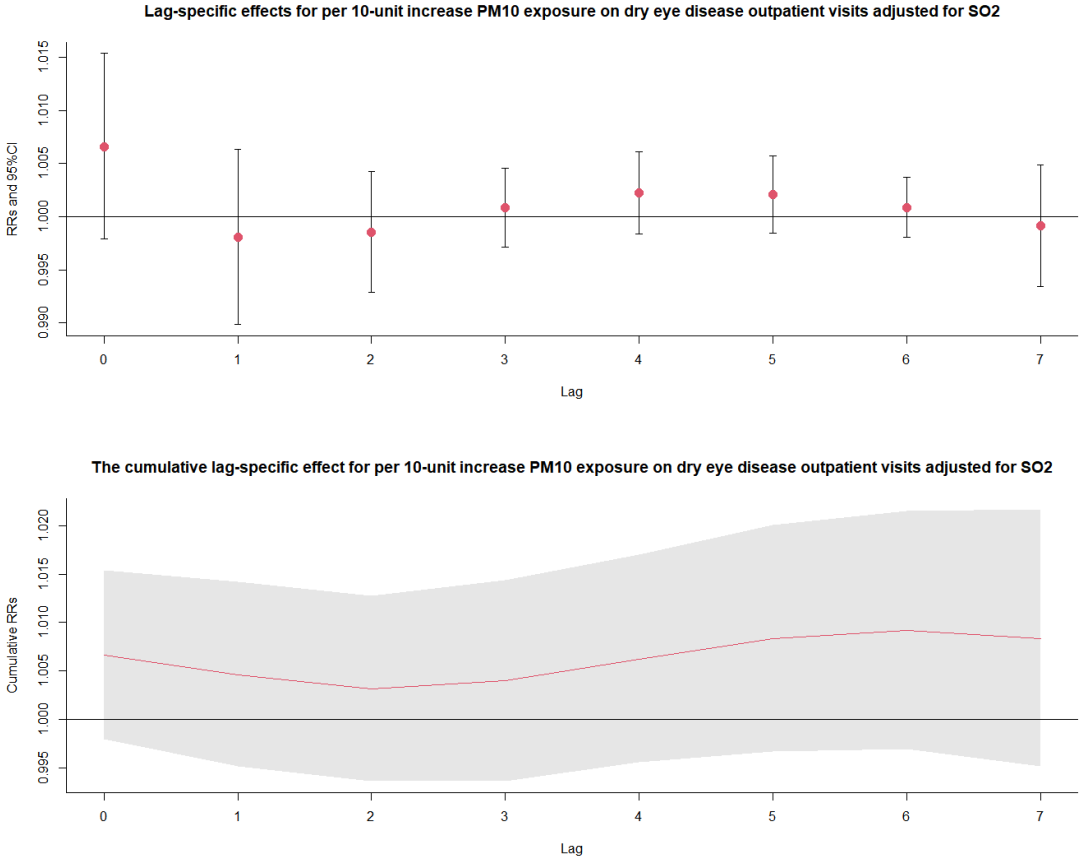

Figure S43. 3D graph and contour map of PM_{10} exposure on dry eye disease outpatient visits after adjusted for SO_2 exposure.

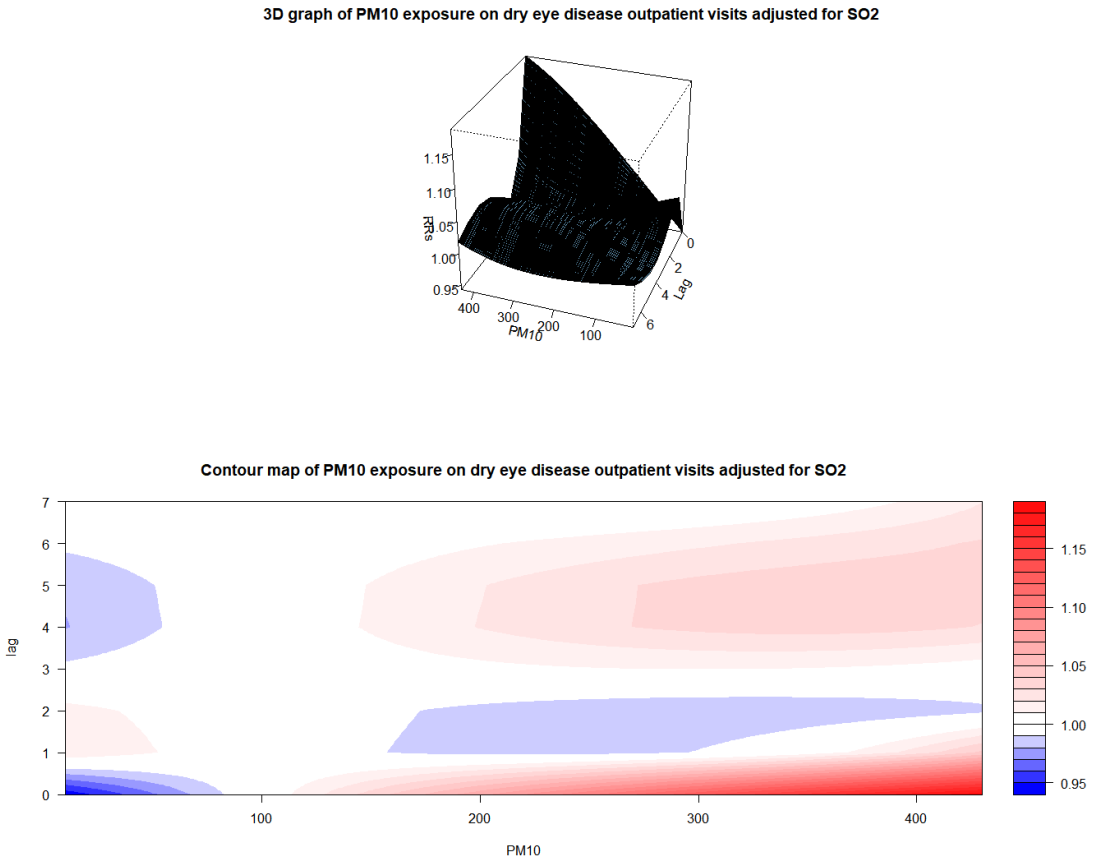

Figure S44. The relative risks (RRs) of per 10 μg/m^3 increase in PM_{10} on dry eye disease outpatient visits at various lag days after adjusted for CO exposure.

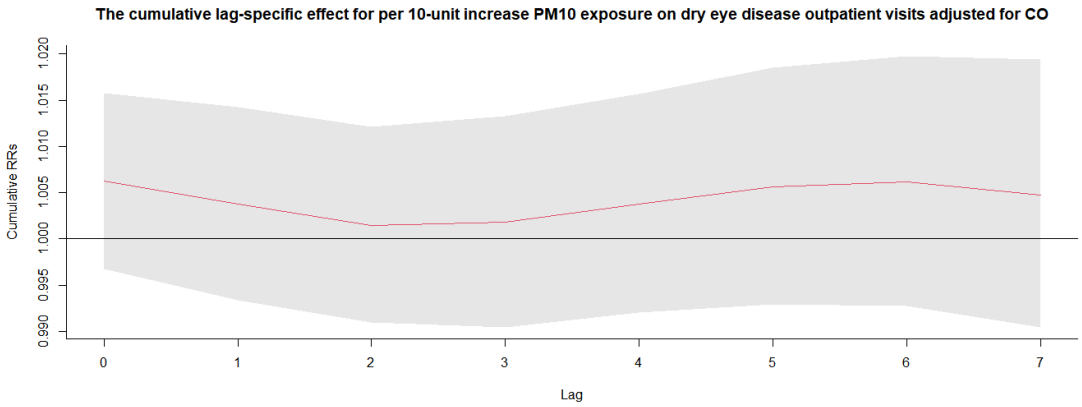

Figure S45. 3D graph and contour map of PM_{10} exposure on dry eye disease outpatient visits after adjusted for CO exposure.

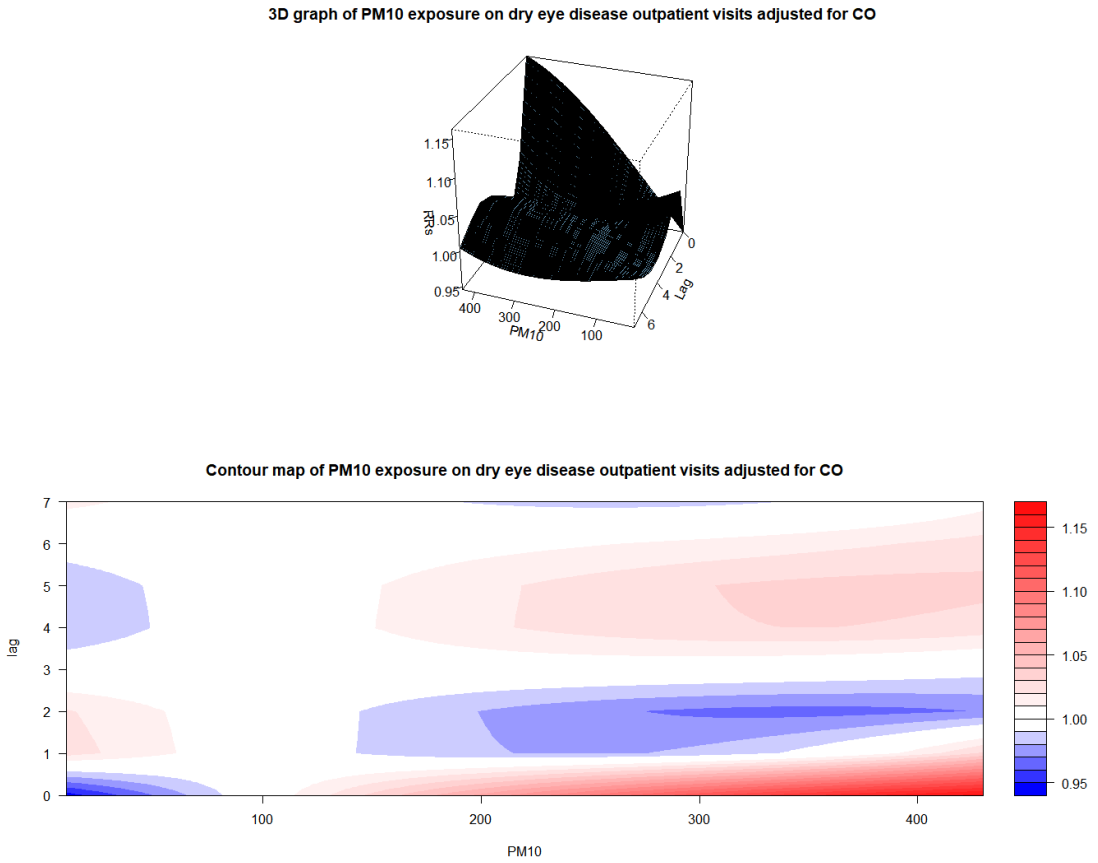

Figure S46. The relative risks (RRs) of per 10 $\mu g/m^3$ increase in PM_{10} on dry eye disease outpatient visits at various lag days after adjusted for O_3 exposure.

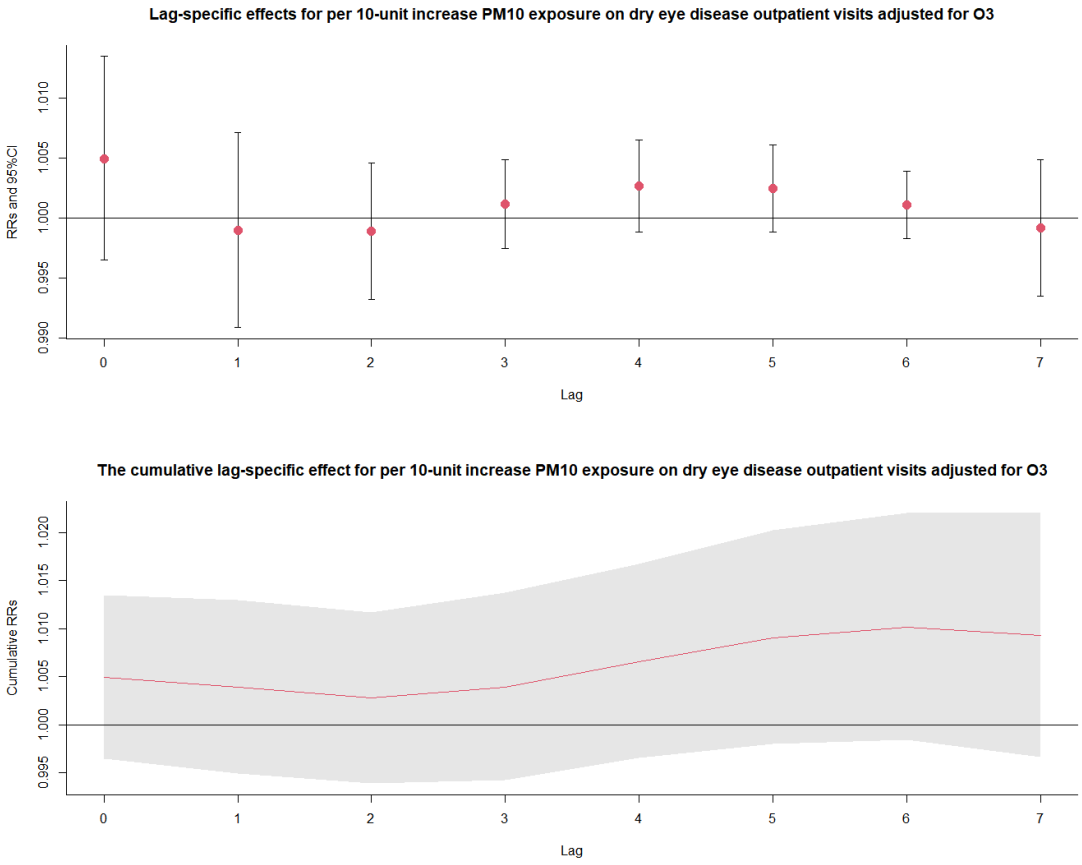

Figure S47. 3D graph and contour map of PM_{10} exposure on dry eye disease outpatient visits after adjusted for O_3 exposure.

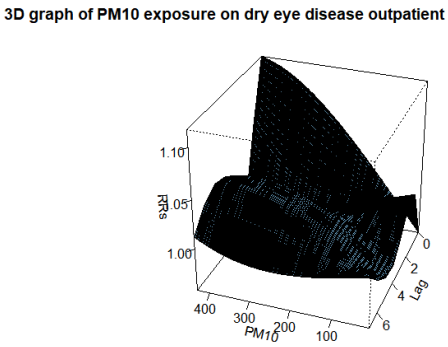

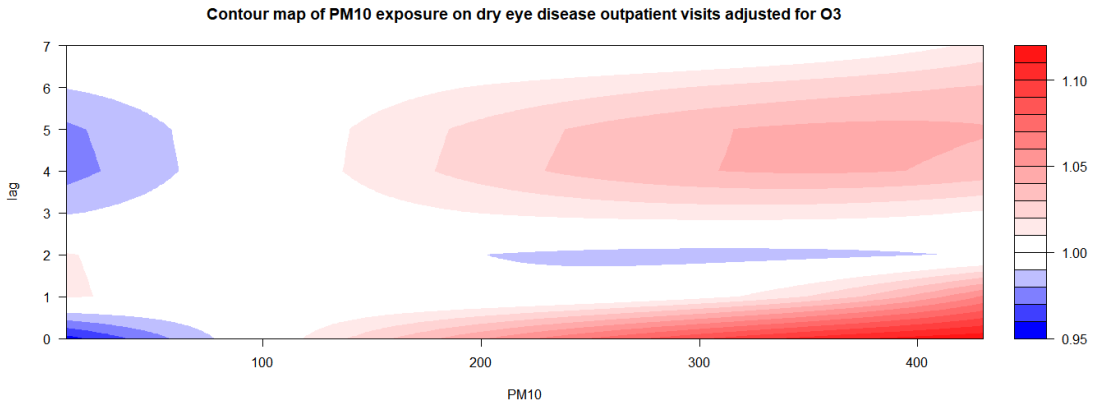

Figure S48. The relative risks (RRs) of per 10 μg/m^3 increase in PM_{10} on dry eye disease outpatient visits at various lag days after adjusted for others exposure.

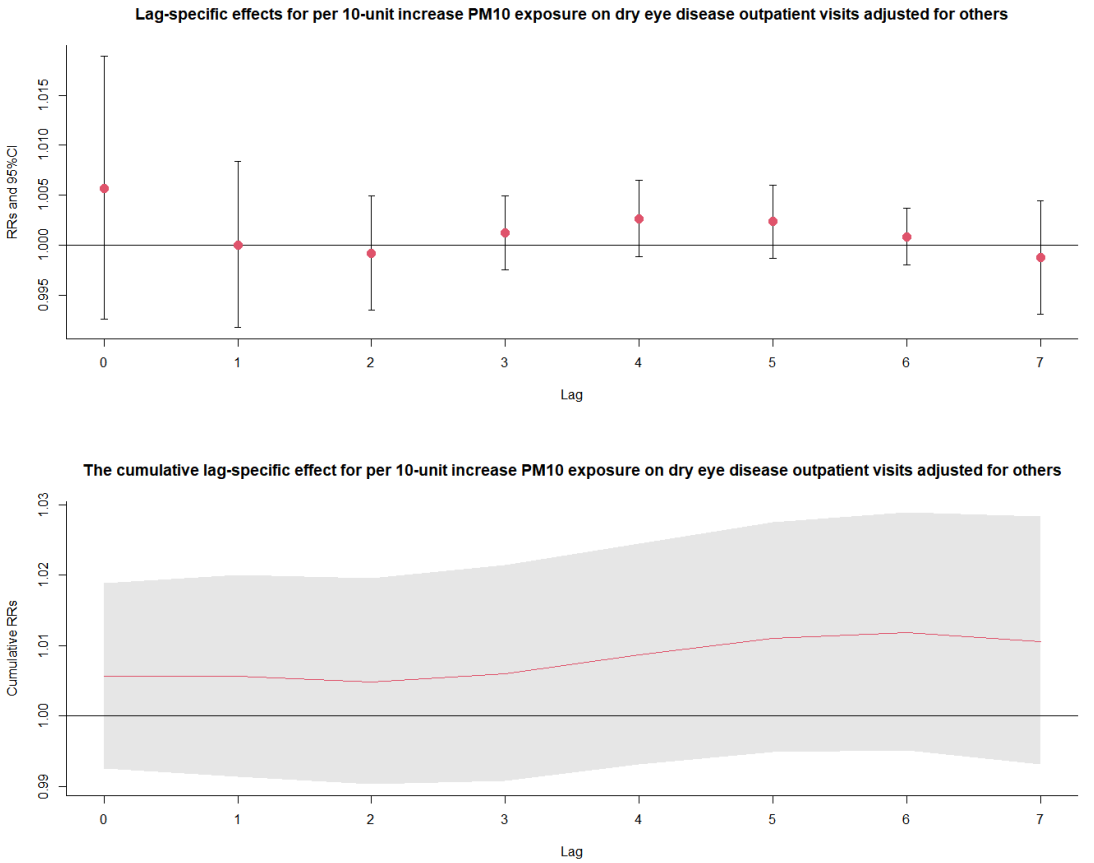

Figure S49. 3D graph and contour map of PM_{10} exposure on dry eye disease outpatient visits after adjusted for others exposure.

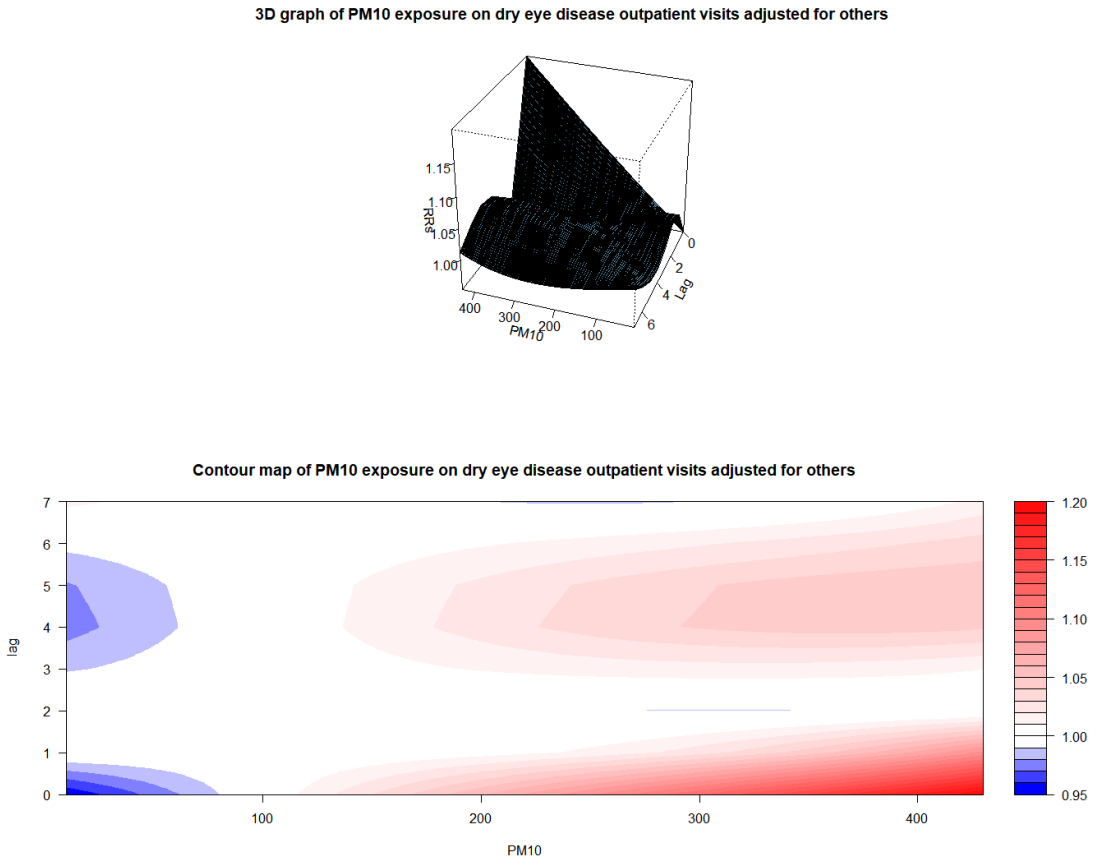

Figure S50. Exposure-response association between dry eye disease outpatient visits and PM_{10} exposure in male patients.

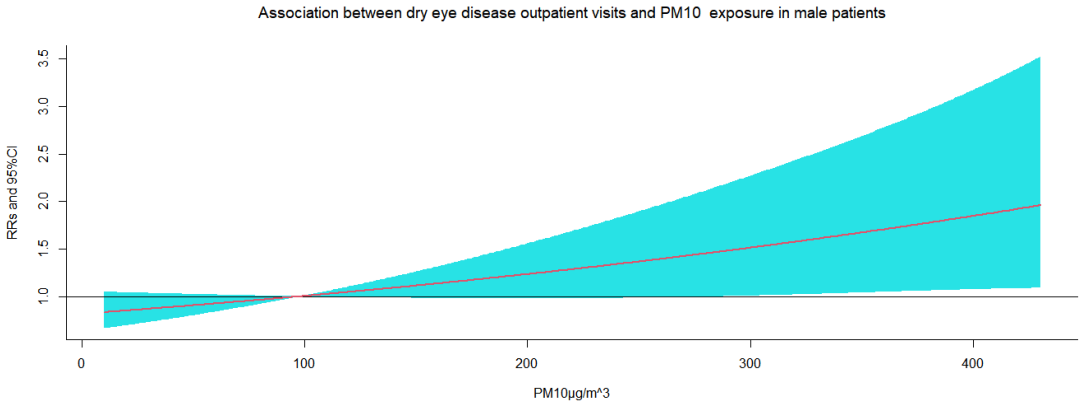

Figure S51. The relative risks (RRs) of per 10 $\mu g/m^3$ increase in PM_{10} on dry eye disease outpatient visits at various lag days in male patients.

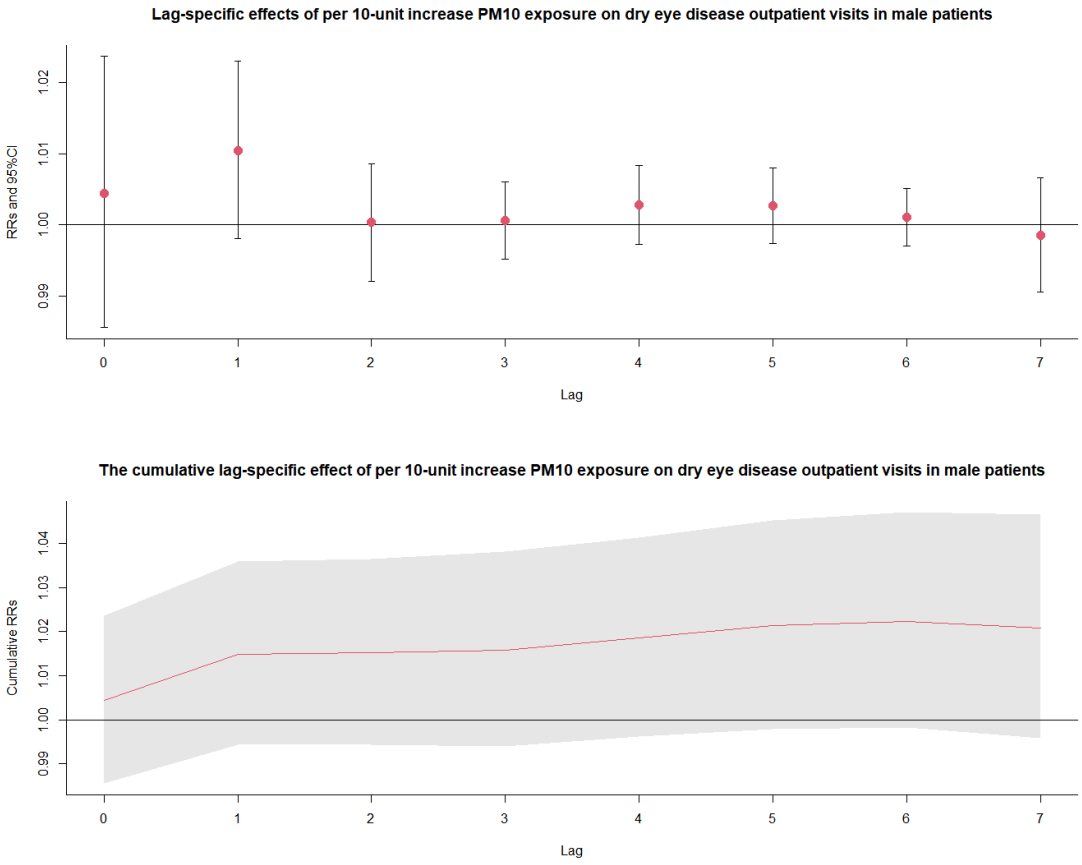

Figure S52. Exposure-response association between dry eye disease outpatient visits and PM_{10} exposure in female patients.

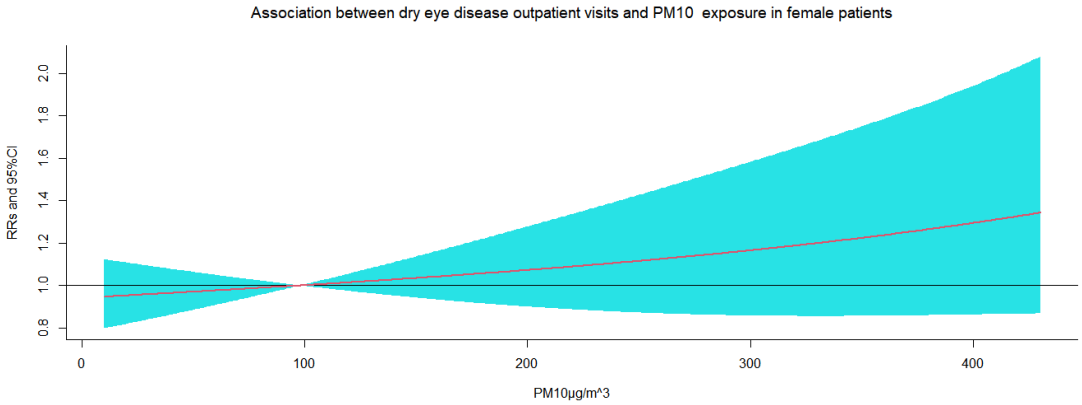

Figure S53. The relative risks (RRs) of per 10 $\mu g/m^3$ increase in PM_{10} on dry eye disease outpatient visits at various lag days in female patients.

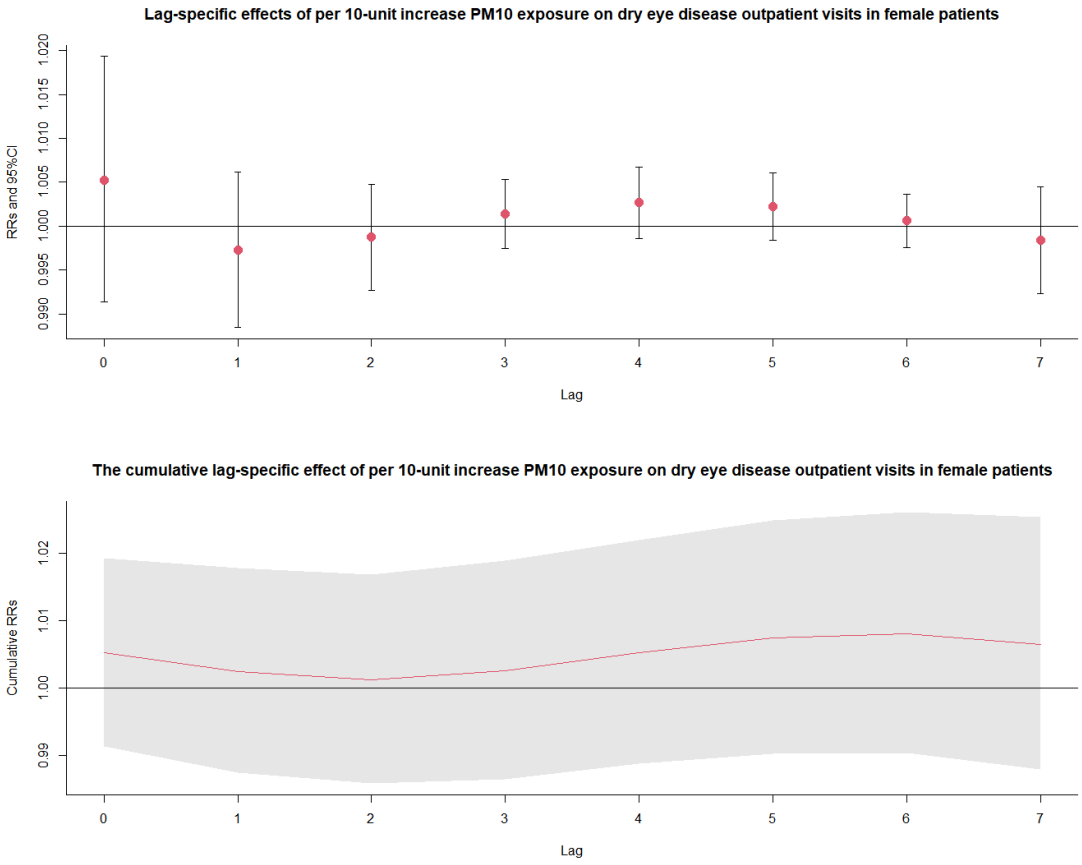

Figure S54. Exposure-response association between dry eye disease outpatient visits and PM_{10} exposure in age 0-5 patients.

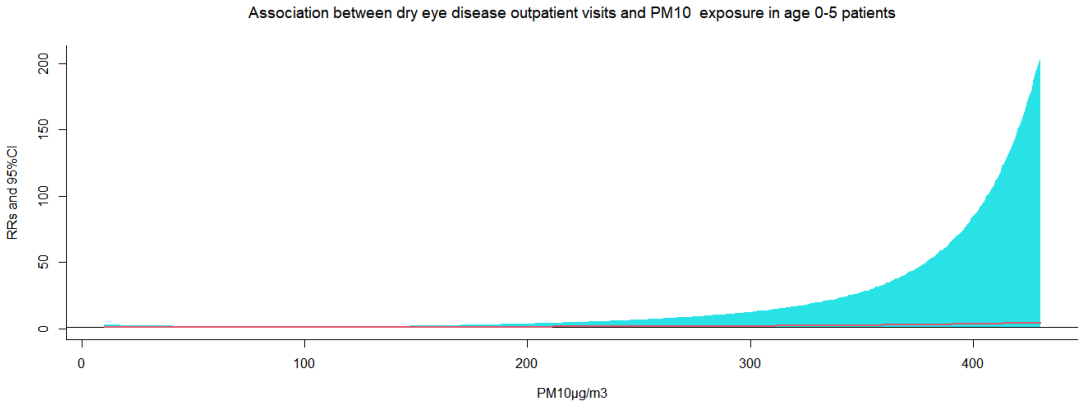

Figure S55. The relative risks (RRs) of per 10 $\mu g/m^3$ increase in PM_{10} on dry eye disease outpatient visits at various lag days in age 0-5 patients.

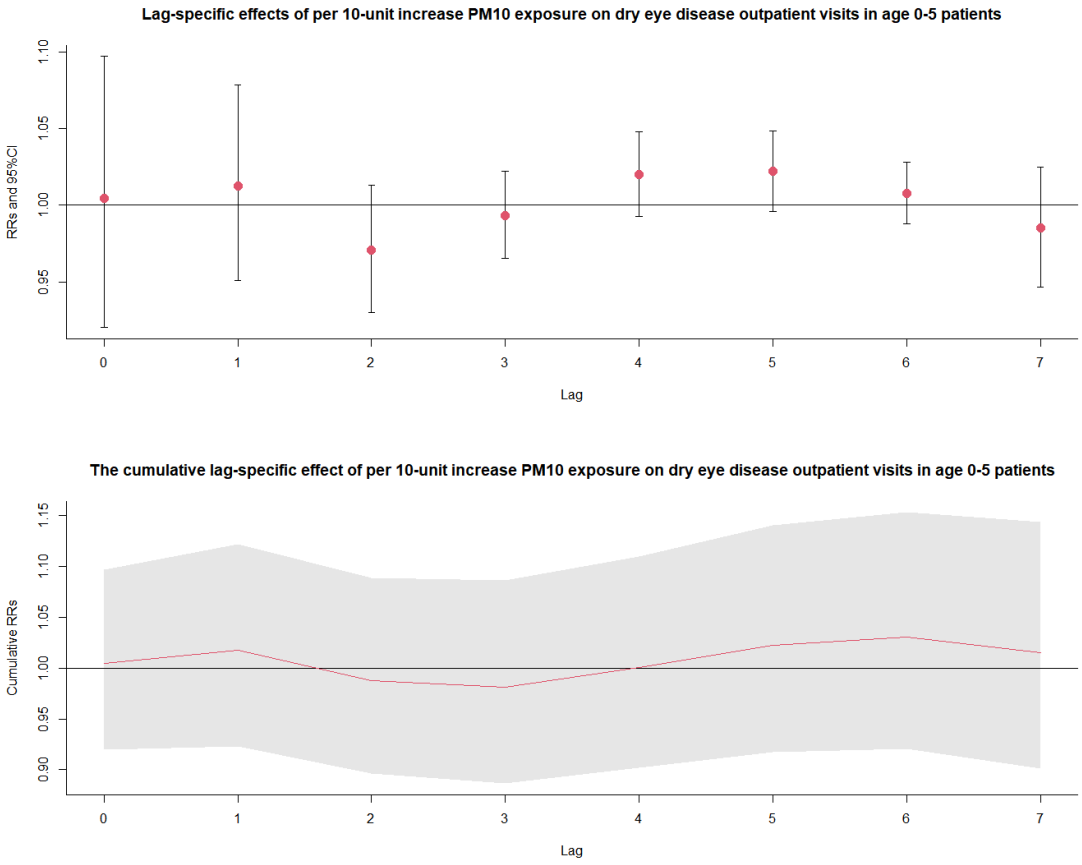

Figure S56. Exposure-response association between dry eye disease outpatient visits and PM_{10} exposure in age 19-64 patients.

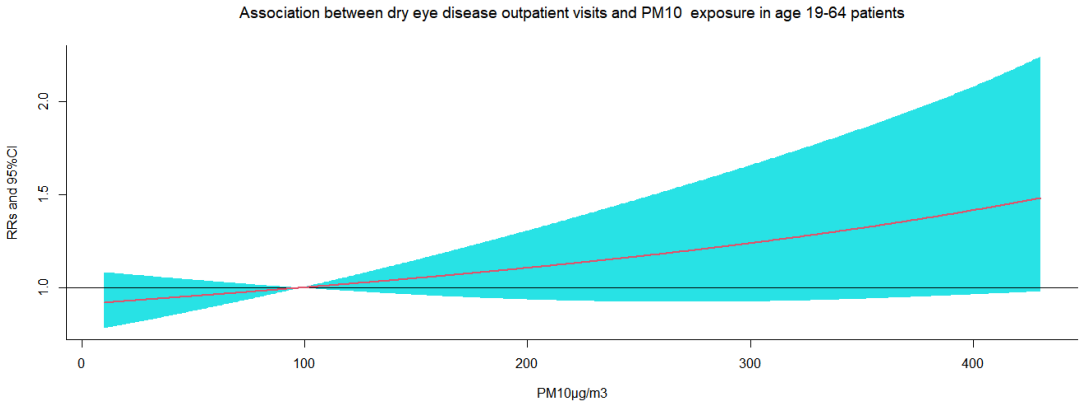

Figure S57. The relative risks (RRs) of per 10 $\mu g/m^3$ increase in PM_{10} on dry eye disease outpatient visits at various lag days in age 19-64 patients.

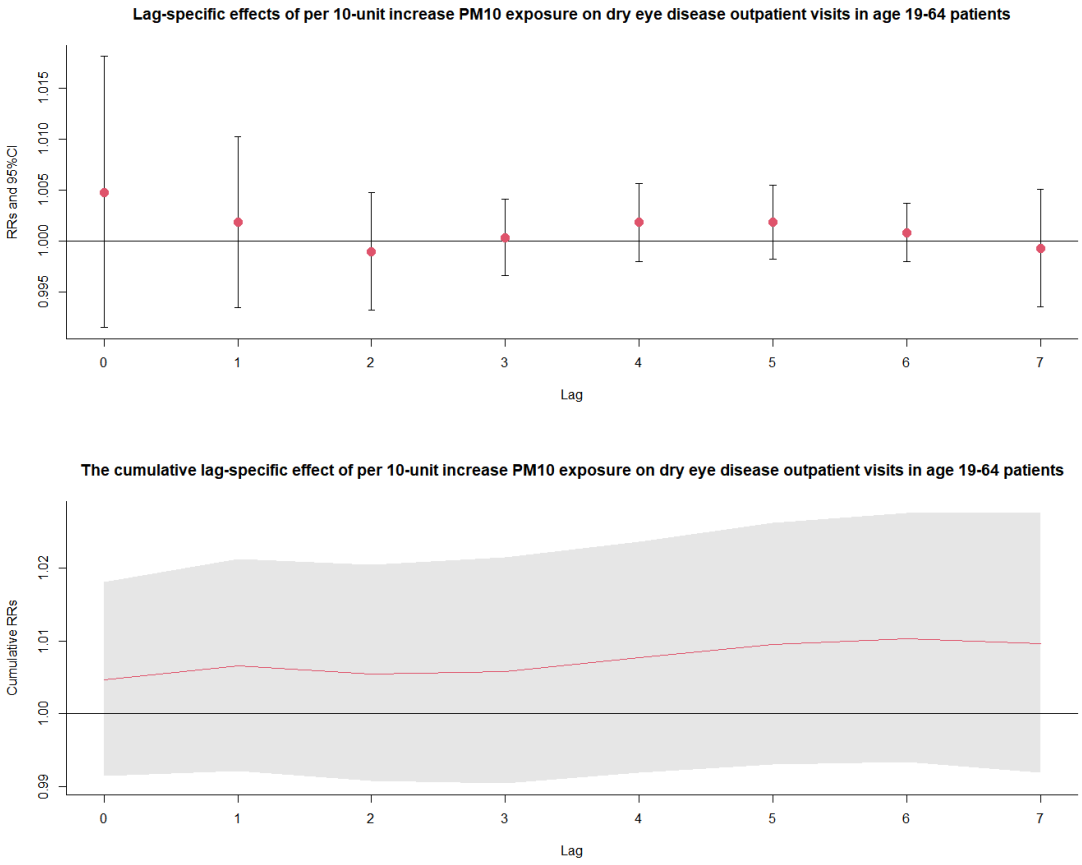

Figure S58. Exposure-response association between dry eye disease outpatient visits and PM_{10} exposure in age ≥65 patients.

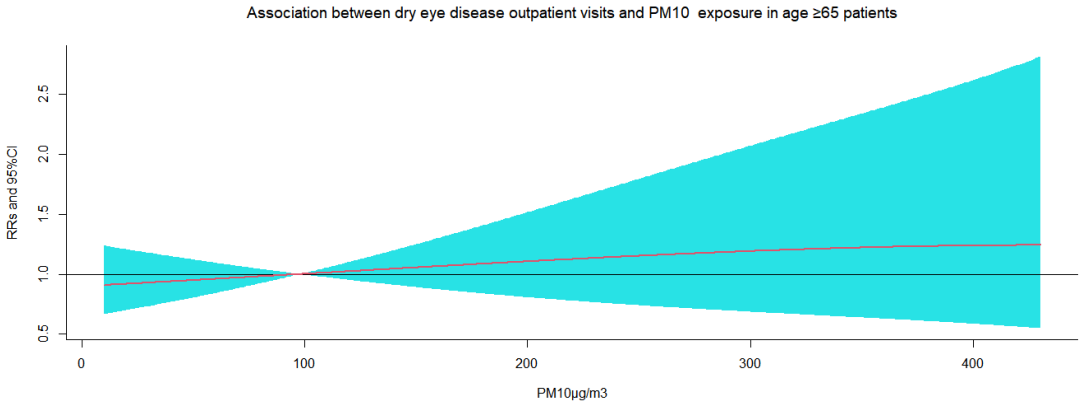

Figure S59. The relative risks (RRs) of per 10 μg/m^3 increase in PM_{10} on dry eye disease outpatient visits at various lag days in age ≥65 patients.

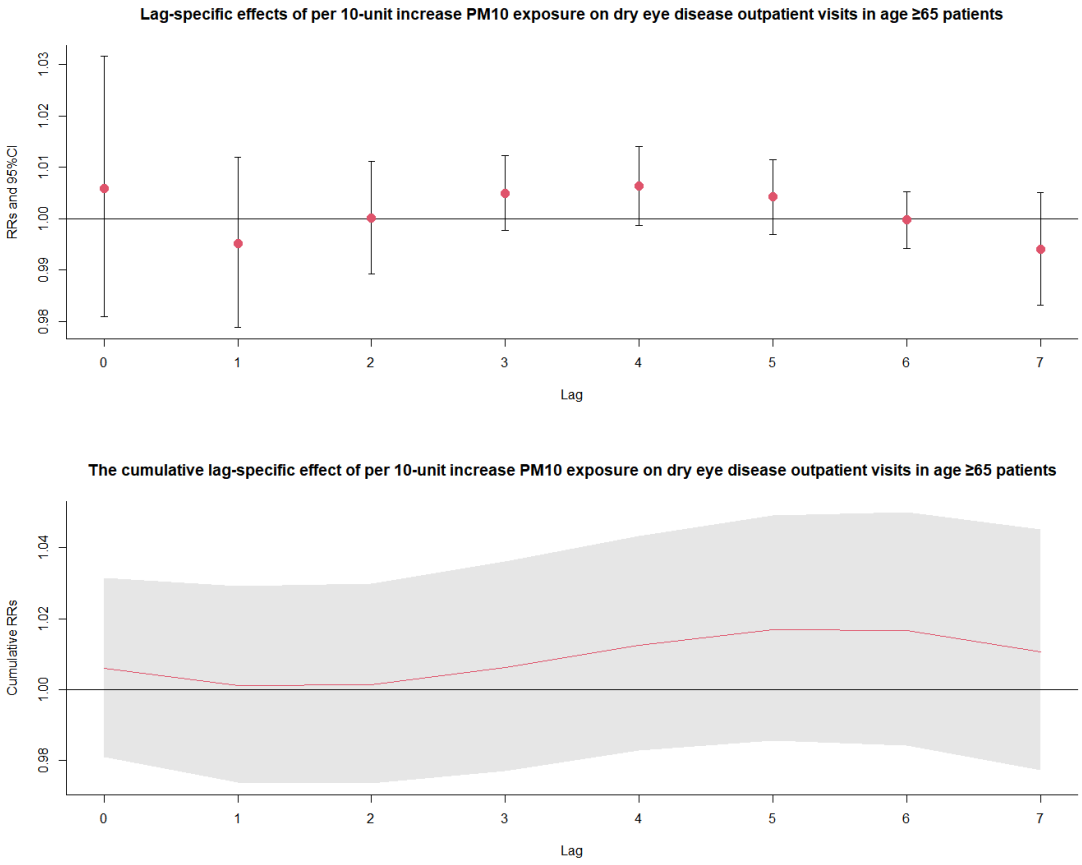

Figure S60. Exposure-response association between dry eye disease outpatient visits and PM_{10} exposure in the warm season.

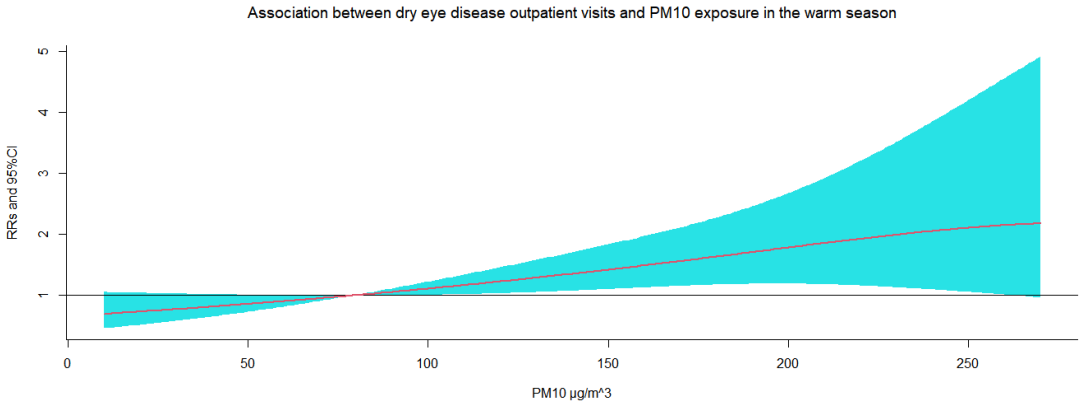

Figure S61. The relative risks (RRs) of per 10 $\mu g/m^3$ increase in PM_{10} on dry eye disease outpatient visits at various lag days in the warm season.

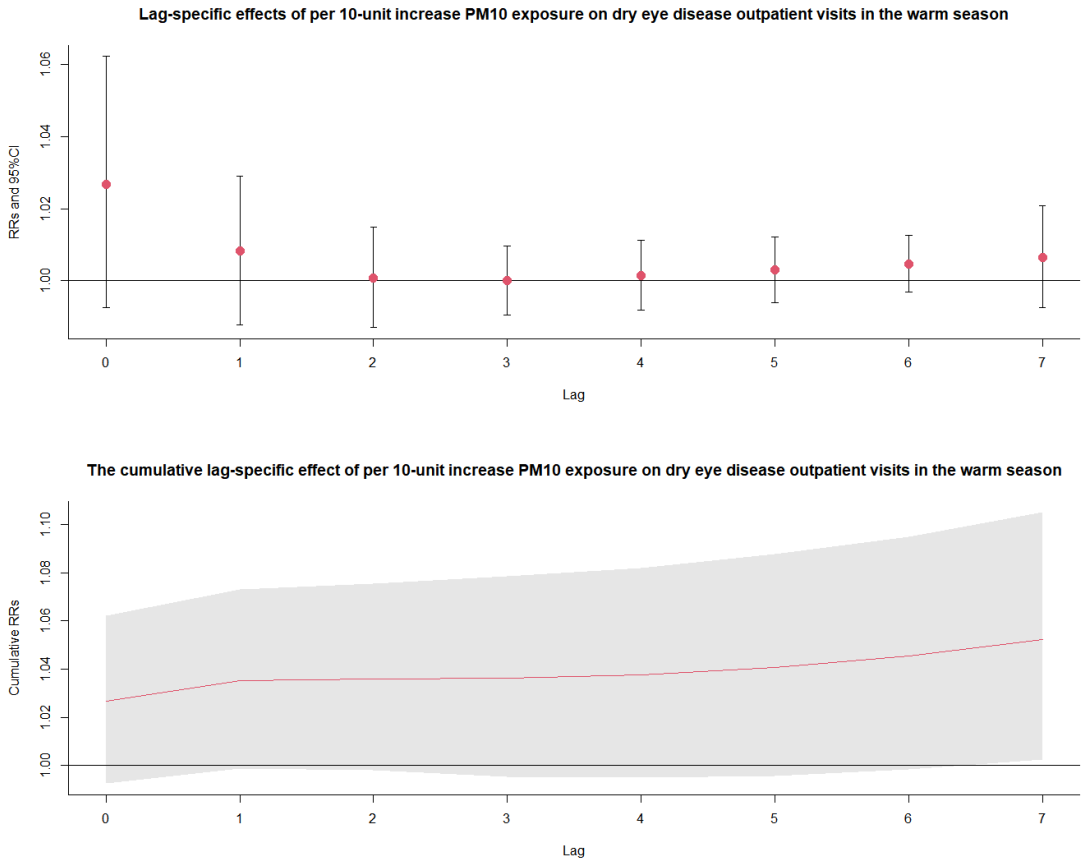

Figure S62. Exposure-response association between dry eye disease outpatient visits and PM_{10} exposure in the cold season.

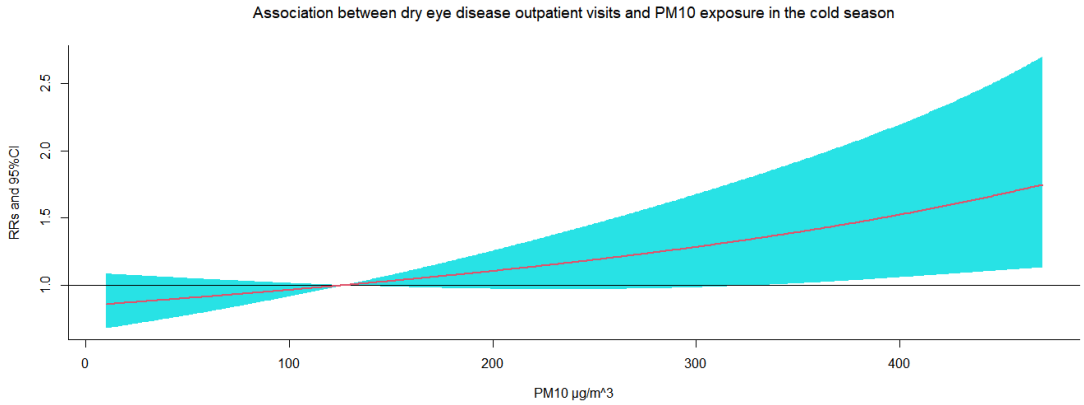

Figure S63. The relative risks (RRs) of per 10 $\mu g/m^3$ increase in PM_{10} on dry eye disease outpatient visits at various lag days in the cold season.

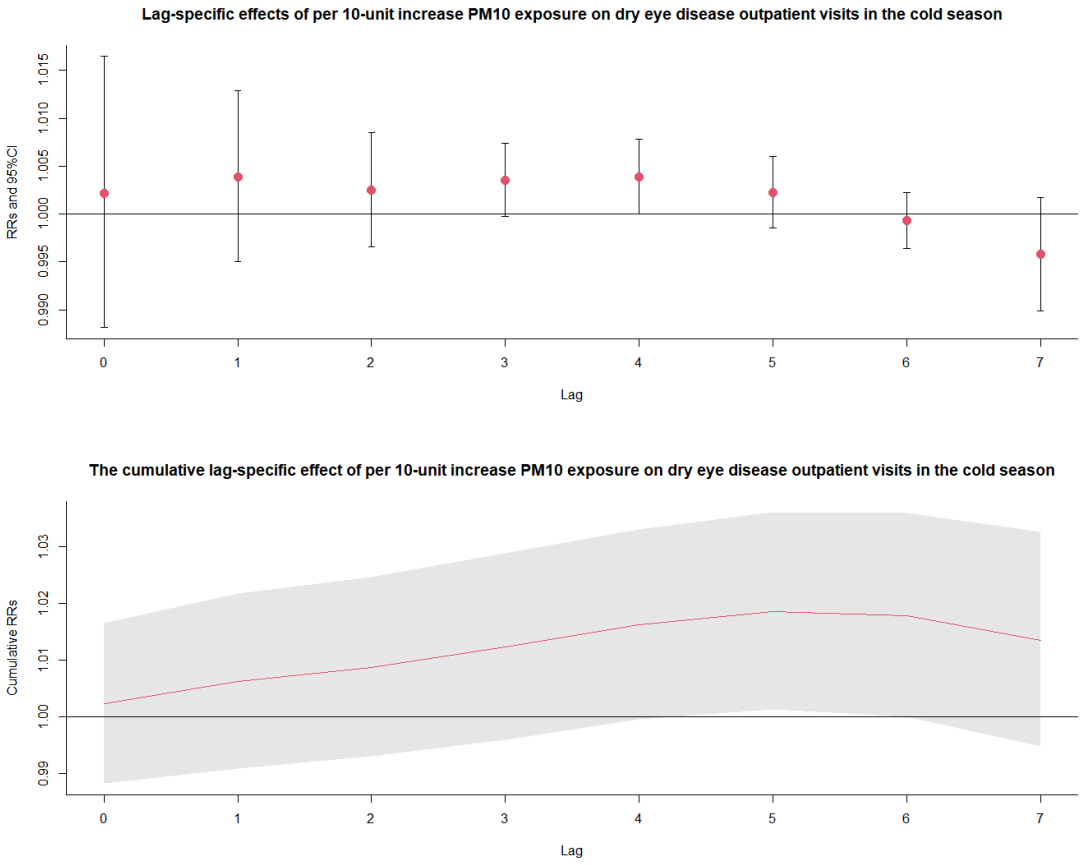

Figure S64. Exposure-response association between dry eye disease outpatient visits and CO exposure.

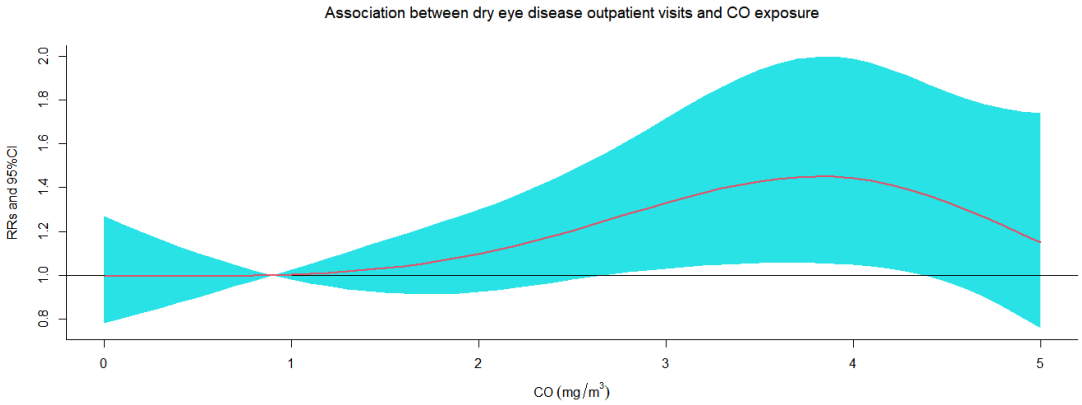

Figure S65. The relative risks (RRs) of per 10 mg/m^3 increase in CO on dry eye disease outpatient visits at various lag days.

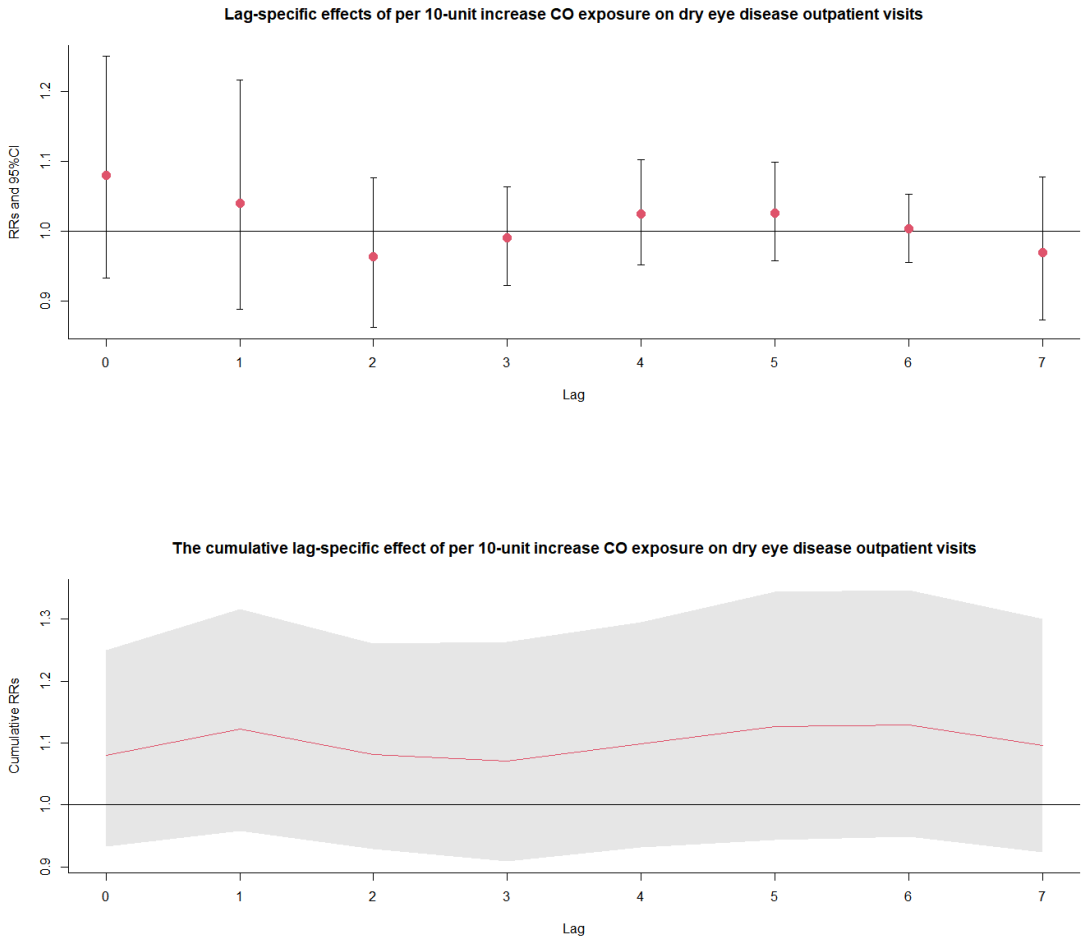

Figure S66. 3D graph and contour map of CO exposure on dry eye disease outpatient visits.

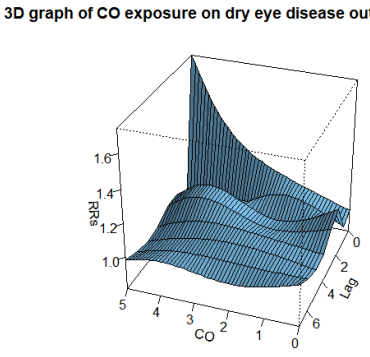

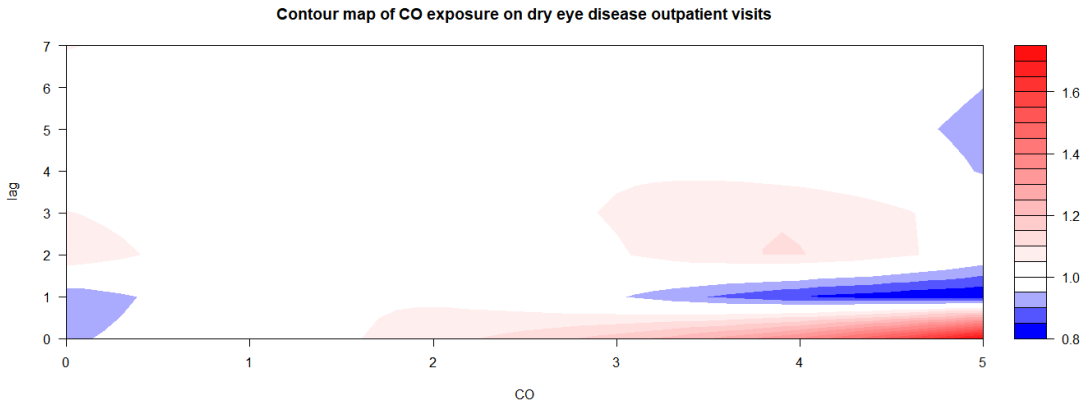

Figure S67. Exposure-response association between dry eye disease outpatient visits and CO exposure after adjusted for other air pollution.

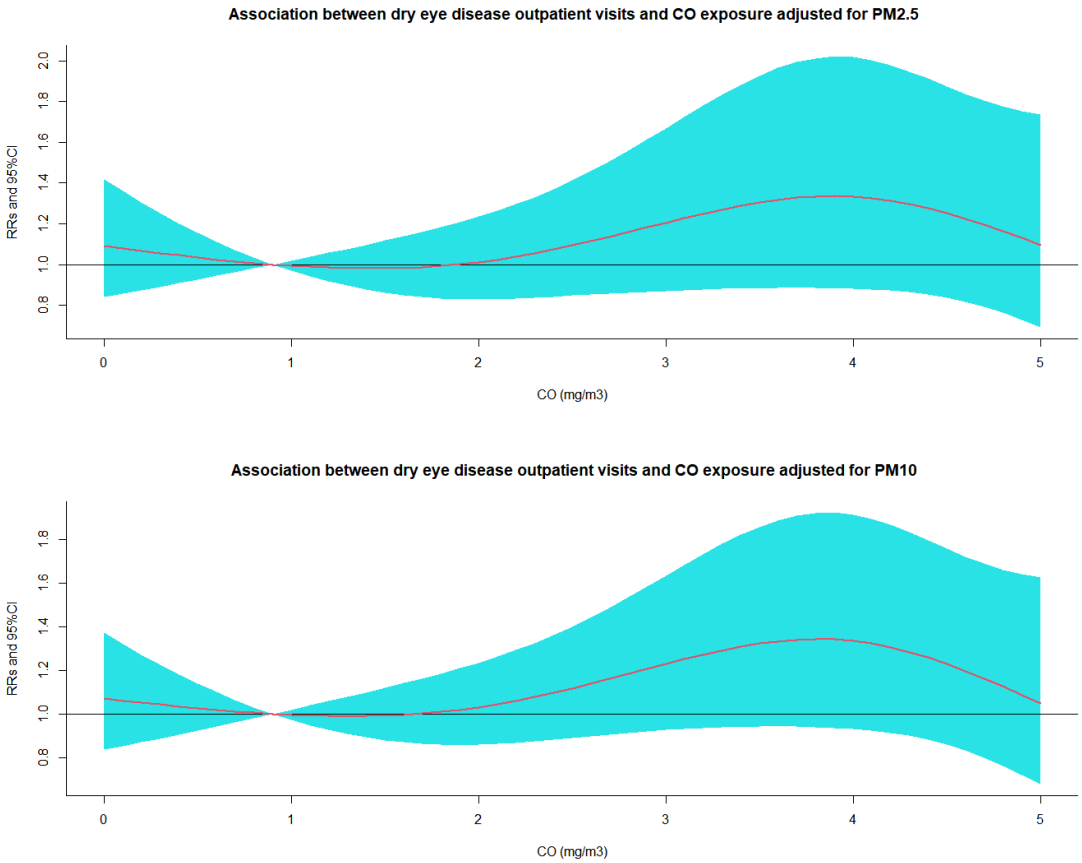

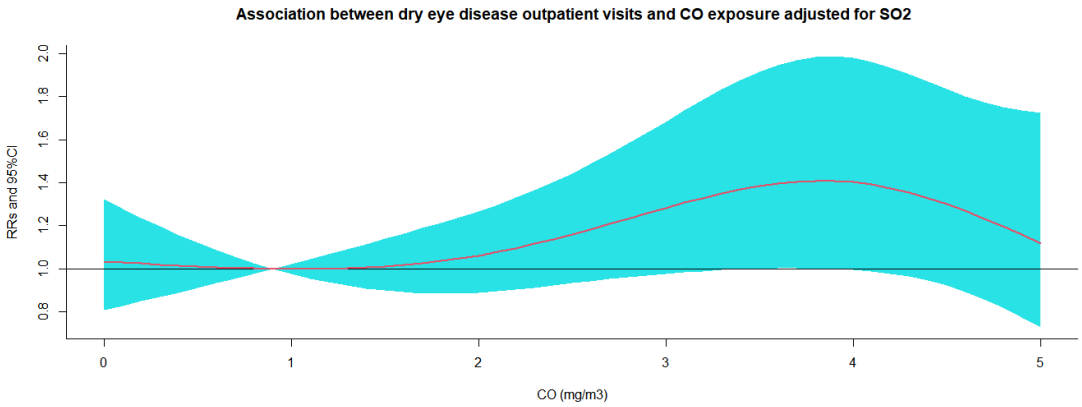
Association between dry eye disease outpatient visits and CO exposure adjusted for SO2
RRs and 95%CI
0.8
1.0
1.2
1.4
1.6
1.8
2.0
0
1
2
3
4
5
CO (mg/m3)

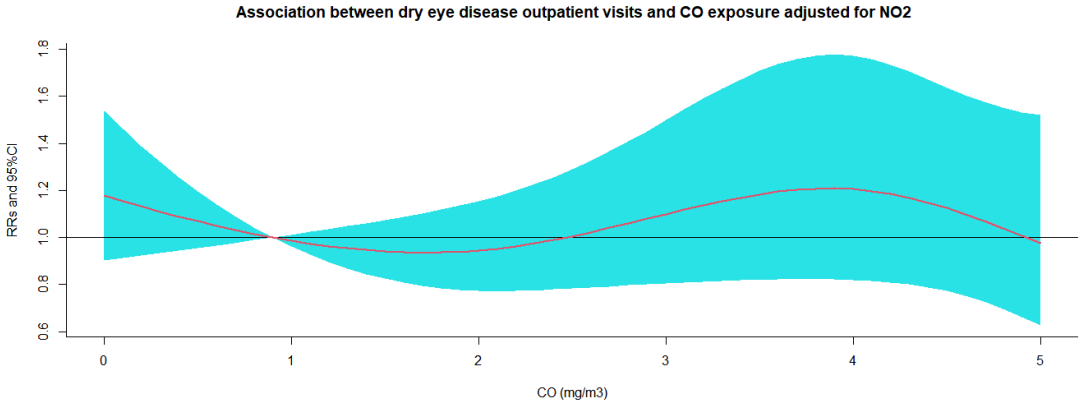
Association between dry eye disease outpatient visits and CO exposure adjusted for NO2
RRs and 95%CI
0.6
0.8
1.0
1.2
1.4
1.6
1.8
0
1
2
3
4
5
CO (mg/m3)

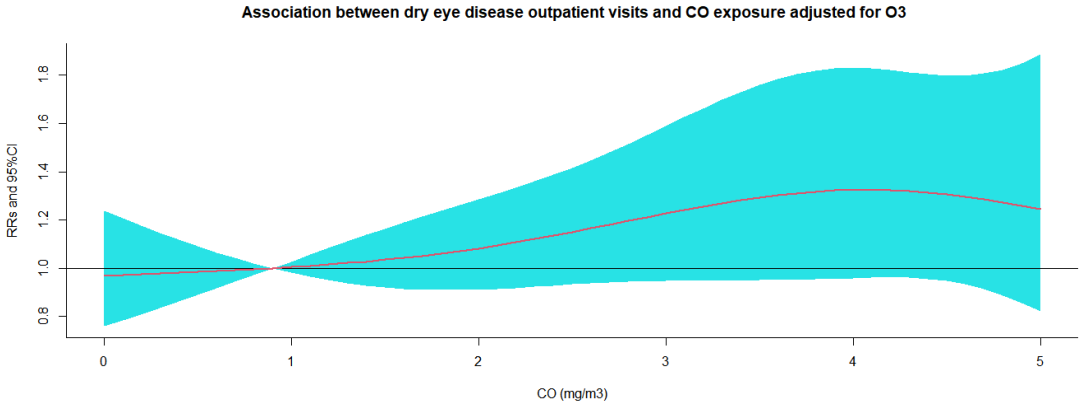
Association between dry eye disease outpatient visits and CO exposure adjusted for O3
RRs and 95%CI
0.8
1.0
1.2
1.4
1.6
1.8
0
1
2
3
4
5
CO (mg/m3)

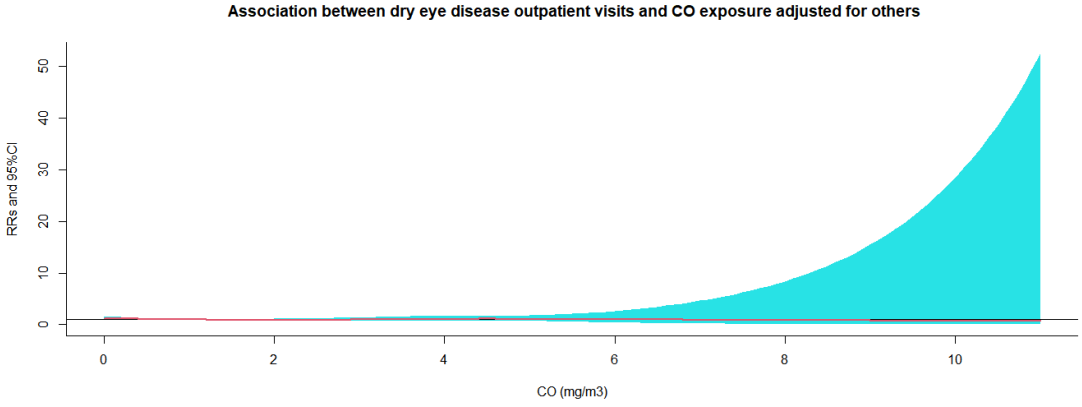
Association between dry eye disease outpatient visits and CO exposure adjusted for others
RRs and 95%CI
0
10
20
30
40
50
0
2
4
6
8
10
CO (mg/m3)

Figure S68. The relative risks (RRs) of per 10 mg/m^3 increase in CO on dry eye disease outpatient visits at various lag days after adjusted for NO_2 exposure.

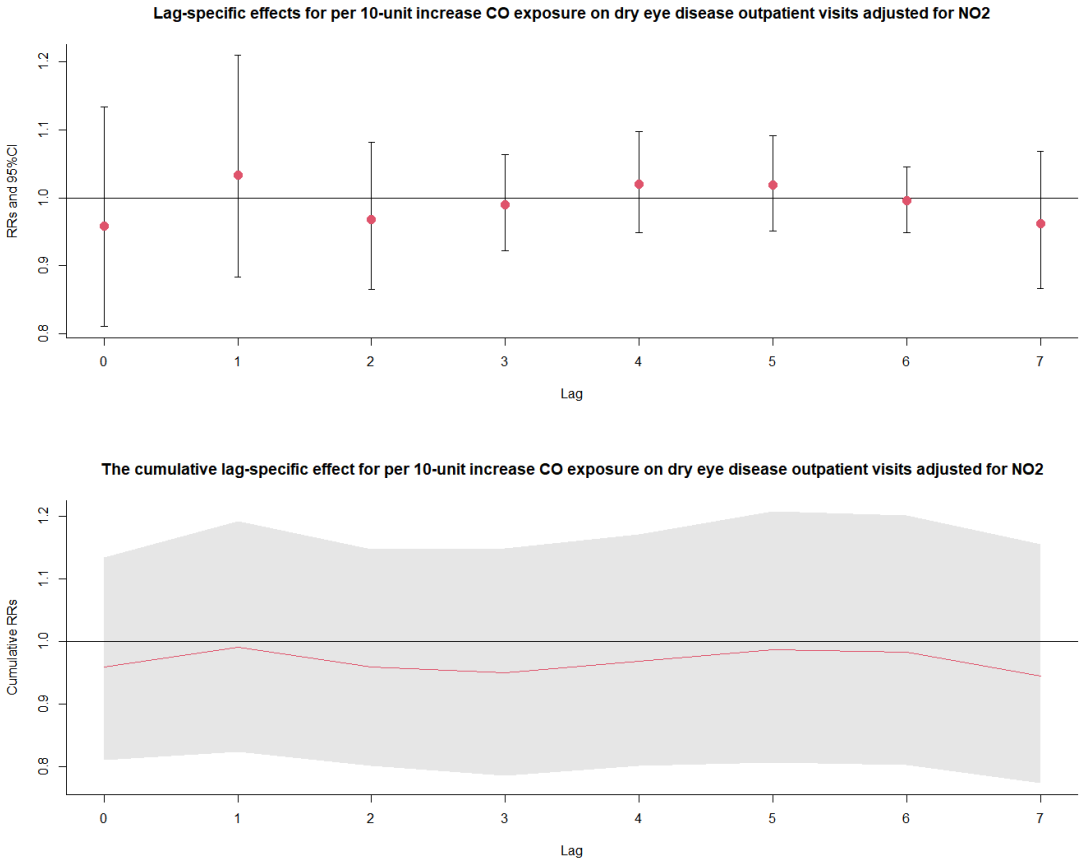

Figure S69. 3D graph and contour map of CO exposure on dry eye disease outpatient visits after adjusted for NO_2 exposure.

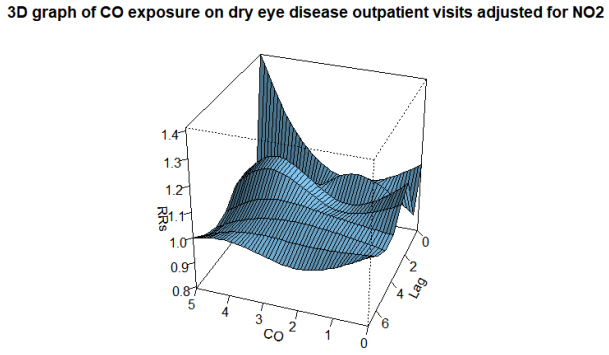

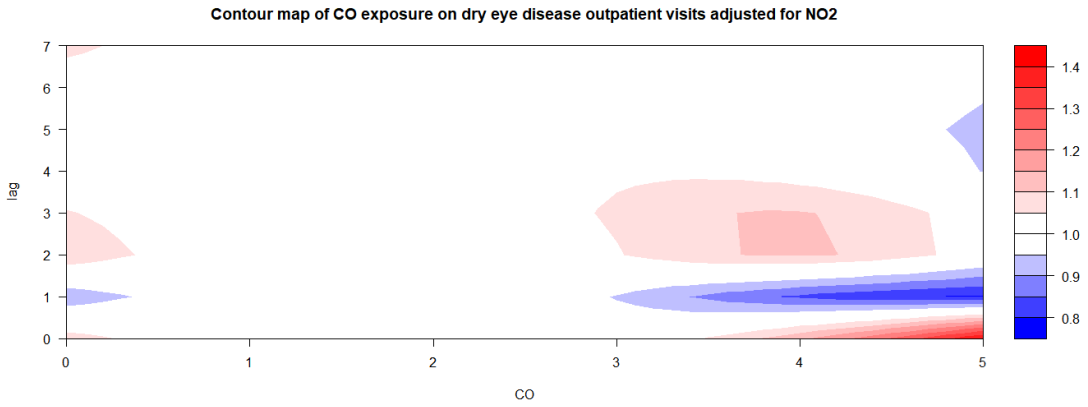

Figure S70. The relative risks (RRs) of per 10 mg/m^3 increase in CO on dry eye disease outpatient visits at various lag days after adjusted for PM_{10} exposure.

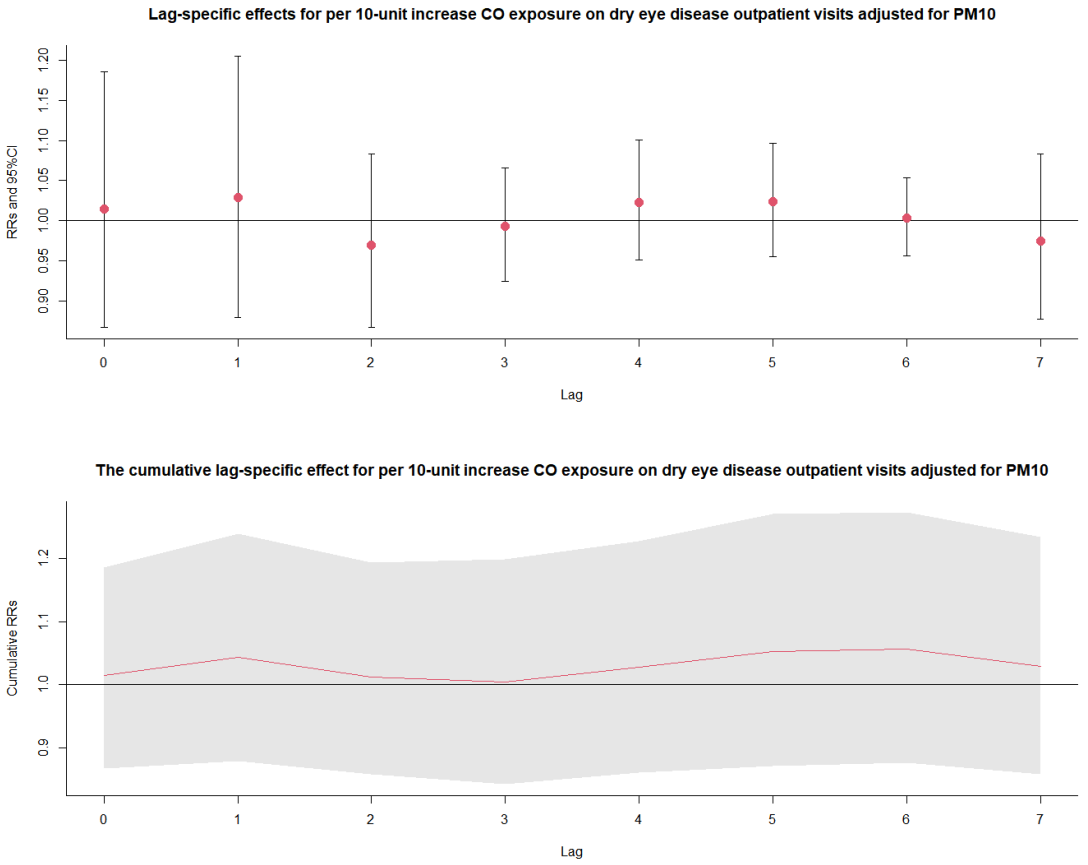

Figure S71. 3D graph and contour map of CO exposure on dry eye disease outpatient visits after adjusted for PM_{10} exposure.

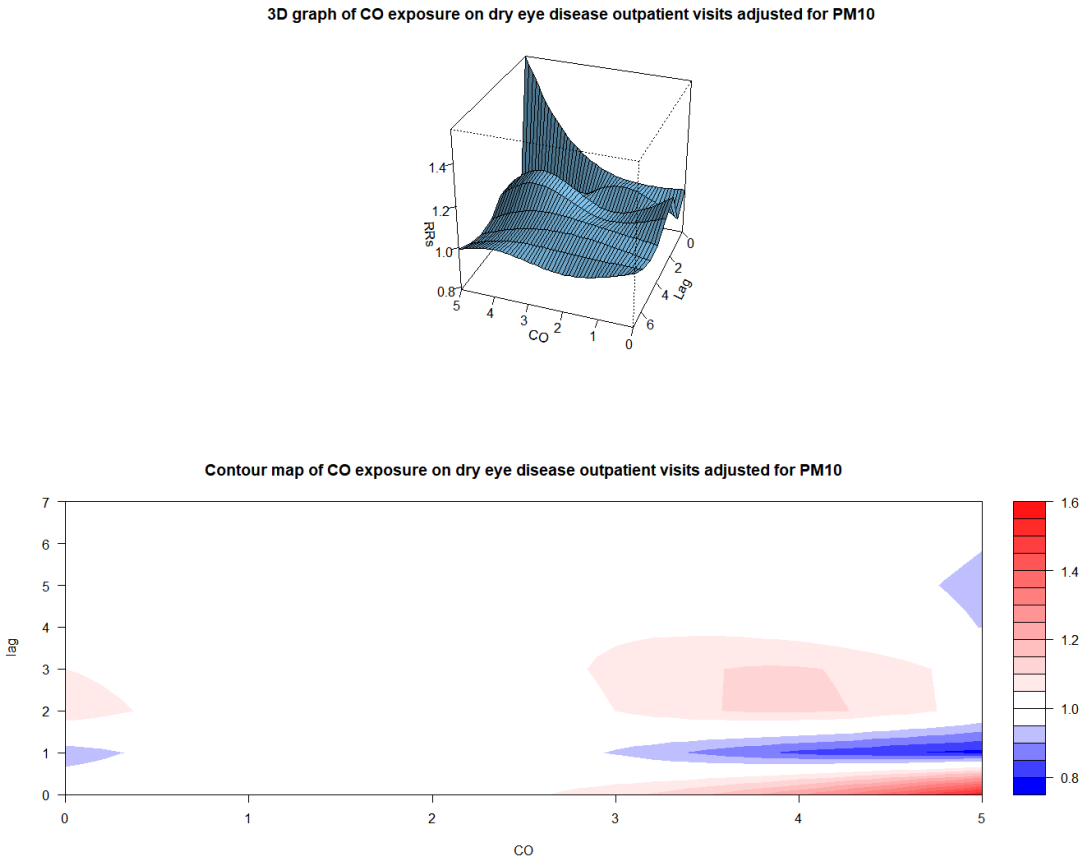

Figure S72. The relative risks (RRs) of per 10 mg/m^3 increase in CO on dry eye disease outpatient visits at various lag days after adjusted for $PM_{2.5}$ exposure.

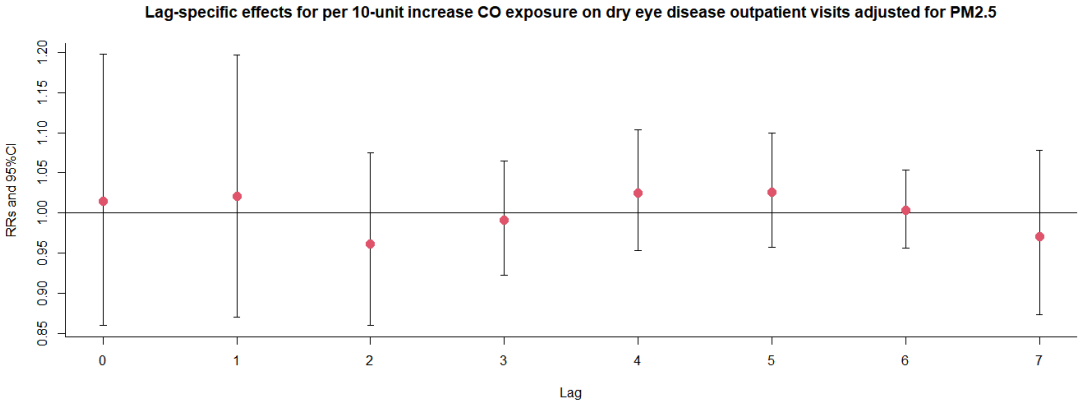

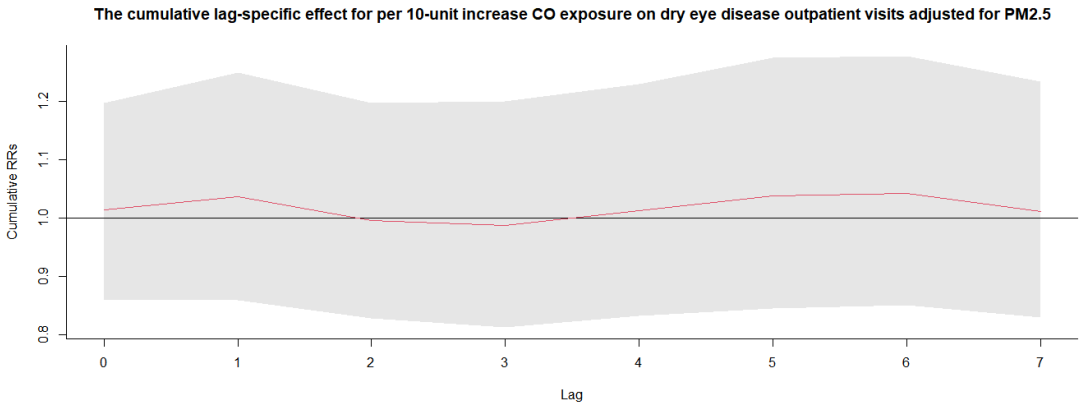

Figure S73. 3D graph and contour map of CO exposure on dry eye disease outpatient visits after adjusted for $PM_{2.5}$ exposure.

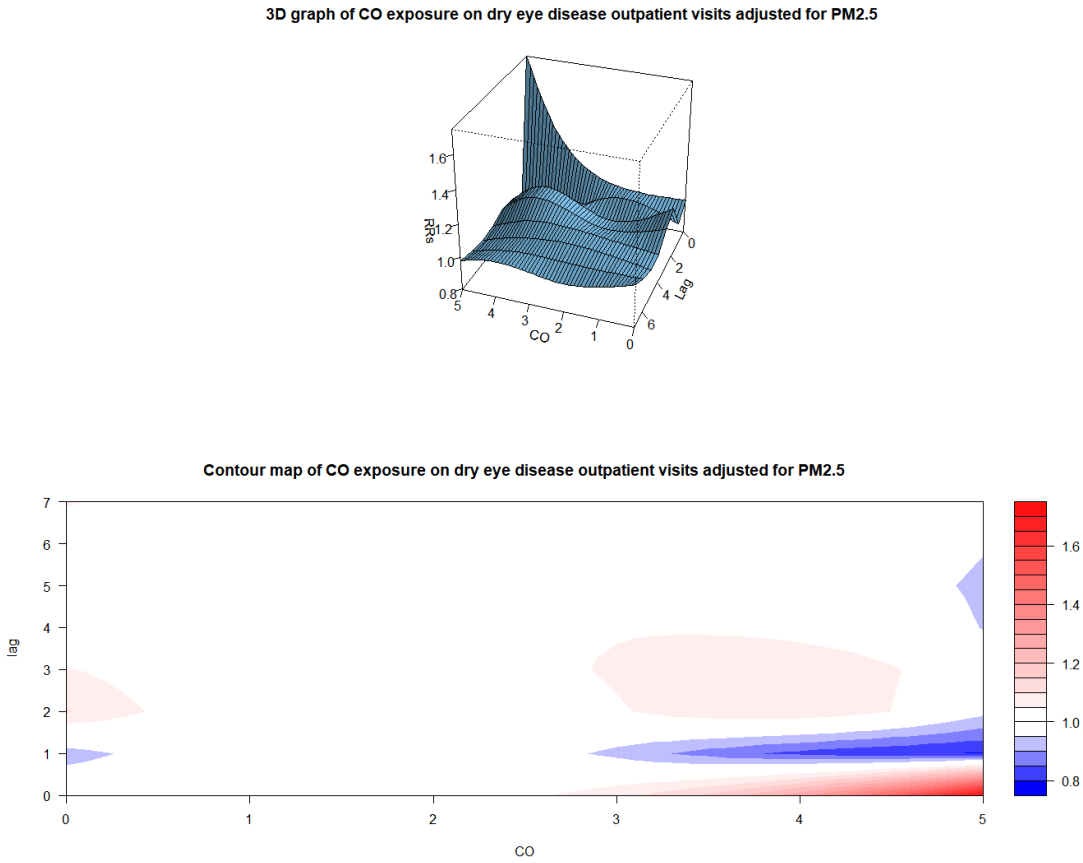

Figure S74. The relative risks (RRs) of per 10 mg/m^3 increase in CO on dry eye disease outpatient visits at various lag days after adjusted for SO_2 exposure.

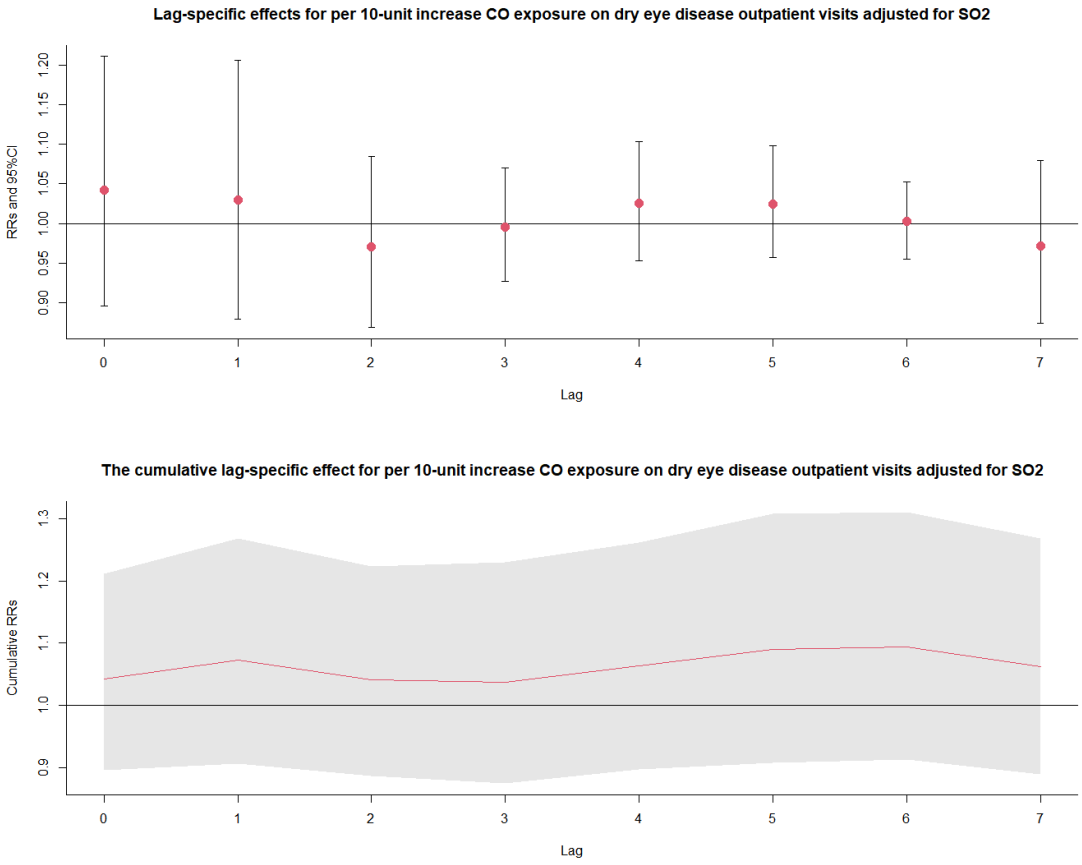

Figure S75. 3D graph and contour map of CO exposure on dry eye disease outpatient visits after adjusted for SO_2 exposure.

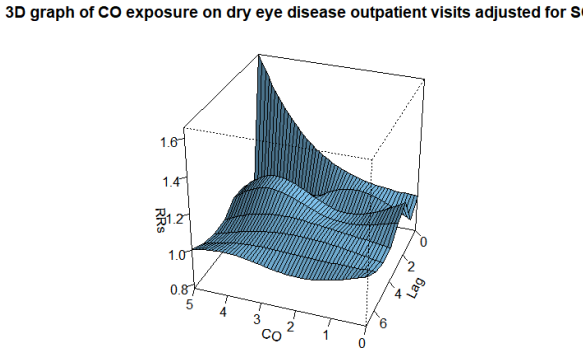

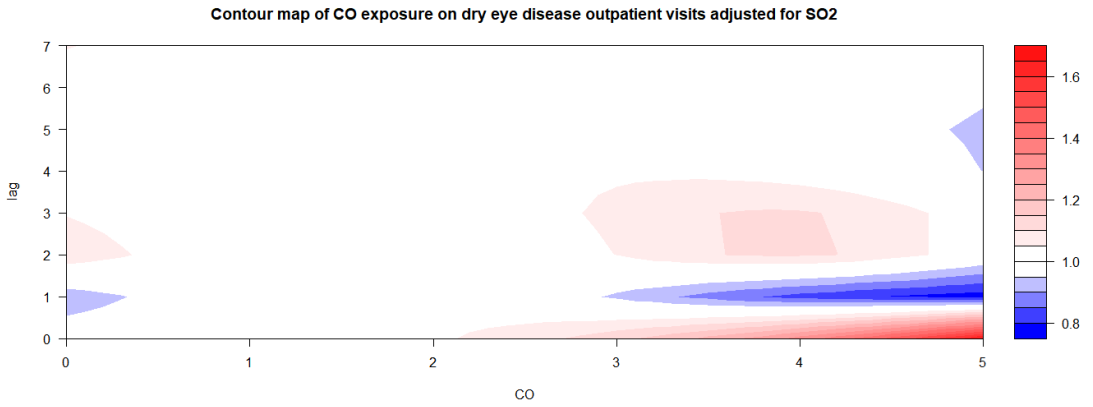

Figure S76. The relative risks (RRs) of per 10 mg/m^3 increase in CO on dry eye disease outpatient visits at various lag days after adjusted for O_3 exposure.

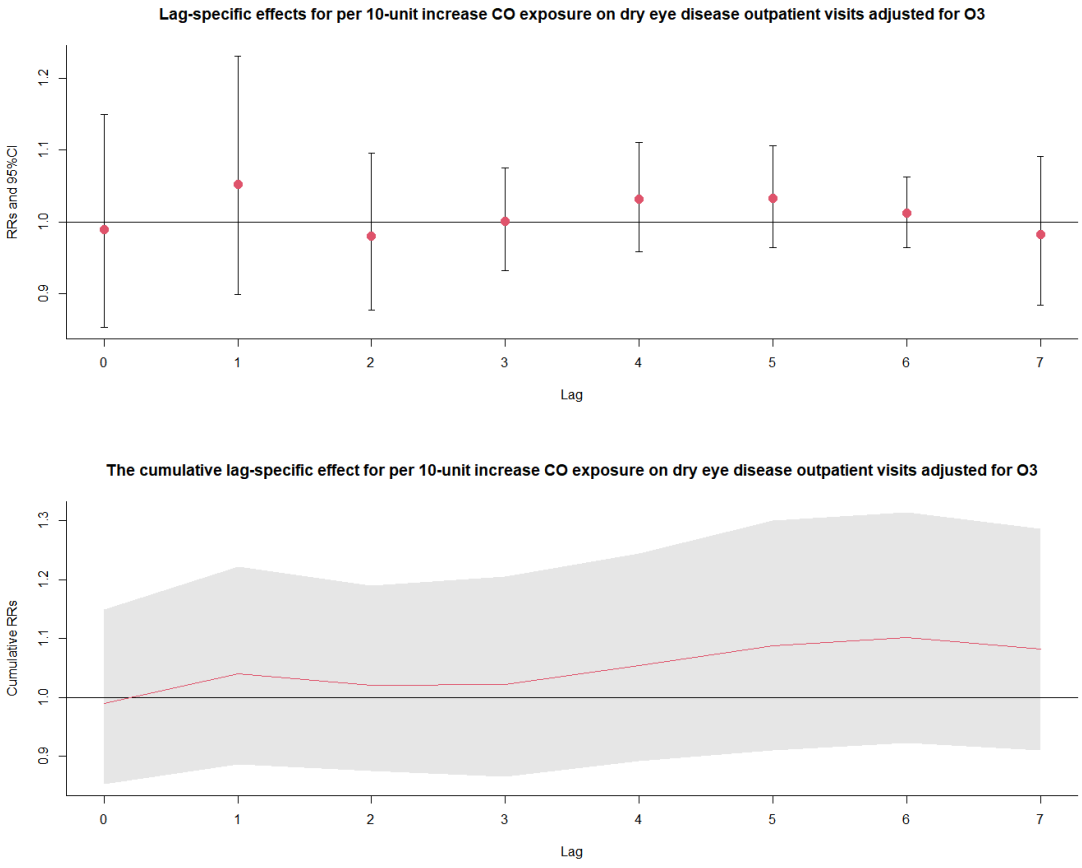

Figure S77. 3D graph and contour map of CO exposure on dry eye disease outpatient visits after adjusted for O_3 exposure.

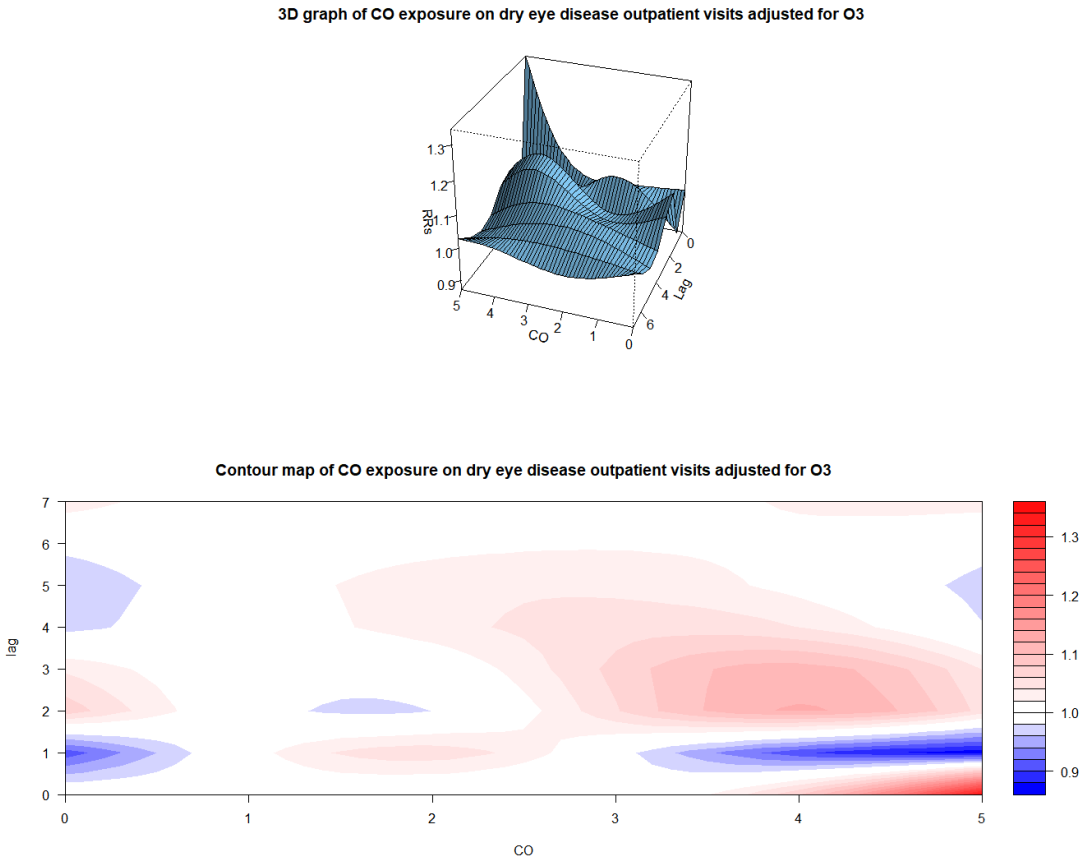

Figure S78. The relative risks (RRs) of per 10 mg/m^3 increase in CO on dry eye disease outpatient visits at various lag days after adjusted for others exposure.

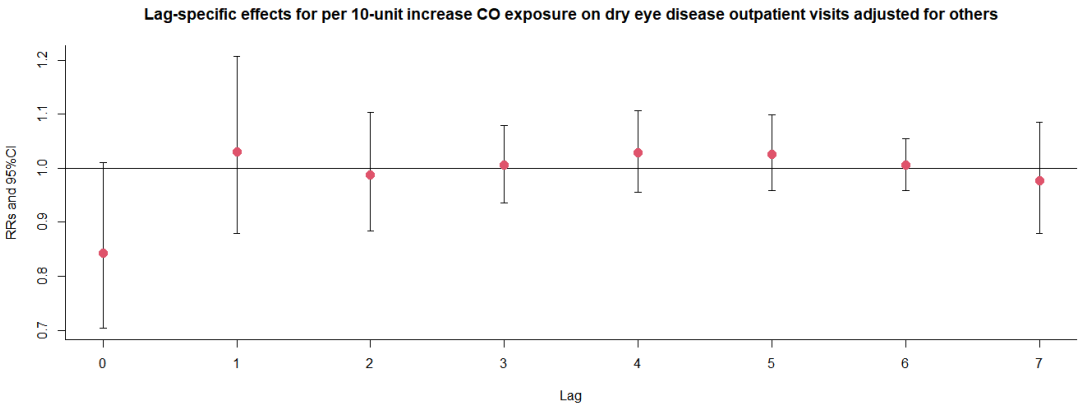

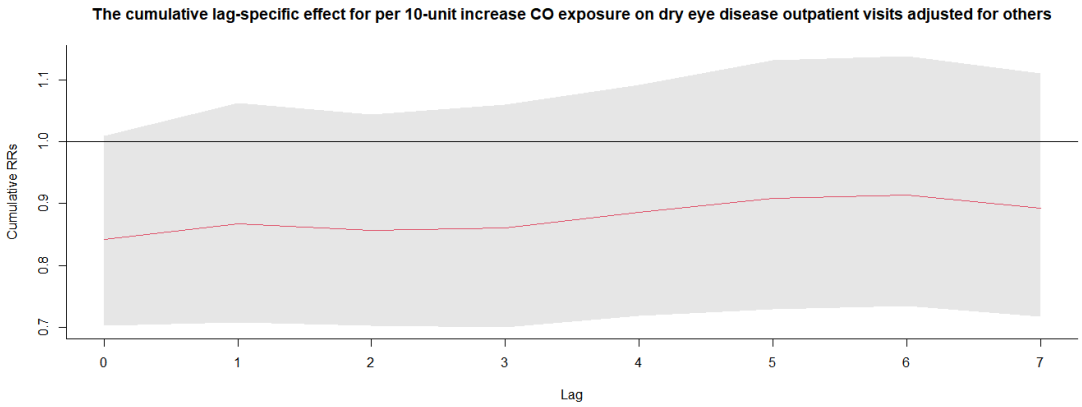

Figure S79. 3D graph and contour map of CO exposure on dry eye disease outpatient visits after adjusted for others exposure.

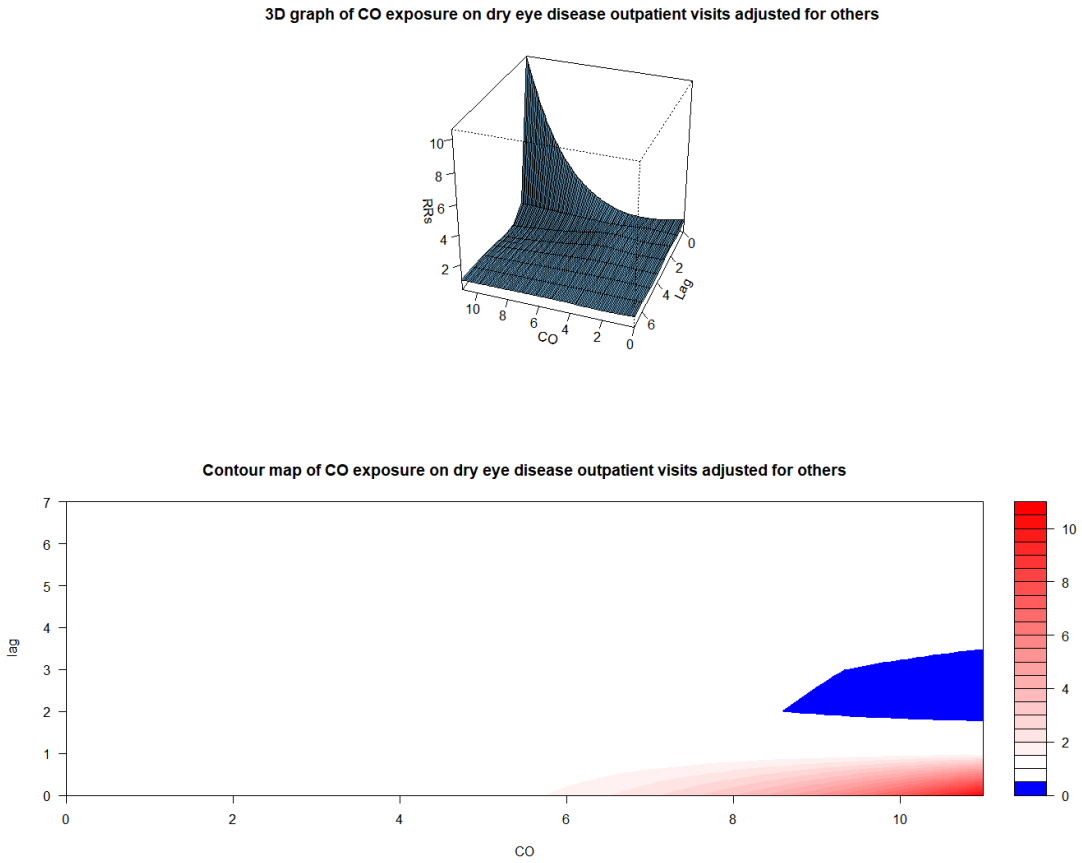

Figure S80. Exposure-response association between dry eye disease outpatient visits and CO exposure in male patients.

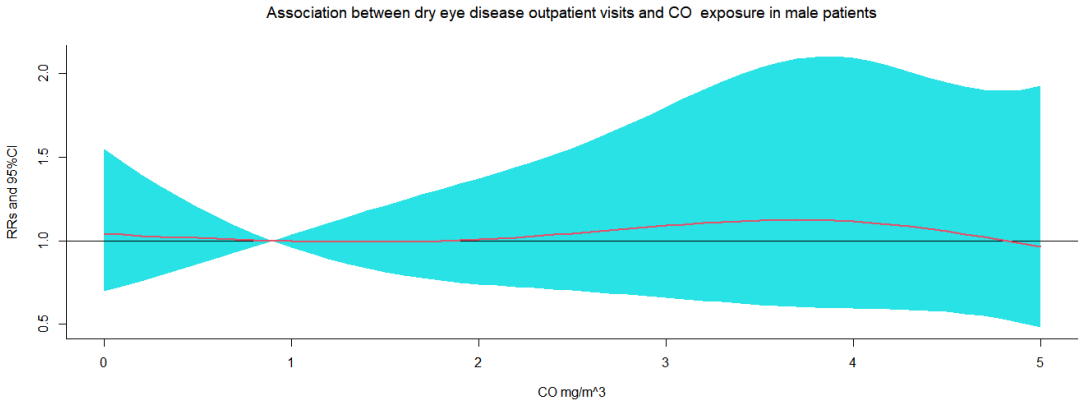

Figure S81. The relative risks (RRs) of per 10 mg/m^3 increase in CO on dry eye disease outpatient visits at various lag days in male patients.

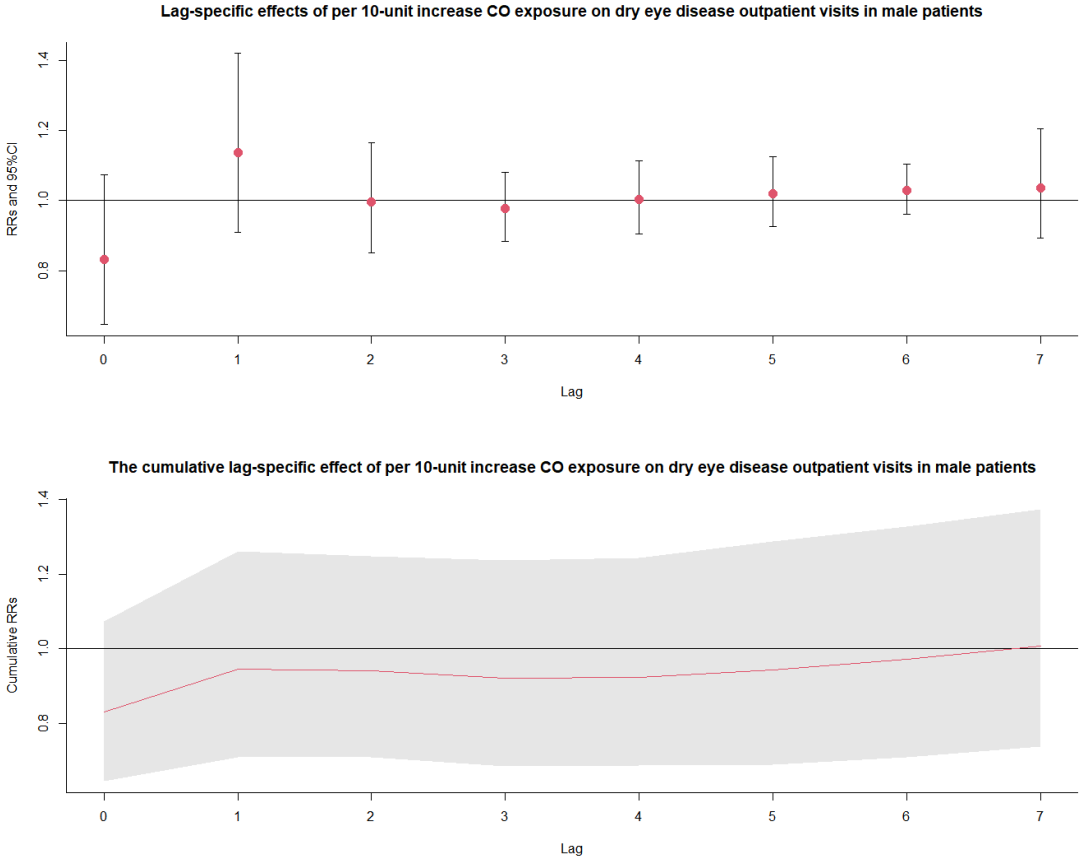

Figure S82. Exposure-response association between dry eye disease outpatient visits and CO exposure in female patients.

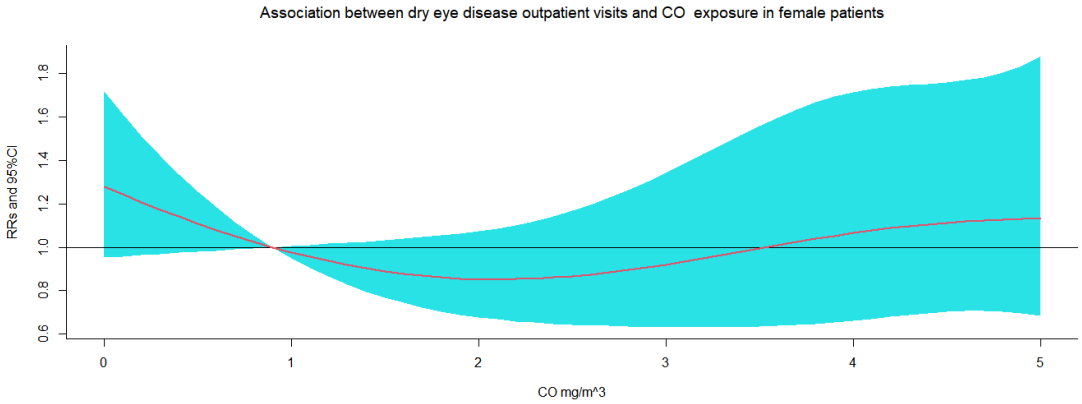

Figure S83. The relative risks (RRs) of per 10 mg/m^3 increase in CO on dry eye disease outpatient visits at various lag days in female patients.

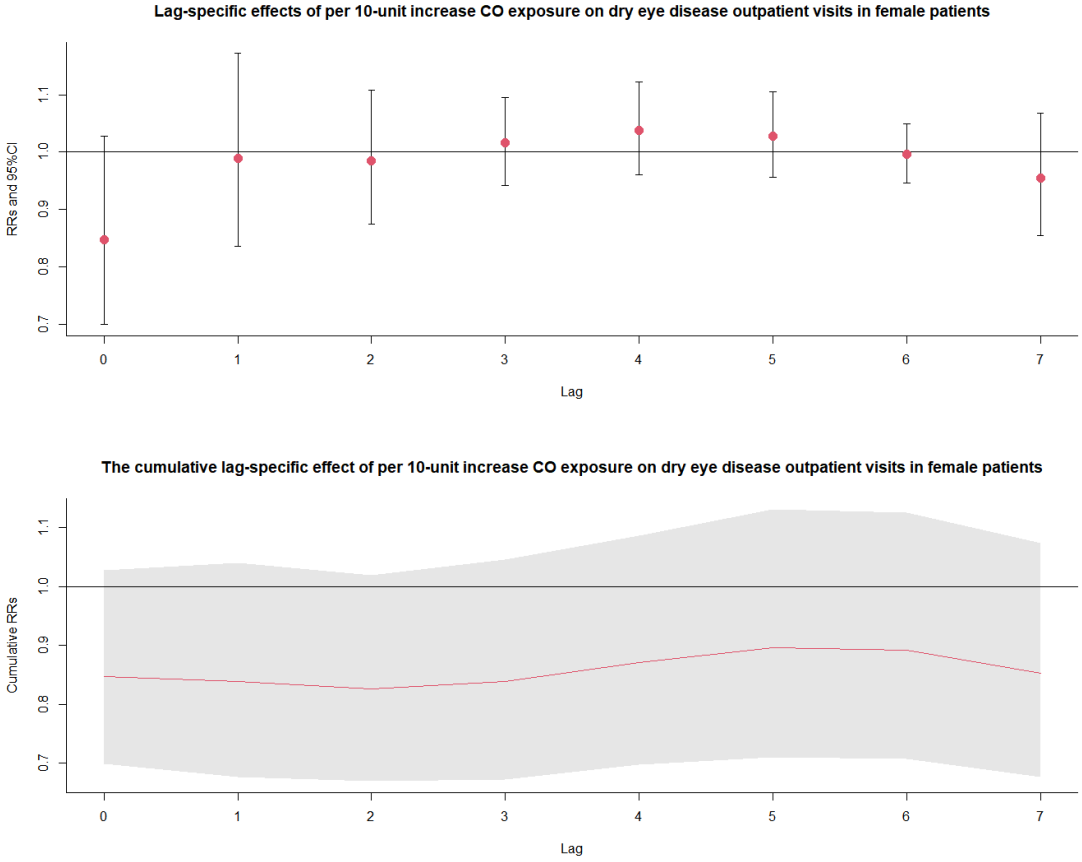

Figure S84. Exposure-response association between dry eye disease outpatient visits and CO exposure in age 0-5 patients.

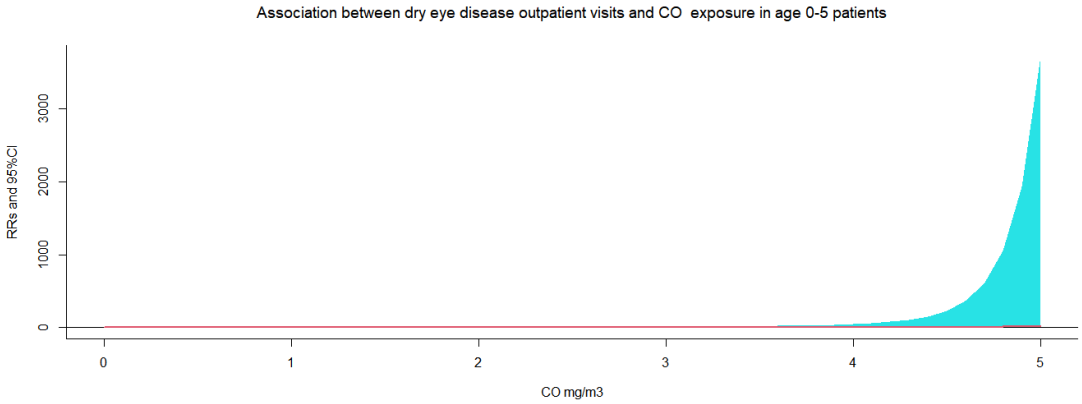

Figure S85. The relative risks (RRs) of per 10 mg/m^3 increase in CO on dry eye disease outpatient visits at various lag days in age 0-5 patients.

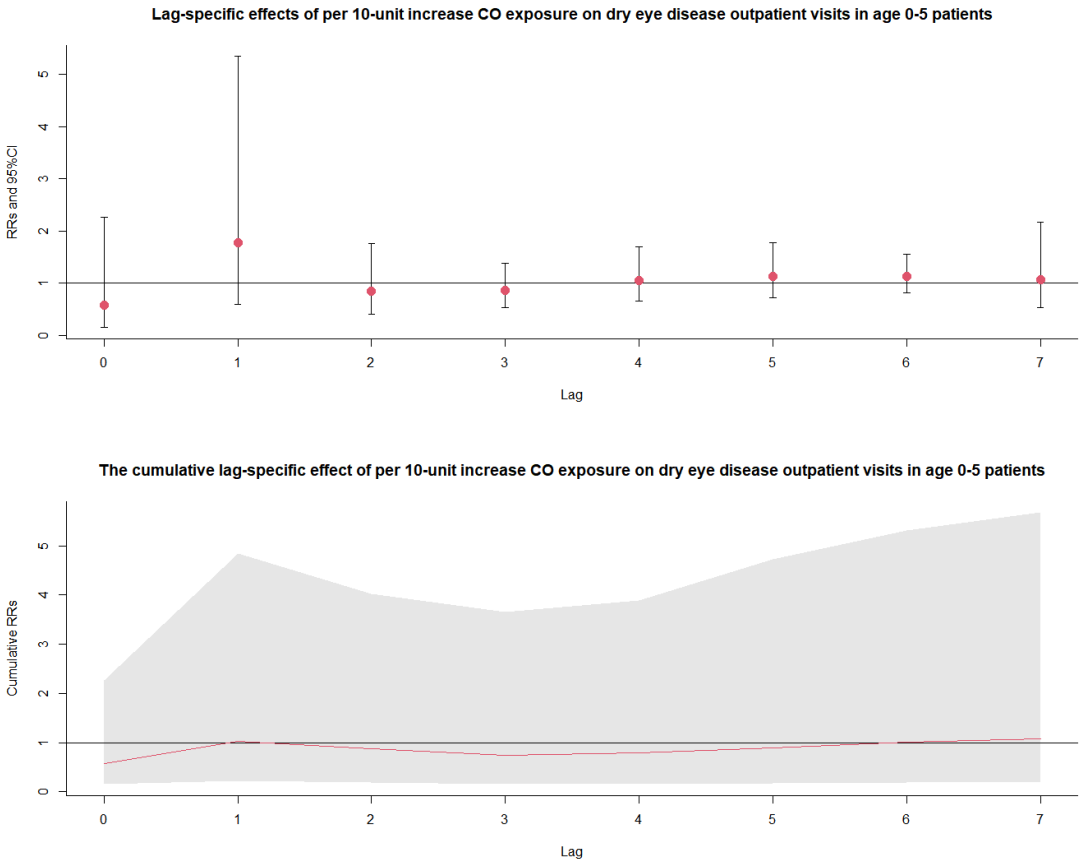

Figure S86. Exposure-response association between dry eye disease outpatient visits and CO exposure in age 6-18 patients.

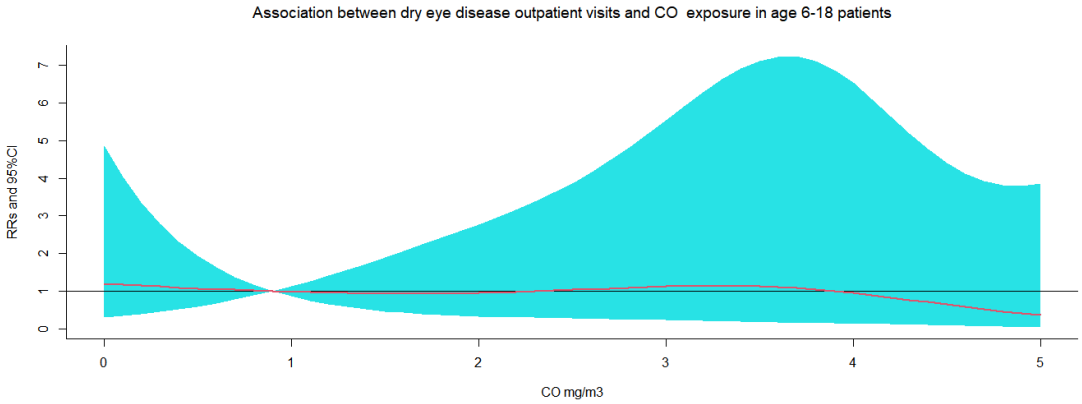

Figure S87. The relative risks (RRs) of per 10 mg/m^3 increase in CO on dry eye disease outpatient visits at various lag days in age 6-18 patients.

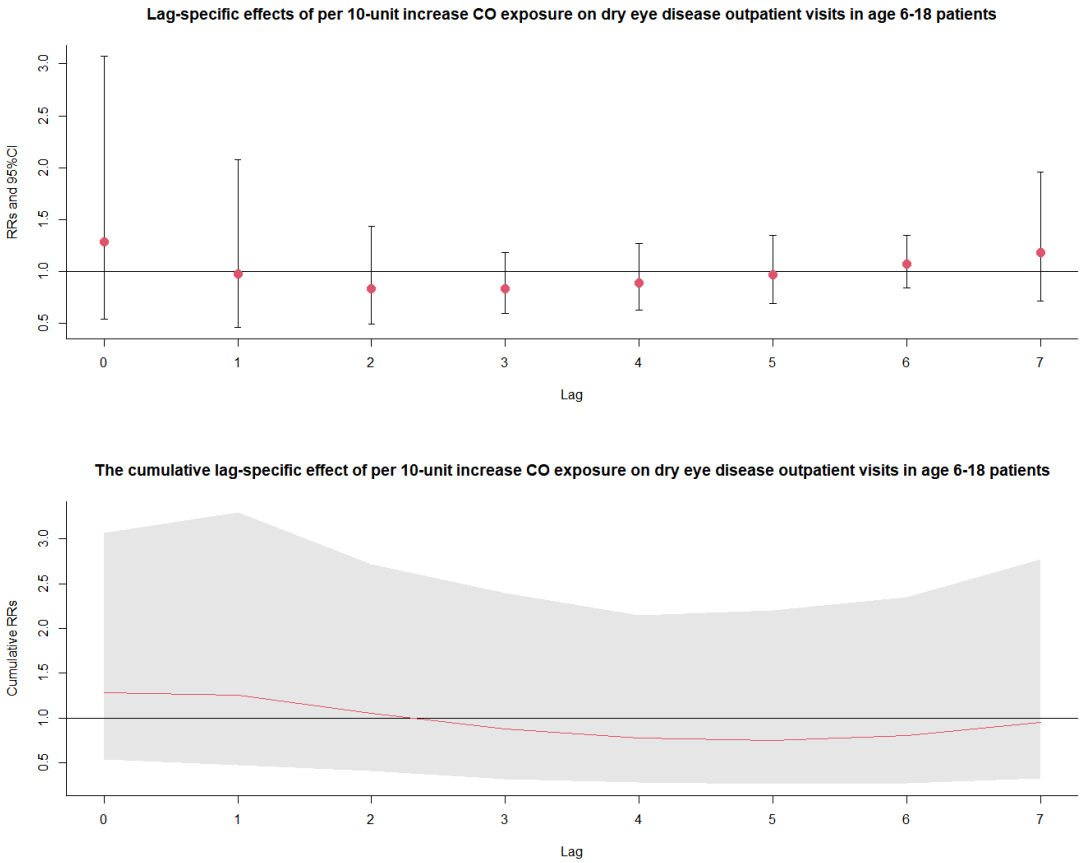

Figure S88. Exposure-response association between dry eye disease outpatient visits and CO exposure in age 19-64 patients.

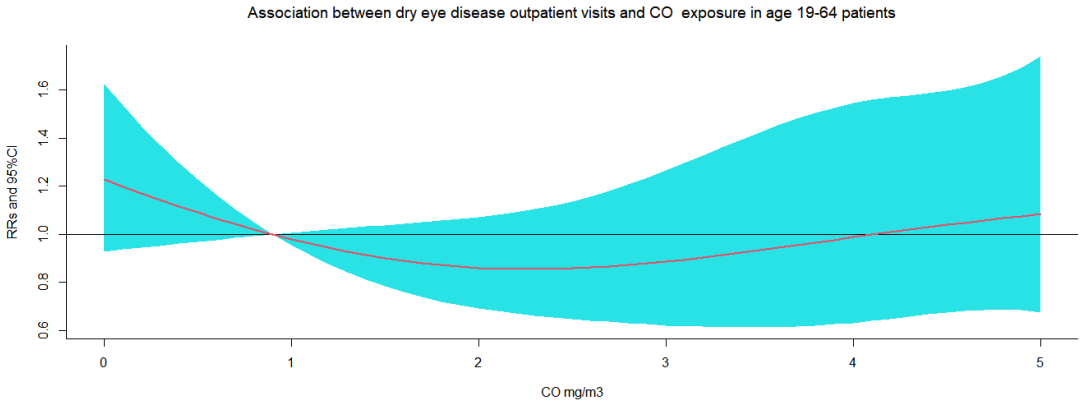

Figure S89. The relative risks (RRs) of per 10 mg/m^3 increase in CO on dry eye disease outpatient visits at various lag days in age 19-64 patients.

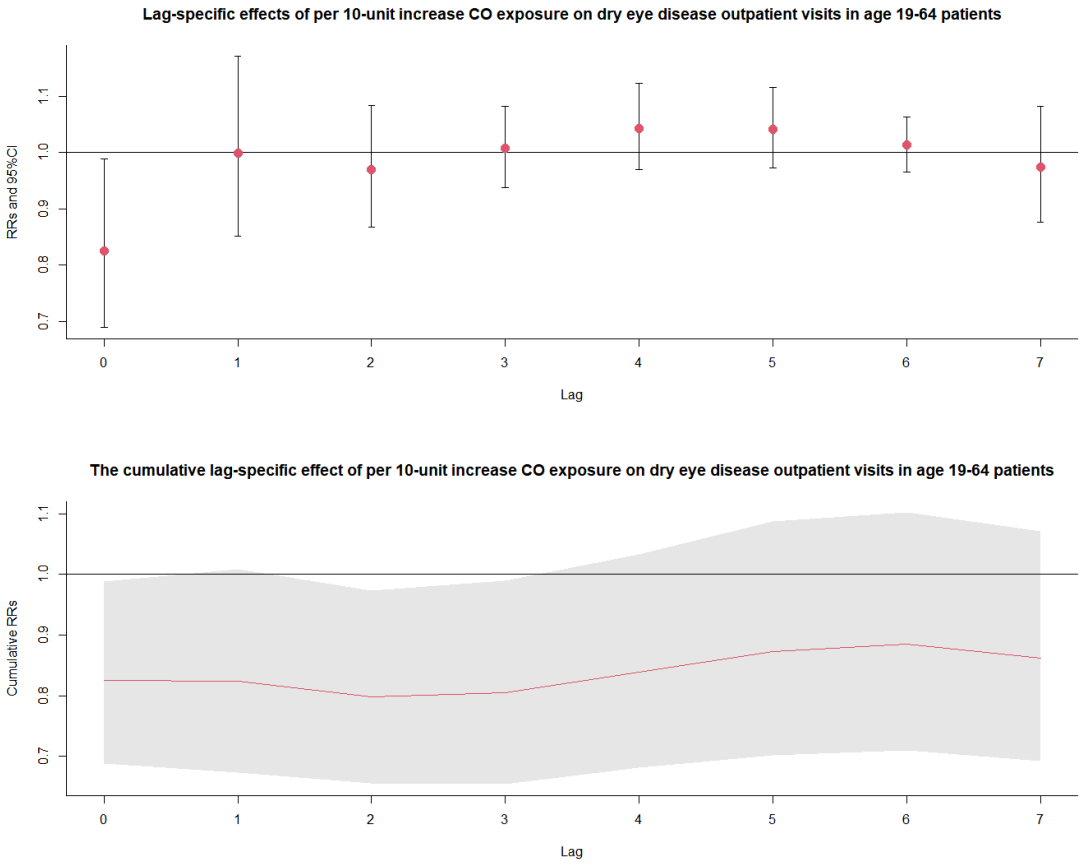

Figure S90. Exposure-response association between dry eye disease outpatient visits and CO exposure in age ≥65 patients.

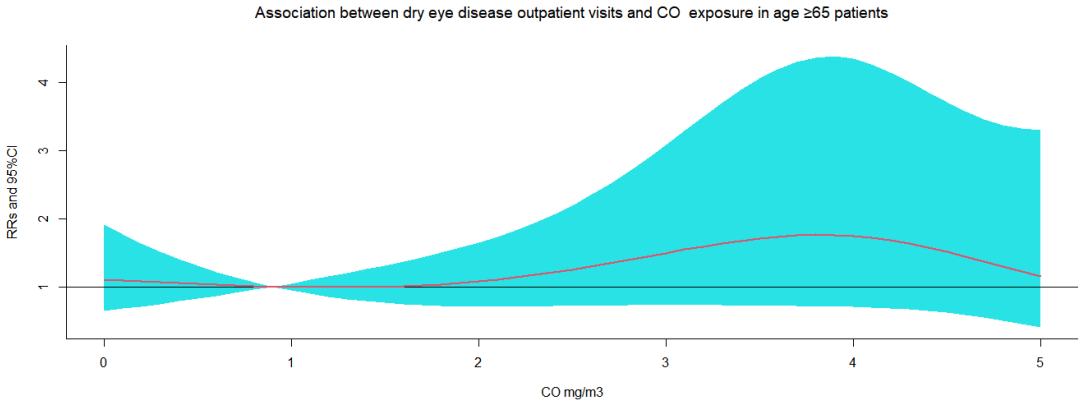

Figure S91. The relative risks (RRs) of per 10 mg/m^3 increase in CO on dry eye disease outpatient visits at various lag days in age ≥65 patients.

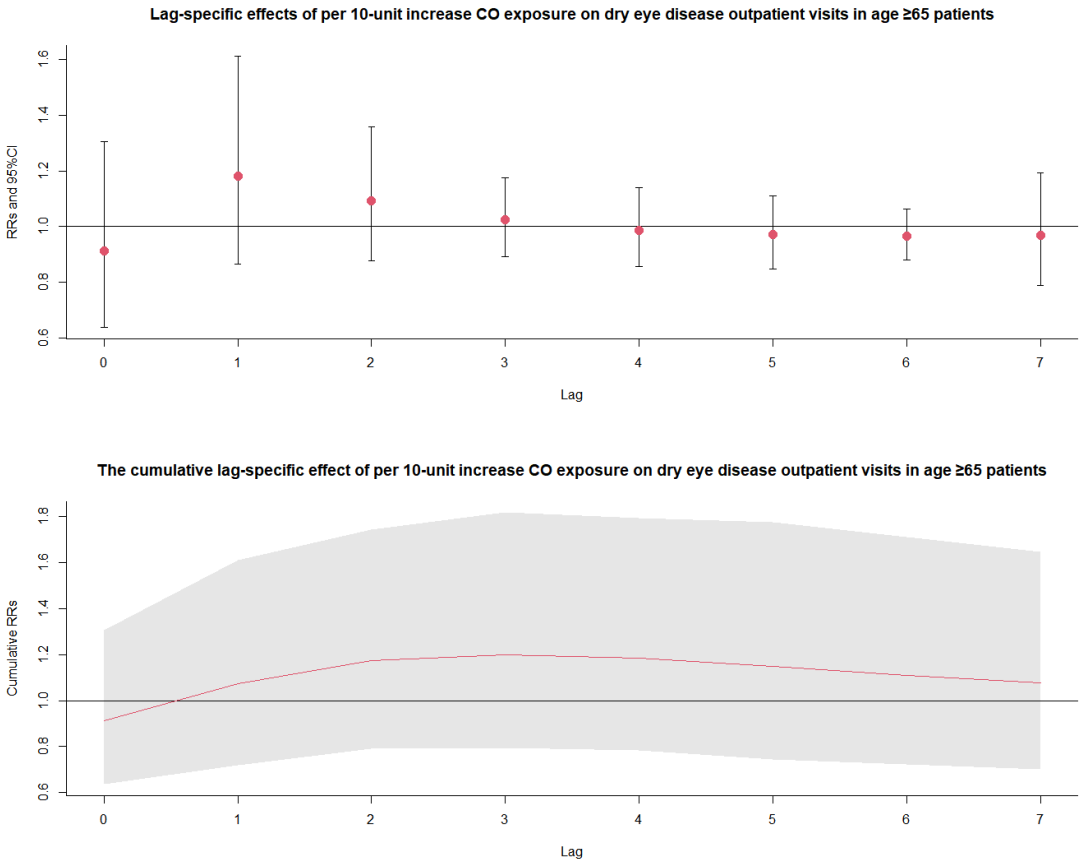

Figure S92. Exposure-response association between dry eye disease outpatient visits and CO exposure in the warm season.

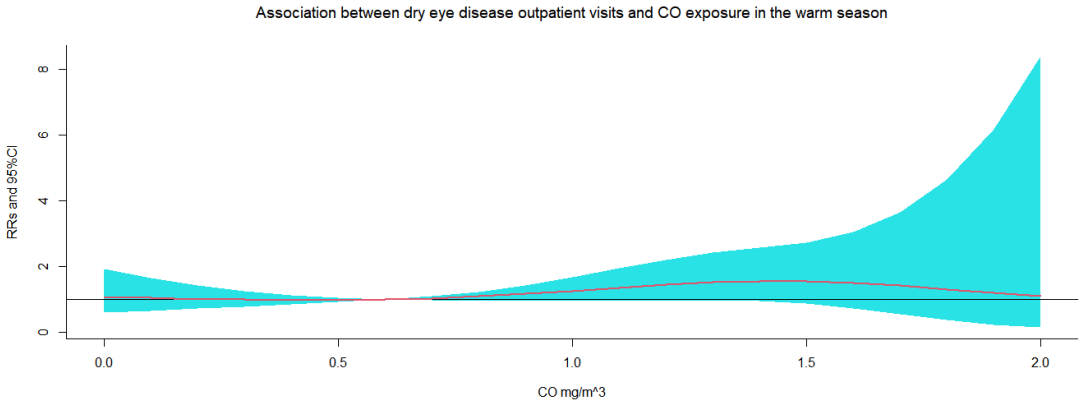

Figure S93. The relative risks (RRs) of per 10 mg/m^3 increase in CO on dry eye disease outpatient visits at various lag days in the warm season.

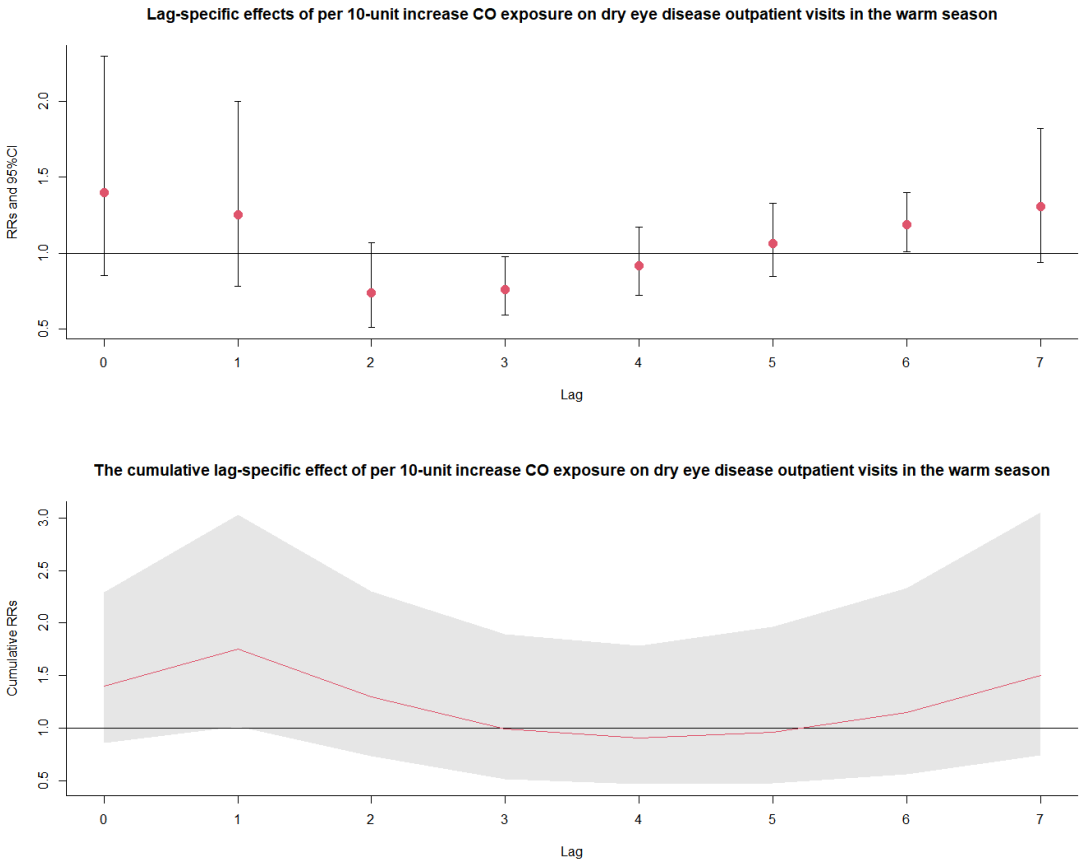

Figure S94. Exposure-response association between dry eye disease outpatient visits and CO exposure in the cold season.

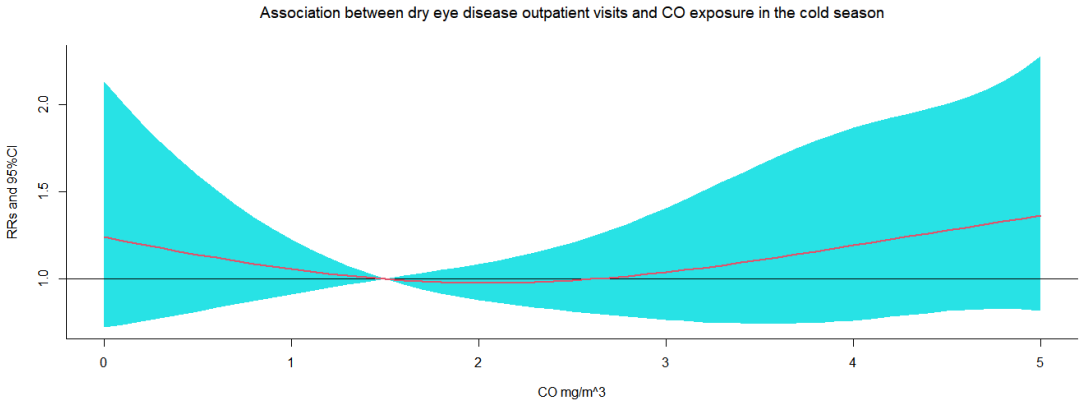

Figure S95. The relative risks (RRs) of per 10 mg/m^3 increase in CO on dry eye disease outpatient visits at various lag days in the cold season.

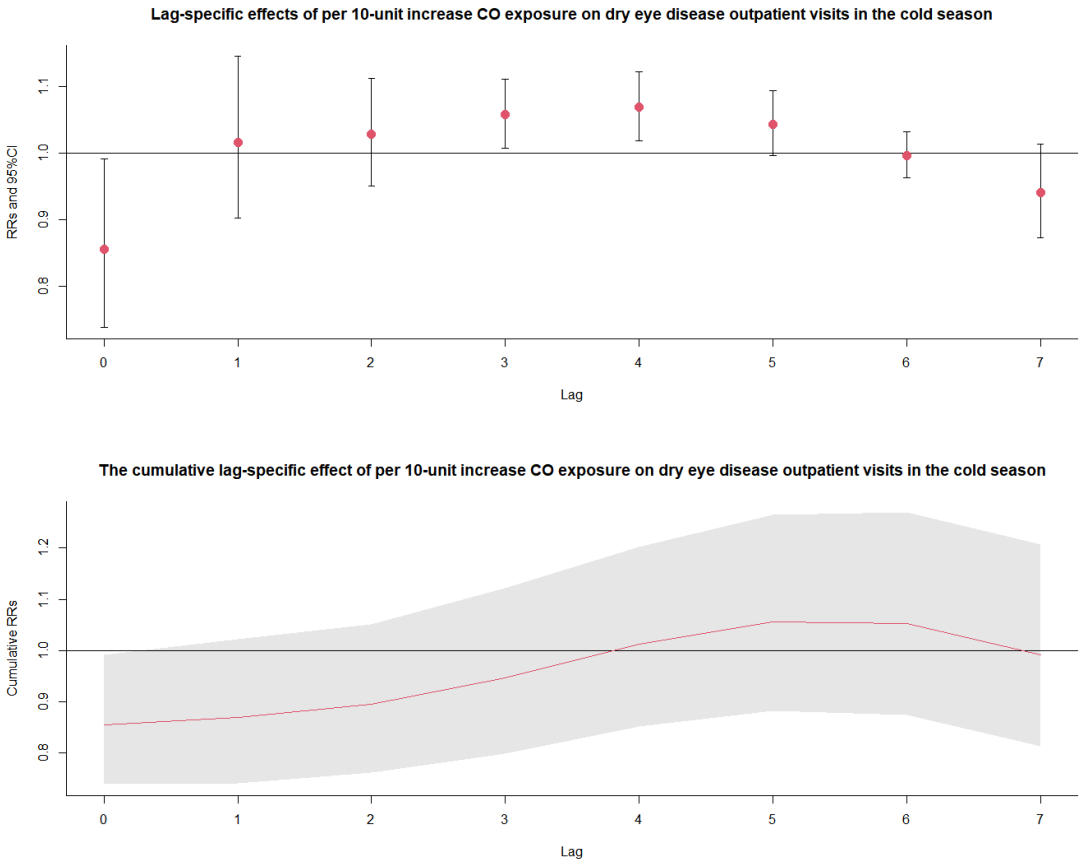

Figure S96. Exposure-response association between dry eye disease outpatient visits and NO_2 exposure.

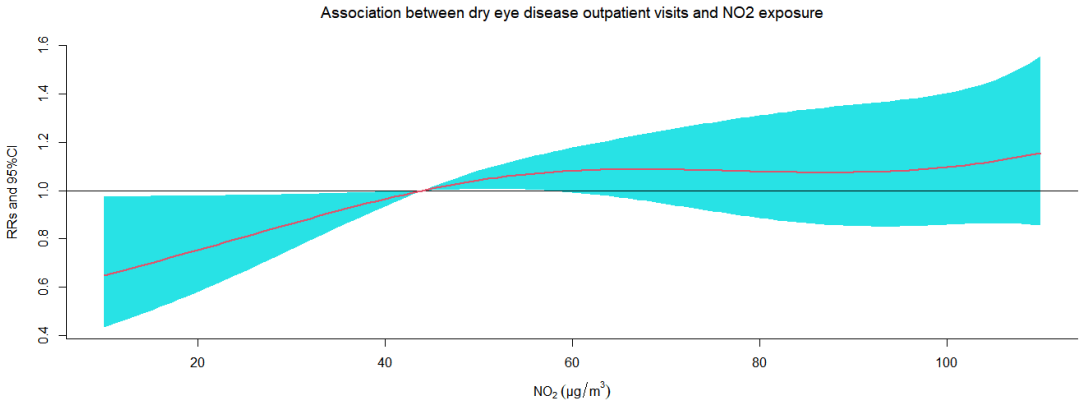

Figure S97. The relative risks (RRs) of per 10 μg/m^3 increase in NO_2 on dry eye disease outpatient visits at various lag days.

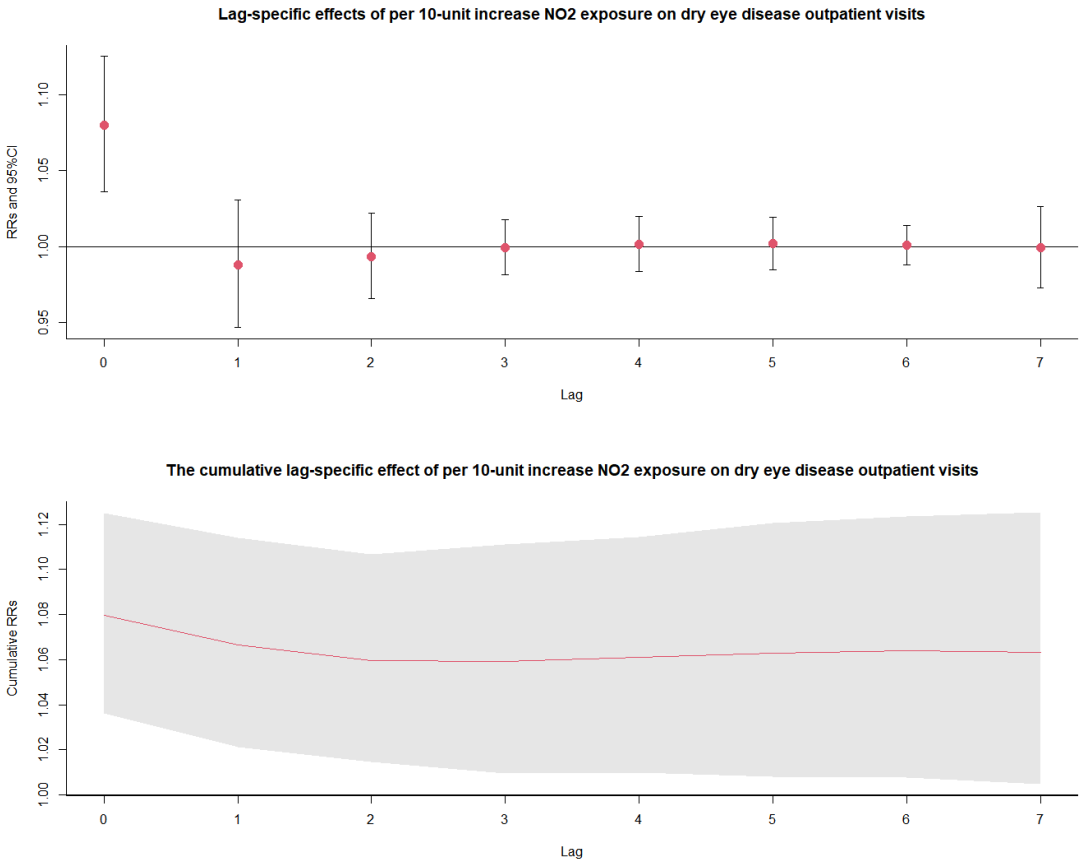

Figure S98. 3D graph and contour map of NO_2 exposure on dry eye disease outpatient visits.

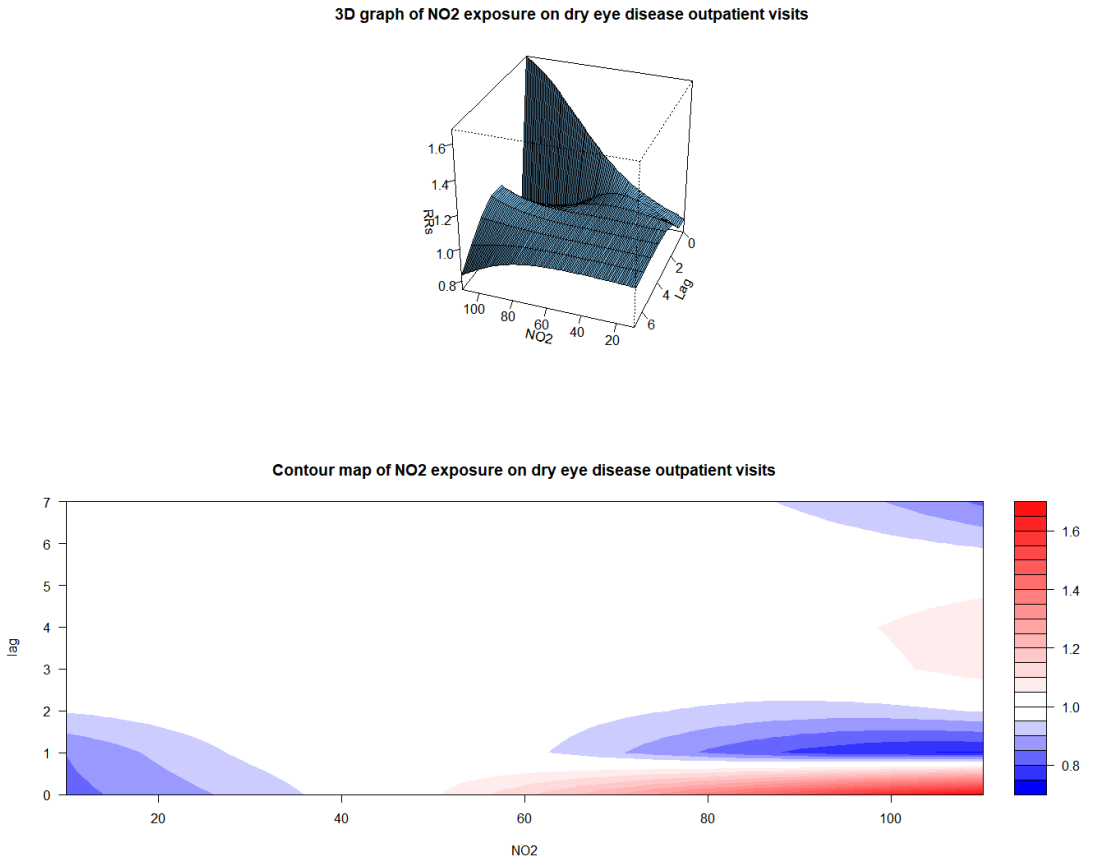

Figure S99. Exposure-response association between dry eye disease outpatient visits and NO2 exposure after adjusted for other air pollution.

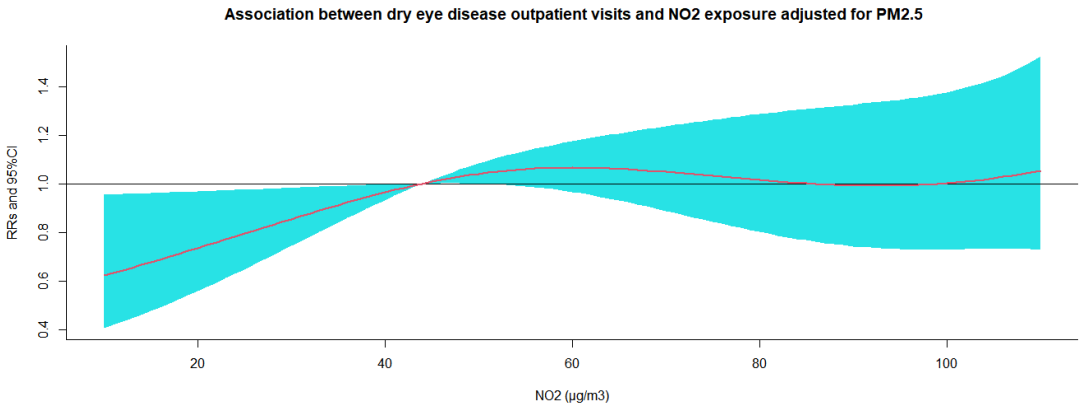

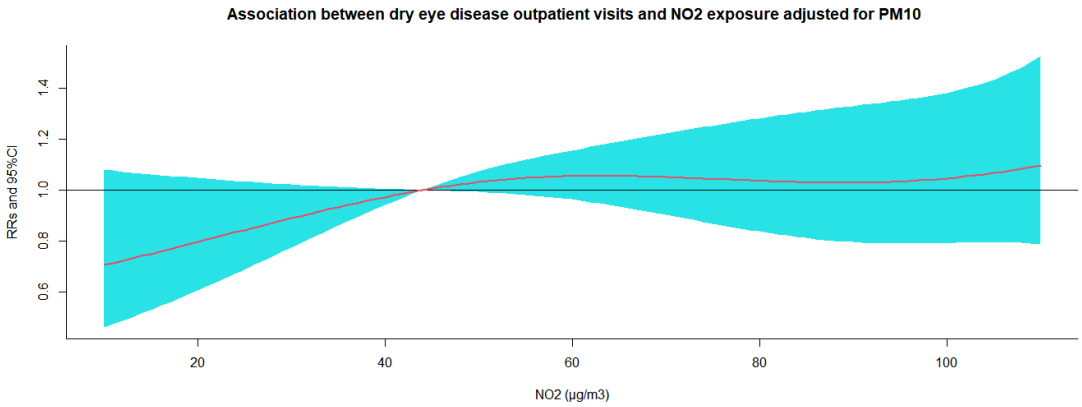
Association between dry eye disease outpatient visits and NO2 exposure adjusted for PM10
RRs and 95%CI
0.6
0.8
1.0
1.2
1.4
20
40
60
80
100
NO2 (μg/m3)

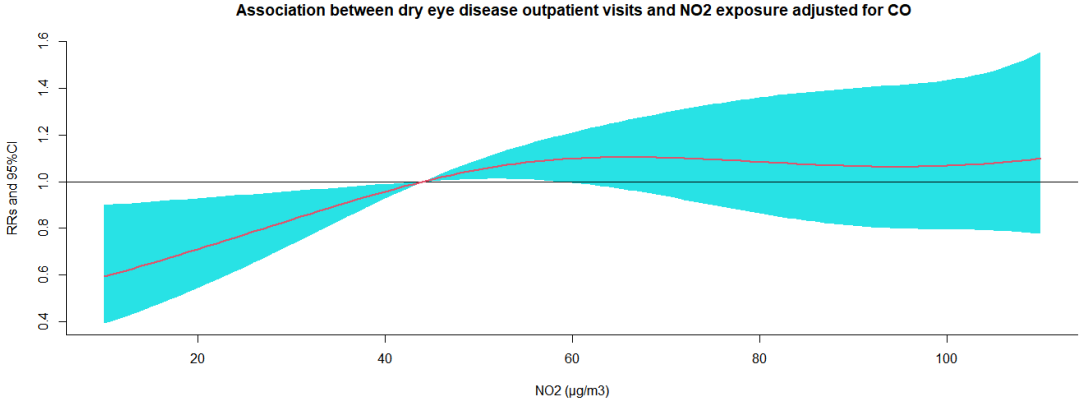
Association between dry eye disease outpatient visits and NO2 exposure adjusted for CO
RRs and 95%CI
0.4
0.6
0.8
1.0
1.2
1.4
1.6
20
40
60
80
100
NO2 (μg/m3)

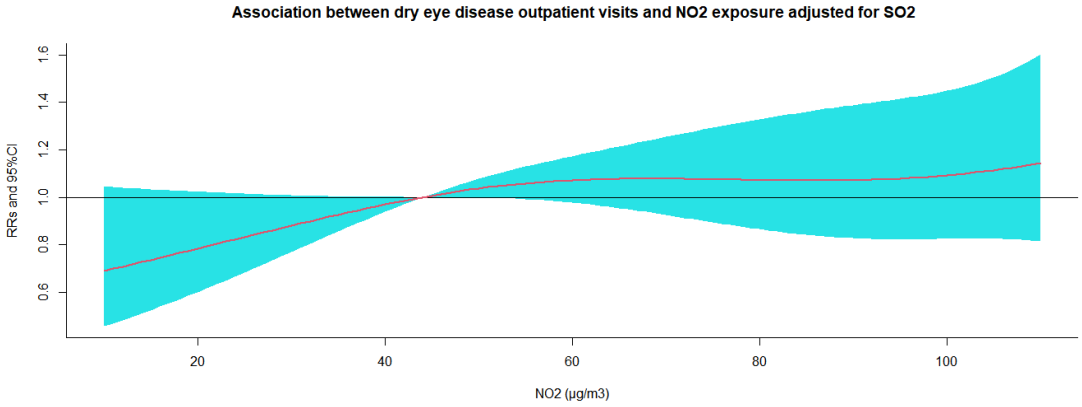
Association between dry eye disease outpatient visits and NO2 exposure adjusted for SO2
RRs and 95%CI
0.6
0.8
1.0
1.2
1.4
1.6
20
40
60
80
100
NO2 (μg/m3)

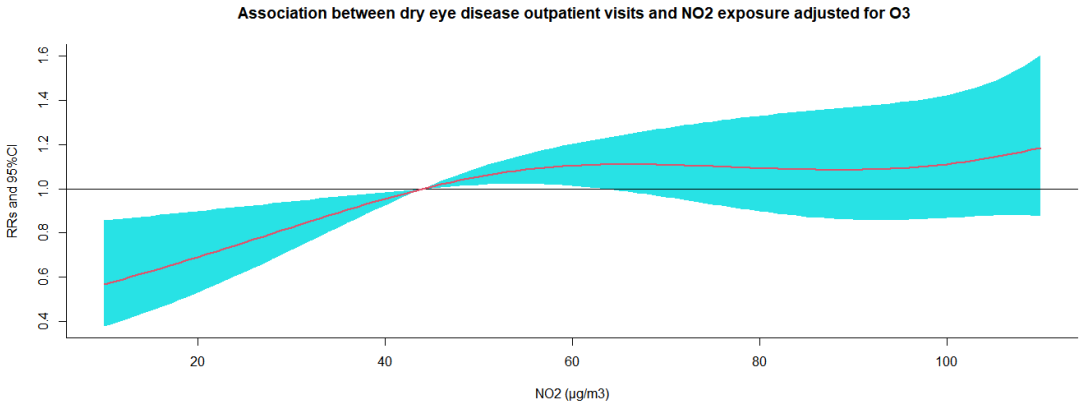
Association between dry eye disease outpatient visits and NO2 exposure adjusted for O3
RRs and 95%CI
0.4
0.6
0.8
1.0
1.2
1.4
1.6
20
40
60
80
100
NO2 (μg/m3)

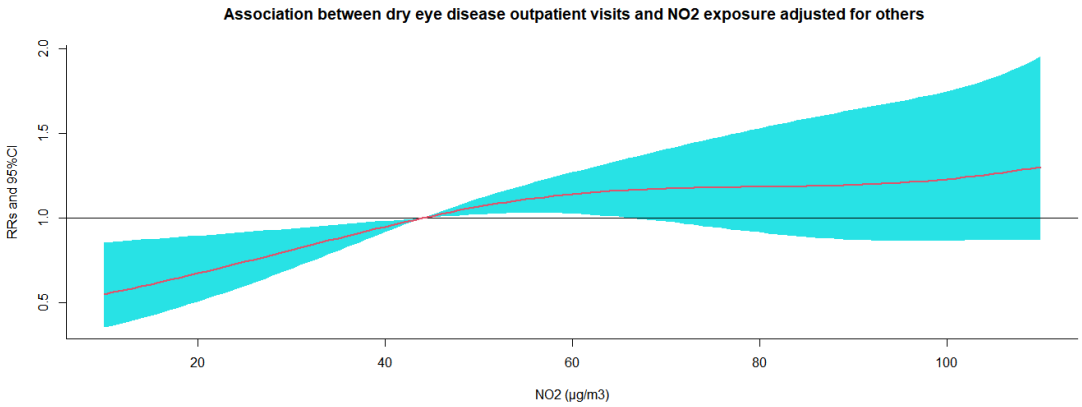

Figure S100. The relative risks (RRs) of per 10 μg/m^3 increase in NO_2 on dry eye disease outpatient visits at various lag days after adjusted for $PM_{2.5}$ exposure.

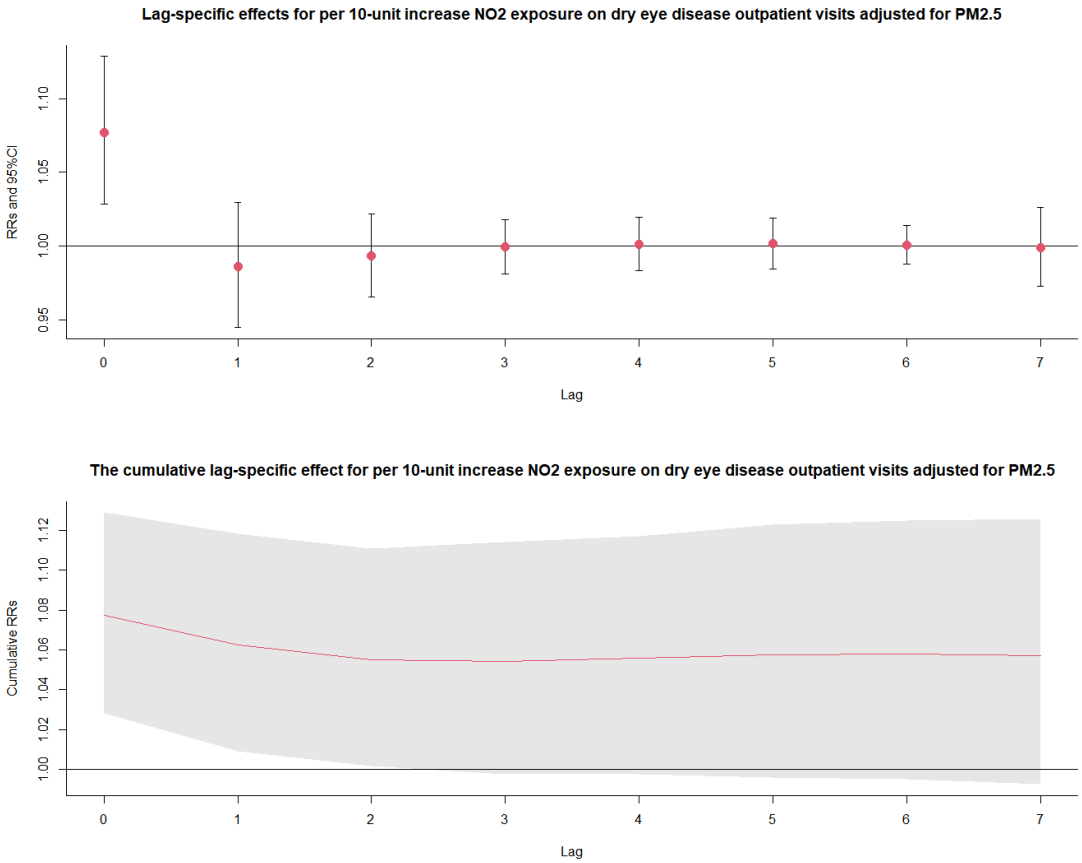

Figure S101. 3D graph and contour map of NO_2 exposure on dry eye disease outpatient visits after adjusted for $PM_{2.5}$ exposure.

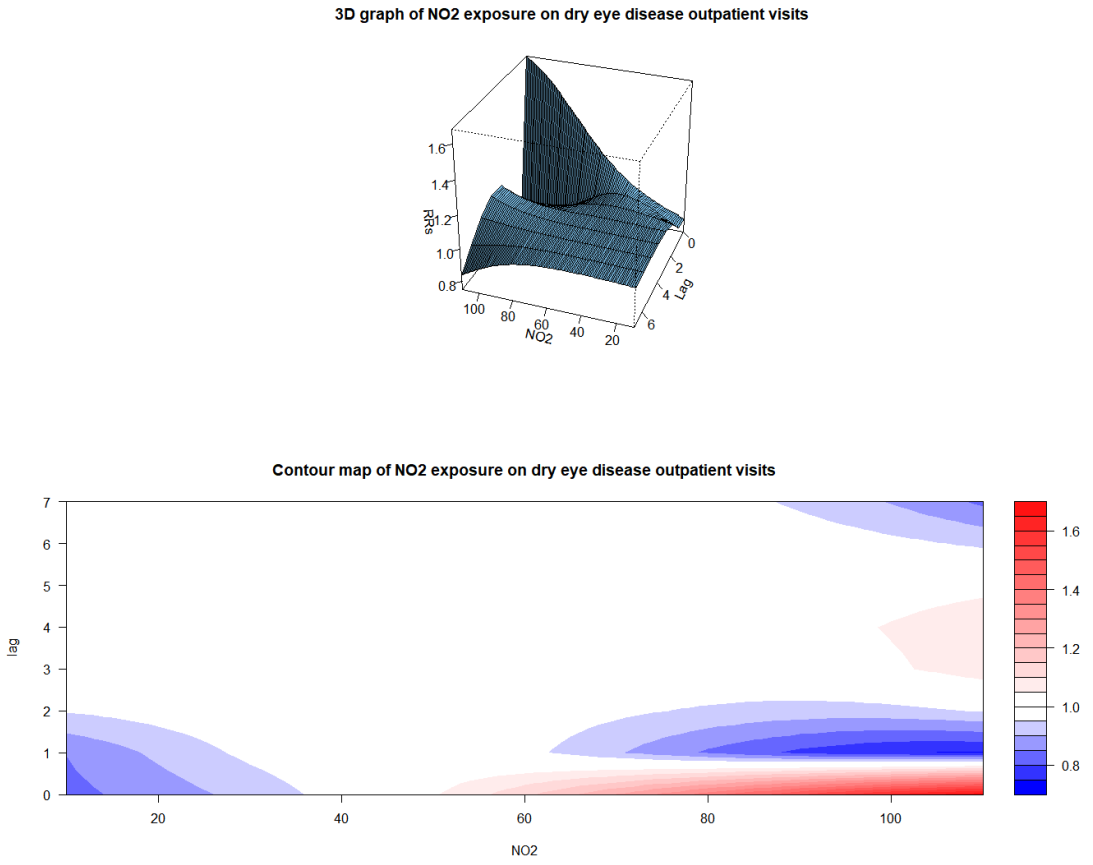

Figure S102. The relative risks (RRs) of per 10 μg/m^3 increase in NO_2 on dry eye disease outpatient visits at various lag days after adjusted for PM_{10} exposure.

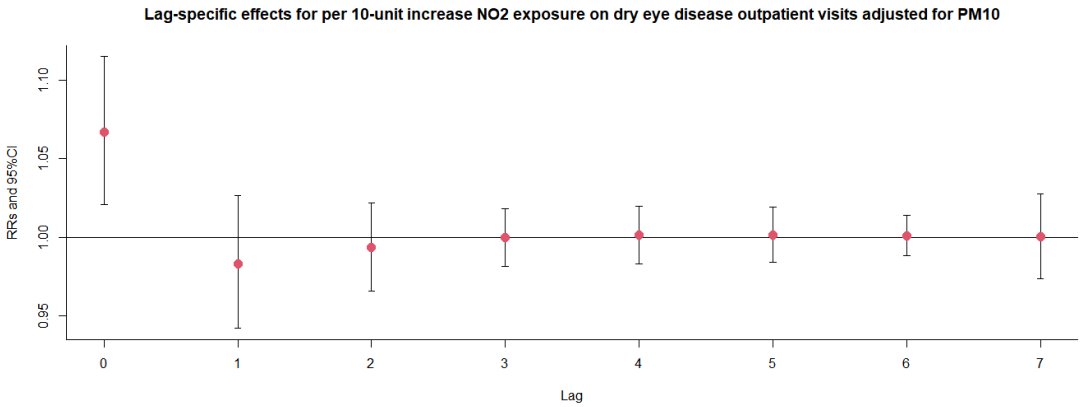

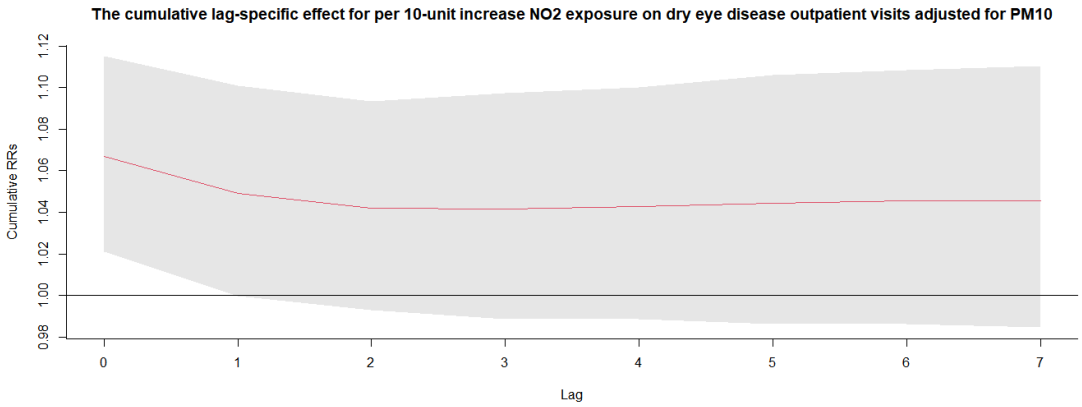

Figure S103. 3D graph and contour map of NO_2 exposure on dry eye disease outpatient visits after adjusted for PM_{10} exposure.

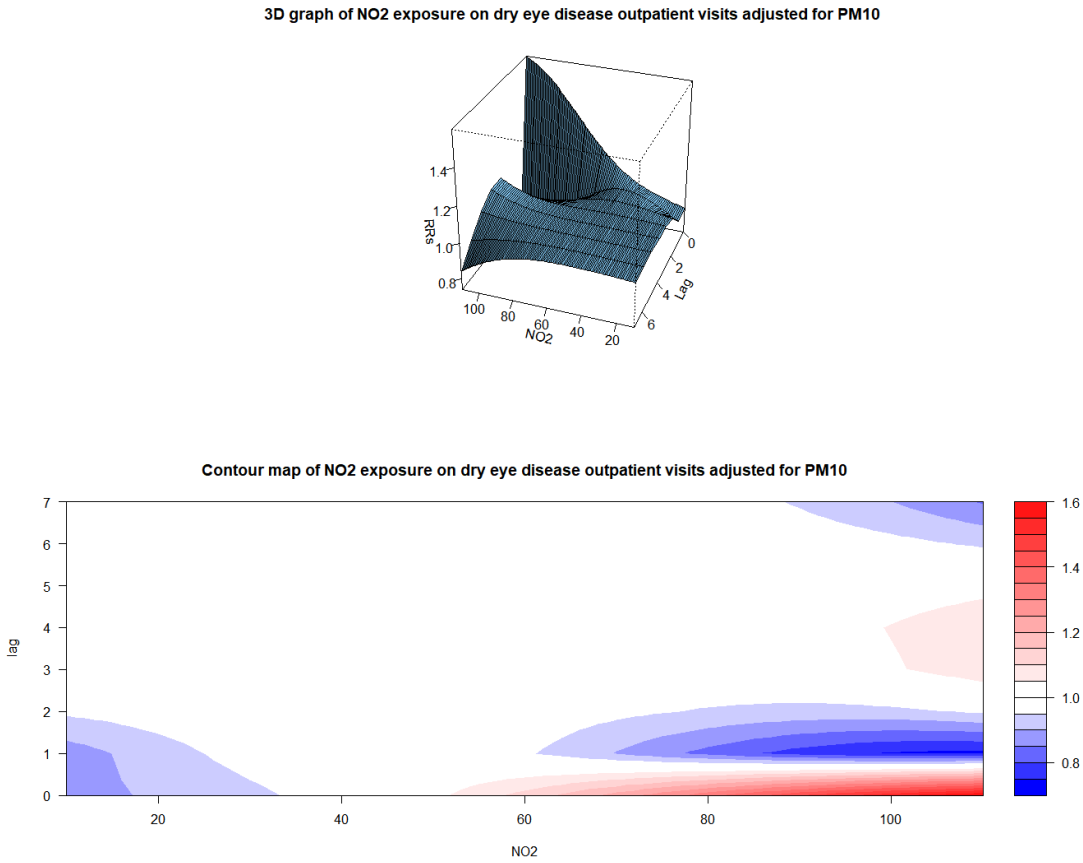

Figure S104. The relative risks (RRs) of per 10 $\mu g/m^3$ increase in NO_2 on dry eye disease outpatient visits at various lag days after adjusted for CO exposure.

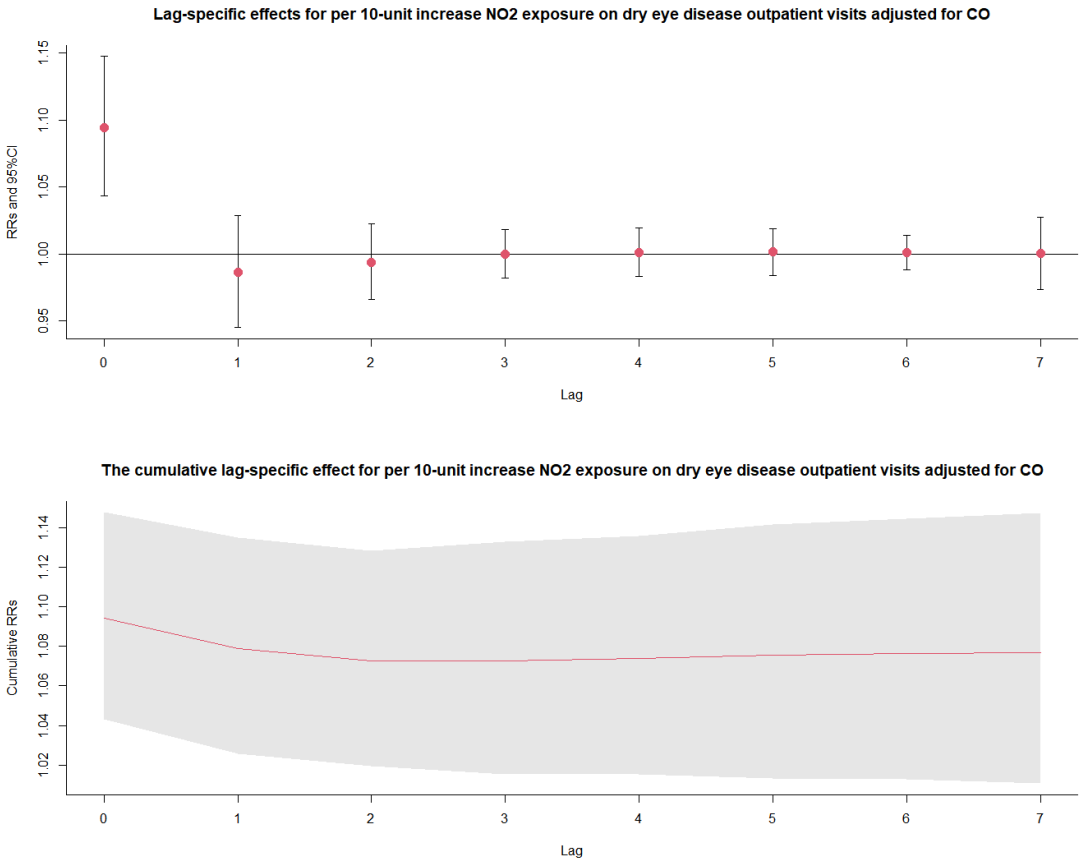

Figure S105. 3D graph and contour map of NO_2 exposure on dry eye disease outpatient visits after adjusted for CO exposure.

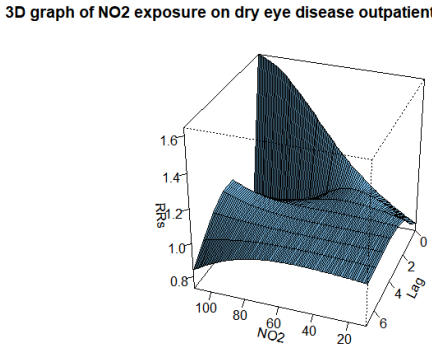

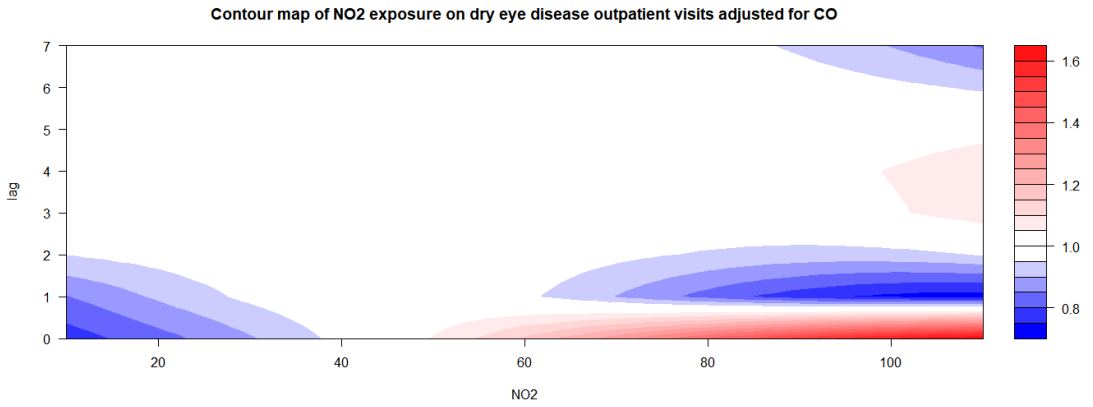

Figure S106. The relative risks (RRs) of per 10 μg/m^3 increase in NO_2 on dry eye disease outpatient visits at various lag days after adjusted for SO_2 exposure.

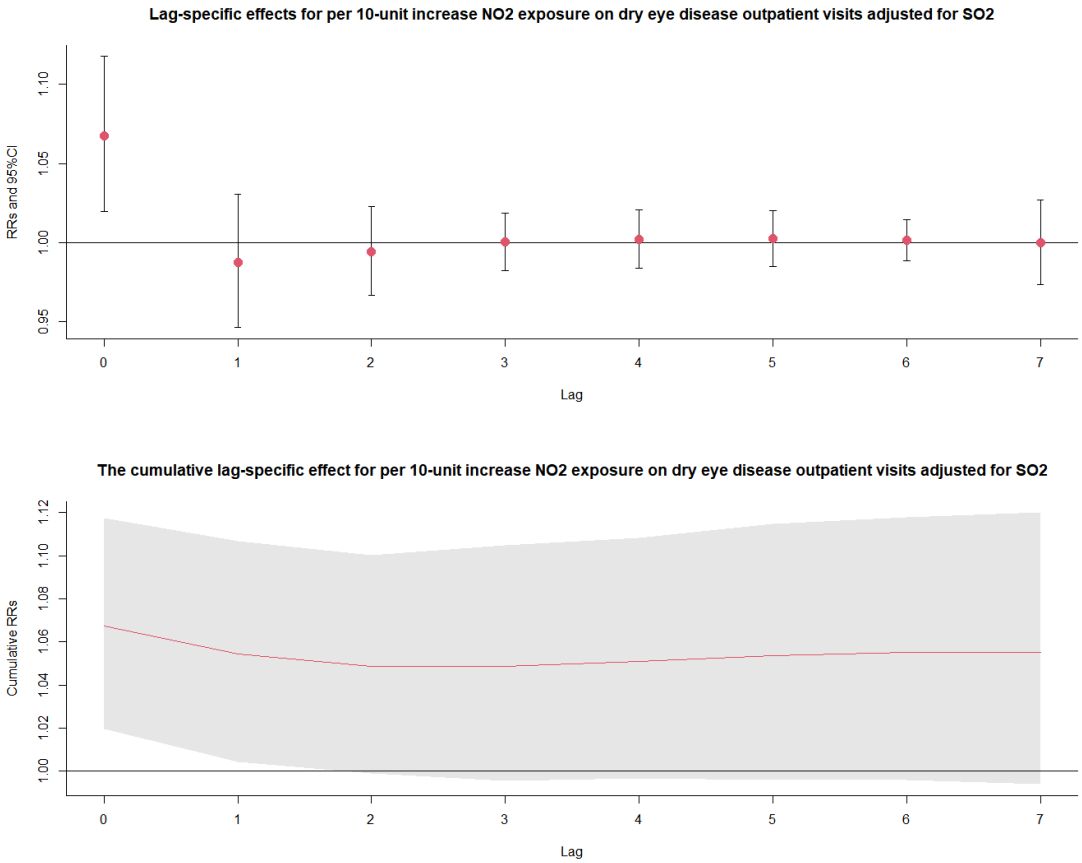

Figure S107. 3D graph and contour map of NO_2 exposure on dry eye disease outpatient visits after adjusted for SO_2 exposure.

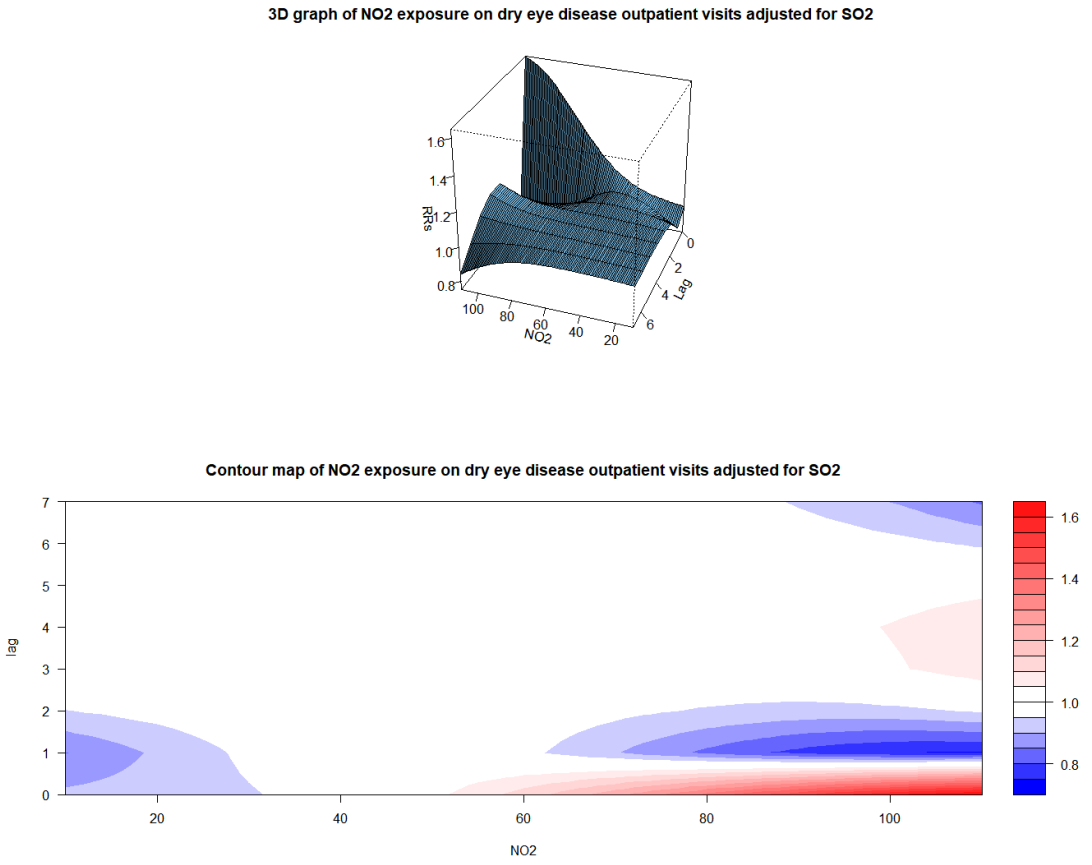

Figure S108. The relative risks (RRs) of per 10 μg/m^3 increase in NO_2 on dry eye disease outpatient visits at various lag days after adjusted for O_3 exposure.

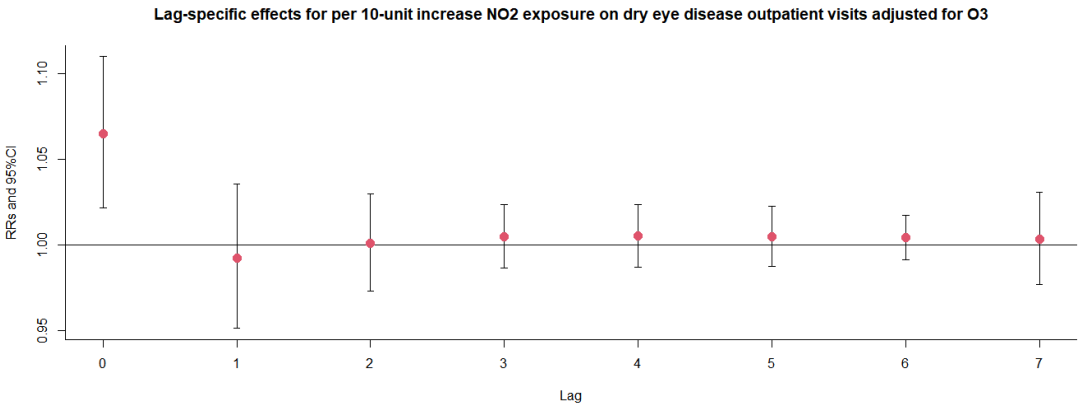

Figure S109. 3D graph and contour map of NO_2 exposure on dry eye disease outpatient visits after adjusted for O_3 exposure.

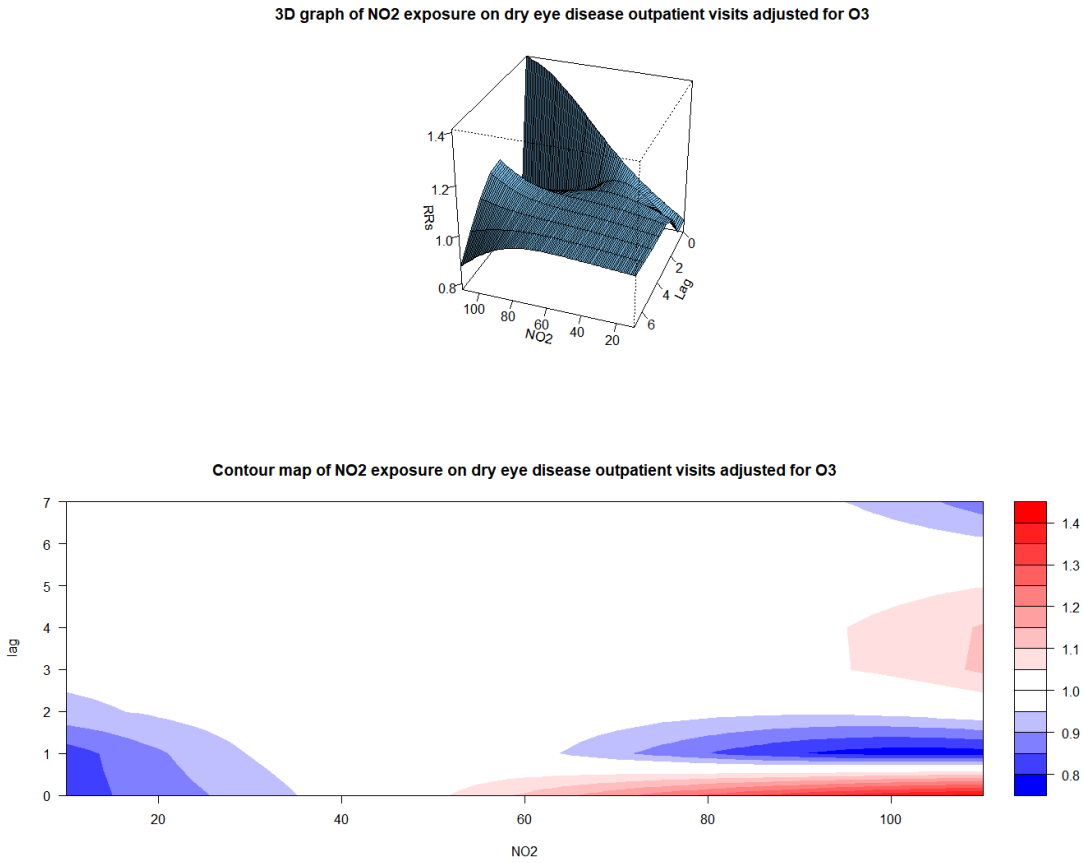

Figure S110. The relative risks (RRs) of per 10 $\mu g/m^3$ increase in NO_2 on dry eye disease outpatient visits at various lag days after adjusted for others exposure.

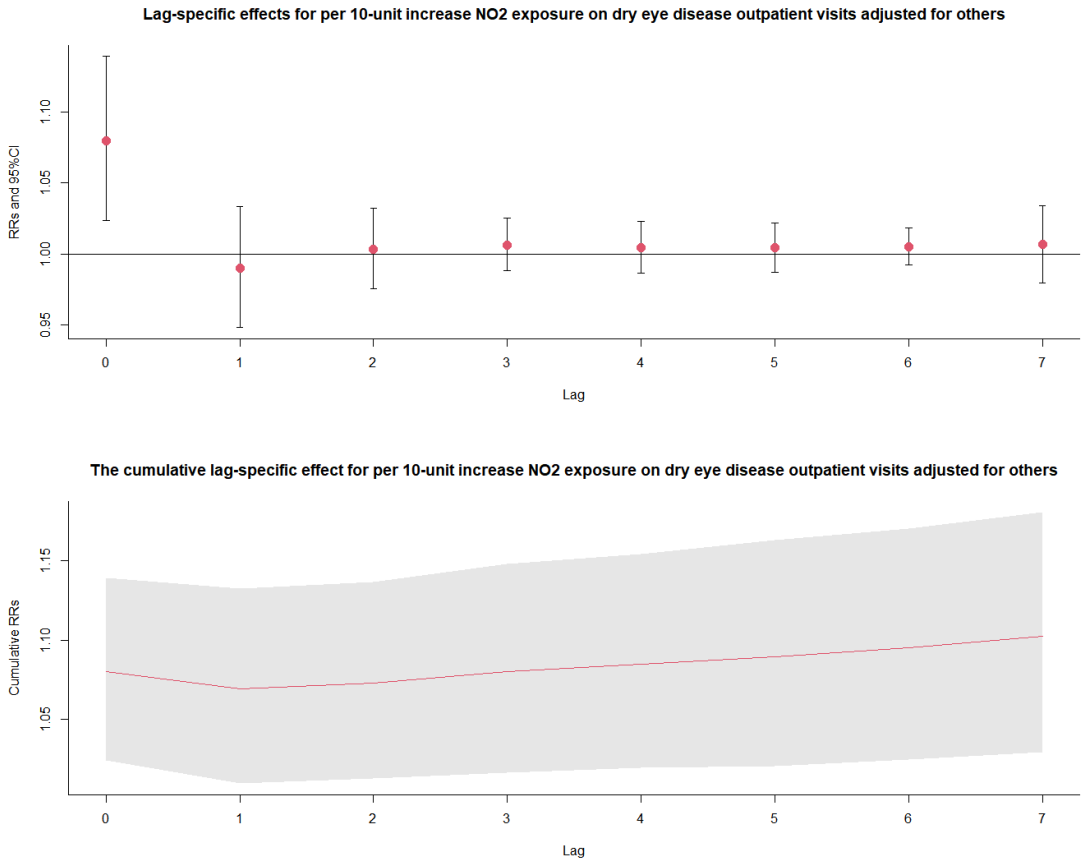

Figure S111. 3D graph and contour map of NO_2 exposure on dry eye disease outpatient visits after adjusted for others exposure.

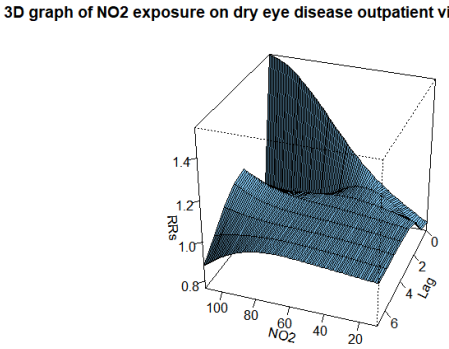

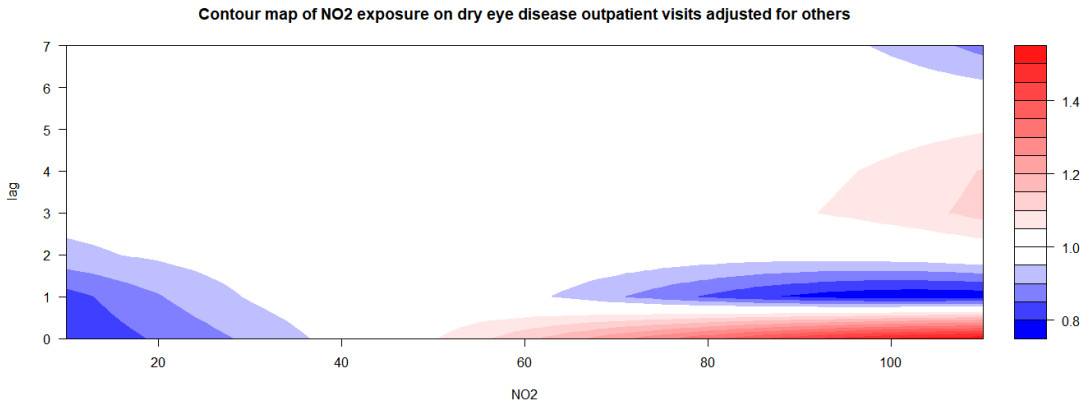

Figure S112. Exposure-response association between dry eye disease outpatient visits and NO_2 exposure in male patients.

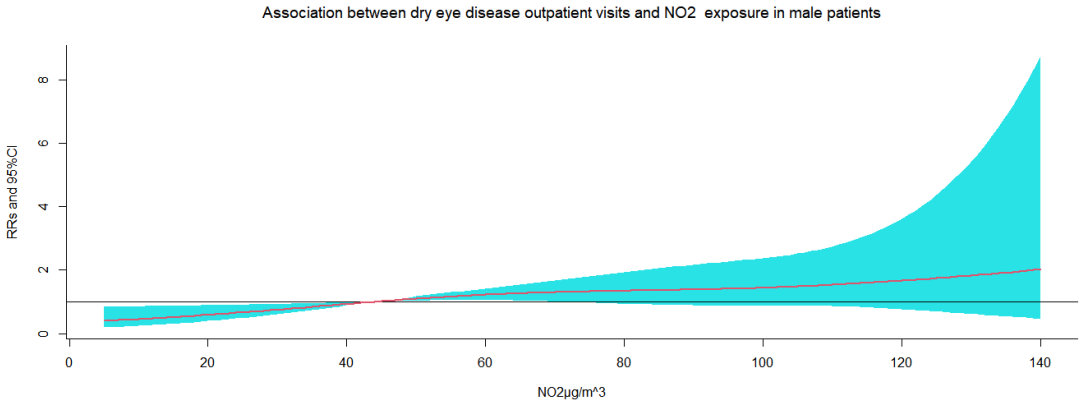

Figure S113. The relative risks (RRs) of per 10 $\mu g/m^3$ increase in NO_2 on dry eye disease outpatient visits at various lag days in male patients.

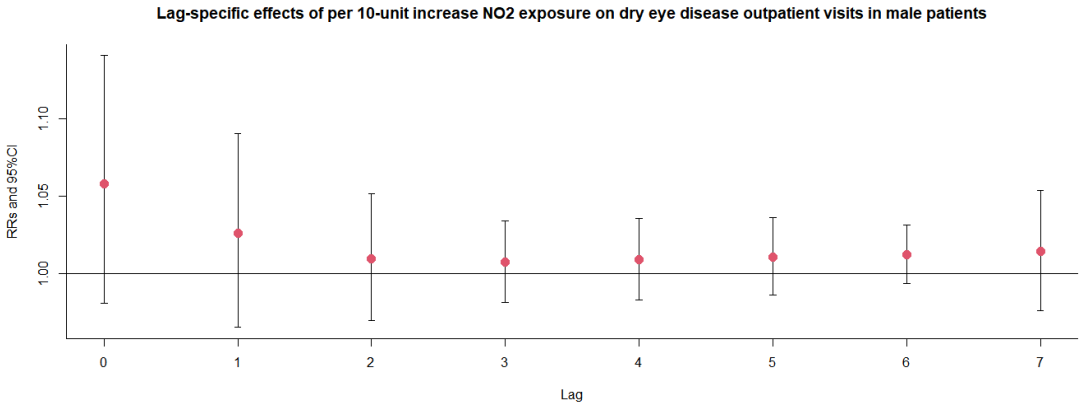

Figure S114. Exposure-response association between dry eye disease outpatient visits and NO_2 exposure in female patients.

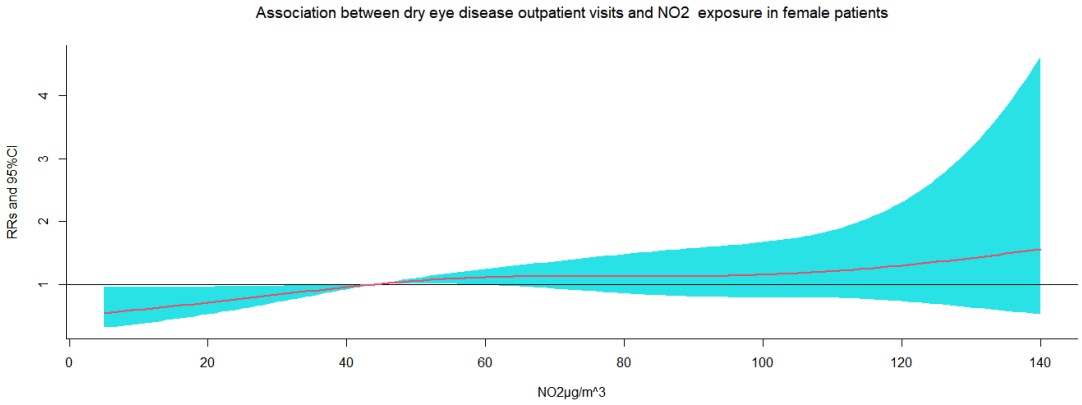

Figure S115. The relative risks (RRs) of per 10 $\mu g/m^3$ increase in NO_2 on dry eye disease outpatient visits at various lag days in female patients.

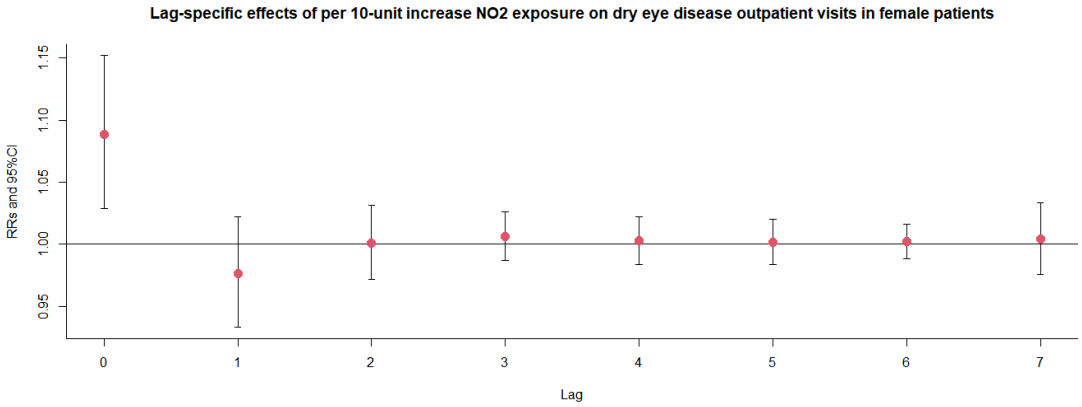

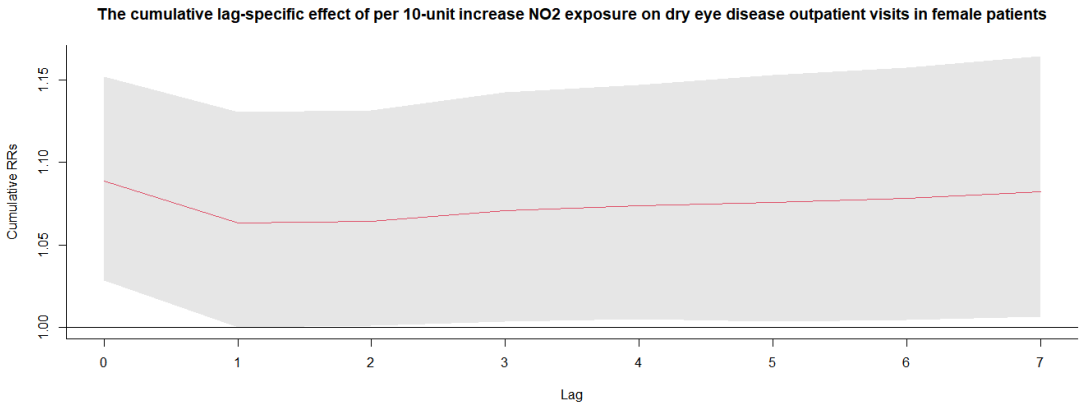

Figure S116. Exposure-response association between dry eye disease outpatient visits and NO_2 exposure in age 0-5 patients.

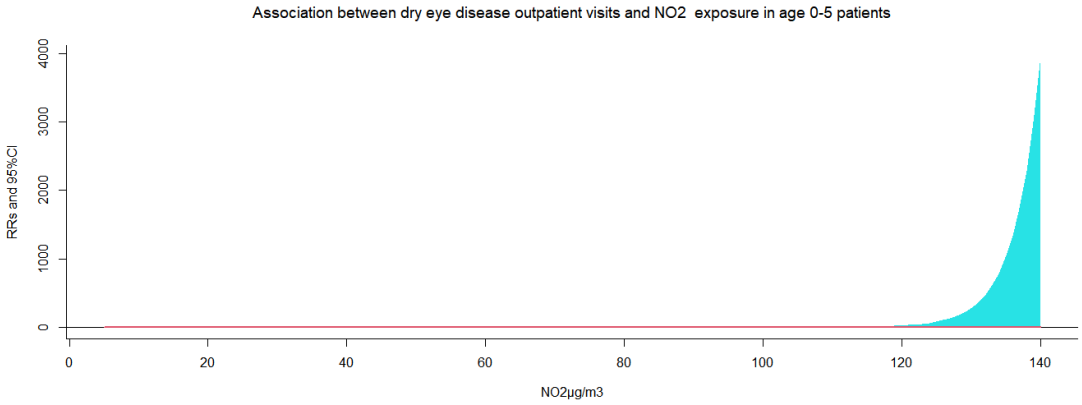

Figure S117. The relative risks (RRs) of per 10 $\mu g/m^3$ increase in NO_2 on dry eye disease outpatient visits at various lag days in age 0-5 patients.

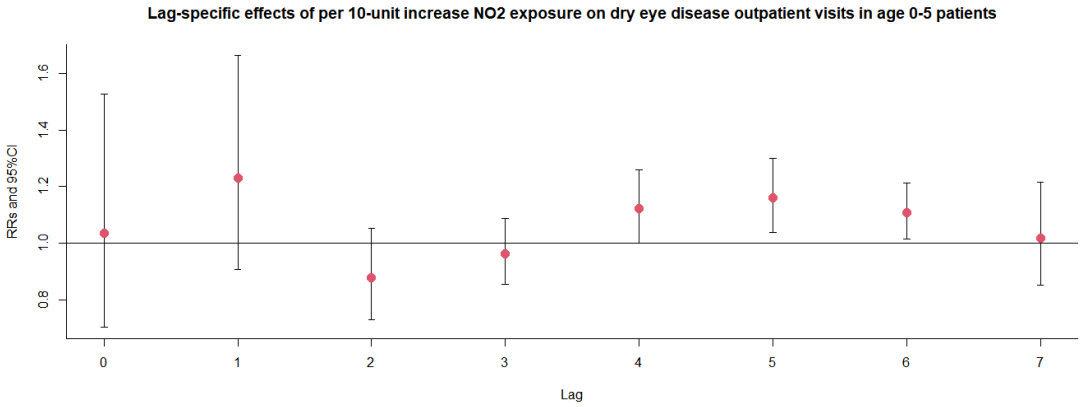

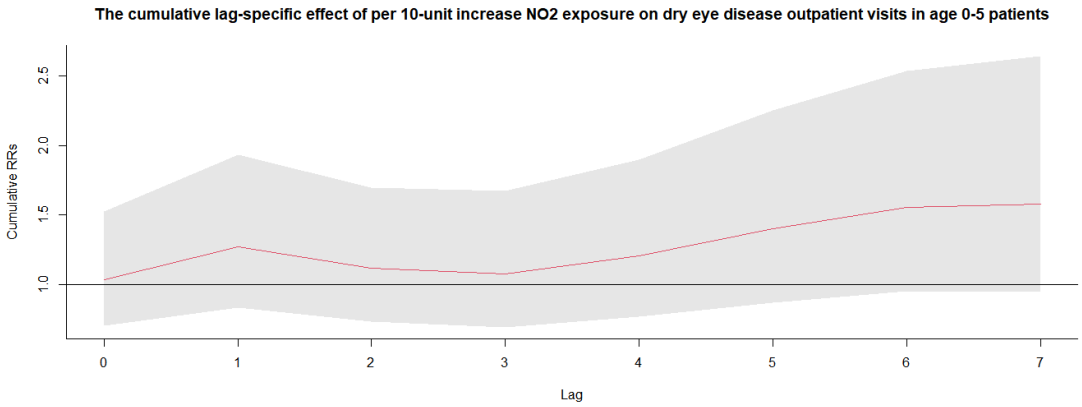

Figure S118. Exposure-response association between dry eye disease outpatient visits and NO_2 exposure in age 6-18 patients.

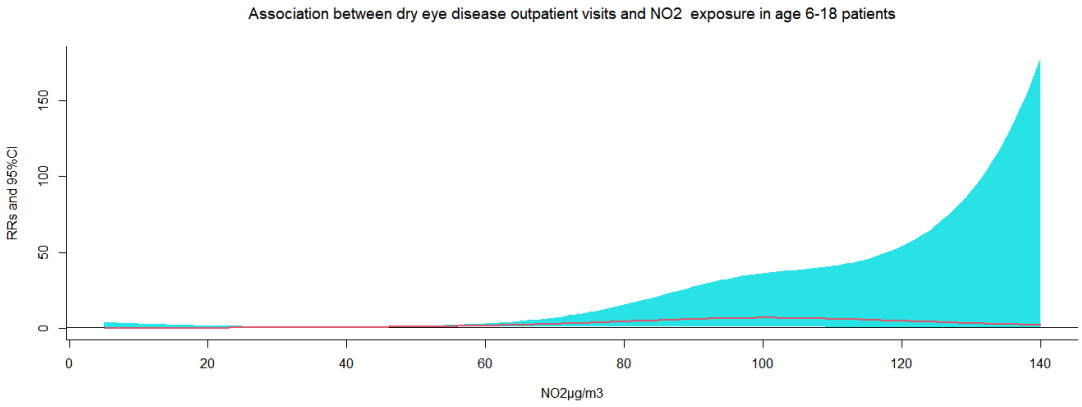

Figure S119. The relative risks (RRs) of per 10 $\mu g/m^3$ increase in NO_2 on dry eye disease outpatient visits at various lag days in age 6-18 patients.

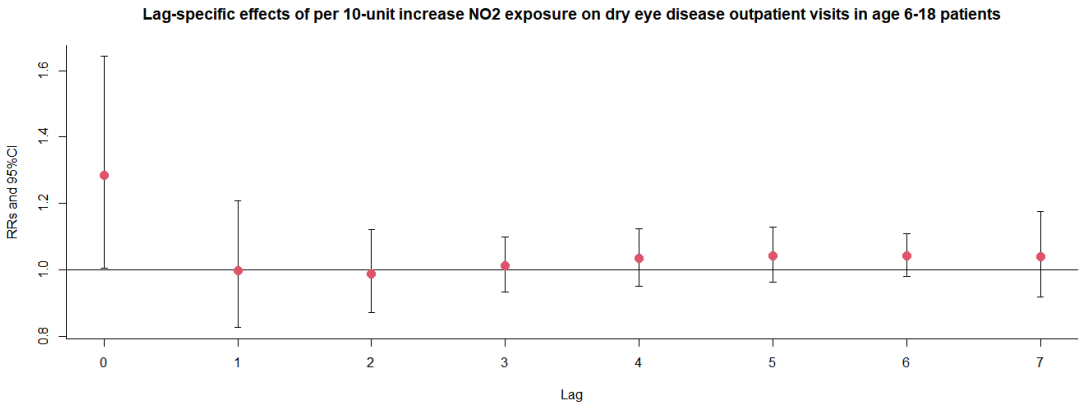

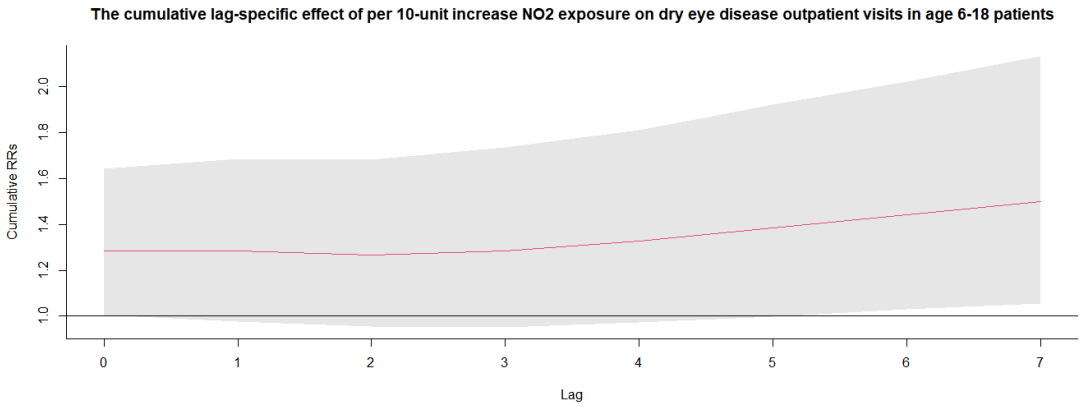

Figure S120. Exposure-response association between dry eye disease outpatient visits and NO_2 exposure in age 19-64 patients.

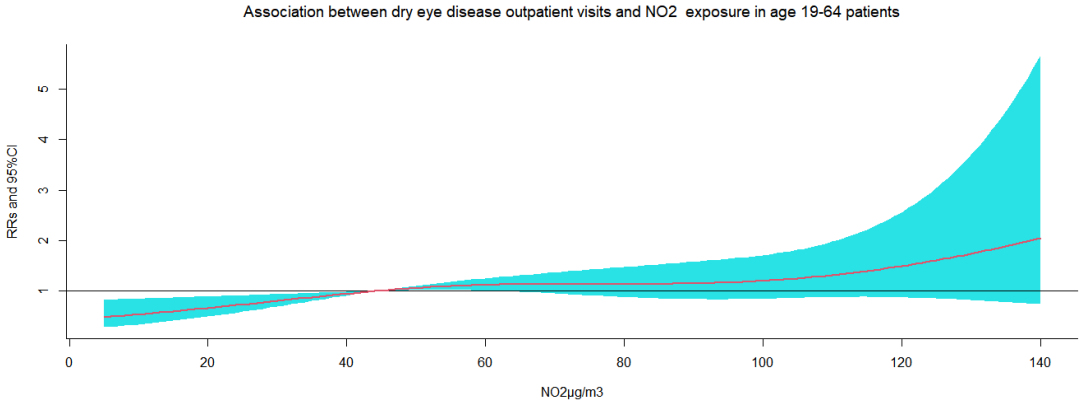

Figure S121. The relative risks (RRs) of per 10 μg/m^3 increase in NO_2 on dry eye disease outpatient visits at various lag days in age 19-64 patients.

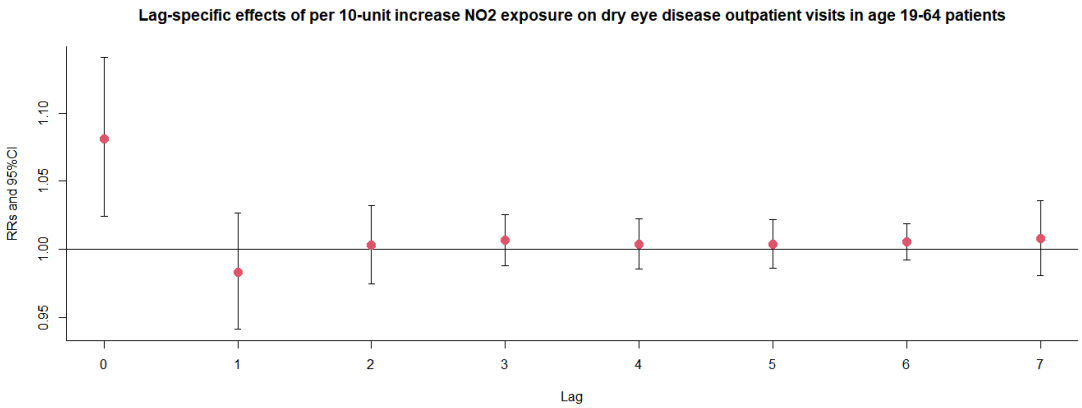

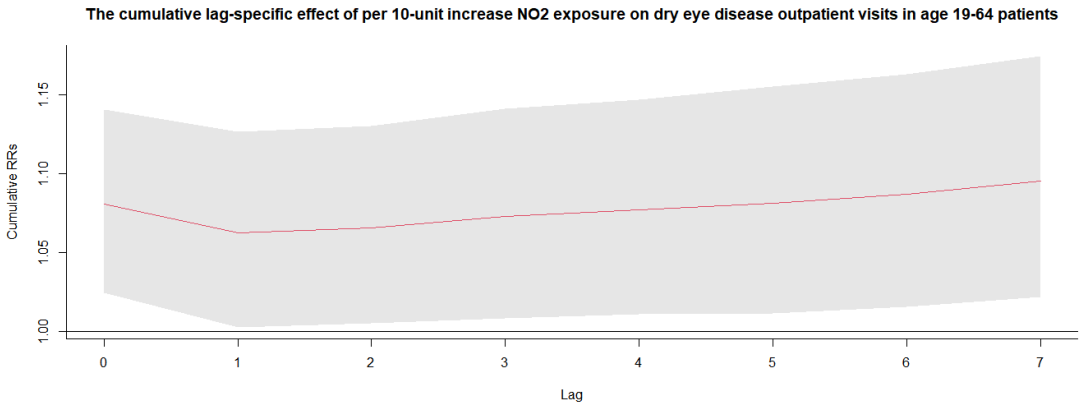

Figure S122. Exposure-response association between dry eye disease outpatient visits and NO_2 exposure in age ≥65 patients.

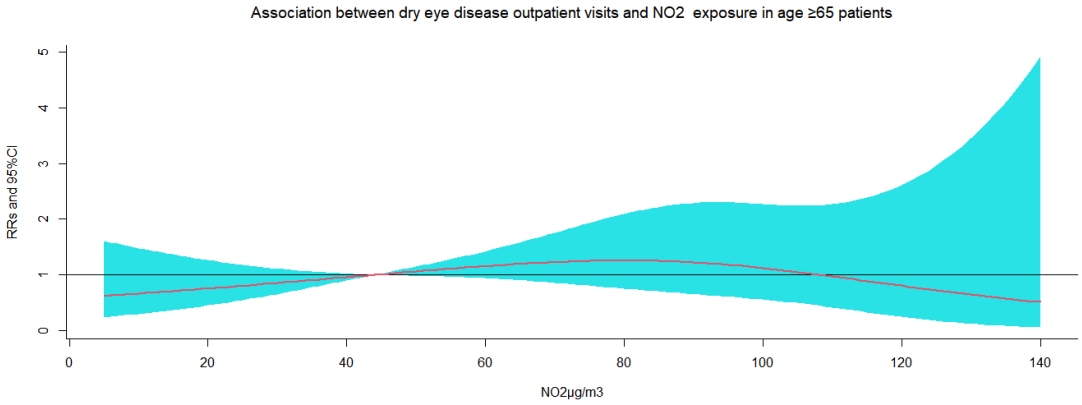

Figure S123. The relative risks (RRs) of per 10 μg/m^3 increase in NO_2 on dry eye disease outpatient visits at various lag days in age ≥65 patients.

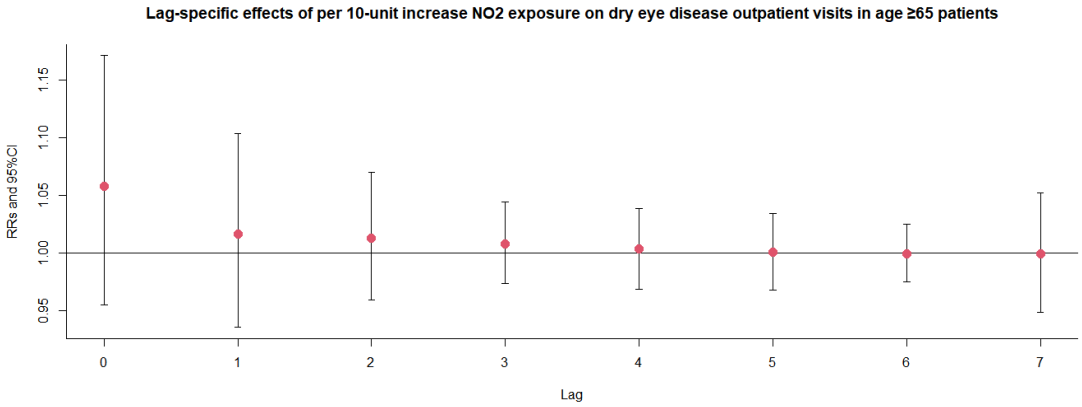

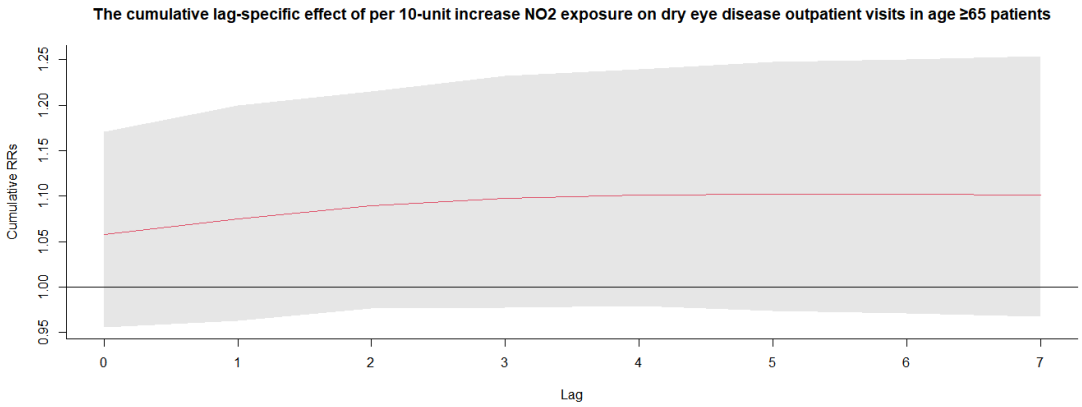

Figure S124. Exposure-response association between dry eye disease outpatient visits and NO_2 exposure in the warm season.

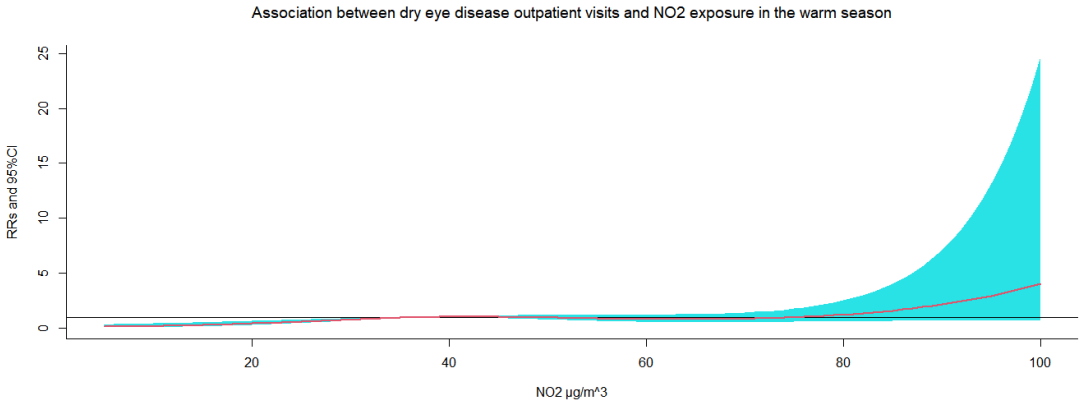

Figure S125. The relative risks (RRs) of per 10 $\mu g/m^3$ increase in NO_2 on dry eye disease outpatient visits at various lag days in the warm season.

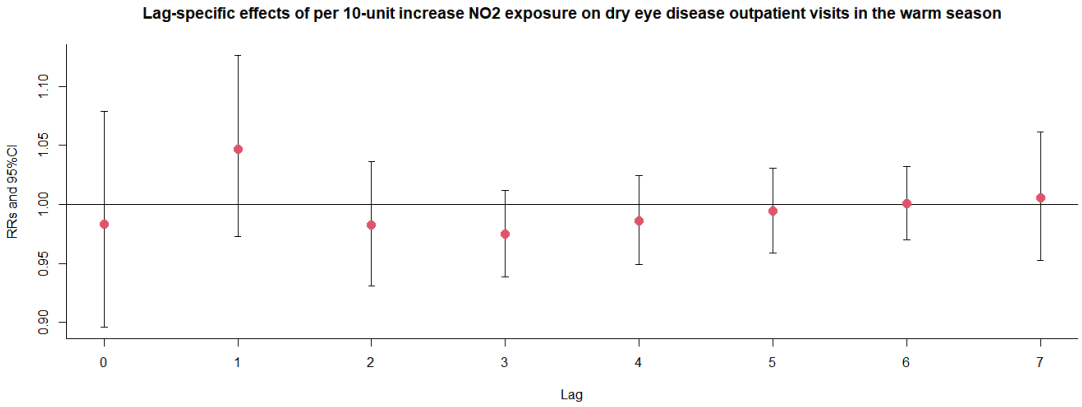

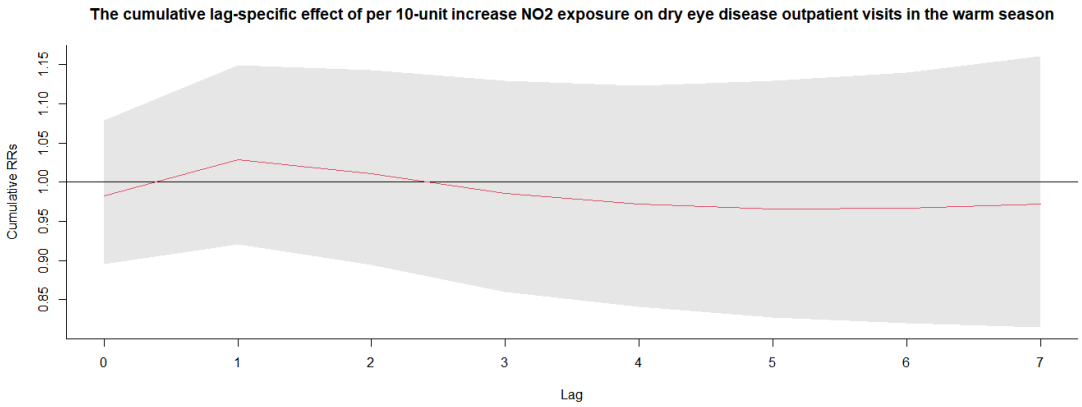

Figure S126. Exposure-response association between dry eye disease outpatient visits and NO_2 exposure in the cold season.

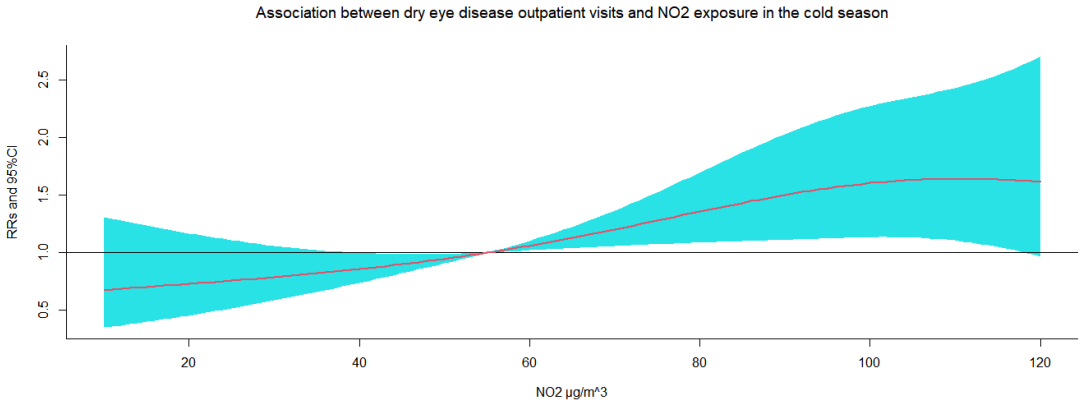

Figure S127. The relative risks (RRs) of per 10 $\mu g/m^3$ increase in NO_2 on dry eye disease outpatient visits at various lag days in the cold season.

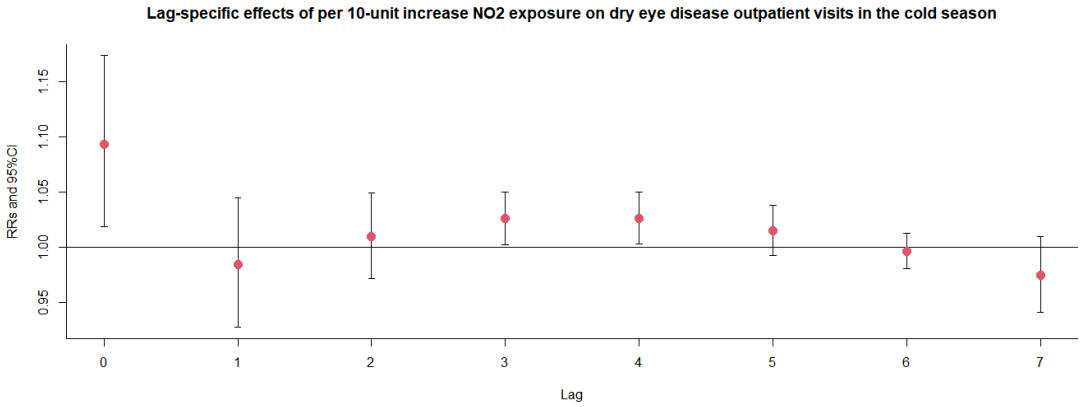

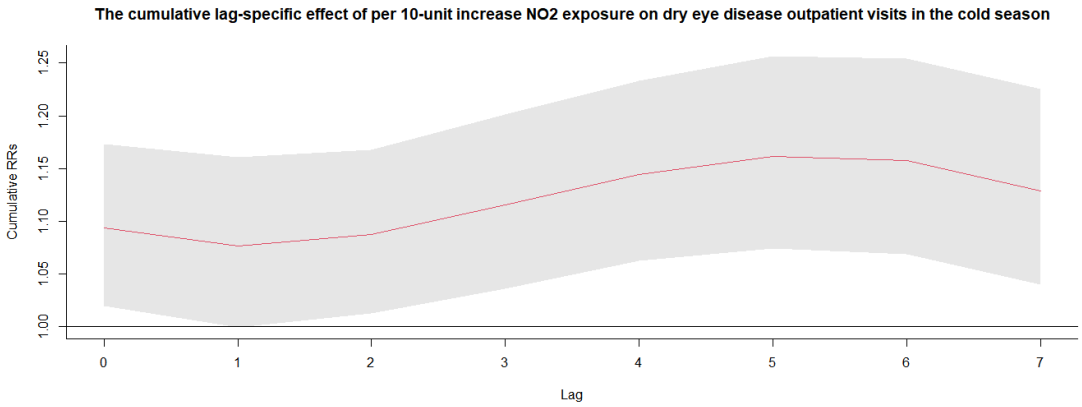

Figure S128. Exposure-response association between dry eye disease outpatient visits and SO_2 exposure.

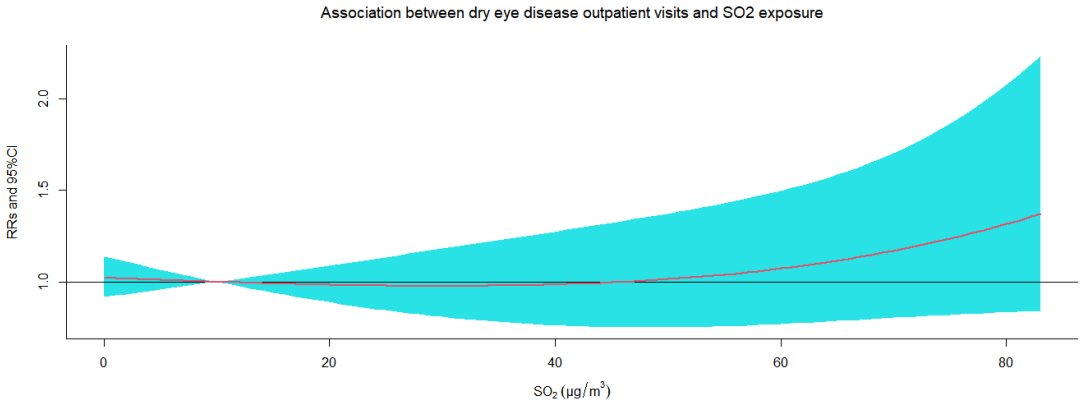

Figure S129. The relative risks (RRs) of per 10 $\mu g/m^3$ increase in SO_2 on dry eye disease outpatient visits at various lag days.

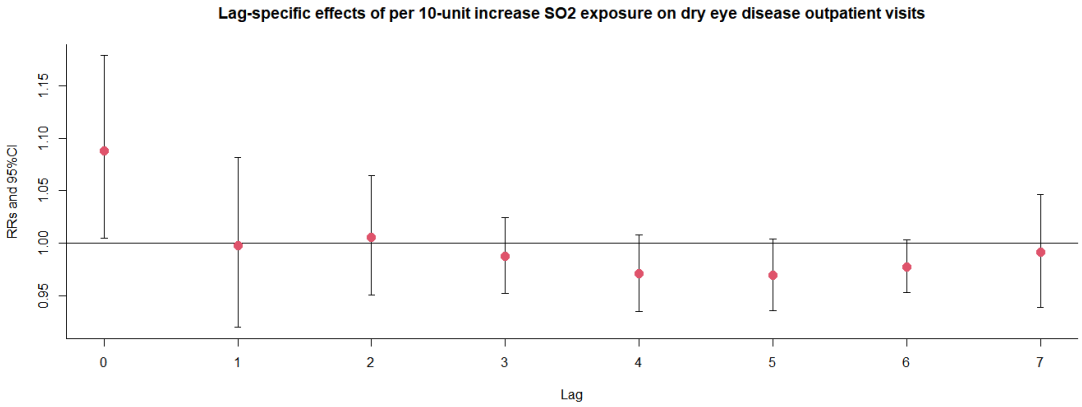

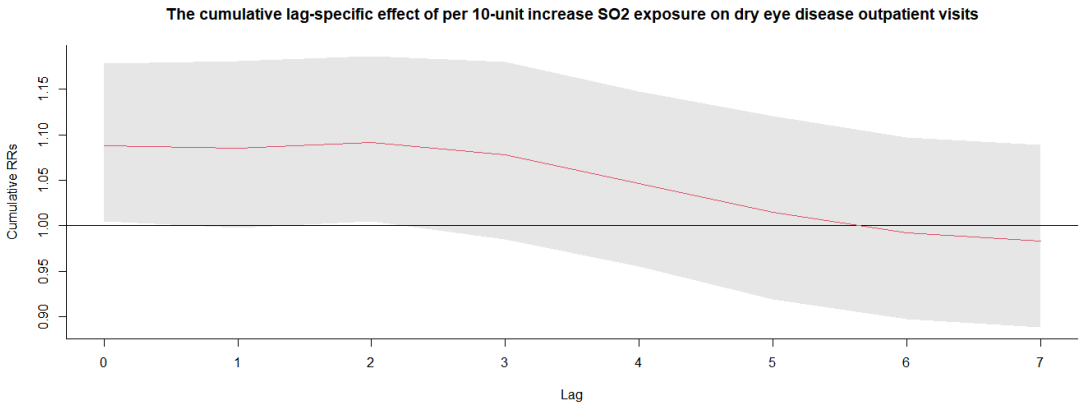

Figure S130. 3D graph and contour map of SO_2 exposure on dry eye disease outpatient visits.

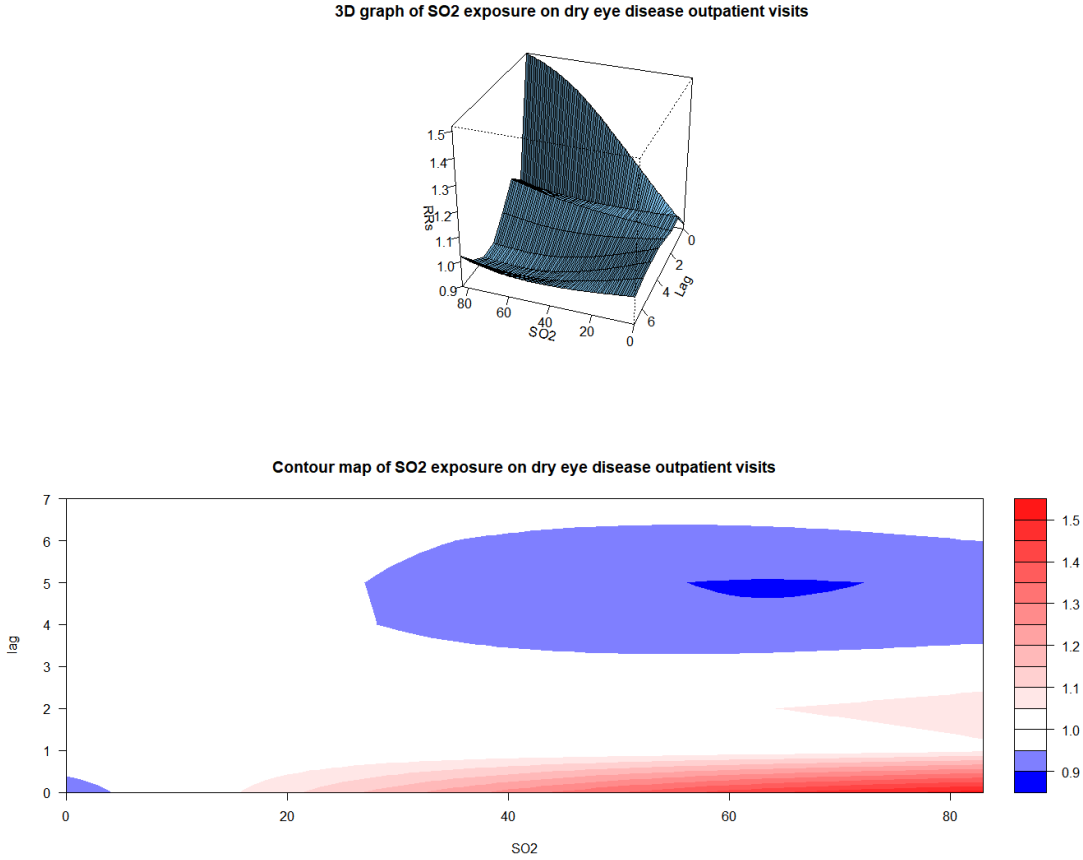

Figure S131. Exposure-response association between dry eye disease outpatient visits and SO_2 exposure after adjusted for other air pollution.

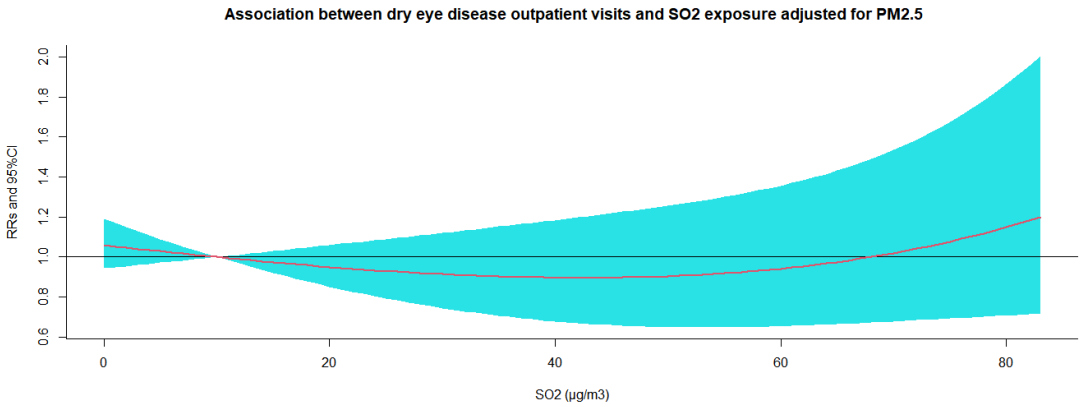
Association between dry eye disease outpatient visits and SO2 exposure adjusted for PM2.5
RRs and 95%CI
0.6
0.8
1.0
1.2
1.4
1.6
1.8
2.0
0
20
40
60
80
SO2 (μg/m3)

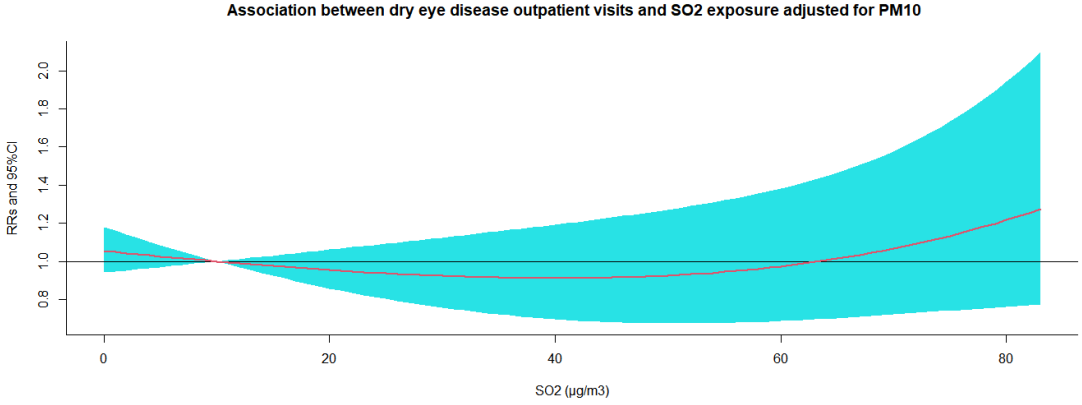
Association between dry eye disease outpatient visits and SO2 exposure adjusted for PM10
RRs and 95%CI
0.8
1.0
1.2
1.4
1.6
1.8
2.0
0
20
40
60
80
SO2 (μg/m3)

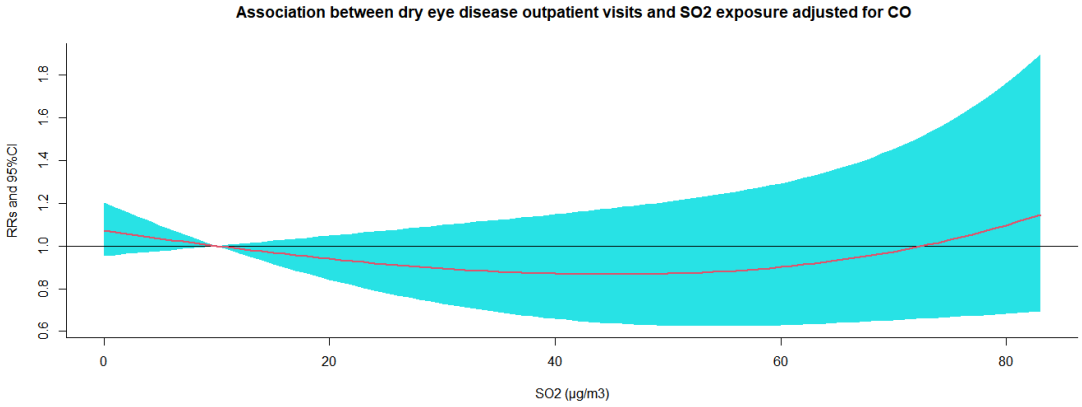
Association between dry eye disease outpatient visits and SO2 exposure adjusted for CO
RRs and 95%CI
0.6
0.8
1.0
1.2
1.4
1.6
1.8
0
20
40
60
80
SO2 (μg/m3)

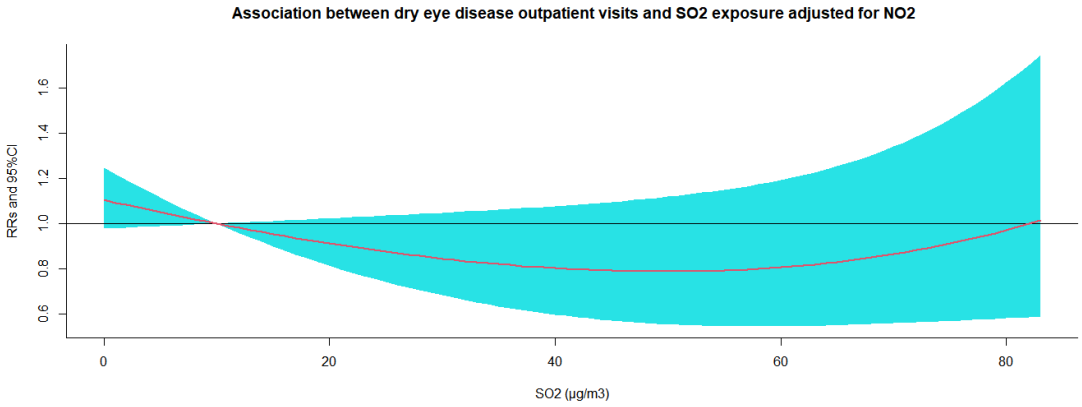
Association between dry eye disease outpatient visits and SO2 exposure adjusted for NO2
RRs and 95%CI
0.6
0.8
1.0
1.2
1.4
1.6
0
20
40
60
80
SO2 (μg/m3)

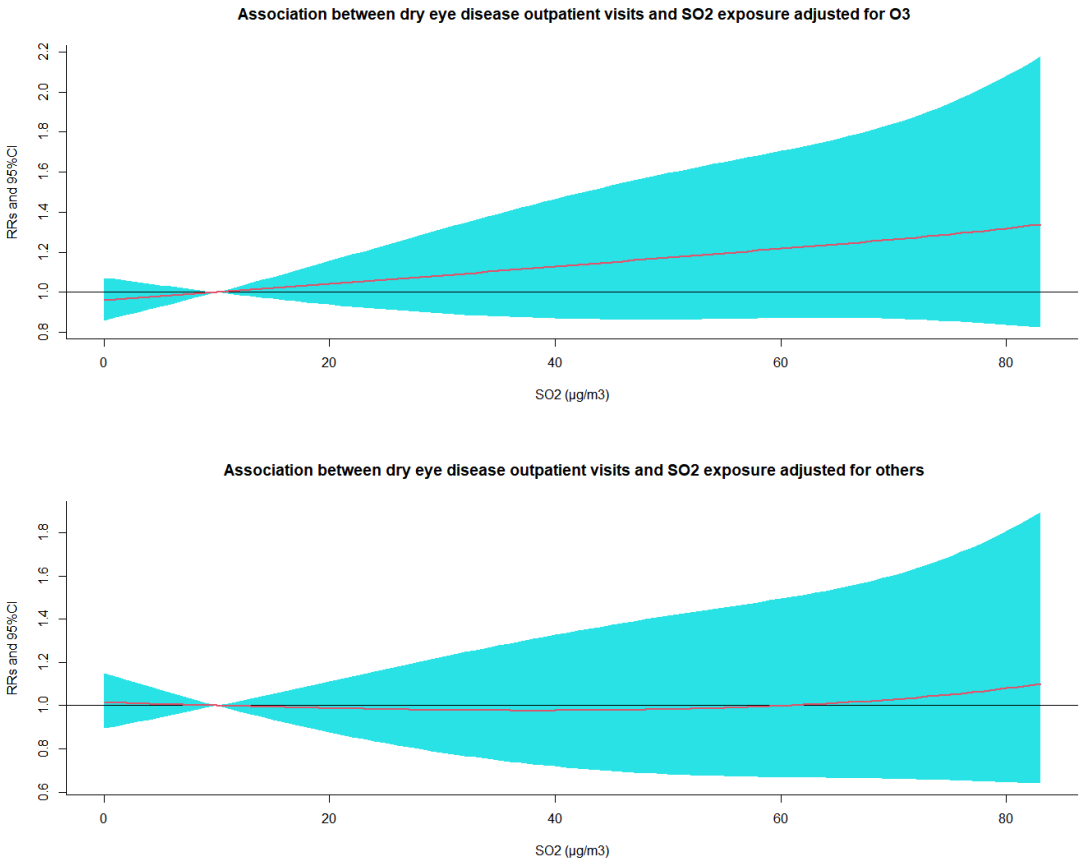

Figure S132. The relative risks (RRs) of per 10 μg/m^3 increase in SO_2 on dry eye disease outpatient visits at various lag days after adjusted for NO_2 exposure.

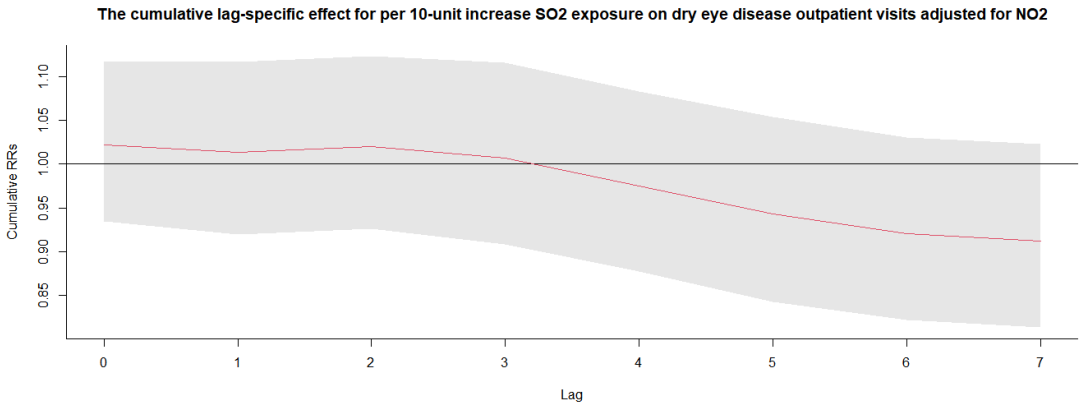

Figure S133. 3D graph and contour map of SO_2 exposure on dry eye disease outpatient visits after adjusted for NO_2 exposure.

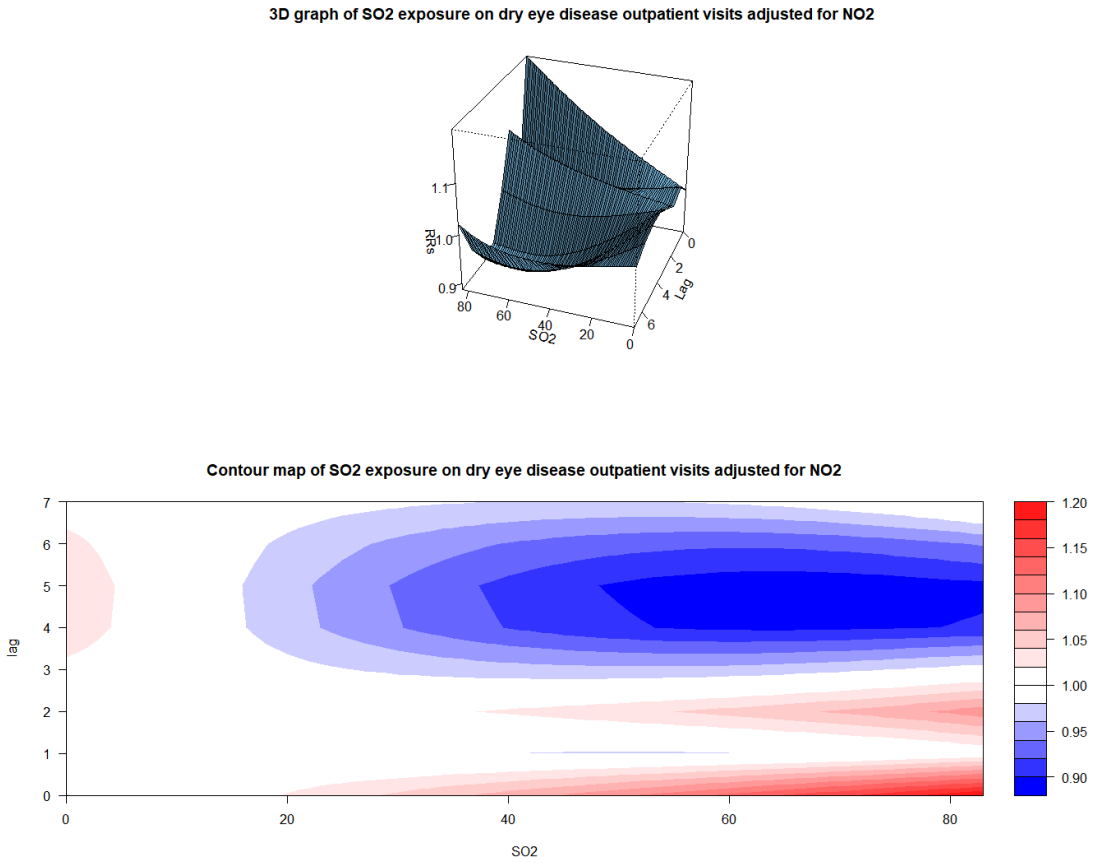

Figure S134. The relative risks (RRs) of per 10 μg/m^3 increase in SO_2 on dry eye disease outpatient visits at various lag days after adjusted for PM_{10} exposure.

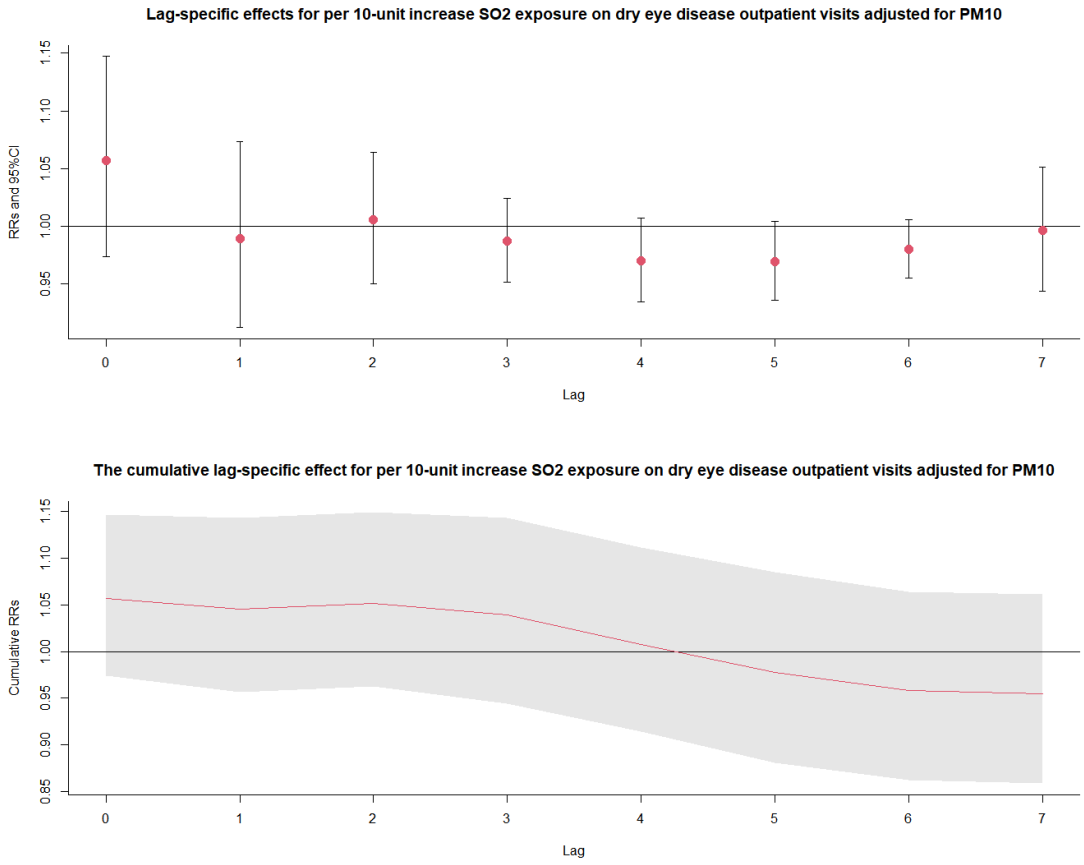

Figure S135. 3D graph and contour map of SO_2 exposure on dry eye disease outpatient visits after adjusted for PM_{10} exposure.

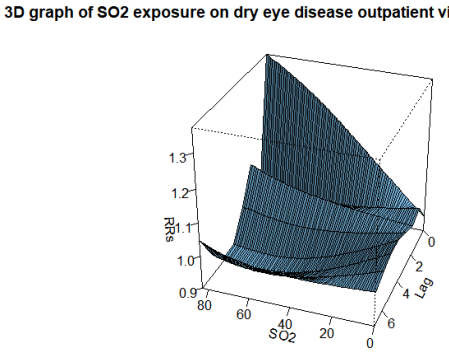

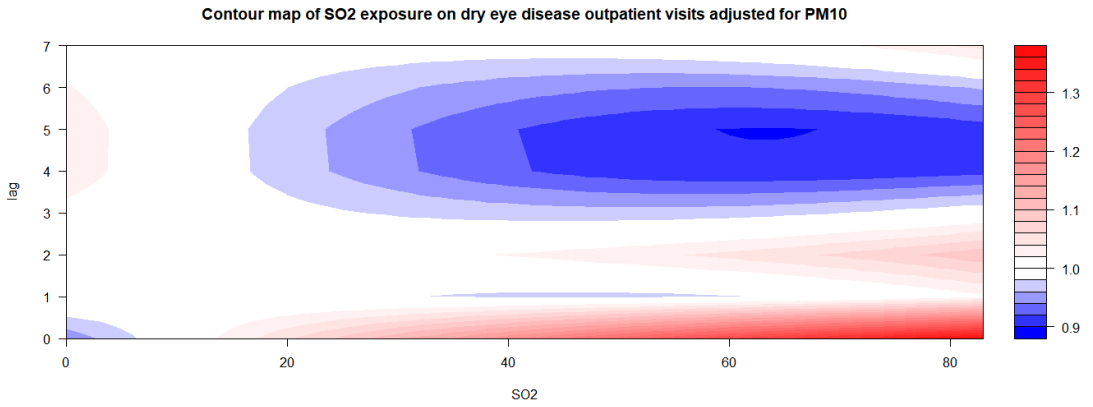

Figure S136. The relative risks (RRs) of per 10 μg/m^3 increase in SO_2 on dry eye disease outpatient visits at various lag days after adjusted for CO exposure.

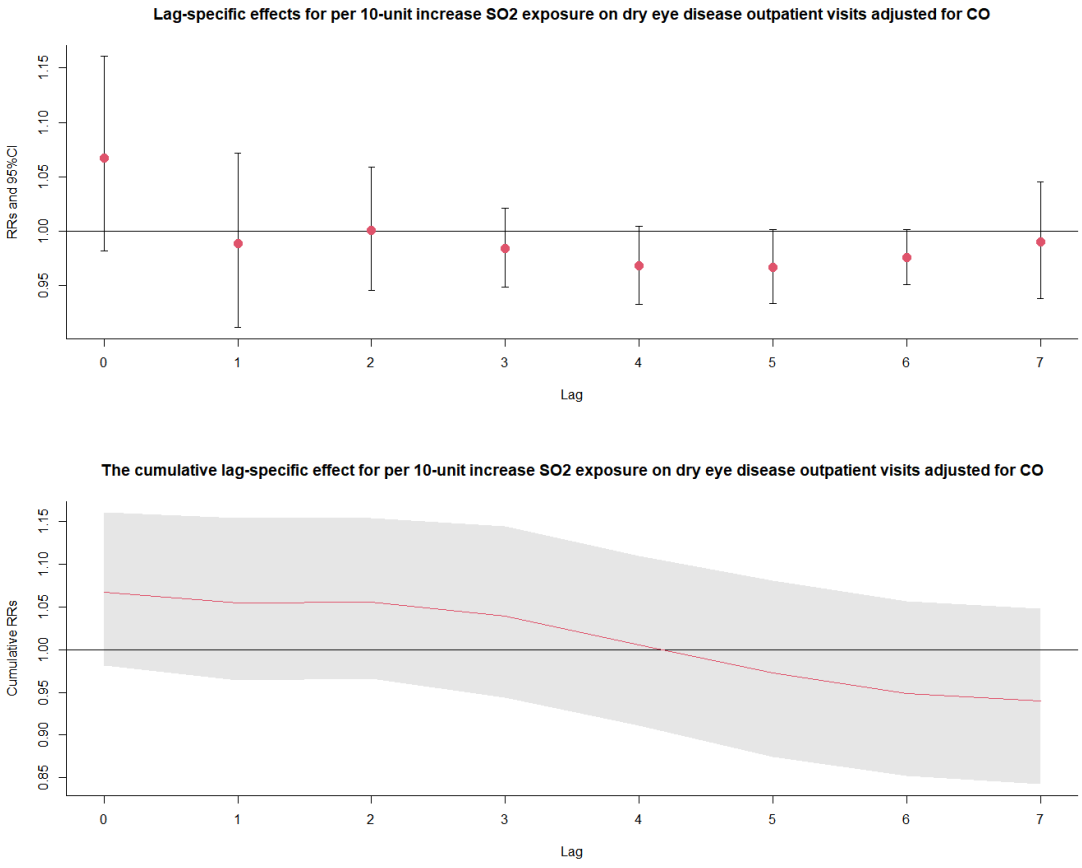

Figure S137. 3D graph and contour map of SO_2 exposure on dry eye disease outpatient visits after adjusted for CO exposure.

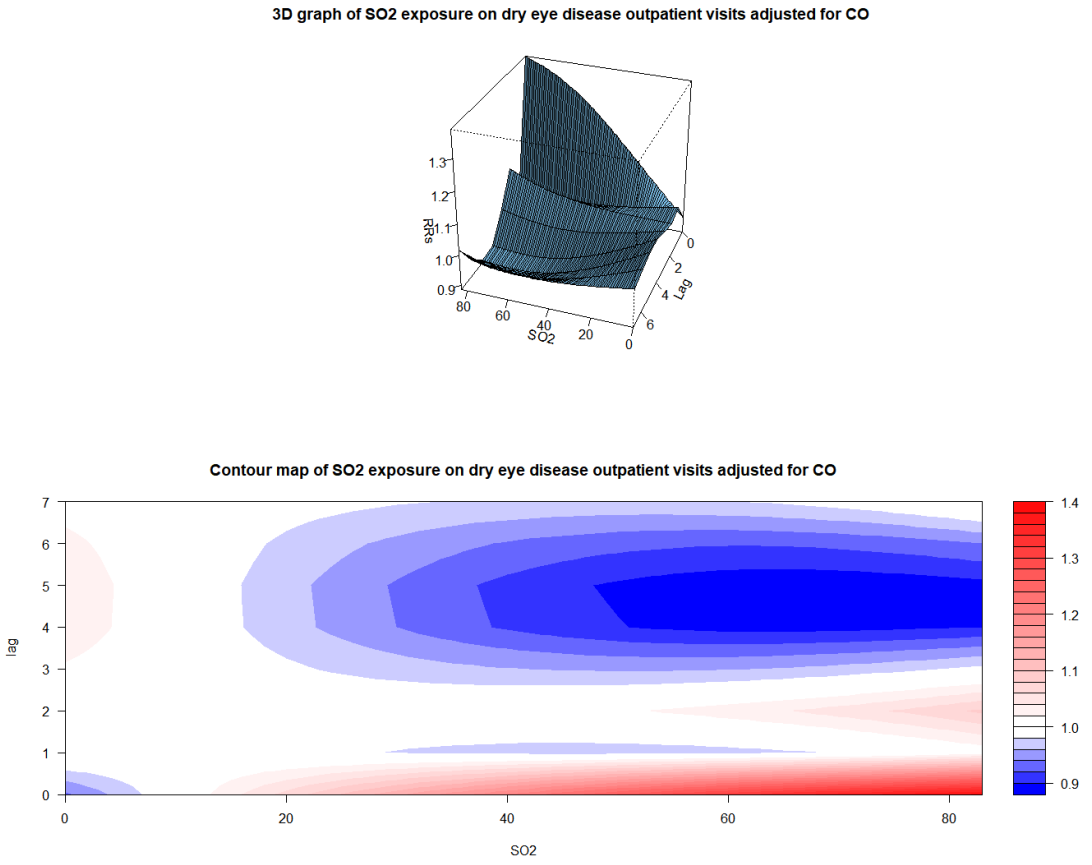

Figure S138. The relative risks (RRs) of per 10 μg/m^3 increase in SO_2 on dry eye disease outpatient visits at various lag days after adjusted for $PM_{2.5}$ exposure.

Figure S139. 3D graph and contour map of SO_2 exposure on dry eye disease outpatient visits after adjusted for $PM_{2.5}$ exposure.

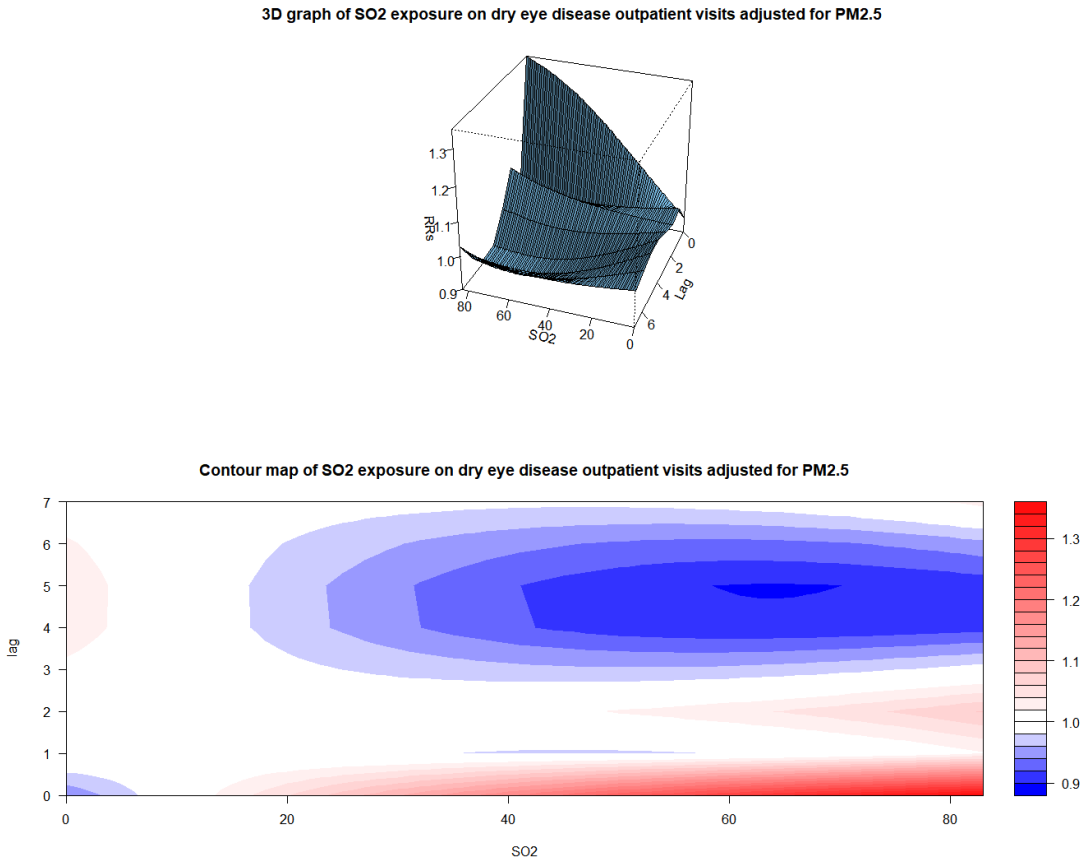

Figure S140. The relative risks (RRs) of per 10 μg/m^3 increase in SO_2 on dry eye disease outpatient visits at various lag days after adjusted for O_3 exposure.

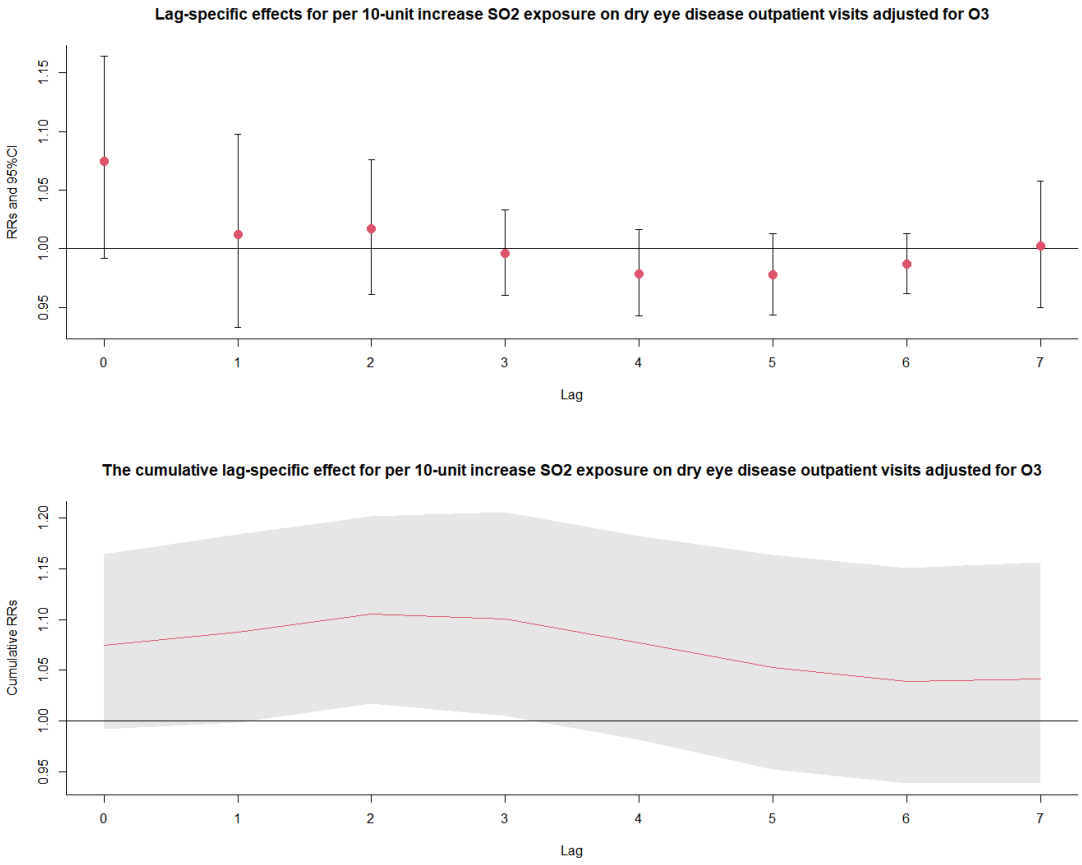

Figure S141. 3D graph and contour map of SO_2 exposure on dry eye disease outpatient visits after adjusted for O_3 exposure.

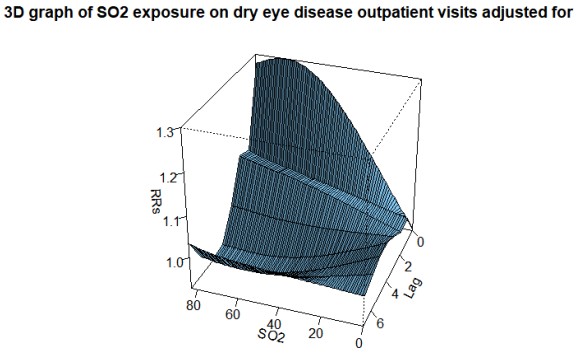

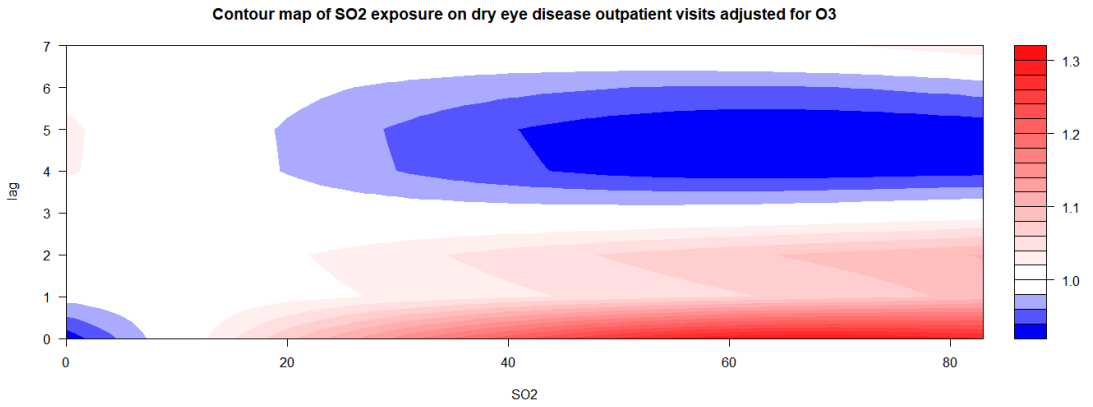

Figure S142. The relative risks (RRs) of per 10 μg/m^3 increase in SO_2 on dry eye disease outpatient visits at various lag days after adjusted for others exposure.

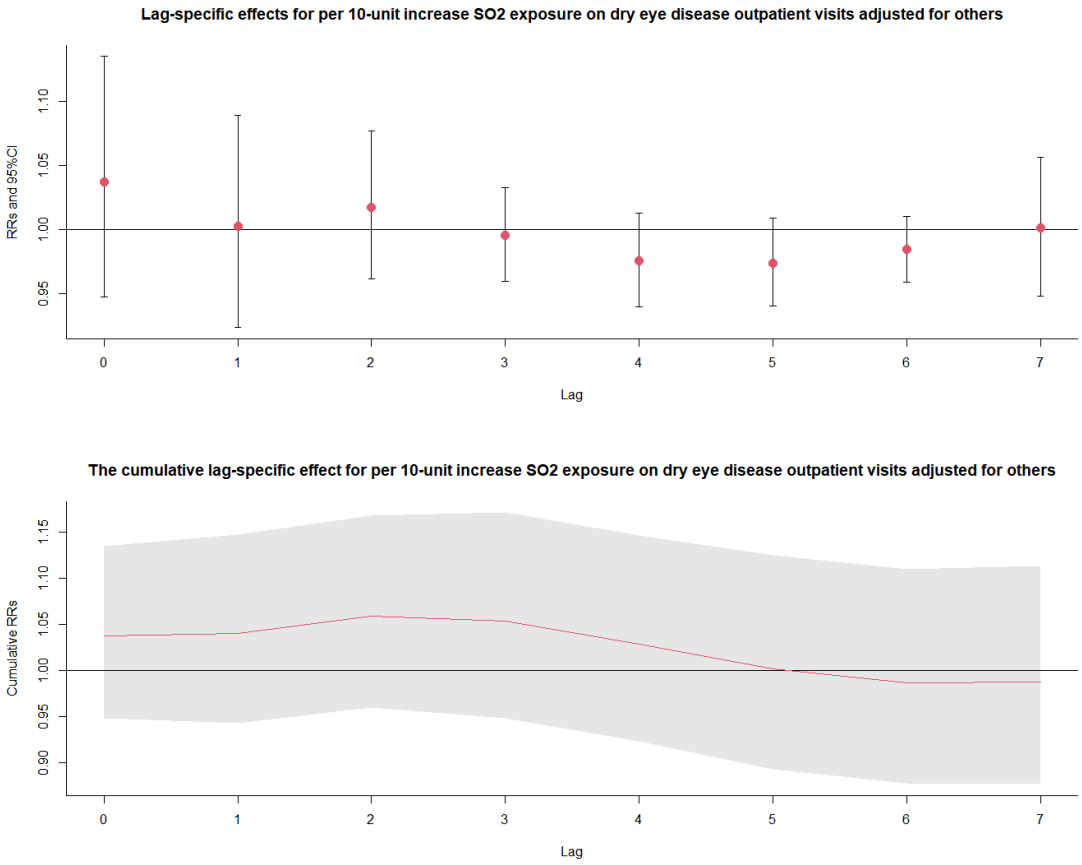

Figure S143. 3D graph and contour map of SO_2 exposure on dry eye disease outpatient visits after adjusted for others exposure.

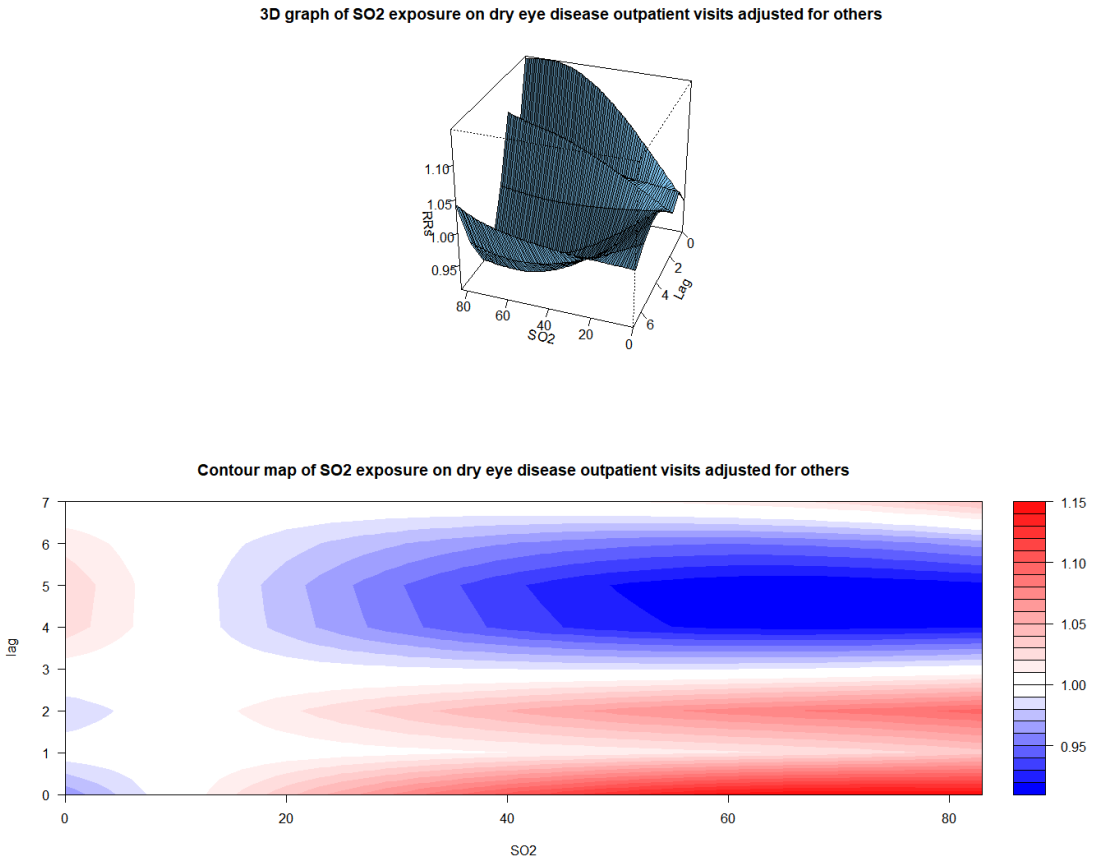

Figure S144. Exposure-response association between dry eye disease outpatient visits and SO_2 exposure in male patients.

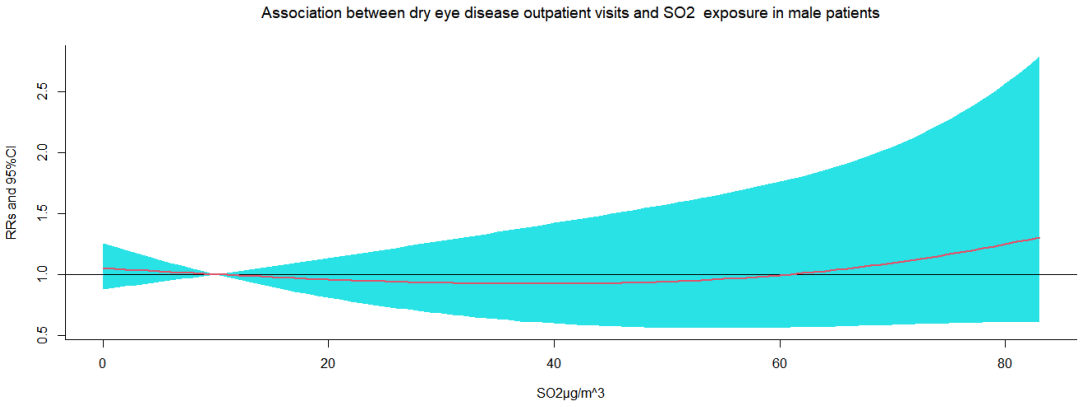

Figure S145. The relative risks (RRs) of per 10 μg/m^3 increase in SO_2 on dry eye disease outpatient visits at various lag days in male patients.

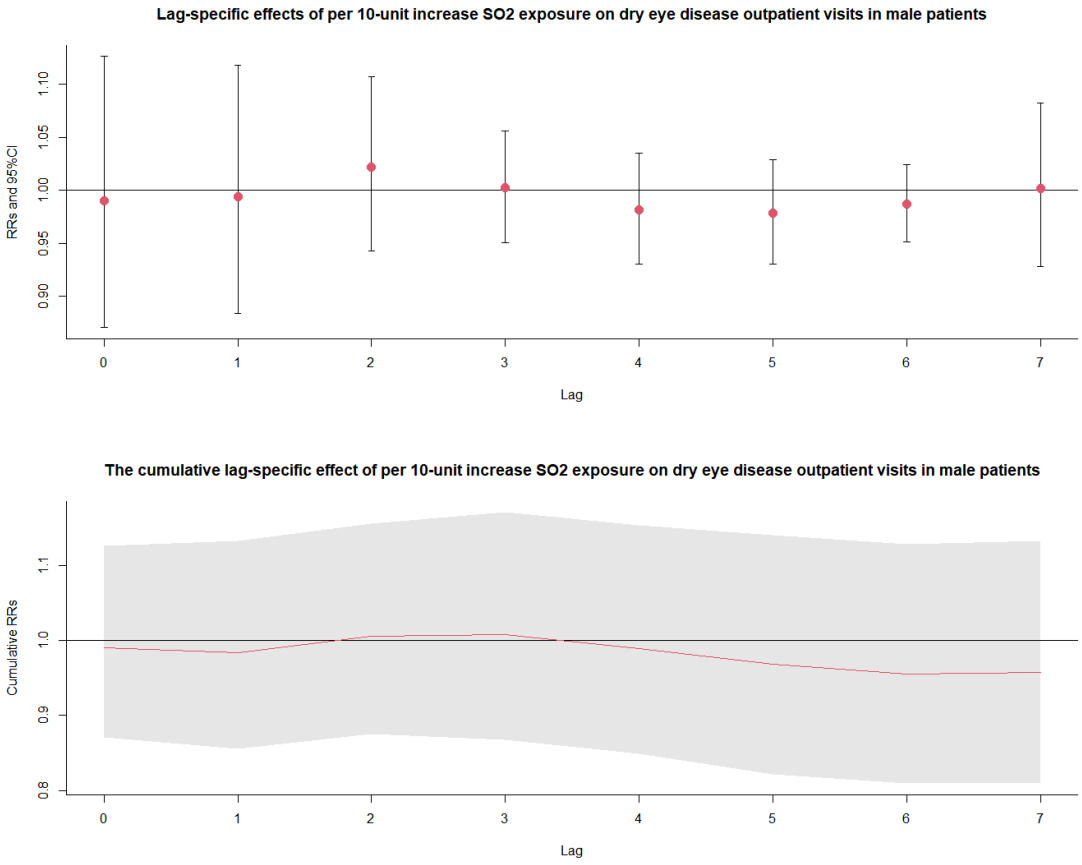

Figure S146. Exposure-response association between dry eye disease outpatient visits and SO_2 exposure in female patients.

Figure S147. The relative risks (RRs) of per 10 $\mu g/m^3$ increase in SO_2 on dry eye disease outpatient visits at various lag days in female patients.

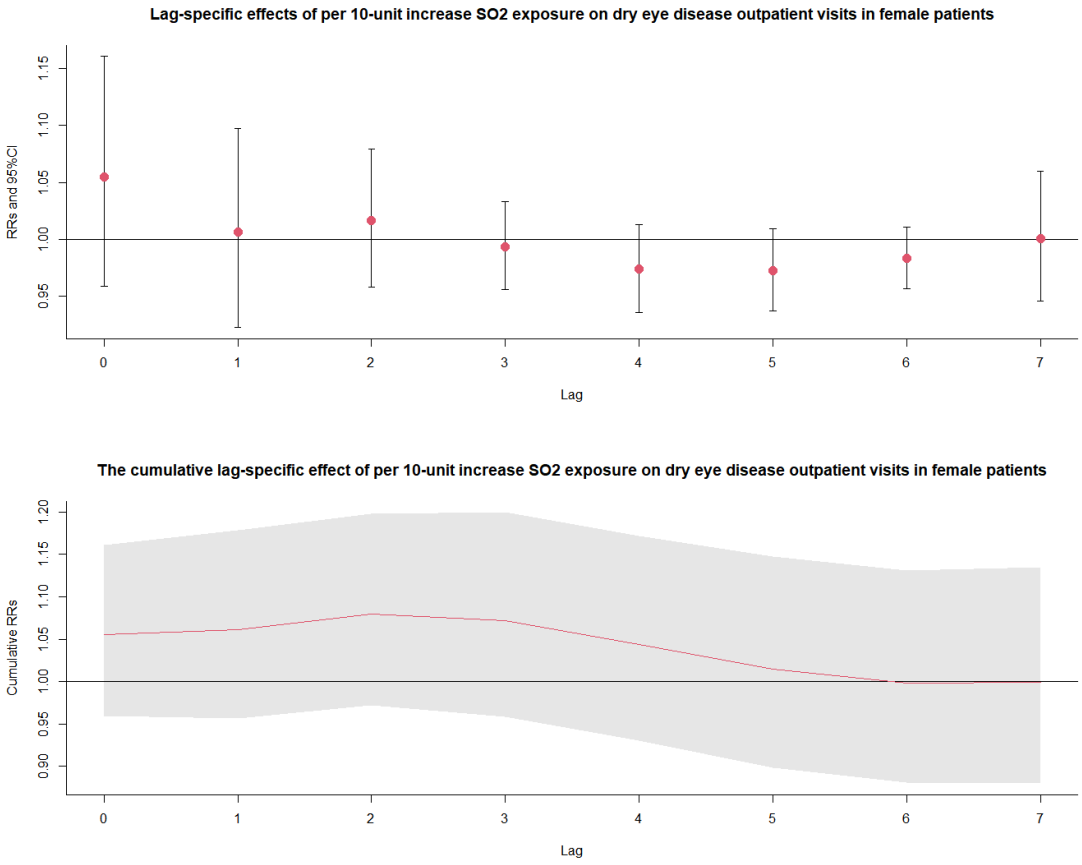

Figure S148. Exposure-response association between dry eye disease outpatient visits and SO_2 exposure in age 0-5 patients.

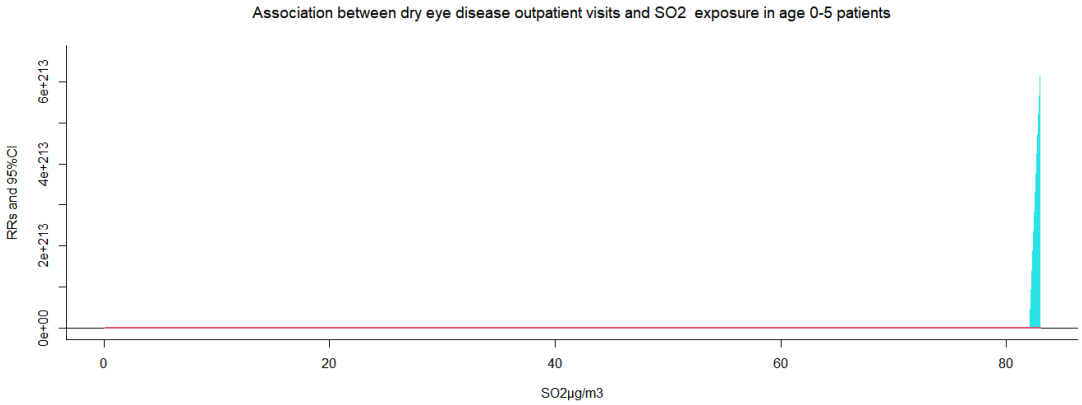

Figure S149. The relative risks (RRs) of per 10 $\mu g/m^3$ increase in SO_2 on dry eye disease outpatient visits at various lag days in age 0-5 patients.

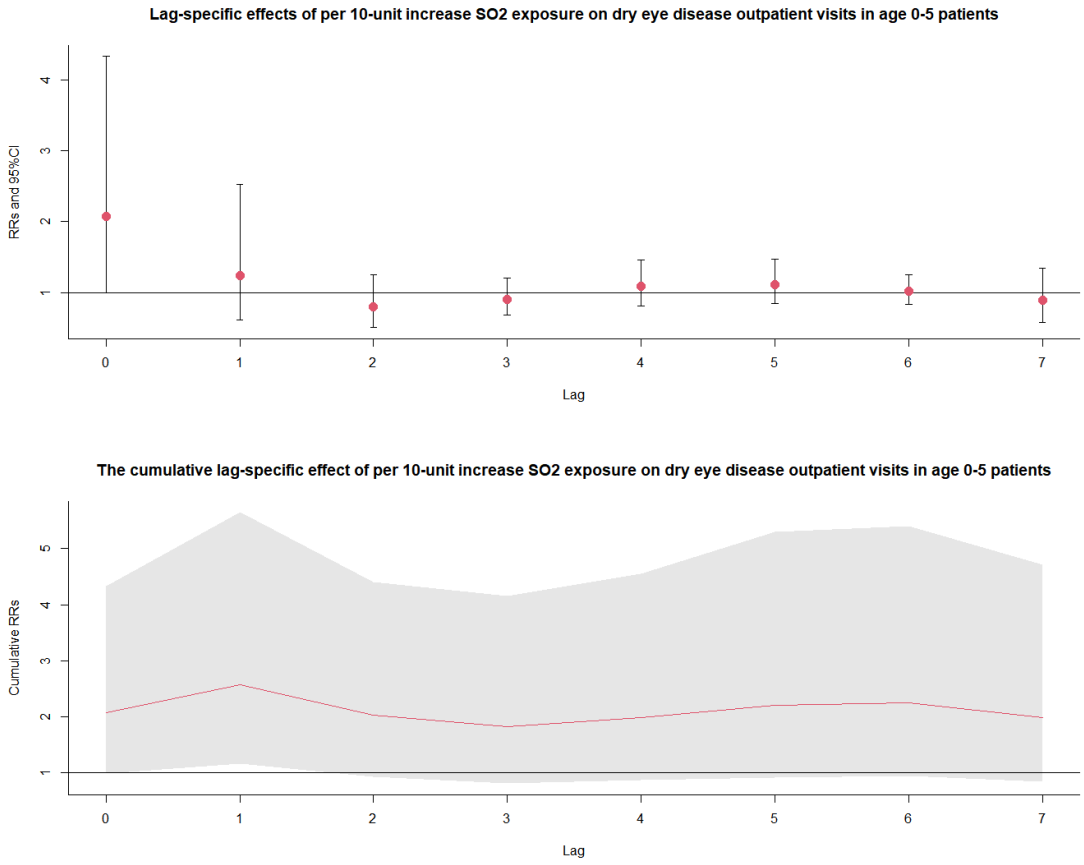

Figure S150. Exposure-response association between dry eye disease outpatient visits and SO_2 exposure in age 6-18 patients.

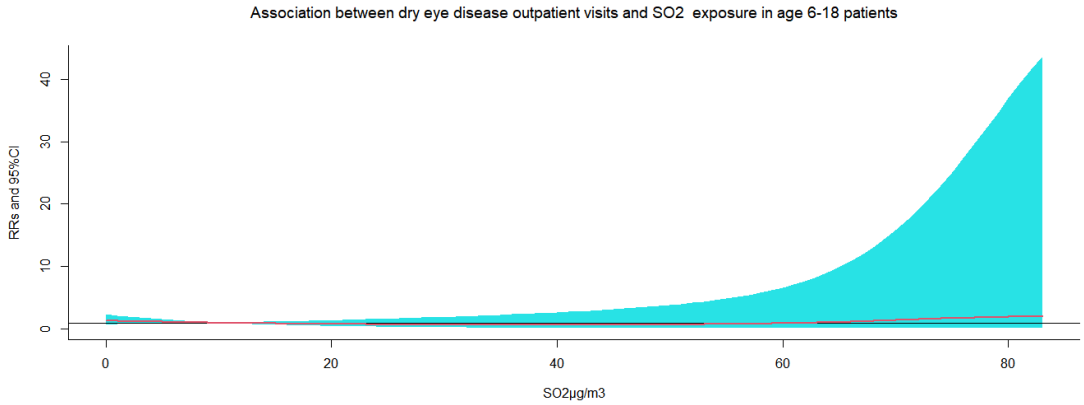

Figure S151. The relative risks (RRs) of per 10 $\mu g/m^3$ increase in SO_2 on dry eye disease outpatient visits at various lag days in age 6-18 patients.

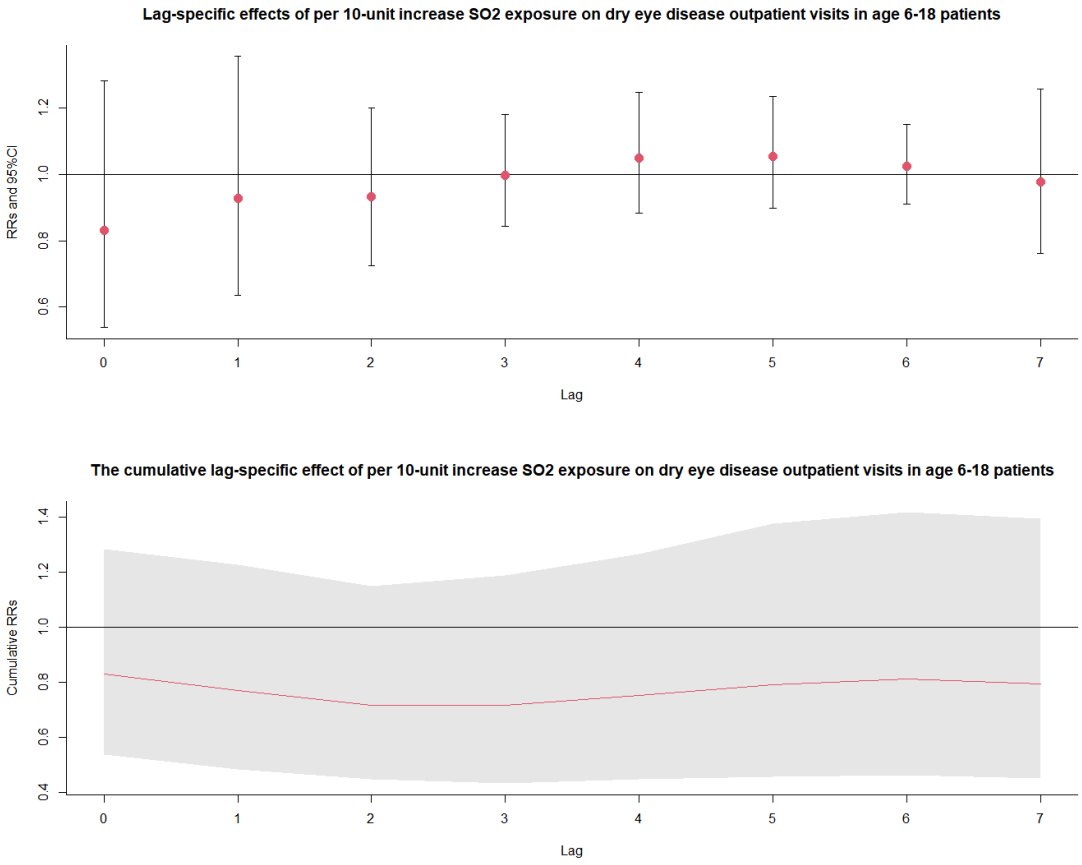

Figure S152. Exposure-response association between dry eye disease outpatient visits and SO_2 exposure in age 19-64 patients.

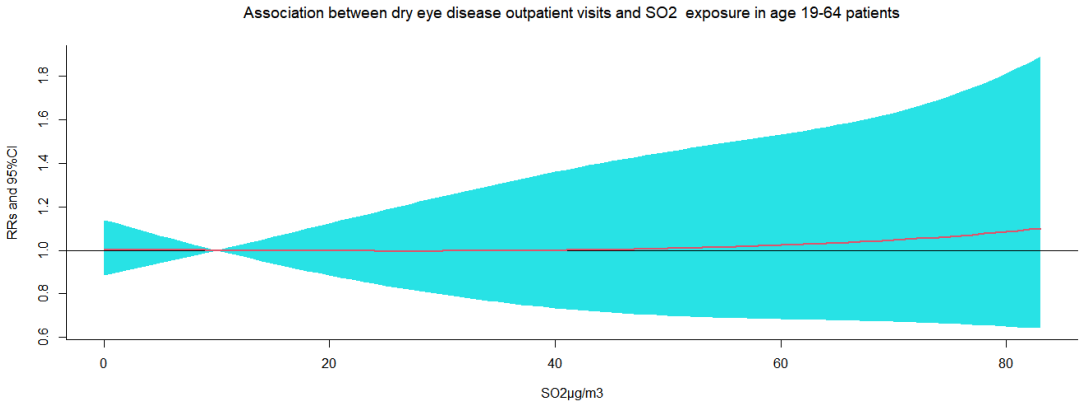

Figure S153. The relative risks (RRs) of per 10 μg/m^3 increase in SO_2 on dry eye disease outpatient visits at various lag days in age 19-64 patients.

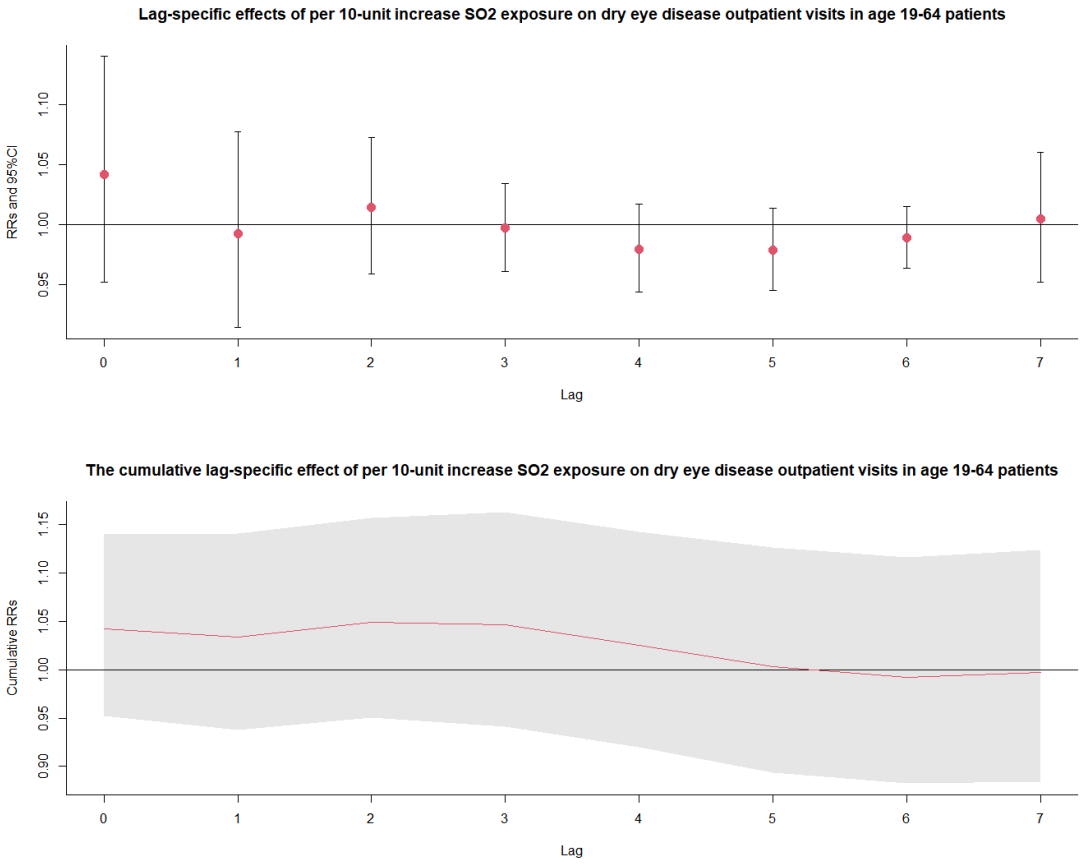

Figure S154. Exposure-response association between dry eye disease outpatient visits and SO_2 exposure in age ≥65 patients.

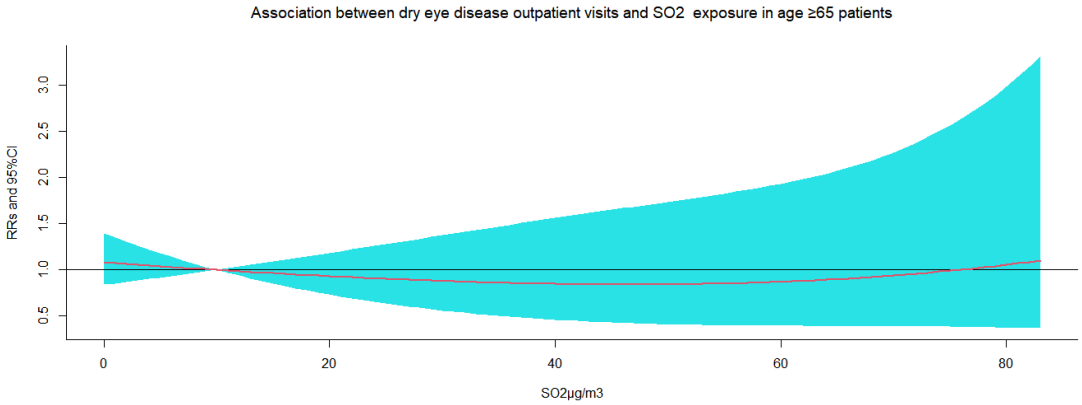

Figure S155. The relative risks (RRs) of per 10 μg/m^3 increase in SO_2 on dry eye disease outpatient visits at various lag days in age ≥65 patients.

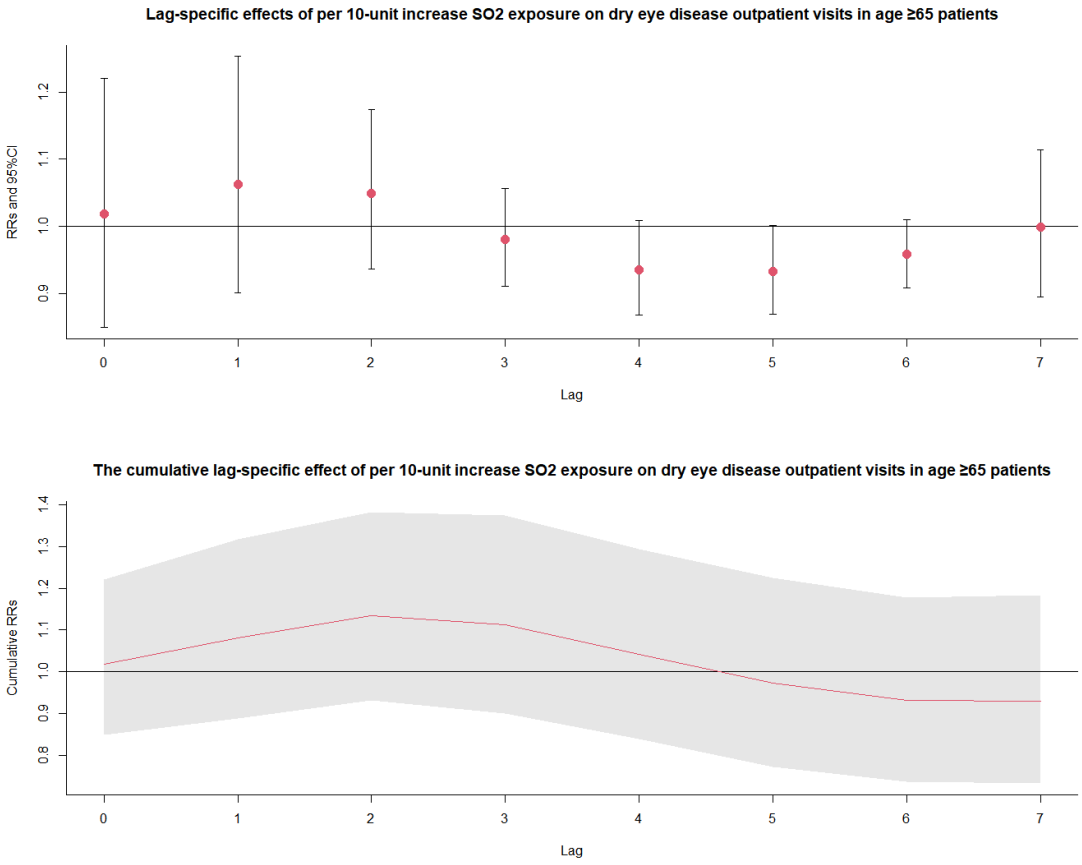

Figure S156. Exposure-response association between dry eye disease outpatient visits and SO_2 exposure in the warm season.

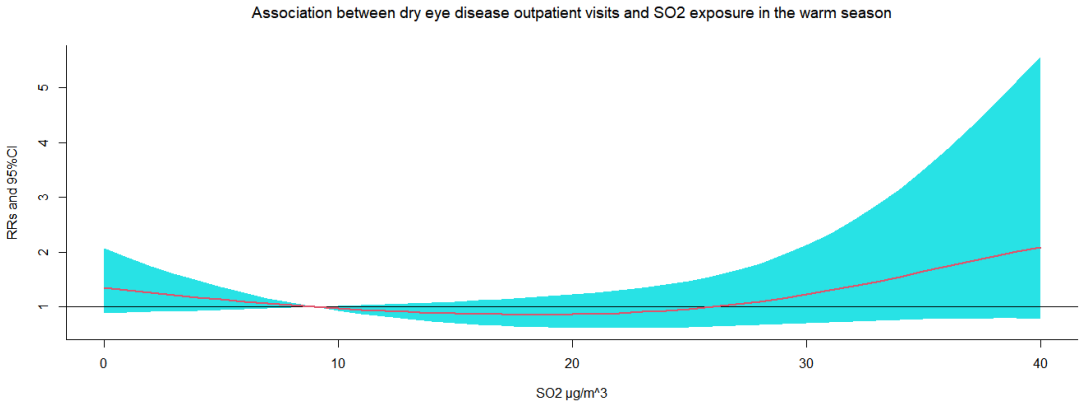

Figure S157. The relative risks (RRs) of per 10 $\mu g/m^3$ increase in SO_2 on dry eye disease outpatient visits at various lag days in the warm season.

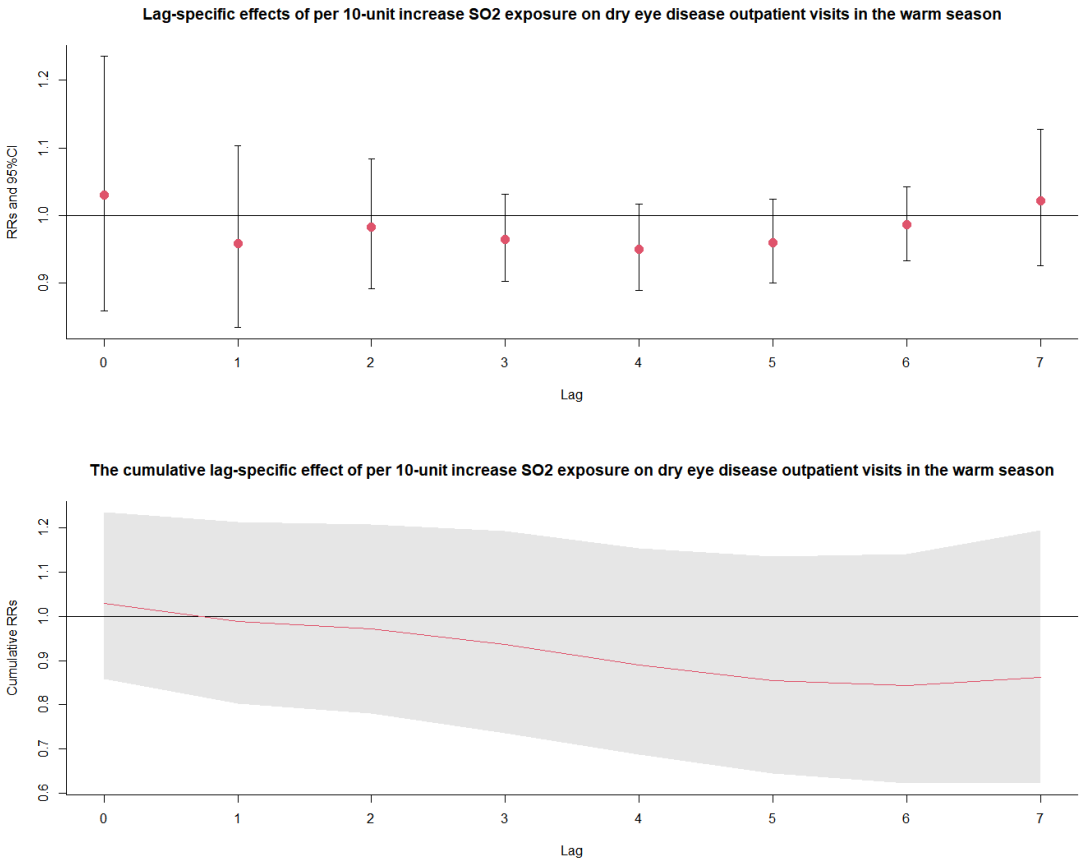

Figure S158. Exposure-response association between dry eye disease outpatient visits and SO_2 exposure in the cold season.

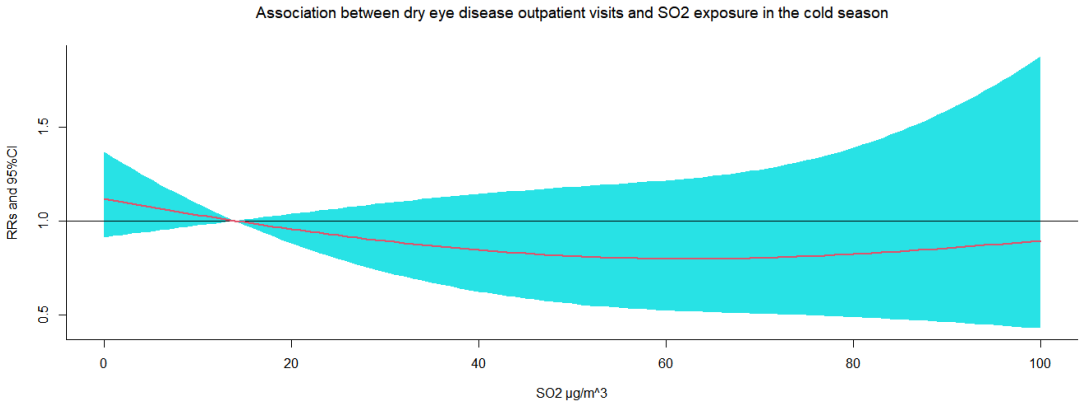

Figure S159. The relative risks (RRs) of per 10 $\mu g/m^3$ increase in SO_2 on dry eye disease outpatient visits at various lag days in the cold season.

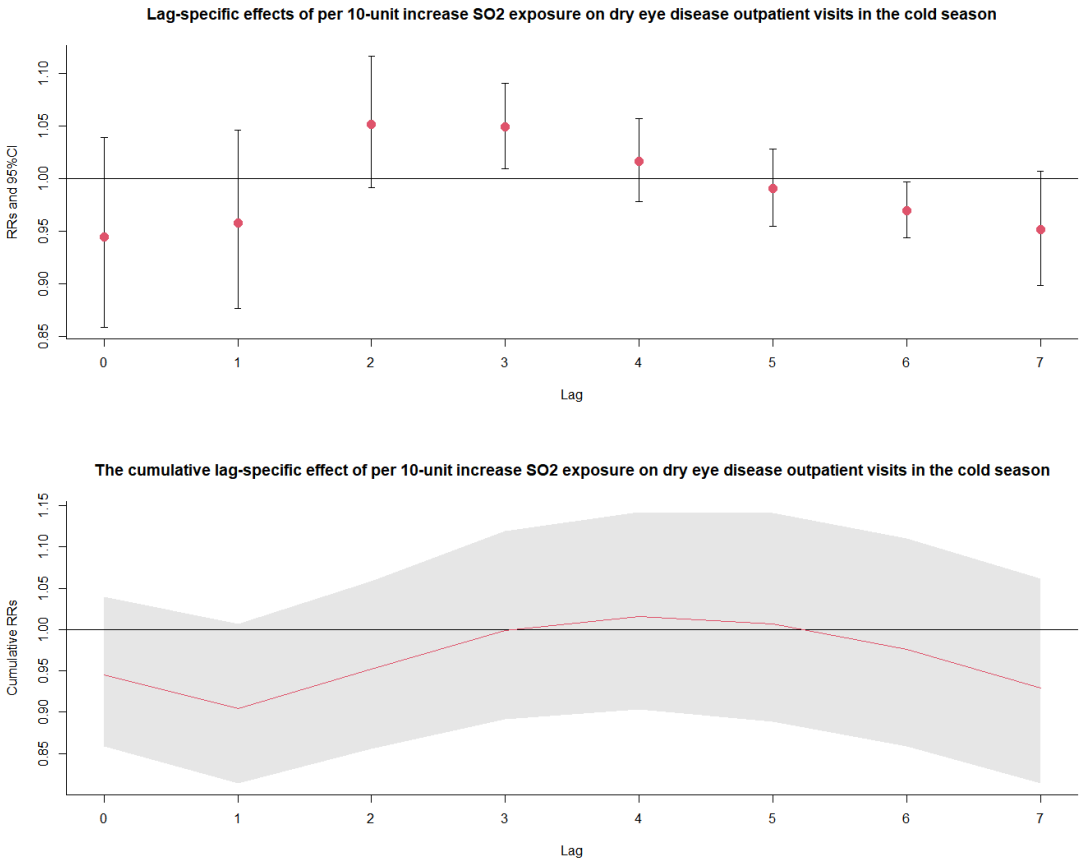

Figure S160. Exposure-response association between dry eye disease outpatient visits and O_3 exposure.

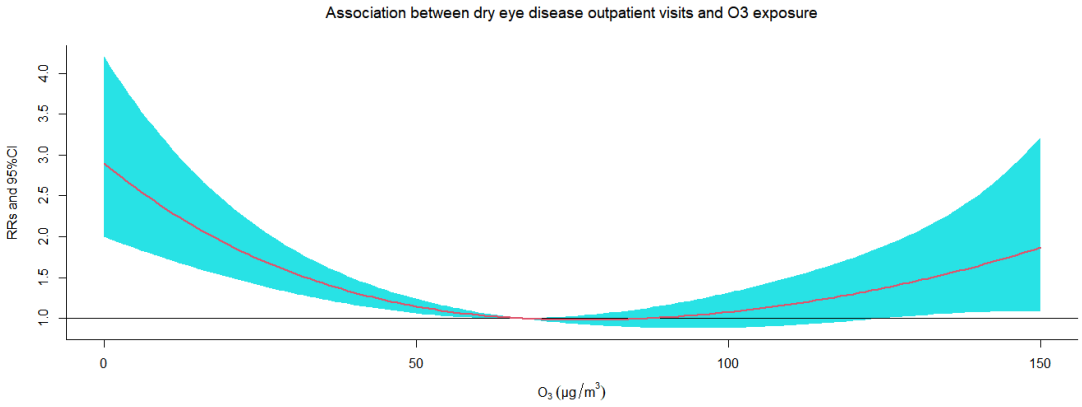

Figure S161. The relative risks (RRs) of per 10 μg/m^3 increase in O_3 on dry eye disease outpatient visits at various lag days.

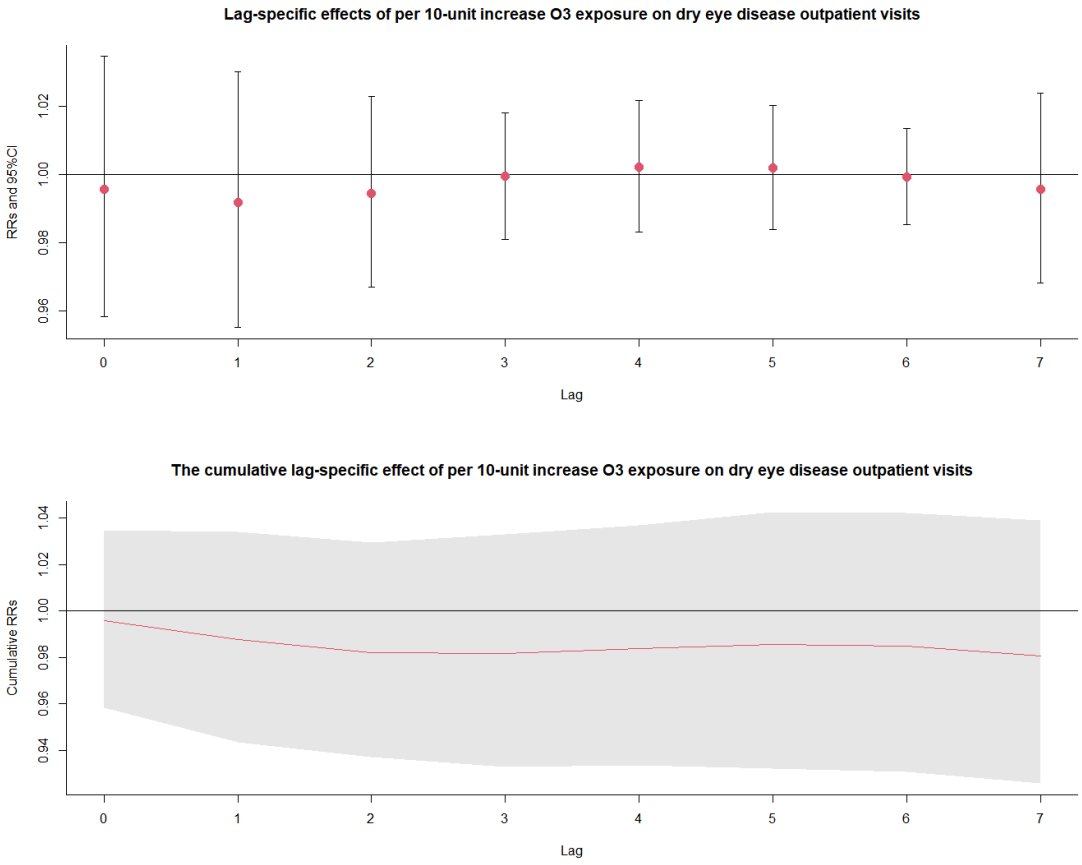

Figure S162. 3D graph and contour map of O_3 exposure on dry eye disease outpatient visits.

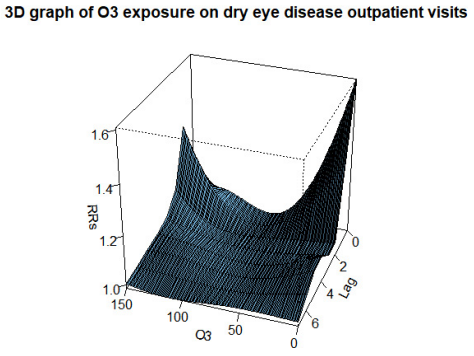

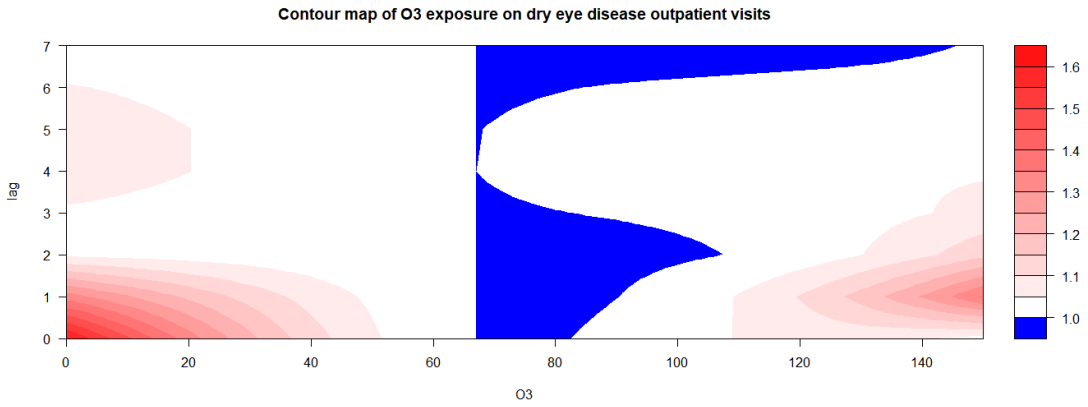

Figure S163. Exposure-response association between dry eye disease outpatient visits and O_3 exposure after adjusted for other air pollution.

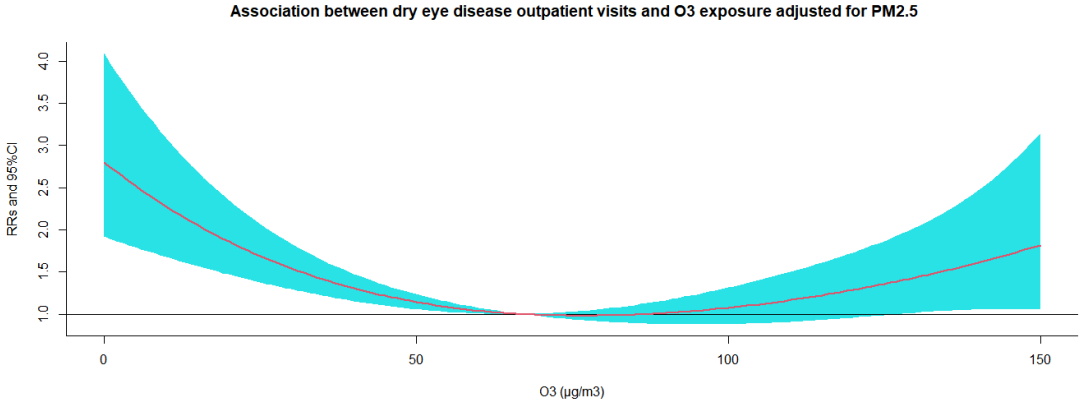

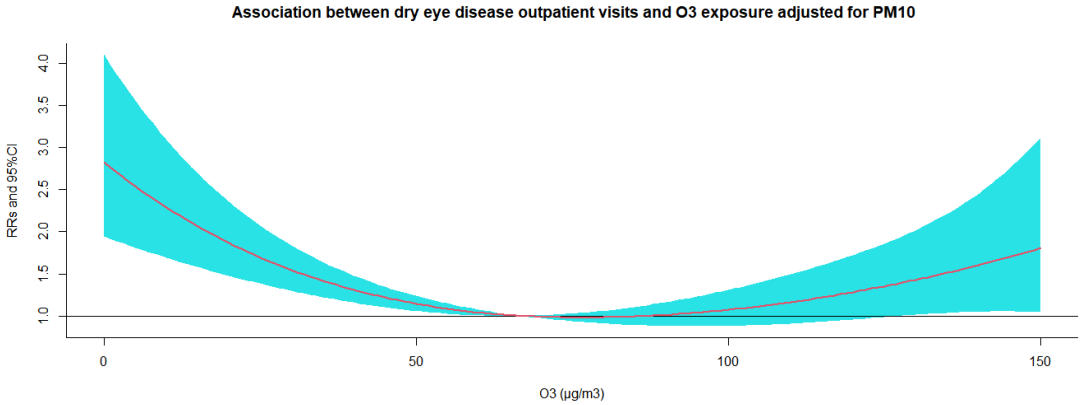

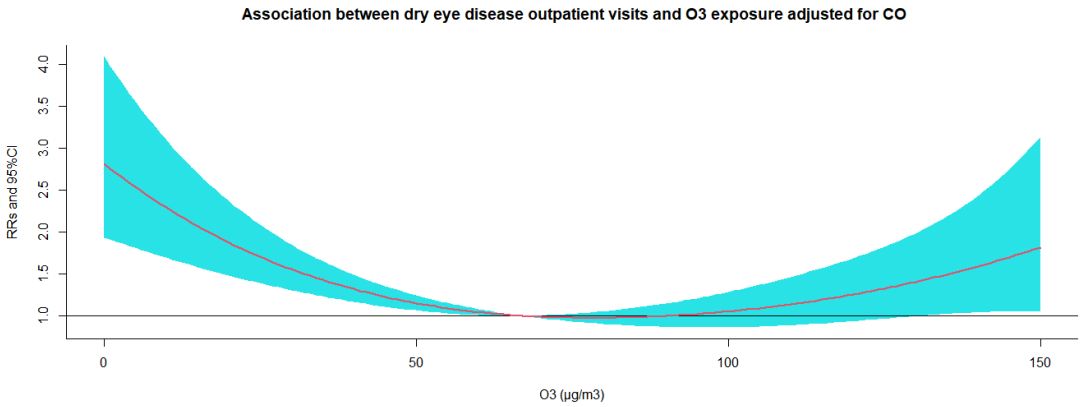
Association between dry eye disease outpatient visits and O3 exposure adjusted for CO
RRs and 95%CI
1.0
1.5
2.0
2.5
3.0
3.5
4.0
0
50
100
150
O3 (µg/m3)

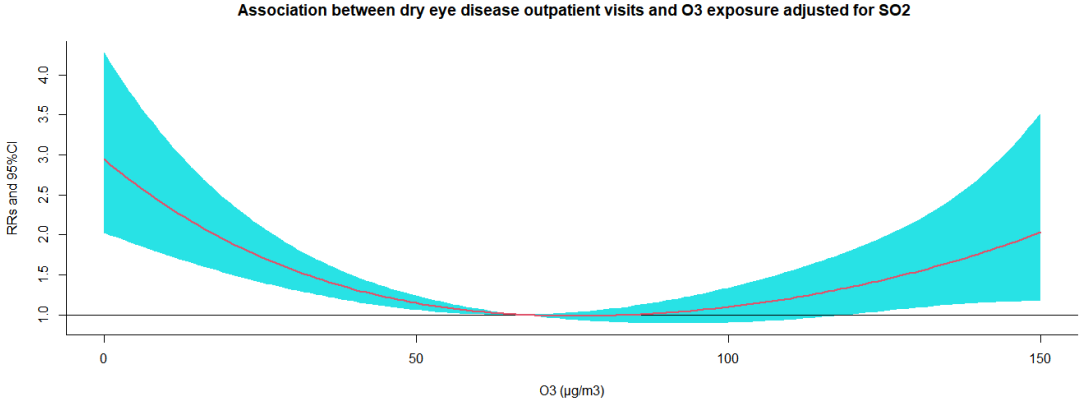
Association between dry eye disease outpatient visits and O3 exposure adjusted for SO2
RRs and 95%CI
1.0
1.5
2.0
2.5
3.0
3.5
4.0
0
50
100
150
O3 (µg/m3)

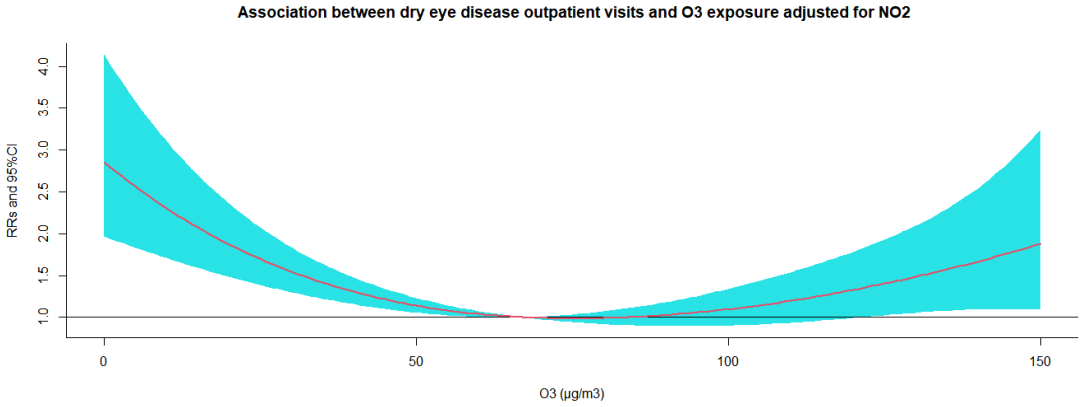
Association between dry eye disease outpatient visits and O3 exposure adjusted for NO2
RRs and 95%CI
1.0
1.5
2.0
2.5
3.0
3.5
4.0
0
50
100
150
O3 (µg/m3)

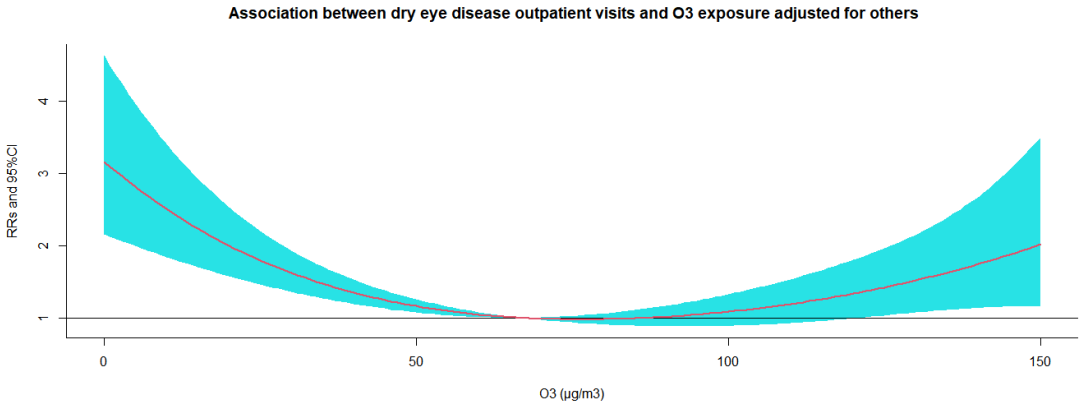
Association between dry eye disease outpatient visits and O3 exposure adjusted for others
RRs and 95%CI
1
2
3
4
0
50
100
150
O3 (µg/m3)

Figure S164. The relative risks (RRs) of per 10 μg/m^3 increase in O_3 on dry eye disease outpatient visits at various lag days after adjusted for NO_2 exposure.

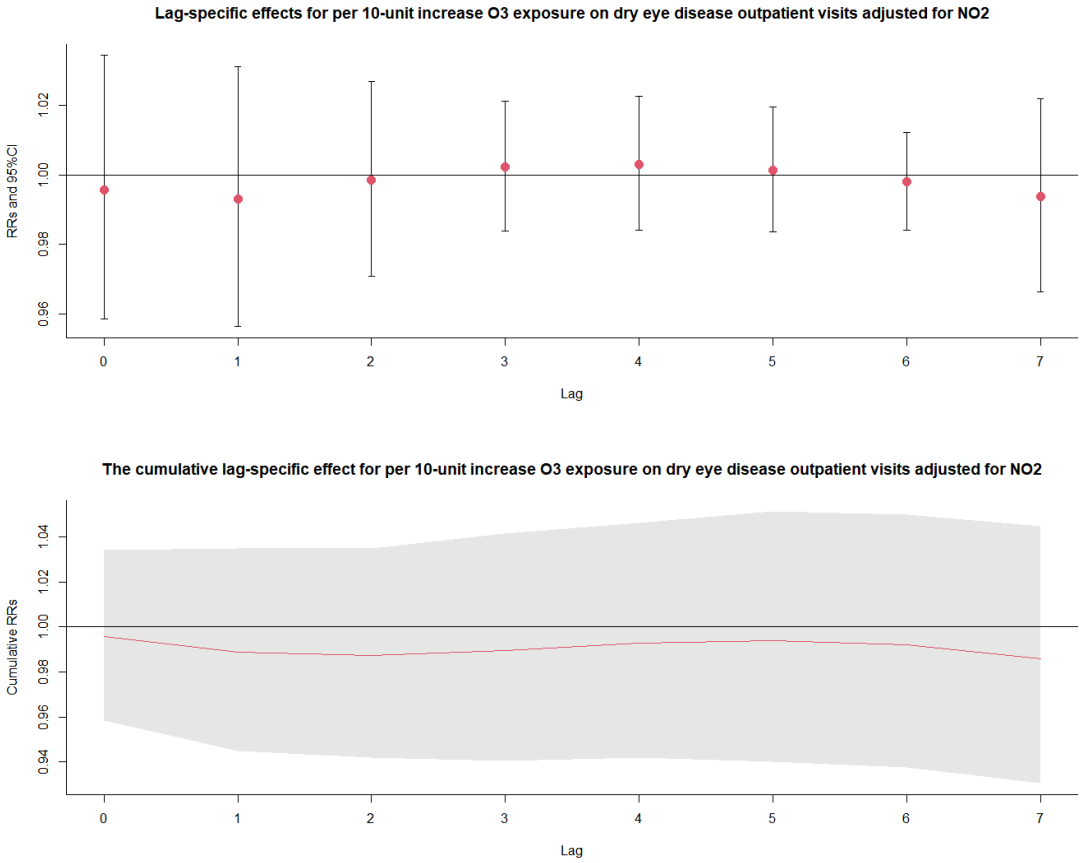

Figure S165. 3D graph and contour map of O_3 exposure on dry eye disease outpatient visits after adjusted for NO_2 exposure.

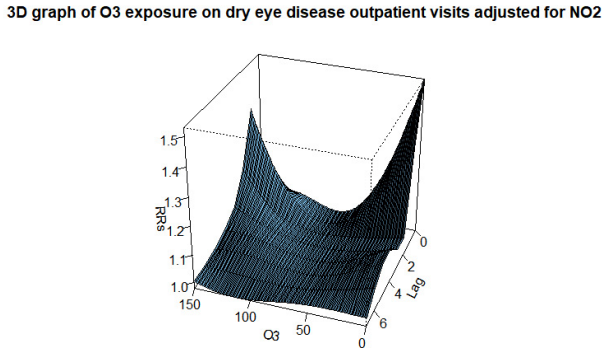

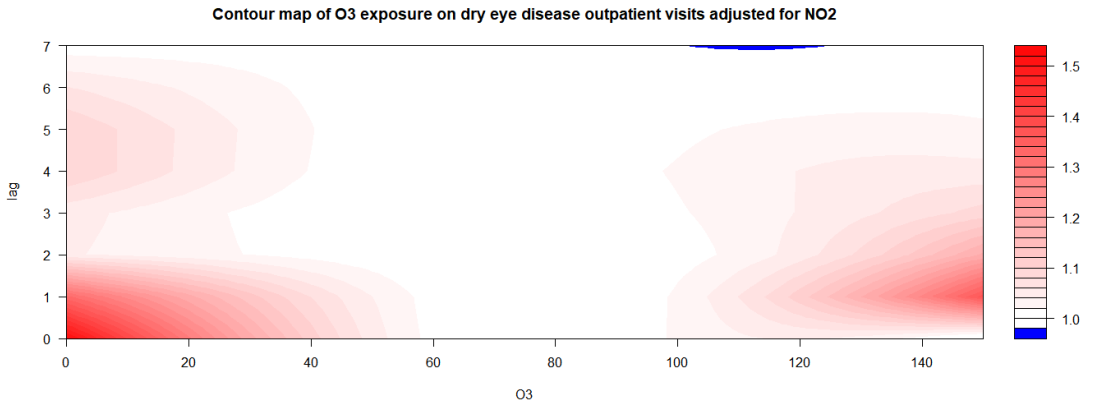

Figure S166. The relative risks (RRs) of per 10 μg/m^3 increase in O_3 on dry eye disease outpatient visits at various lag days after adjusted for PM_{10} exposure.

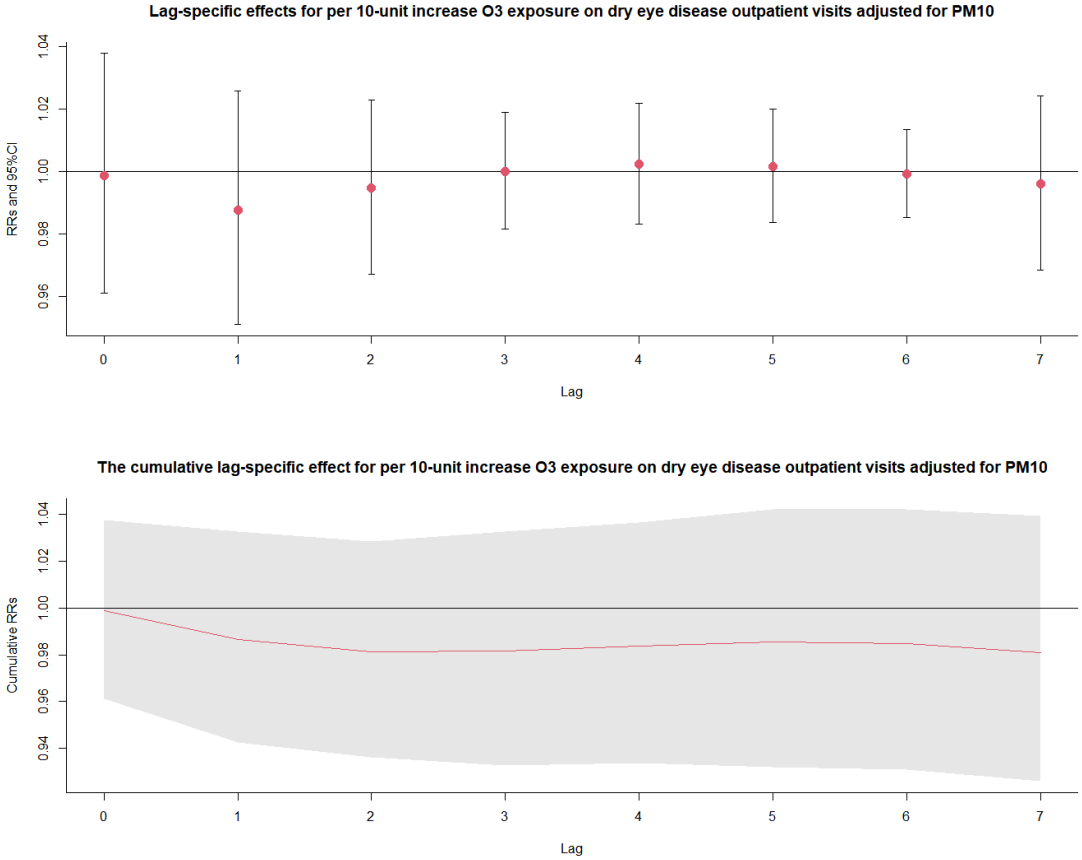

Figure S167. 3D graph and contour map of O_3 exposure on dry eye disease outpatient visits after adjusted for PM_{10} exposure.

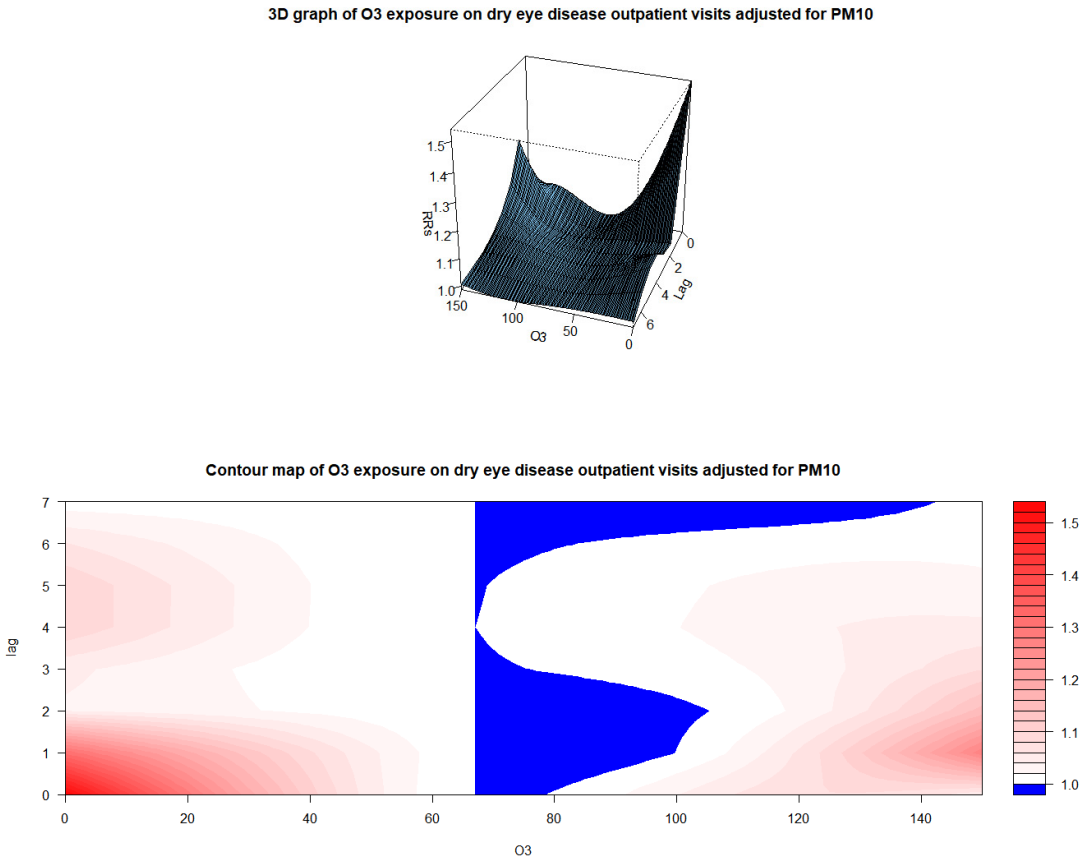

Figure S168. The relative risks (RRs) of per 10 μg/m^3 increase in O_3 on dry eye disease outpatient visits at various lag days after adjusted for CO exposure.

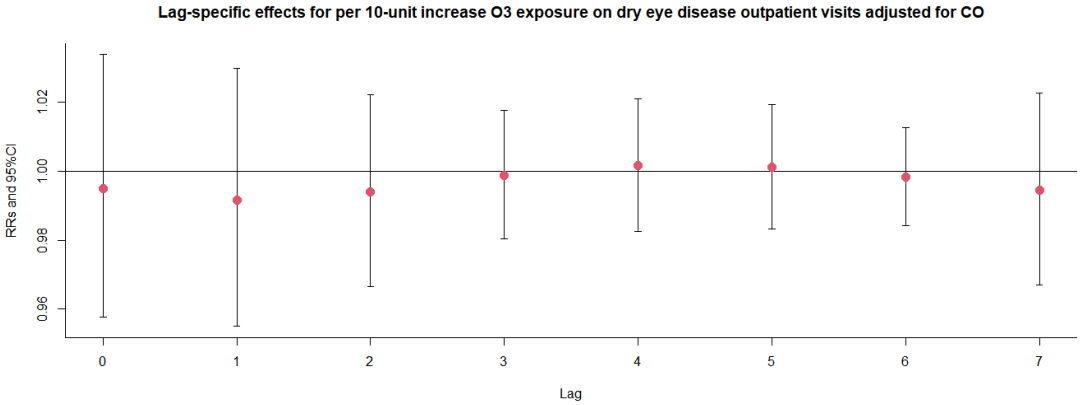

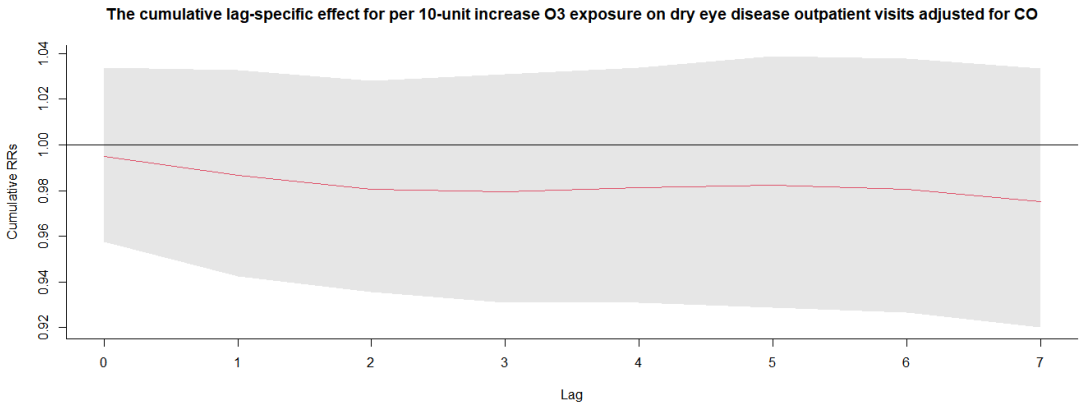

Figure S169. 3D graph and contour map of O_3 exposure on dry eye disease outpatient visits after adjusted for CO exposure.

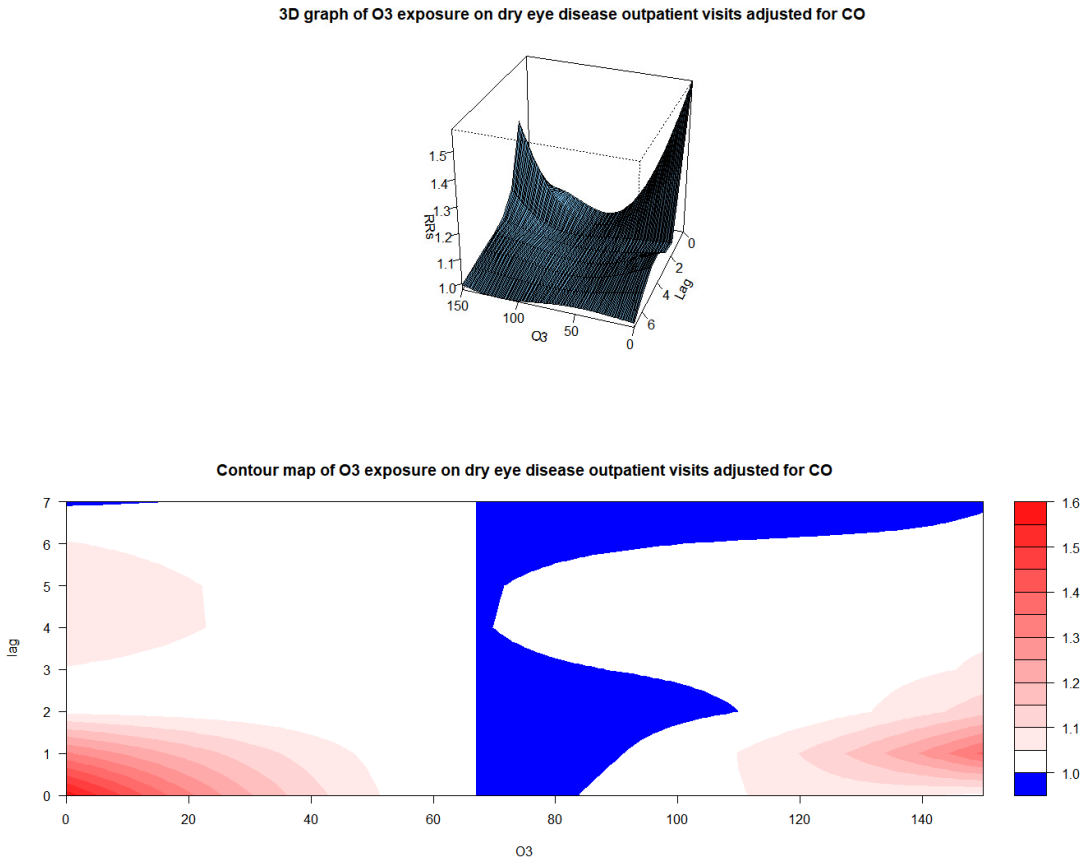

Figure S170. The relative risks (RRs) of per 10 $\mu g/m^3$ increase in O_3 on dry eye disease outpatient visits at various lag days after adjusted for $PM_{2.5}$ exposure.

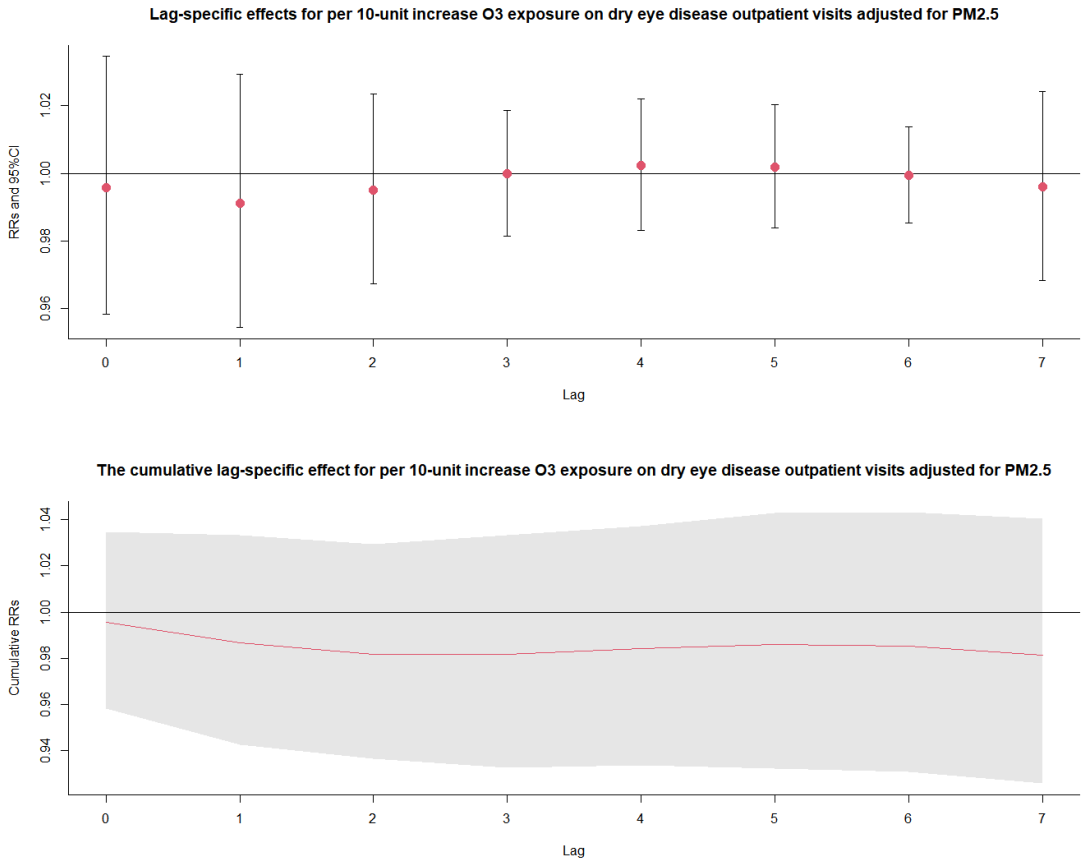

Figure S171. 3D graph and contour map of O_3 exposure on dry eye disease outpatient visits after adjusted for $PM_{2.5}$ exposure.

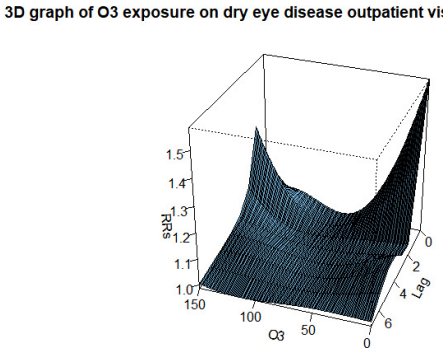

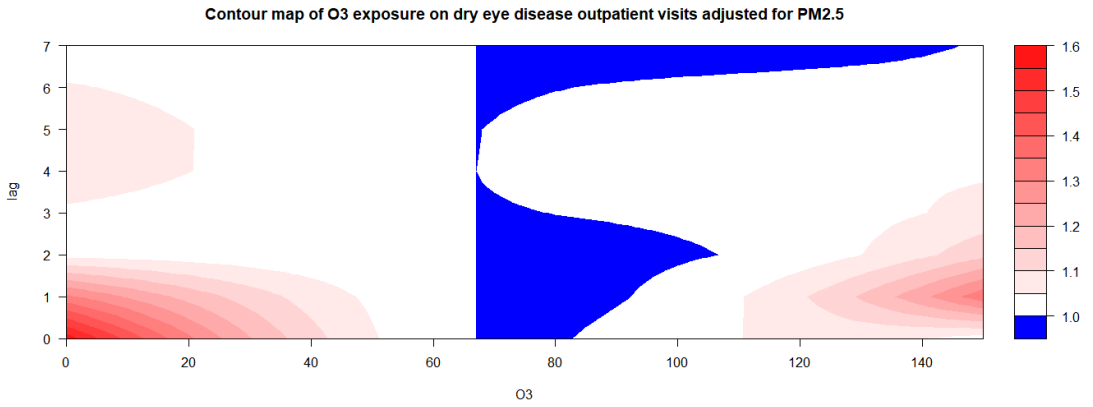

Figure S172. The relative risks (RRs) of per 10 μg/m^3 increase in O_3 on dry eye disease outpatient visits at various lag days after adjusted for SO_2 exposure.

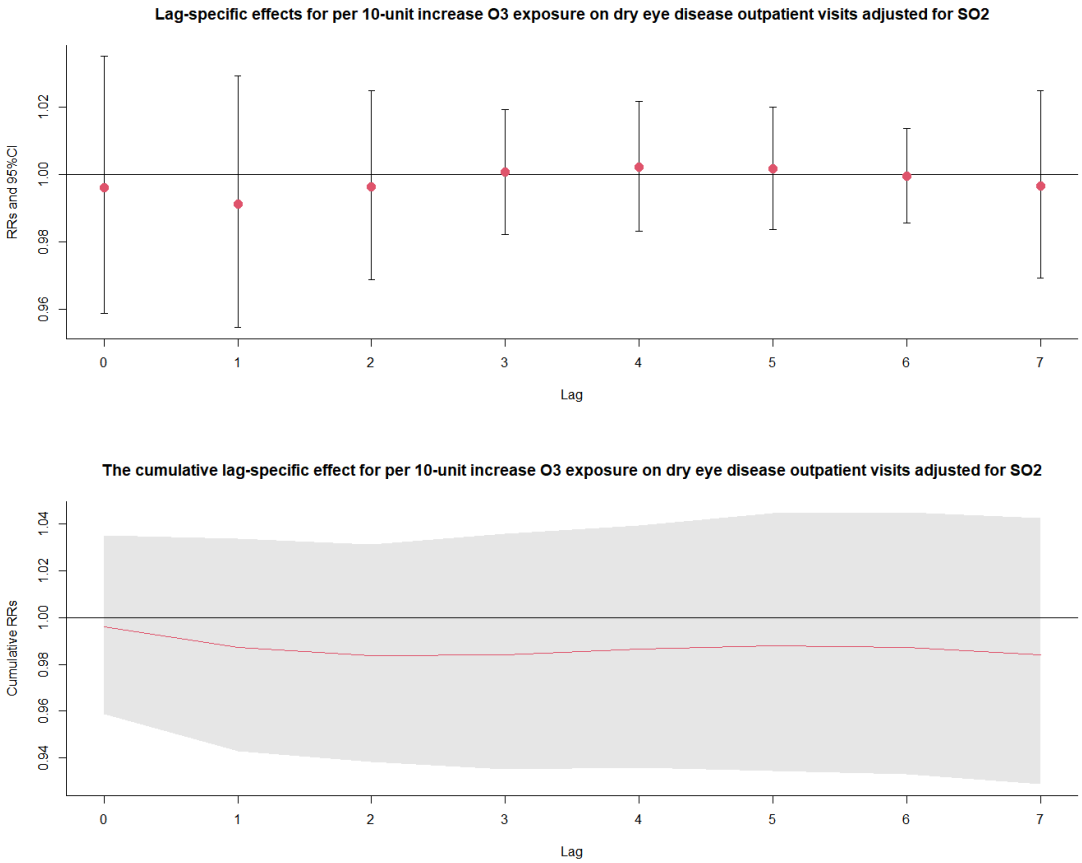

Figure S173. 3D graph and contour map of O_3 exposure on dry eye disease outpatient visits after adjusted for SO_2 exposure.

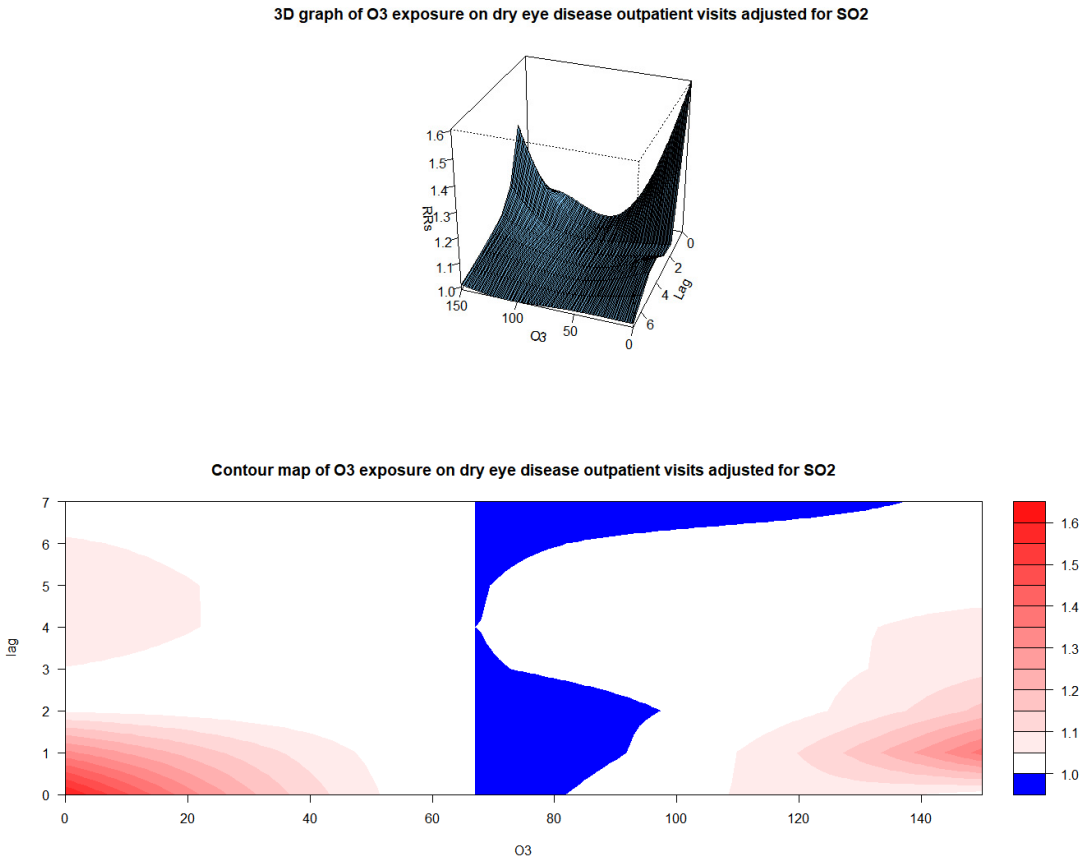

Figure S174. The relative risks (RRs) of per 10 μg/m^3 increase in O_3 on dry eye disease outpatient visits at various lag days after adjusted for others exposure.

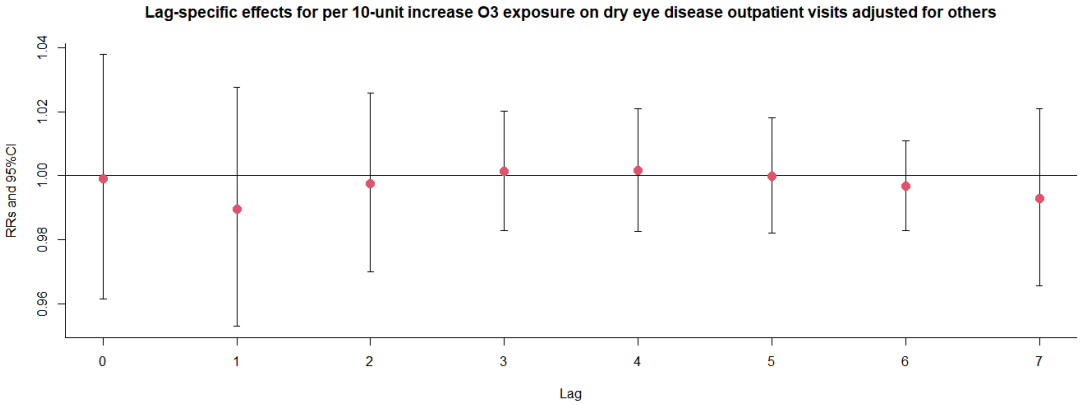

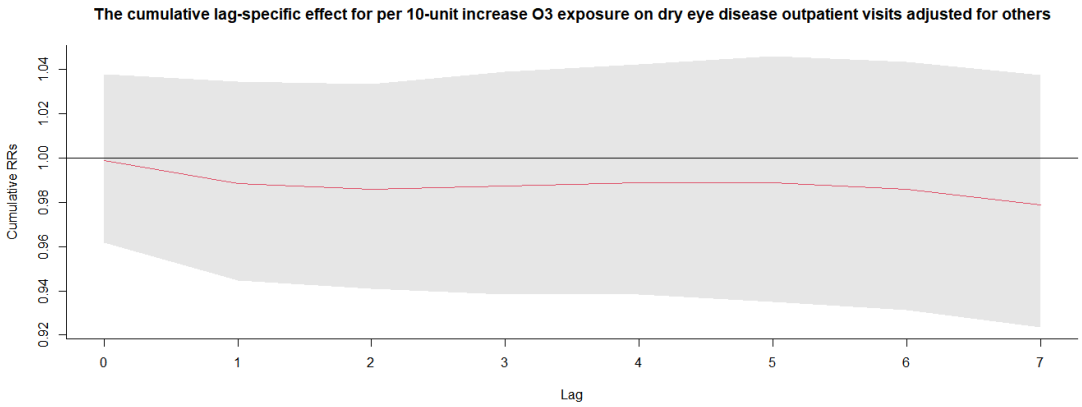

Figure S175. 3D graph and contour map of O_3 exposure on dry eye disease outpatient visits after adjusted for others exposure.

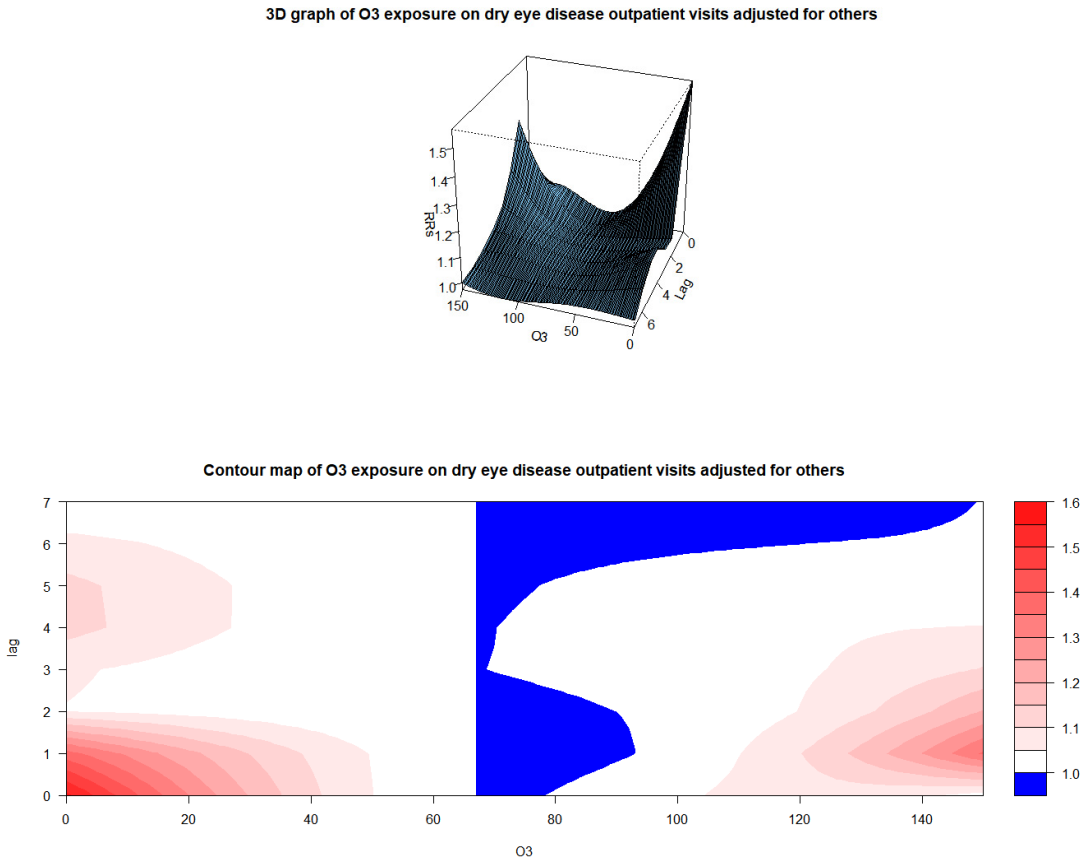

Figure S176. Exposure-response association between dry eye disease outpatient visits and O_3 exposure in male patients.

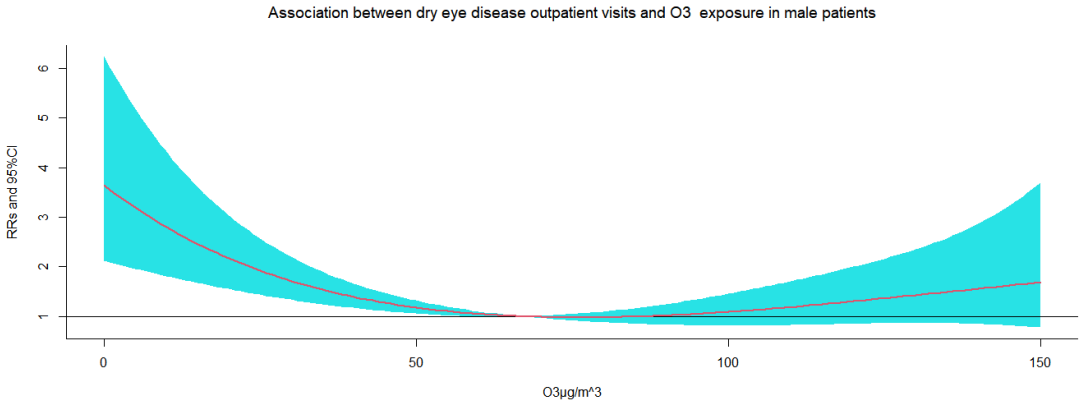

Figure S177. The relative risks (RRs) of per 10 μg/m^3 increase in O_3 on dry eye disease outpatient visits at various lag days in male patients.

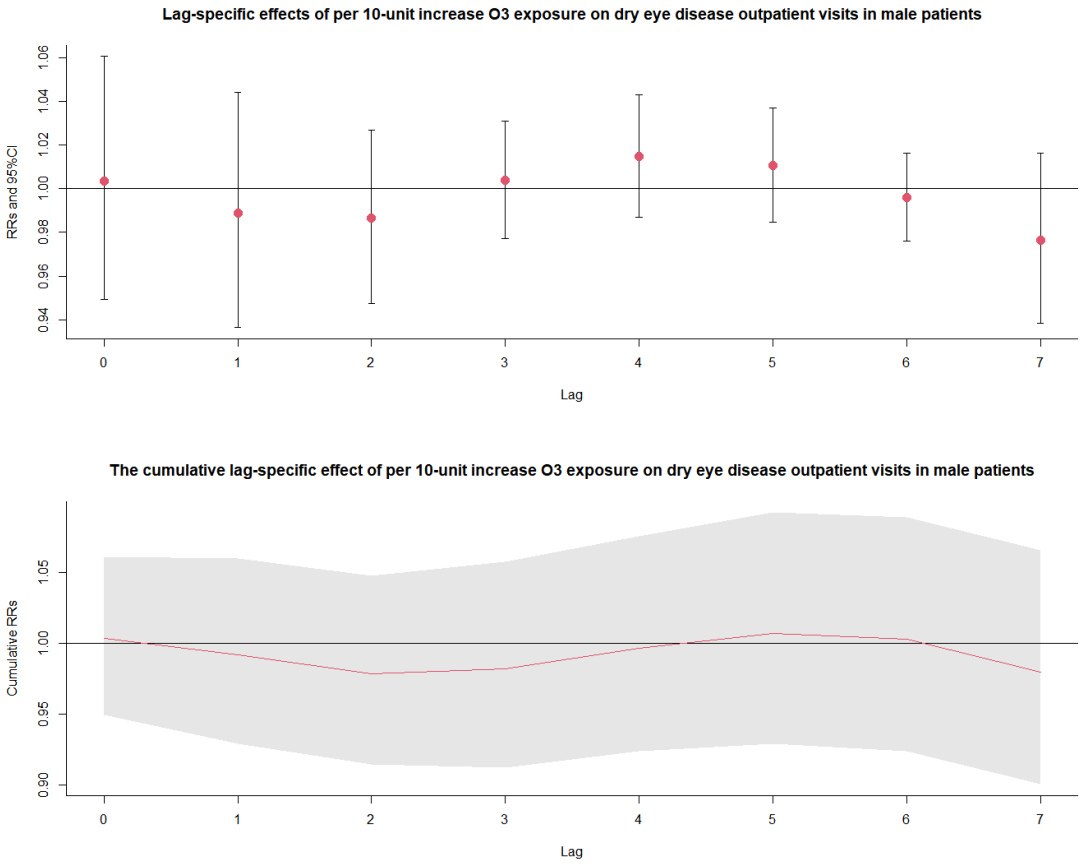

Figure S178. Exposure-response association between dry eye disease outpatient visits and O_3 exposure in female patients.

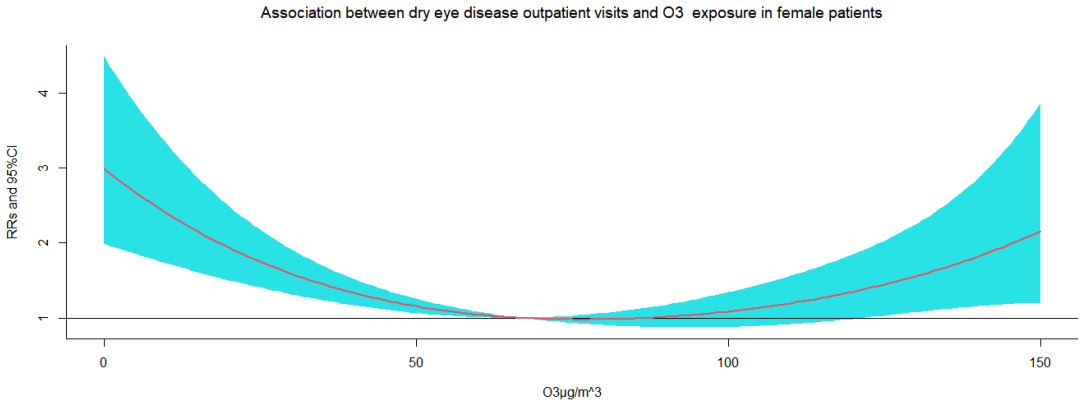

Figure S179. The relative risks (RRs) of per 10 μg/m^3 increase in O_3 on dry eye disease outpatient visits at various lag days in female patients.

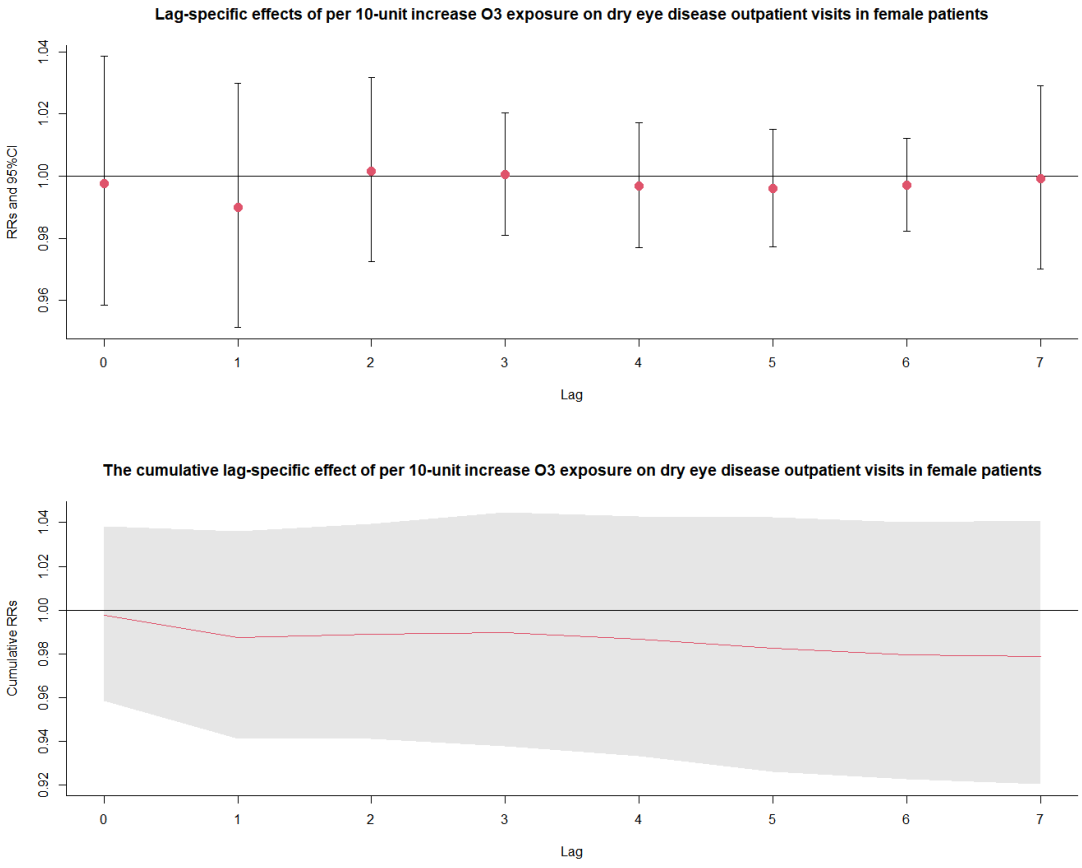

Figure S180. Exposure-response association between dry eye disease outpatient visits and O_3 exposure in age 0-5 patients.

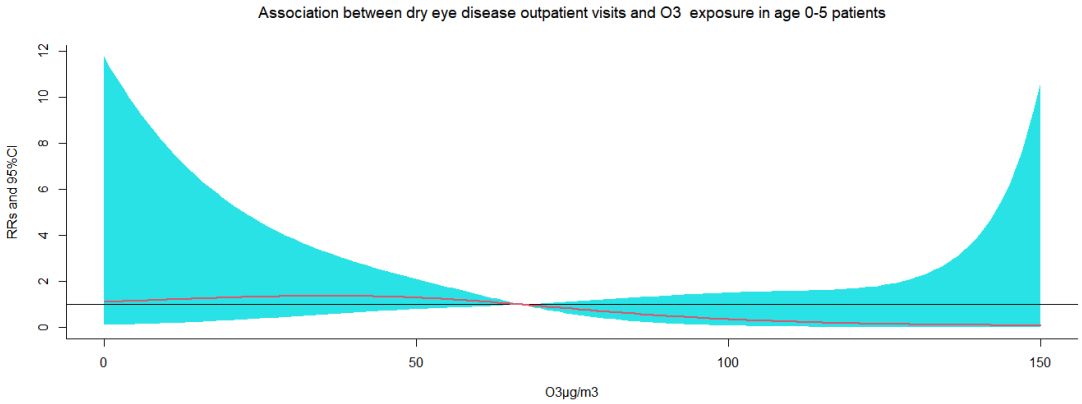

Figure S181. The relative risks (RRs) of per 10 μg/m^3 increase in O_3 on dry eye disease outpatient visits at various lag days in age 0-5 patients.

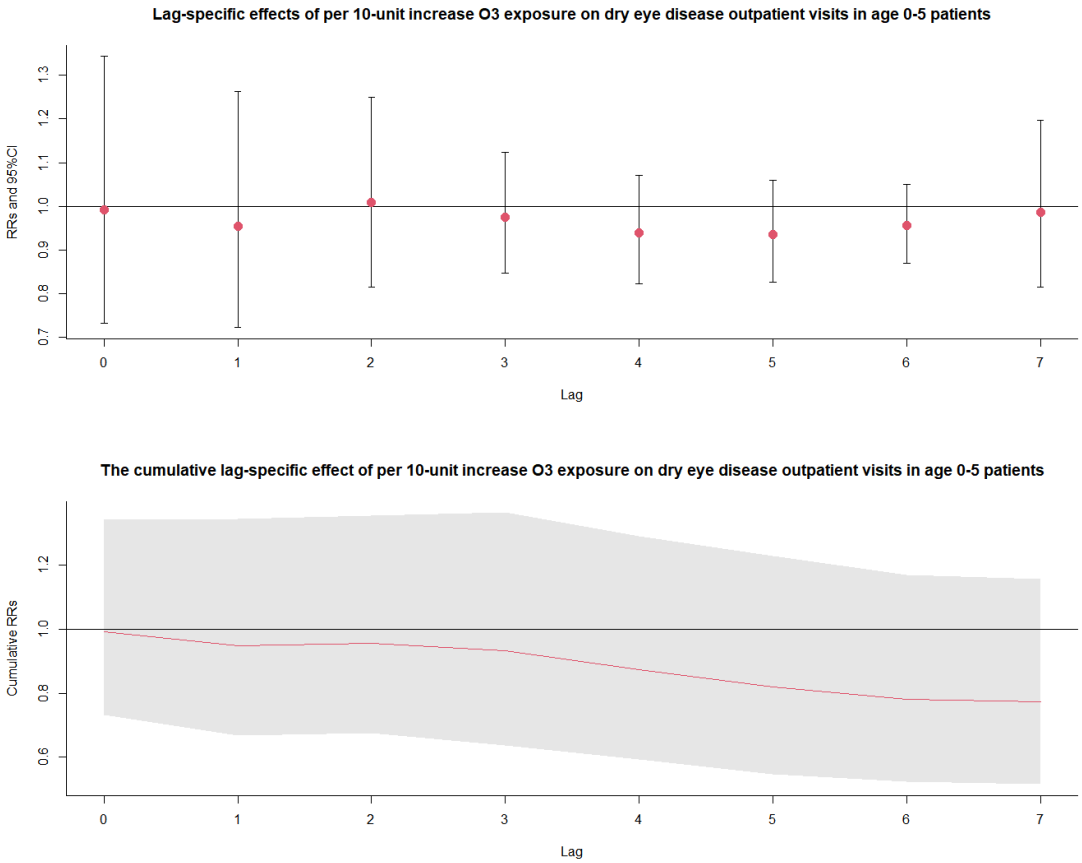

Figure S182. Exposure-response association between dry eye disease outpatient visits and O_3 exposure in age 6-18 patients.

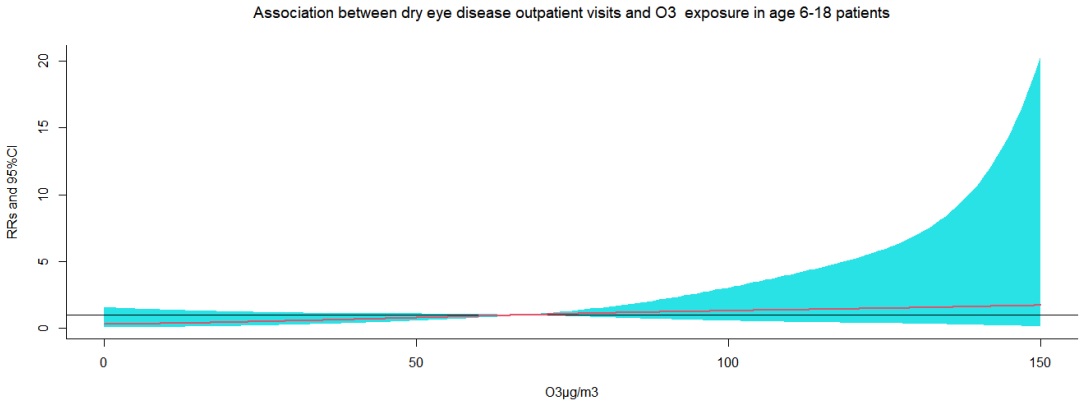

Figure S183. The relative risks (RRs) of per 10 μg/m^3 increase in O_3 on dry eye disease outpatient visits at various lag days in age 6-18 patients.

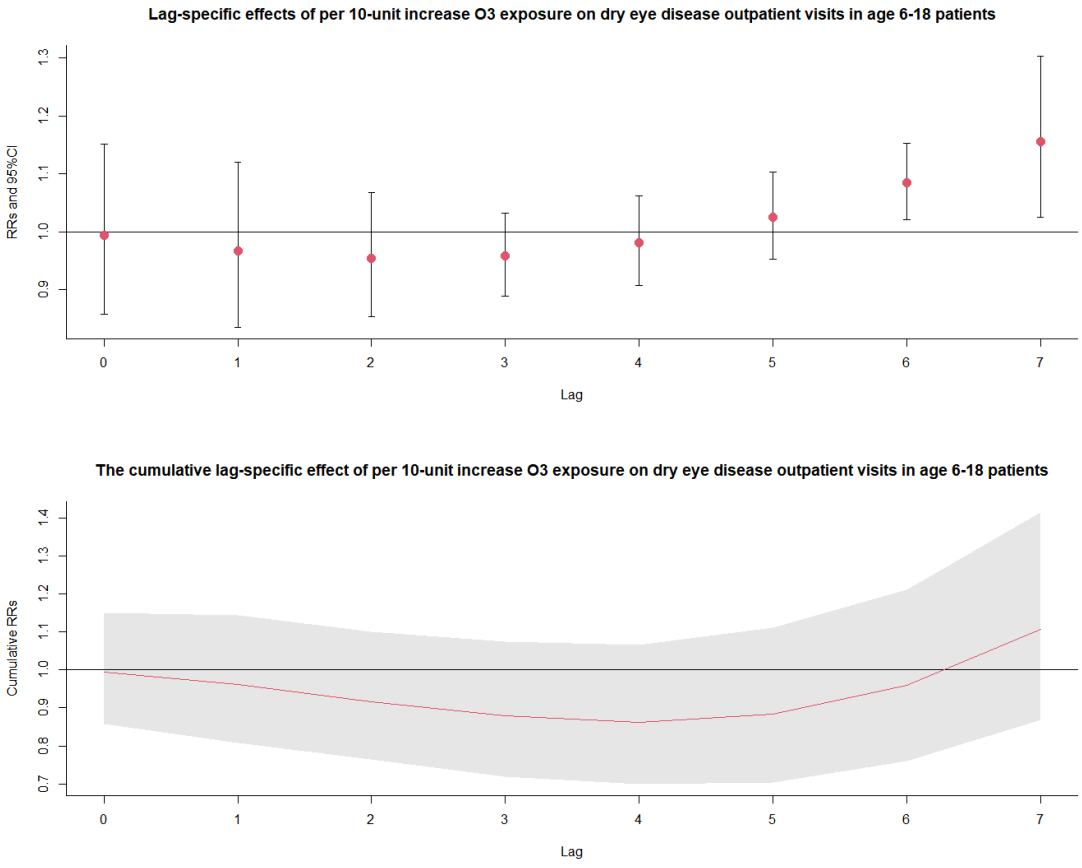

Figure S184. Exposure-response association between dry eye disease outpatient visits and O_3 exposure in age 19-64 patients.

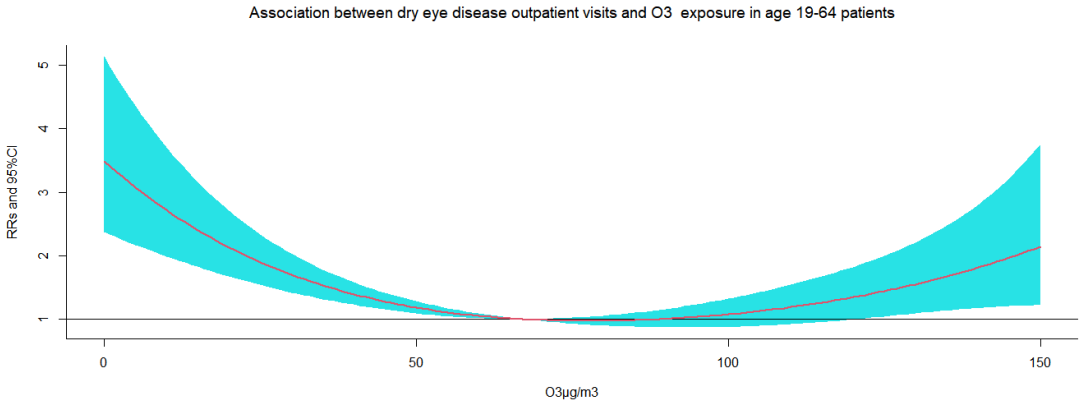

Figure S185. The relative risks (RRs) of per 10 μg/m^3 increase in O_3 on dry eye disease outpatient visits at various lag days in age 19-64 patients.

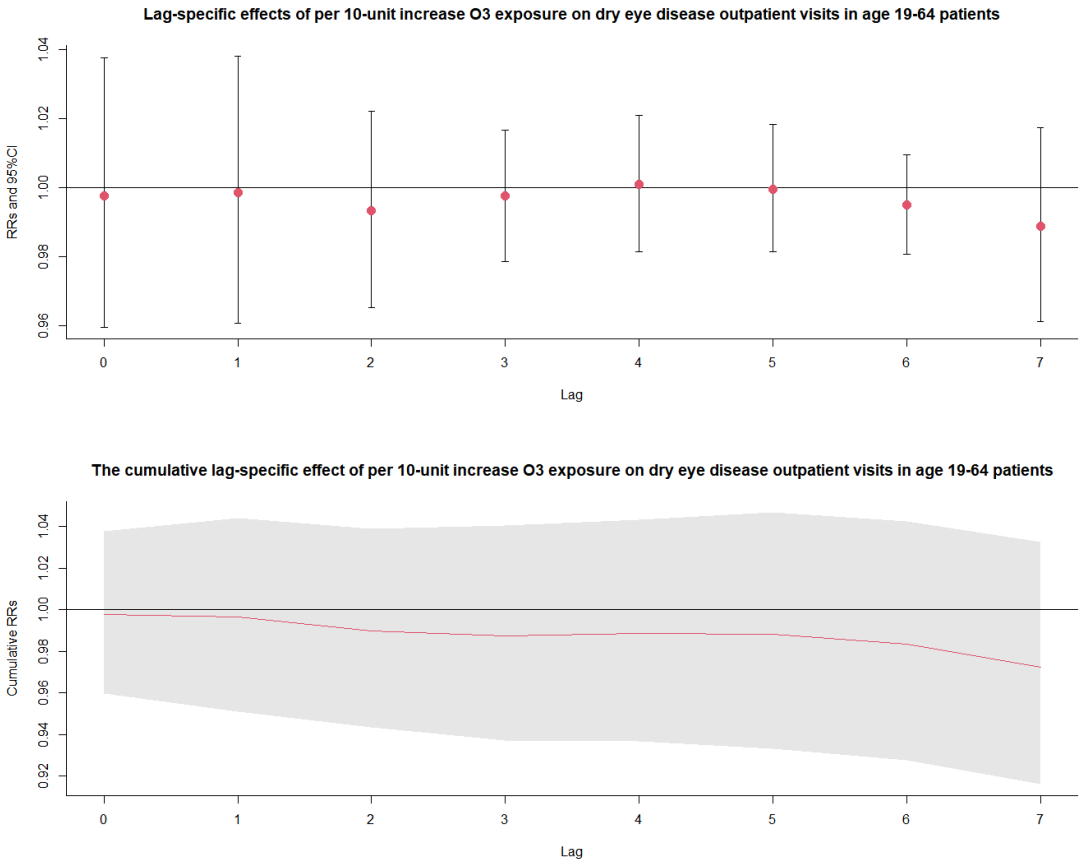

Figure S186. Exposure-response association between dry eye disease outpatient visits and O_3 exposure in age ≥65 patients.

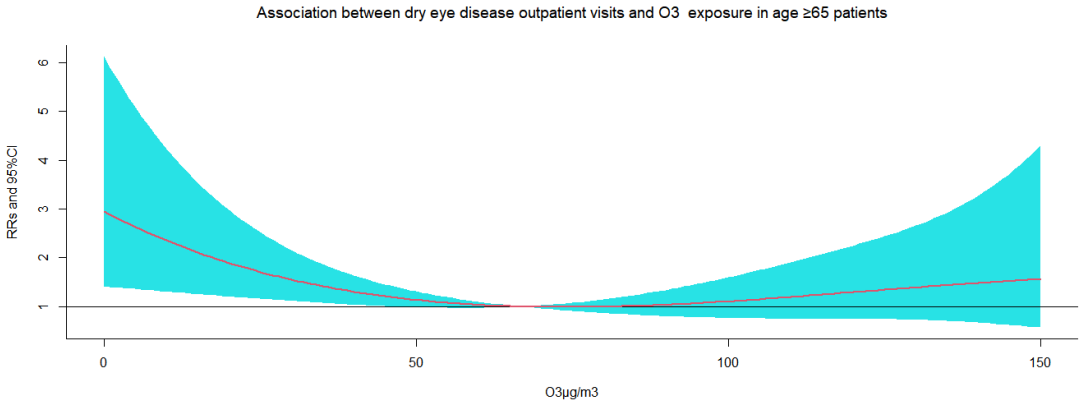

Figure S187. The relative risks (RRs) of per 10 μg/m^3 increase in O_3 on dry eye disease outpatient visits at various lag days in age ≥65 patients.

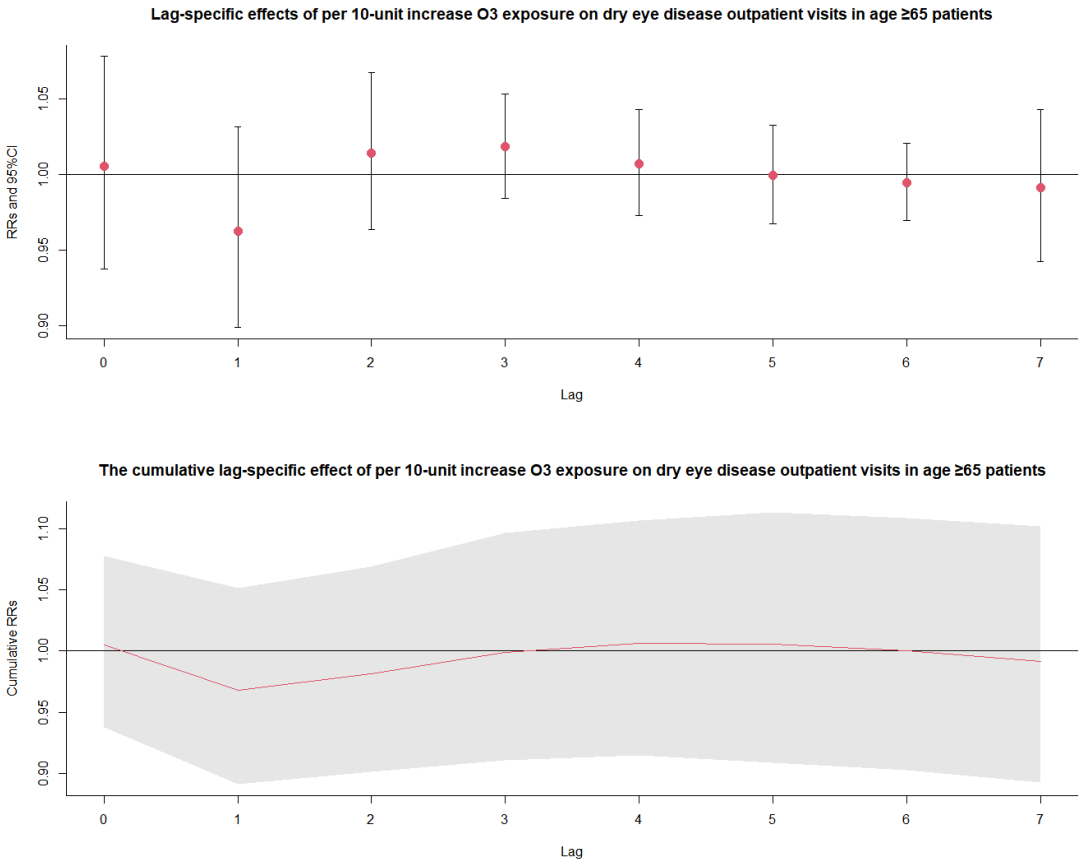

Figure S188. Exposure-response association between dry eye disease outpatient visits and O_3 exposure in the warm season.

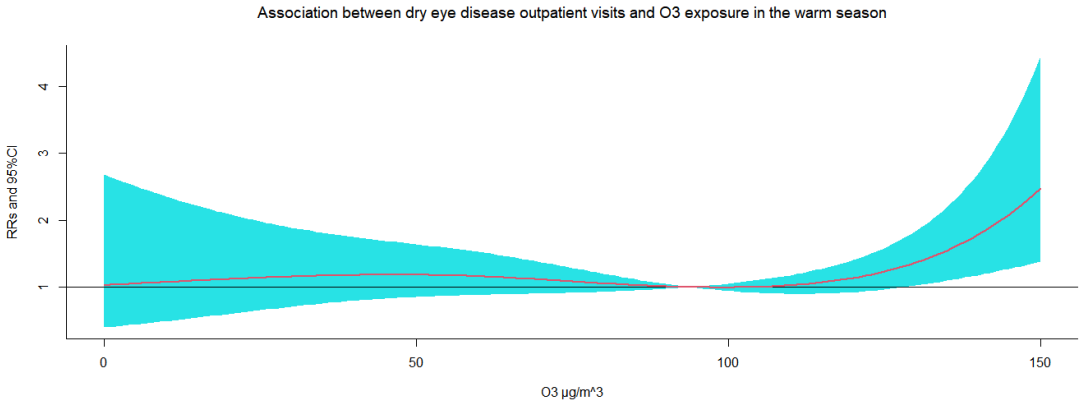

Figure S189. The relative risks (RRs) of per 10 µg/m^3 increase in O_3 on dry eye disease outpatient visits at various lag days in the warm season.

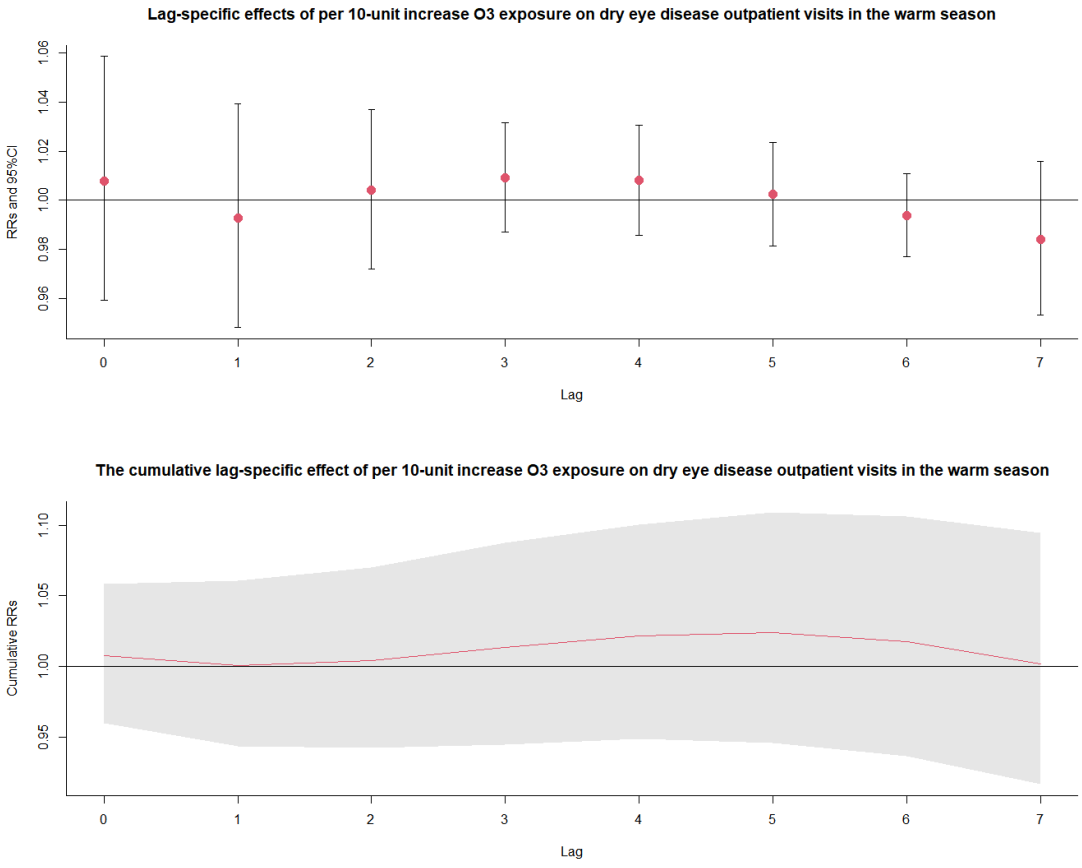

Figure S190. Exposure-response association between dry eye disease outpatient visits and O_3 exposure in the cold season.

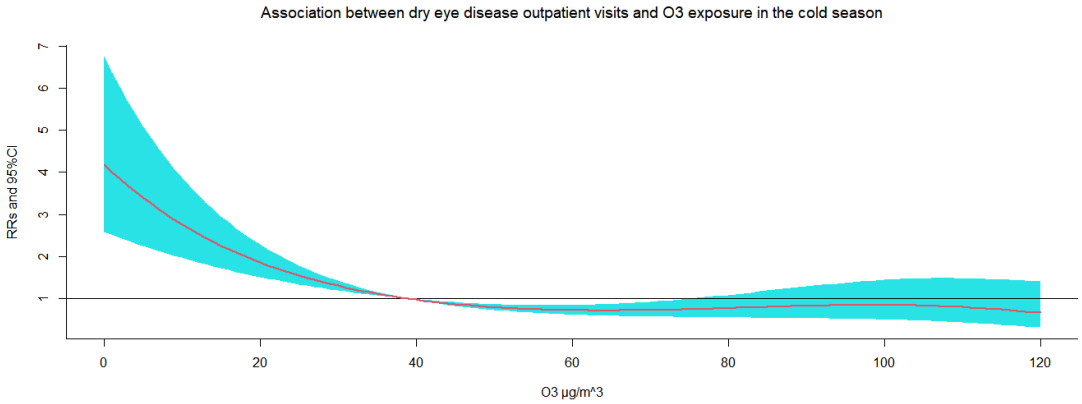

Figure S191. The relative risks (RRs) of per 10 µg/m^3 increase in O_3 on dry eye disease outpatient visits at various lag days in the cold season.

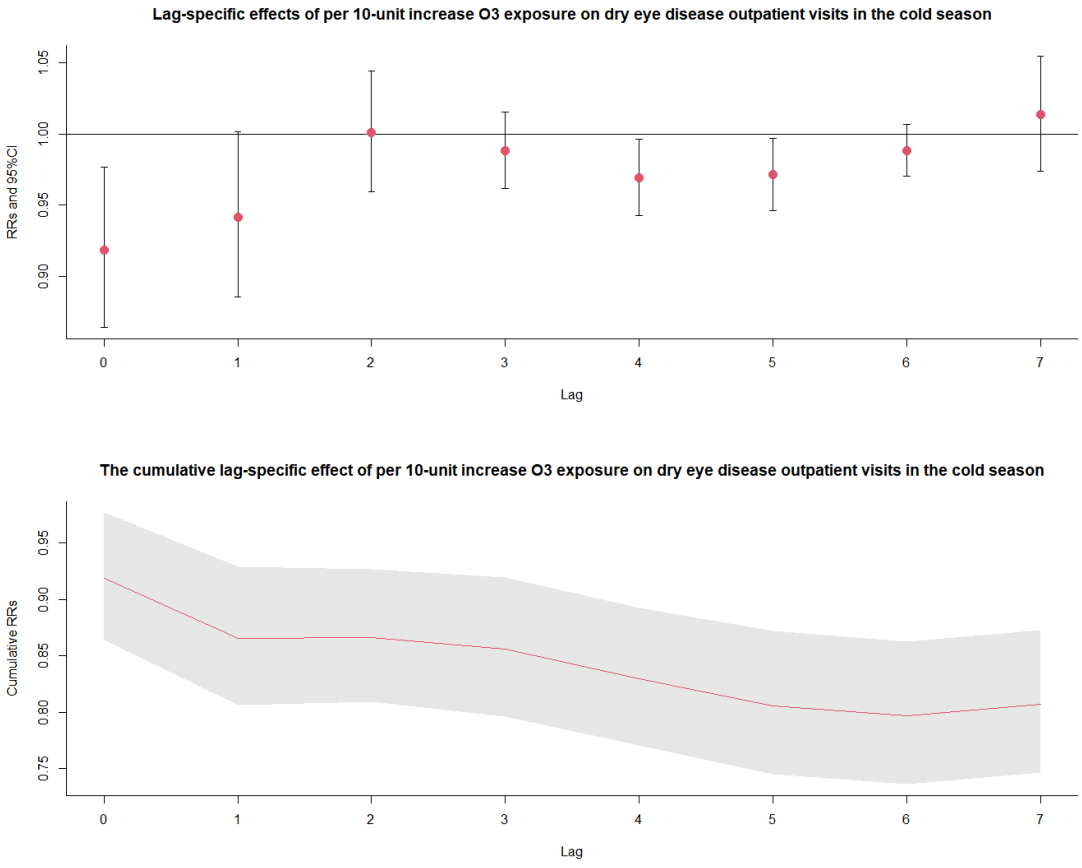

Figure S192. Overall exposure-response association and meteorological conditions: Multi-pollutant model.

Overall exposure-response association and $PM_{2.5}$ exposure distribution: Multi-pollutant model

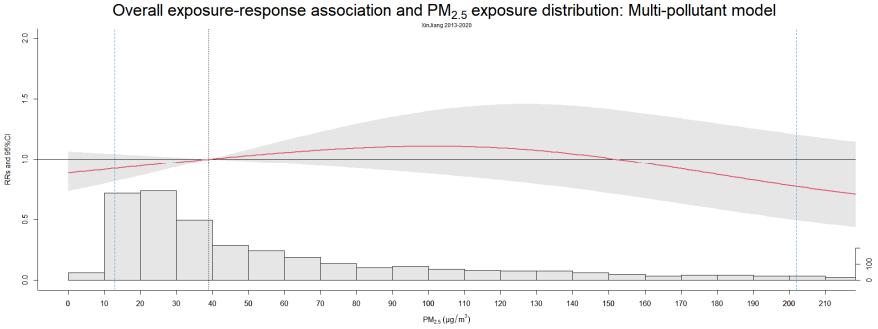

Overall exposure-response association and PM_{10} exposure distribution: Multi-pollutant model

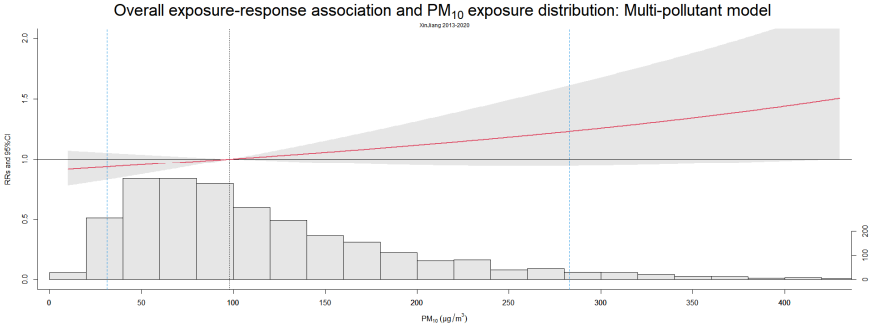

Overall exposure-response association and CO exposure distribution: Multi-pollutant model

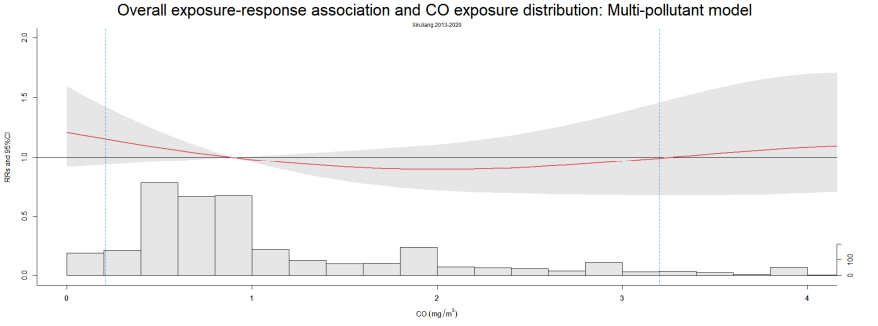

Overall exposure-response association and NO_2 exposure distribution: Multi-pollutant model

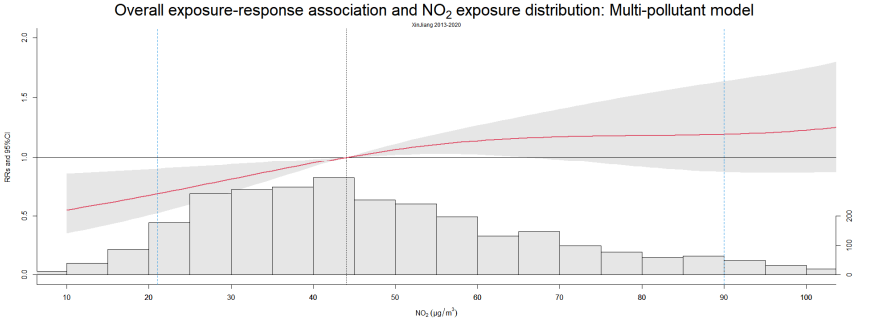

Overall exposure-response association and SO_2 exposure distribution: Multi-pollutant model

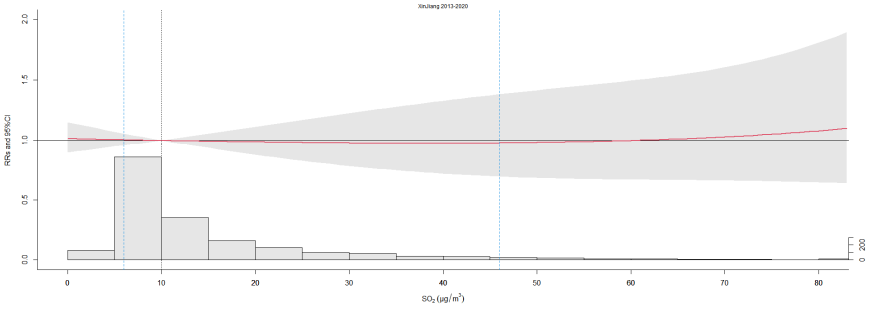
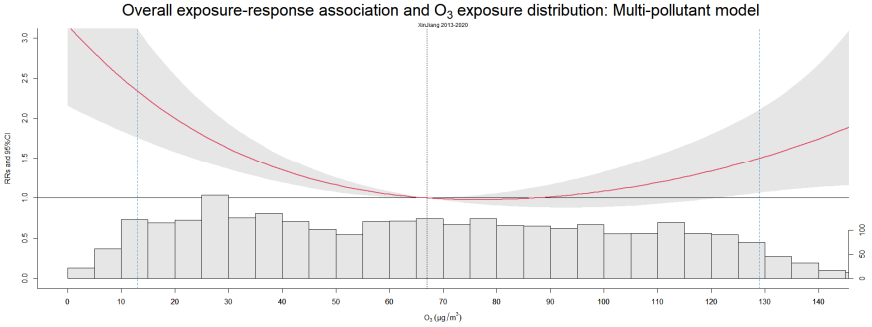
Overall exposure-response association and O_3 exposure distribution: Multi-pollutant model